POST SYMBIOTIC ANALYSIS OF THE *BRADYRHIZOBIUM JAPONICUM*-SOYBEAN SYMBIOSIS: PROTEOMICS AND MUTAGENESIS OF PROTOCATECHUATE 3,4-DIOXYGENASE PARALOGS

A Dissertation presented to

the Faculty of the Graduate School

at the University of Missouri-Columbia

In Partial Fulfillment

of the Requirements for the Degree

Doctor of Philosophy

---

by

Kent N. Strodtman

Dr. David W. Emerich, Dissertation Supervisor

MAY 2012

The undersigned, appointed by the dean of the Graduate School, have examined the dissertation entitled

POST SYMBIOTIC ANALYSIS OF THE *BRADYRHIZOBIUM JAPONICUM*-SOYBEAN SYMBIOSIS: PROTEOMICS AND MUTAGENESIS OF PROTOCATECHUATE 3,4-DIOXYGENASE PARALOGS

presented by Kent N. Strodtman,

a candidate for the degree of doctor of philosophy,

and hereby certify that, in their opinion, it is worthy of acceptance.

Professor David W. Emerich

Professor Scott C. Peck

Professor Gary Stacey

Professor Jay J. Thelen

Professor Judy D. Wall

ACKNOWLEDGEMENTS

I truly wish to express my sincerest gratitude and appreciation to my graduate advisor Dr. David W. Emerich. Without his guidance and encouragement in developing my capabilities as a scientist, educator, and mentor I would not be as prepared as I am to enter into the next phase of my career. He was a guide and voice of reason when I was frustrated, but allowed me to venture in my own creativity and ideas when they came. In doing so he allowed me the greatest freedom and independence of thought and discovery in his lab and for this I will forever be grateful.

I would like to thank Dr. Emerich and all the members of my committee for their guidance and their labs technical help in my research. Dr. Annamraju Sarma I only knew for a short time in the Emerich laboratory, but in that short time he left a lasting impression and gave me the tools to effectively prepare proteomic samples from *B. japonicum*. I am particularly grateful to Dr. Bill Franck formerly of Dr. Stacey's lab, Dr. Severin Stevenson and Dr. Yadong Huong of Dr. Thelen's lab, and all the members of Dr. Judy Wall's lab. I would like to thank Dr. Elizabeth Hoyos of Dr. Doug Randall's lab for gratefully sharing lab space and equipment with the Emerich laboratory and for being a wonderful colleague.

Dr. David Emerich and Dr. Francis Schmidt were both key to my development as an educator in the classroom and I would not be nearly as well prepared for the next stage of my career without their mentoring for my time as the Zahler Teaching Fellow. I would also like to thank all the other members of the Biochemistry Department that I was fortunate enough to work within the various teaching laboratories and classes. I would also like to thank all the TA's and PLA's who I worked with.

I would like to acknowledge all the work the various undergraduates in the Emerich lab have done towards helping me complete my dissertation research. Particularly I would like to thank Nicole Hams and Taylor Zak who worked tirelessly on their own research while, also, helping me. Their work ethic and humor every day helped to make being in the lab pure joy.

I would like to finally thank my family. My parents, in-laws, siblings, and extended family have been a constant support and source of encouragement has been the backbone of this journey for me. To my wife, Erin, and children you have borne the brunt of directly sharing in the burden that being a graduate student can have on a family. With all my gratitude and sincerity, I thank you.

This work is dedicated to my late sister Heidi Jeanne Strodtman.

If I am even half of what you thought I was I will truly have lived a blessed life, rest in peace.

TABLE OF CONTENTS

LIST OF TABLES

Table **Page**

LIST OF FIGURES

Figure **Page**

ABSTRACT

Symbiotic nitrogen fixation between *Bradyrhizobium japonicum* and soybean is the predominant pathway by which the abundant, inert supply of atmospheric dinitrogen is made available in the form of reduced nitrogen, the most limiting nutrient in agricultural production. In a microaerobic environment huge amounts of energy are required to fuel this process and a steady supply of carbon substrates is needed from the symbiotic legume partner to fuel nitrogenase. What source(s) of carbon that are made available to supply nitrogen fixation is poorly understood beyond simple sugars and dicarboxylic acids in *B. japonicum*. The extension of the duration of nitrogen fixation could lead to greater agricultural production. Many aspects of *B. japonicum* persistence in soil, infection, and nodule formation and function have been researched. The least studied aspects of leguminous nitrogen fixation of determinant species are the events that occur beyond the cessation of the symbiosis. Heinrich Anton de Bary, defined symbiosis as " the living together of unlike organisms" in 1879. Upon senescence of the plant what cellular changes occur to the bacteria? In order to better understand the metabolism of *B. japonicum* bacteroids past peak nitrogen fixation proteomics was done over 119 days. Additionally proteins of the periplasm were isolated and analyzed as this cellular compartment serves as a regulator of metabolites and enivormental signals to the bacterium. A metabolic pathway of interest, β-ketoadipate pathway, was analyzed for symbiotic phenotype by mutating both sets of genes encoding *pcaHG*. Finally to better understand if the bacteroids of *B. japonicum* were dedifferentiating into their free-living form, scanning and transmission electron micrographs were taken of post-peak nitrogen

fixing soybean nodules with the discovery of appendages being created by *B. japonicum* in the post-symbiotic state.

Chapter I

Introduction

Adapted from:
Nitrogen Fixation in Crop Production (2009)
American Socity of Agronomy, Inc.
Crop Science Society of America, Inc.
Soil Science Society of America, Inc.

Ch5: Nodule Metabolism

Kent N. Strodtman and David W. Emerich
Department of Biochemistry
University of Missouri

The function of plant root nodules is the fixation of atmospheric dinitrogen into ammonium by the symbiotic form of the rhizobia, called the bacteroid, for assimilation by the plant into proteins, nucleic acids and other nitrogenous compounds. Although the function can be simply stated, the molecular events that must occur to accomplish this goal are complex and many critical steps remain incompletely characterized or unknown. Biochemical, molecular, and genetic analyses have been limited by the complexity of the interaction. The myriad forms of communication and interactions between the plant and the bacteroid are mutually, interdependently controlled from the first initial recognition events in the soil until the nodule undergoes senescence. The plant and the bacteroid must also have the requisite transporters to exchange metabolites between the two symbionts. Nodule physiology is dictated by the low oxygen environment created during nodule development and by the compounds provided to the bacteroids from the plant for maintenance of the bacteroid and more importantly to provide the energy for the nitrogen fixation process. Nodule metabolism encompasses a myriad of process, but this review is limited to aspects of carbon, oxygen and nitrogen metabolism.

Cellular Differentiation and Compartmentation

Symbiotic nitrogen fixation requires the creation of a new plant organ called the nodule. The reduction of atmospheric dinitrogen to ammonium requires differentiation of both the invading bacteria and the host plant cells. Although determinant and indeterminant nodules are structurally unique, fundamentally they can both be considered to be composed of cortical, uninfected, and infected nodule cells. The cortical cells impose a barrier to oxygen diffusion. The uninfected cells provide metabolic support to the nitrogen fixation process, which occurs in the infected cells. The infected cells contain the differentiated bacteroids housed within membrane structures called symbiosomes. Symbiosome membrane originates from the plasma membrane with modifications during cellular differentiation. The symbiosome membrane serves as the interface between eukaryotic and prokaryotic symbionts and thus would be expected to possess transporters for nutrient exchange. Within the symbiosome membrane are differentiated rhizobial cells, bacteroids, which express nitrogenase, the enzyme that catalyzes the reduction of atmospheric dinitrogen to ammonium. The integration of the cellular roles of the infected and uninfected cell types has relied on the measurement of enzyme activities or the expression of unique genes referred to as nodulins. The cellular activities of the bacteroids have been characterized by measurement of enzyme activities, transcription of symbiotically-specific genes, but also the use of genetic mutants. While these approaches will continue to be primary means of experimentation, the use of plant mutants, and anti-sense technology, coupled with global technologies will provide new approaches for exploring symbiotic functioning.

Global Technologies

Large scale expression profiling and proteomic analayses of both the plant and bacteroid portions of the nodule from several symbioses have been reported. As expected many of the genes and proteins identified previously by classical methods of investigation were identified by these new technologies. Also as expected, many new genes and proteins were identified. For example, in *Medicago truncatula* nodules, of the 765 identified plant genes that were differentially expressed during the nodulation process, 41 were previously known nodulation genes, and the remainder had not been previously related to symbiosis (El Yahyaoui et al., 2004). In agreement with biochemical reports, genes for sucrose synthase, β-amylase, a hexose transporter, glycolytic enzymes, malate dehydrogenase and phosphoenolpyruvate carboxylase are up-regulated in nodules (Colebatch et al., 2004; El Yahyaoui et al., 2004; Kouchi et al., 2004; Tesfaye et al., 2006). Many transcription factors/cellular regulators have been found to be differentially regulated during symbiosis, the majority of which have not been assigned specific functional roles. The development of the dual-genome microarray containing sequences of both *Sinorhizobium meliloti* and *M. truncatula* provides a way to simultaneously analyze both symbionts (Barnett et al., 2004).

In bacteroids of *S. meliloti*, a total of 982 genes (Becker et al., 2004) and 1,288 genes (Barnett et al., 2004) were differentially expressed and in *Bradyrhizobium japonicum* a total of 1,234 genes (Chang et al., 2007) and 2,778 genes (Pessi et al., 2007) were differentially expressed. The variation in the number of expressed genes reflects differences in experimental conditions and methodologies. Among the up-regulated genes common to all are the genes previously identified for nitrogenase and supporting

metabolic activities. However, a large number of differentially expressed genes were not in common when the experimental results are compared. These differences will require further experimentation to reconcile the discrepancies.

As with the microarray data, the proteomic studies show considerable agreement with past biochemical and genetic reports, yet they also reveal many additional annotated and unannotated proteins expressed during symbiosis. Proteomic analysis of *B. japonicum* and *S. meliloti* bacteroids has revealed a considerable proportion of the protein mass was dedicated to protein refolding. Nitrogenase has been estimated to comprise at least 10 % of all of the cellular protein mass, but chaperones contribute at least as much protein mass (Djordjevic, 2004; Sarma and Emerich, 2005). Djordjevic (2004) reported the presence of several enzymes of glycolysis in the proteome of *S. meliloti* bacteroids, a pathway which was not thought to be functional during symbiosis. A small protein proteome of less than 20 kDa mass of *M. truncatula* nodules and bacteroids revealed a number of ribosomal and histone-like protein in both symbionts (Zhang et al., 2006).

Proteomic analysis of *M. truncatula* nodules identified 377 plant proteins (Larrainzar et al., 2007). While many of these proteins have been identified in the various transcriptomic analyses to date, many have not. Comparison of the transcriptomic and proteomic analyses demonstrates the dynamic cellular nature of complex systems.

Much of this global information has yet to be clearly articulated into specific metabolic and regulatory processes. Part of the delay is that a large portion of all expressed genes are classified as ‘unknown’, ‘hypothetical’ or poorly annotated, i.e. ‘dehydrogenase’, ‘glycohydrolase’. As with all new technologies, their underlaying value is to not only provide additional information to be analyzed, but new perspectives as to

how it should be analyzed and interpreted. Global technologies will spawn new hypotheses which can be tested by additional biochemical and genetic experimentation.

O_2 Metabolism

The unique physiology and metabolism of the nodule originates with the oxygen lability of nitrogenase, which has only a short half-life in the presence of oxygen. The nodule has a gas diffusion barrier in the outer cortex to reduce oxygen tension within the nodule interior. Vandenbosch and Newcomb (1988) found leghemoglobin, an abundant heme protein that functions to control the oxygen concentration in the interior of the *Glycine max* nodules, in the cytoplasm of both central nodule cell types although there was considerably more located within the infected cells. Using immumogold labeling they found labeling within the nuclei, but not in the organelles nor in the symbiosome space. Vandenbosch and Newcomb (1988) noted that their antibody did not distinguish between holo- and apoprotein and they speculated that the uninfected cells contained primarily apoprotein until the heme was transported from the infected cells via plasmodesmata. Leghemoglobin was identified in the proteome of the symbiosome membrane of *Pisum sativum* (Saalbach et al., 2002) and *Lotus japonicus* (Wienkoop and Saalbach, 2003), but not in *M. truncatula* (Catalano et al., 2004).

The mechanism by which oxygen travels from the leghemoglobin in the plant cytoplasm to the bacteroids within the symbiosome is not known (Garrocho-Villegas et al., 2007). However, hemoglobins have been reported to interact with proteins and membrane lipids and thus the symbiosome membrane may facilitate oxygen transfer from leghemoglobin to the bacteroids (Garrocho-Villegas et al., 2007). No proteins which

could function as an oxygen carrier were noted in a limited proteome analysis of the symbiosome space of pea nodules (Saalbach et al., 2002).

Kuzma et al. (1999) reported that the primary limitation of oxygen to the overall nitrogen fixation process occurs with the bacteroid and not within the plant cells. The free oxygen concentration in nodules has been estimated between 5 and 60 ηM (Hunt and Layzell, 1993). Although the dissolved oxygen concentration is low, the oxygen flux through the nodule is high to permit the generation of ATP needed by nitrogenase and its supporting reactions (Garrocho-Villegas et al., 2007). Oresnik and Layzell (1994) estimated the adenylate energy charge of the plant and bacteroid fractions of soybean nodule and reported the rate of ATP consumption of the bacteroid fraction was ~60% greater than that of the central nodule fraction.

The oxygen concentration within nodules must be precisely maintained to allow symbiotic nitrogen fixation. The effects on nitrogen fixation in whole nodules by variation of oxygen concentration in the nodule environment has been documented (Hunt et al., 1989). The low oxygen environment and unique composition of plant-derived nutrients within the nodule has been difficult to replicate *ex planta*. Generally, the acetylene reduction assay is used to set the oxygen concentration in *ex planta* bacteroids assays. Acetylene is an alternative substrate for nitrogenase, which is reduced to ethylene in a two-electron reaction. The acetylene reduction assay provides a convenient and facile index of nitrogen fixation. However, the assay has limitations and may not accurately reflect nitrogenase activity under all conditions (Peoples and Herridge, 1990; Shah et al., 1975). Oxygen concentration has not been systematically included as a variable parameter when monitoring nitrogen fixation activity and/or associated metabolic

parameters. For example, differences in optimal oxygen concentrations have been noted occasionally such as that for glucose utilization in French bean bacteroids (Trinchant et al., 1981), and aldehyde utilization (Peterson and Larue, 1981) and alanine excretion (Waters et al., 1998) in soybean bacteroids. These examples illustrate the experimental limitations of attempting to understand a complex, dynamic symbiotic interaction *ex planta*.

Although the role of leghemoglobin is to maintain oxygen tension, it is also a significant contributor of activated oxygen species in the nodule, which can interrupt biological function (Dalton, 1995). The active oxygen species generated in nodules leads to the oxidation of ferrous leghemoglobin to ferric leghemoglobin thereby destroying its ability to maintain oxygen tension (Becana and Klucas, 1990). Becana and Klucas (1990) identified four mechanisms by which ferric leghemoglobin can be restored in nodules: a flavin-containing ferric leghemoglobin reductase; direct chemical reduction by NAD(P)H, ascorbate and cysteine; reduction via transfer of electrons from NAD(P)H to free flavins, and reduction by an unidentified low molecular weight heat stable molecule. Soybean oxyleghemoglobin was also shown to scavenge nitric oxide and peroxynitrite (Herold and Puppo, 2005b). Herold and Puppo (2005a,b) suggested that the sequestering of nitric oxide by leghemoglobin may serve to recycle the inactive forms of leghemoglobin to the active state, and also could contribute to preventing the activation of plant defense mechanisms.

Nodules also contain abundant anti-oxidants to protect against activated oxygen species such as the ascorbate-glutathione pathway and superoxide dismutase (Dalton, 1995). Matamoros et al. (2006) demonstrated the biosynthesis of ascorbic acid occurred

by the L-galactose/D-mannose pathway (Valpuesta and Botella, 2004) within the infected zones of both determinant and indeterminant nodules. The components of the ascorbate-glutathione pathway, which reduces H_2O_2 to H_2O, are highly elevated and are coordinately expressed with nitrogenase (Dalton et al., 1986). Ascorbate peroxidase was found in the cytoplasm of both infected and uninfected cells of soybean root nodules and accumulated to ~1% of the total nodule protein (Dalton et al., 1993). All four enzymes of the ascorbate-glutathione pathway were present in the soluble fraction of plant nodule cells and in isolated mitochondria, but were absent in the peroxysome (Dalton et al., 1993). Immunogold labeling indicated that ascorbate peroxidase was present in the cytosol of infected and uninfected cells but not in the symbiosome space. NADPH recycling is an inherent part of the ascrobate-glutathione cycle and Marino et al. (2007) identified an NADP-isocitrate dehyrdrogenase in pea nodules to participate in this recycling in addition to glucose 6-phosphate dehydrogenase and 6-phosphogluconate dehydrogenase. Frendo et al. (2005) created anti-sense plants of *M. truncatula* which were unable to express glutathione and homoglutathione and found that these plants formed fewer nodules, although the early infection events were not altered.

Superoxide dismutases catalyze the conversion of superoxide radicals to dioxygen and hydrogen peroxide. All legume nodules contain a CuZn superoxide dismutase and an Fe superoxide dismutase has been found in nodules of several legume species (Becana et al., 2000). A Mn superoxide dismutase was demonstrated in the root and nodule mitochondria proteomes of soybean (Hoa et al., 2004).

Catalases, which catalyze the decomposition of hydrogen peroxide into water and oxygen, are located mostly in peroxisomes and glyoxysomes and are especially abundant

in determinant nodules where it reduces hydrogen peroxide generated by uricase and other oxidases (Becana et al., 2000). Transcripts for peroxidases, which catalyze the dehydrogenation of various substances in the presence of hydrogen peroxide, were found to be significantly up-regulated in nodules relative to root tissues in *L. japonicus* (Colebatch et al., 2004). Proteomic analysis of the symbiosome membrane of *L. japonicus* did not identify a superoxide dismutase or a catalase, but did identify a peroxidase (Wienkoop and Saalbach, 2003).

Bacteroids contain manganese and/or iron superoxide dismutases depending upon the organism (Becana et al., 1989; Puppo et al., 1982). Santos et al. (2000) deleted the cytoplasmic superoxide dismutase (*sod*A) of *S. meliloti* and reported that the resulting nodules were symbiotically defective demonstrating the important role of this enzyme. An Fe/Mn superoxide dismutatse was found in the *B. japonicum* bacteroid proteome (Sarma and Emerich, 2005). Peroxide metabolism in bacteroids is not well understood, but does not appear to proceed through the ascorbate-glutathione cycle. Bacteroids contain high levels of catalase, but no guaiacol peroxidases (Becana et al., 1989). Ardissone et al. (2004) purified and characterized three catalases from *S. meliloti* and speculated that the disparity of properties of each permits the organism to function in diverse environments. Mutation of the first and second steps of glutathione biosynthesis in *S. meliloti* resulted in the inability to nodulate, and a drastic reduction in nitrogen fixation, respectively (Harrison et al., 2005).

Clearly, reactive oxygen species can have deleterious effects on symbiotic nitrogen fixation. In contrast to their deleterious effects, Pauly et al. (2006) have

suggested that reactive oxygen species and reactive nitrogen species may perform important regulatory roles during symbiosis.

Carbohydrate Metabolism by Plant Nodule Cells

The nodule receives the photosynthetically produced carbohydrates, sucrose and glucose from the leaves and metabolizes them to organic acids, primarily malate, which is provided to the bacteroids for deriving the energy and low potential electrons needed by nitrogenase. Soybean nodules contain relatively high levels of sucrose, but low levels of glucose and fructose (Reibach and Streeter, 1983; Streeter, 1980; Streeter, 1981). The uninfected cells may be the primary sites of sucrose metabolism to dicarboxylates (Kavroulakis et al., 2000).

Several sugar transporters have been identified in *L. japonicus* and *M. truncatula* nodules via transcriptomics and proteomics, but the location of most of these with regard to cell type is not known (Barnett et al., 2004; Colebatch et al., 2004; El Yahyaoui et al., 2004; Kouchi et al., 2004; Tesfaye et al., 2006). A sucrose/proton co-transporter has been localized to the vascular bundles of *L. japonicus* nodules (Colebatch et al., 2004; Flemetakis et al., 2006). Uninfected, but not infected cells of *Vicia faba*, which forms indeterminant nodules, can actively take up glucose and sucrose from the apoplast (Peiter and Schubert, 2003). Kouchi et al. (2004) reported that one hexose transporter, GENF047b10, in *L. japonicus*, increased markedly from 2 and 4 days after infection but returned to the levels of uninfected roots by day 12.

Sucrose synthase, the first step of sucrose catabolism, results in the production of fructose and UDP-glucose (Figure 1). Sucrose synthase from soybean nodules has a

greater affinity for UDP than for UDP-glucose, and also the strong inhibition by UDP, favors the cleavage reaction over the synthetic direction (Morrell and Copeland, 1985). Sucrose synthase was up-regulated in nodules of the well studied leguminous symbioses (Hohnjec et al., 1999; Kuster et al., 1993; Perlick and Puhler, 1993; Silvente et al., 2002; Thummler and Verma, 1987) and has been demonstrated to be essential for nitrogen fixation in pea (Gordon et al., 1999). In developing soybean nodules, transcripts for sucrose synthase were abundant in all nodule tissues, whereas in mature nodules they were much lower with the greatest abundance localized to the parenchyma and pericycle cells of the vascular bundles (Kavroulakis et al., 2000). Kouchi et al. (1988) reported that sucrose synthase enzyme activity in infected soybean nodule cells was more than twice that of uninfected cells. Sucrose synthase transcripts were up-regulated in *M. truncatula* at 4 and 10 days post infection (El Yahyaoui et al., 2004).

The invertases have been suggested to be needed for starch production (Flemetakis et al., 2006) but in *M. truncatula* nodules, Tesfaye et al. (2006) found that neutral invertase was significantly up-regulated relative to sucrose synthase during nodule development.

In *L. japonicus* nodules, the activities of both alkaline and neutral invertases and sucrose synthase were elevated and the transcripts of each were elevated in both infected and uninfected cells (Flemetakis et al., 2006). In soybean nodules, Kouchi et al. (1988) reported that alkaline and acid invertase activity of soybean nodules was at least twice as great in infected cells compared to uninfected cells. Anthon and Emerich (1990) found the two invertases of soybean nodules showed contrasting developmental profiles relative

to the development of nitrogenase activity; acid invertase declined whereas alkaline invertase increased.

UDP-glucose derived from sucrose synthase can be converted to glucose 1-phosphate via UDP-glucose pyrophosphorylase, which was found to be very active in soybean nodule cytosol (Anthon and Emerich, 1990; Copeland et al., 1989c) as was phosphoglucomutase which converts glucose 1-phosphate to glucose 6-phosphate (Copeland et al., 1989c; Reibach and Streeter, 1983). The enzymes for glycolysis and the pentose phosphate pathway have been measured in extracts from a wide variety of nodules (Anthon and Emerich, 1990; Copeland et al., 1995; Copeland et al., 1989c; Gordon and James, 1997; Henson et al., 1982; Hong and Copeland, 1990; Irigoyen et al., 1990; Romanov et al., 1995). Up-regulated transcripts for the glycolytic enzymes have been observed in *L. japonicus* (Colebatch et al., 2004; Kouchi et al., 2004) and *M. truncatula* (El Yahyaoui et al., 2004; Tesfaye et al., 2006). Hexokinase and fructokinase activities were both present in soybean nodules (Copeland et al., 1989c). ATP-dependent phosphofructokinase activity increased sharply at the same time as the rapid decline in aldolase activity in developing soybean nodules (Anthon and Emerich, 1990). The presence of these enzymes and their developmental time course are consistent with the sucrose synthase pathway with the exception of pyrophosphate-dependent phosphofructokinase activity which declined as the ATP-dependent activity increased. Whether the level of the pyrophosphate-dependent activity was sufficient for the sucrose synthase pathway has not been determined. An advantage of the sucrose synthase pathway compared to the invertase pathway is that it requires one ATP per sucrose

compared to two ATP per sucrose via the invertase pathway. Considering the microaerobic nature of the nodule, this may represent an appreciable energy savings.

The pentose phosphate pathway does provide a route around aldolase converting fructose 6-phosphate to glyceraldehyde 3-phosphate without requiring the hydrolysis of ATP or pyrophosphate via their respective fructokinase reactions (Figure 2). Hong and Copeland (1990) recorded appreciable activity of the pentose phosphate pathway enzymes of nodules from seven diffferent plants. This certainly permits the possibility that the pentose phosphate pathway contributes to the primary metabolism of sucrose to triose phosphates. The components of the pentose phosphate pathway are not common in the transcriptomes and proteomes of leguminous nodules. The pentose phosphate pathway may not only participate in the metabolism of sucrose to trioses, but also regenerates NADPH for the ascorbate-glutathione cycle (Marino et al., 2007).

Copeland et al. (1989) demonstrated that the activities of all of the enzymes of the three carbon portion of glycolysis were elevated in soybean nodules relative to roots. Kouchi et al. (1988) found glyceraldehyde 3-phosphate dehydrogenase and phosphoglycerate kinase were more abundant in the infected and uninfected plant cells than in the outter cortex of soybean nodules. All of the genes/proteins for the three carbon portion of glycolysis have been identified in the transcriptomes and proteomes of *L. japonicus* and *M. truncatula* (Bestel-Corre et al., 2002; Colebatch et al., 2004; Larrainzar et al., 2007; Tesfaye et al., 2006). However, the activity of pyruvate kinase activity was low in infected and uninfected cells and the cortex of soybean nodules (Kouchi et al., 1988).

Phosphoenolpyruvate (PEP) can be rapidly converted into malate, rather than pyruvate, via the sequential action of PEP carboyxlase (PEPC) and malate dehydrogenase. Malate was the most abundant dicarboxylate (Stumpf and Burris, 1979) in soybean nodules and is believed to be the primary energy source provided to bacteroids. PEPC requires bicarbonate rather than CO_2 as a substrate. Carbonic anhydrase transcripts were strongly up-regulated in *L. japonicus* (Colebatch et al., 2004) and in *M. truncatula* at 4 and 10 days post infection (El Yahyaoui et al., 2004). Kavroulakis et al. (2000) reported that carbonic anhydrase transcripts were present in all tissues of developing soybean nodules, but absent in the central tissues of mature nodules. They hypothesized that in younger nodules CO_2 recycling was the primary function of carbonic anhydrase whereas in older nodules its function was to remove CO_2 from the nodule tissues. In developing nodules, the majority of transcripts found in soybean nodules were localized to the parenchymateous cells and vasular bundles (Kavroulakis et al., 2000). Gálvez et al. (2000) showed that carbonic anhydrase was expressed inversely to external oxygen concentration.

PEPC can provide up to 25% of the carbon needed for malate and aspartate synthesis (Vance and Gantt, 1992). The activity of PEPC was greater in nodules than in roots of alfalfa, lentil, mung bean and soybean (Choptra et al., 2002; Miller et al., 1987; Pathirana et al., 1992; Vance and Gantt, 1992). Normura et al. (2006) used anti-sense to down-regulate PEPC activity by 90% and found that the levels of sucrose synthase and asparagine aminotransferase were also reduced by ≥50%, whereas glutamine synthetase and glutamate synthase were unchanged. The transgenic plants showed signs of nitrogen deficiency that were relieved by exogenous nitrogen.

PEPC activity in soybean nodules was activated by a PEPC kinase that phosphorylates a serine residue in response to photosynthate supply (Wadham et al., 1996; Zhang and Chollet, 1997), making PEPC less sensitive to inhibition by malate (Schuller et al., 1990; Schuller and Werner, 1993; Zhang et al., 1995). Since malate was one of the more abundant organic acids in nodules (Stumpf and Burris, 1979), PEPC is likely to be highly phosphorylated *in planta*.

Malate dehydrogenase and PEPC were both up-regulated in nodules as determined by proteomic and transcriptomic analyses (Colebatch et al., 2004; El Yahyaoui et al., 2004; Kouchi et al., 2004; Saalbach et al., 2002; Wienkoop and Saalbach, 2003) and these enzyme activities correlate with nodule effectiveness (Haser et al., 1992; Suganuma et al., 2004; Vance et al., 1994). A nodule-enhanced malate dehydrogenase has been detected in pea and alfalfa, which becomes highly expressed during symbiosis (Appels and Haaker, 1988; Fedorova et al., 1999; Miller et al., 1998).

Fermentative Metabolism

Pyruvate decarboxylase, pyruvate kinase, malic enzyme, lactate dehydrogenase and alcohol dehydrogenase have been found in the cytosols of several plant nodules and for the most part, these enzymes have not been extensively studied (McCloud et al., 2001; Peterson and Evans, 1978; Peterson and Larue, 1981; Smith et al., 1994; Suganuma et al., 1987; Tajima and Larue, 1982; Vance and Heichel, 1991). Peterson and La Rue (1981) demonstrated that acetaldehyde could result in acetylene reduction rates equivalent to those of succinate when each was added exogenously to isolated bacteroid suspensions, but the oxygen concentration for optimal aldehyde-dependent activity was

considerably lower than that for optimal activity with dicarboxylic acids. These authors found a number of two and three carbon compounds that could support acetylene reduction, albeit at lower levels of activity than compared to succinate, and all required much lower oxygen concentrations than that needed for optimum activity with succinate.

Symbiosome Membrane

The symbiosome can be considered a special form of lytic comparment of the infected plant cell (Mellor, 1989). It forms a dual role of segregating the prokaryotic and eukaryotic symbionts and providing a mechanism for the exchange of selected nutritients. Since the symbiosome membrane is inverted, due to endocytosis of the bacteroids into the infected plant cell, solute movement across the symbiosome membrane toward the bacteroid resembles plant export. The selective permeability of the symbiosome membrane provides bacteroids with a defined regimen of metabolites from which they extract energy for nitrogen fixation.

Symbiosome membranes are produced by the host plant consisting of infection-thread membrane, Golgi, Endoplasmic Reticulum and *de novo* lipid synthesis (Roth and Stacey, 1989). The fatty acid composition of the membrane in soybean nodules was more similar to that of the Endoplasmic Reticulum than the Golgi (Bassarab et al., 1989). Catalano et al. (2007) have identified a SNARE protein in the symbiosome membrane of *M. truncatula* suggesting a role in infection thread and/or symbiosome development.

Proteins have been identified in the symbiosome membranes of *G. max* (Panter et al., 2000; Werner, 1992), *M. truncatula* (Catalano et al., 2004), and *P. sativum* (Saalbach et al., 2002) by both biochemical and proteomic analyses. The first proteins identified

were from soybean and included: Nodulin 24, Nodulin 26, Nodulin 53, thiol protease, subtilisin protease, protein disulfide isomerase, calcium-dependent protein kinase, heat shock protein 60 and BiP protein, which is a widely distributed and highly conserved Endoplasmic Reticulum luminal protein that has been implicated in co-translational folding of nascent polypeptides, and in the recognition and disposal of misfolded polypeptides. The identities of 51 proteins in *M. truncatula* (Catalano et al., 2004) and 20 proteins in *P. sativum* (Saalbach et al., 2002) symbiosome membranes have been determined, many of which support a role for the symbiosome membrane in protein folding and import (Panter et al., 2000). Simonsen and Rosendahl (1999) have directly demonstrated that isolated pea symbiosomes can import plant-translated proteins.

Symbiosomes from a variety of legume nodules all have been demonstrated to rapidly transport dicarboxylates (Udvardi and Day, 1997). The high affinity malate and succinate transporters operate as a uniport for the monovalent dicarboxylate anion. Symbiosome and bacteroid membranes from soybean nodules can not effectively transport sucrose, fructose or glucose in toward the bacteroids (Day et al., 2001; Lodwig et al., 2003), although French bean symbiosomes effectively transport glucose through both sets of membranes (Herrada et al., 1989). Trinchant et al. (1981) demonstrated that glucose supported acetylene reduction activity in bacteroids isolated from French beans at rates similar to that of succinate. However, optimal glucose-supported activity occurred at a significantly lower oxygen concentration than that for dicarboxylate-supported activity. Oxalate has also been shown to be transported across the symbiosome and bacteroid membranes from Broad bean and support acetylene reduction activity, also at oxygen concentrations lower than those for succinate (Trinchant et al., 1981).

The energy for transport originates, at least partially, from vacuolar ATPase proteins that have been reported by two separate proteomic investigations (Catalano et al., 2004; Saalbach et al., 2002). Udvardi and Day (1989) demonstrated that the ATPase of the symbiosome membrane generates a membrane electrical potential with the interior possessing a positive charge which would permit the operation of voltage-driven channels (Roberts and Tyerman, 2002; Rosendahl et al., 2001).

Amino acids are not effectively transported across the symbiosome membranes of *G. max*, *Phaseolus vulgaris* and *Vicia faba* (White et al., 2007), but an H^+/aspartate export transporter has been identified in pea (Rosendahl et al., 2001; Rudbeck et al., 1999). A voltage-gated monovalent cation channel capable of transporting ammonium to the plant has been reported in several plants (Kaiser et al., 1998; Mouritzen and Rosendahl, 1997; Roberts and Tyerman, 2002; Tyerman et al., 1995; Whitehead et al., 1995).

Symbiosome Space

The symbiosome space, the region between the symbiosome membrane and the bacteroids varies greatly in terms of volume among symbioses and has a much lower density than the infected plant cell cytoplasm. Proteins identified in the soybean symbiosome space via biochemical methods include: acid phosphatase, α-mannosidase II, proteases, protease inhibitors, α-glucosidase, aspartate aminotransferase, and trehalase (Werner, 1992). Curiously, three of the identified proteins are sugar hydrolases.

Saalbach et al. (2002) used proteomic methods to identify 46 proteins in the symbiosome space of pea nodules. Among the proteins found were chaperonins, heat

shock proteins, protein disulfide isomerase, and ATP synthase components, which would be expected based on the protein composition of the symbiosome membrane. However, both nitrogenase proteins were found in the symbiosome space of pea nodules and the majority (21 of the 27) of the identified proteins were annotated as bacterial in origin, primarily *Rhizobium leguminosarum*, the endophyte of pea indicating lysis of the pea bacteroids occurred. This emphasizes the difficulty associated with obtaining uncontaminated preparations of subcellular components of nodules. None the less, the combined biochemical and proteomic analyses demonstrate that the symbiosome membrane and symbiosome space are highly active metabolic compartments of the nodule.

Bacteroid Periplasm

The periplasmic space is the compartment between the plasma membrane and the outer membrane of Gram-negative bacteria, which may constitute up to 40% of the total cell volume. The periplasm actively acquires and transport nutrients, synthesizes peptidoglycan, promotes electron transport, inactivates substances toxic to the cell, and senses the environment (Ames, 1988). The periplasm of non-symbiotic rhizobia retains their integrity from the extracellular environment, but the symbiosome represents a unique 'intracellular' environment. At present there are insufficient experimental results to determine how these two spaces are inter-related during symbiosis. However, communication and nutrient transport between the prokaryotic and eukaryotic nodule symbionts requires the co-operative interaction of the periplasm and the symbiosome spaces.

Methods have been developed to isolate proteins in the periplasm (de Maagd and Lugtenberg, 1986; Glenn, 1979; Streeter, 1989; Streeter and Salminen, 1990), but there are only a few reports on the enzyme activities and protein contents of the periplasmic space. The periplasmic nitrate reductase from *B. japonicum* was recently isolated and characterized (Delgado et al., 2003). The two electron reduction of NO_3^- to NO_2^- was coupled to quinol oxidation which in turn was possibly coupled to proton translocation and energy generation. The results of the study suggested that the periplasmic nitrate reductase was the enzyme responsible for anaerobic growth of free-living *B. japonicum* under nitrate respiring conditions (Delgado et al., 2003), but may also be responsible for the formation of nitrosylleghemoglobin from nitric oxide (Meakin, 2007). The nitrosylleghemoglobin compromises leghemoglobins' ability to effectively bind oxygen. Bernardelli et al. (2001) have shown that glucose metabolism occurs extracellularly via a periplasmic PQQ-dependent glucose dehydrogenase that oxidizes glucose to gluconate in *S. meliloti* bacteroids. Three *R. leguminosarum* periplasmic proteins were identified as components of the symbiosome space of pea: a general L-amino acid-binding protein; DppA protein (dipeptide transporter), and an unspecified periplasmic binding protein (Saalbach et al., 2002).

Periplasmic, secreted, or membrane spanning proteins can be identified by creating fusions between target genes and *pho*A, the gene encoding the *Escherichia coli* alkaline phosphatase first described by Manoil and Beckwirth (1985). Long et al. (1988) used this method to screen 1,250 *S. meliloti* mutants, identifying 25 symbiotically defective mutants that formed Fix^- nodules on alfalfa. Thirteen mutants were defective in synthesizing exopolysaccharide. The remaining twelve mutants comprised nine

membrane proteins, including the *dct*A gene (dicarboxylic acid transporter), and three periplasmic proteins required for symbiosis. ExoR, a global regulator of transcription, was localized to the periplasm via PhoA fusions, and by fractionation and western blotting (Wells et al., 2007). The periplasmic localization of ExoR defined it as a novel class of protein that influences the activity of transcription factors in the cytoplasm (Wells et al., 2007). *B. japonicum* PhoA mutant studies have identified genes of signal peptidases, *sipS*, *sipF,* and *sipX* (Muller, 2004; Muller, 1995). Mutants of *sip*S mutants form ineffective nodules during symbiosis, mutants of *sip*F have some nitrogen fixation activity, but the bacteroids appear deformed, while mutants of *sip*X form an effective symbiotic interaction.

Bacteroid Transport

Carbon Compounds

The energy for nitrogenase is provided through the metabolism of photosynthetically-derived compounds (Figure 3). These compounds are metabolized to the level of organic acids and transported through the symbiosome membrane, move through the symbiosome and the periplasmic spaces and across the bacteroid membrane. The rapid transport of dicarboxylic acids and their metabolic importance has been well demonstrated via biochemical and genetic results (Lodwig et al., 2003; Poole and Alloway, 2000; Prell and Poole, 2006; White et al., 2007).

Although most evidence demonstrates that dicarboxylates are the energy sources for nitrogen fixation, other carbon sources may perform roles during symbiosis. Glucose has been demonstrated to be transported across the bacteroid and symbiosome

membranes (Herrada et al., 1989) of French bean. Trinchant et al. (1981) reported that glucose and sucrose supported nitrogen fixation activity in French bean bacteroids, but the concentration of oxygen needed for optimal sucrose- or glucose-dependent activity was much lower than that demonstrated for succinate. In contrast, sucrose and glucose were transported across the soybean bacteroid membrane via passive diffusion (Udvardi et al., 1990) and provide only ~ 20% increase in soybean bacteroid respiration (Ruiz-Argüeso et al., 1979). Udvardi et al. (1990) found that fructose was transported across the *B. japonicum* bacteroid membrane by two separate transporters, one of which achieved rates of fructose transport comparable to that of succinate transport. Kinnback et al. (1987) identified enzymes of mannose metabolism in the symbiosome space of soybean nodules, specifically α-mannosidase II, but transport of mannose by bacteroids has not been demonstrated.

Pyruvate alone can support nitrogen fixation, respiration and hydrogen evolution by anaerobically isolated soybean bacteroids (Bergersen and Turner, 1967a) and pyruvate utilizing enzymes have been measured in *B. japonicum* bacteroids and also found in the proteome (Copeland et al., 1989a; Copeland et al., 1989c; Kim and Copeland, 1996; Sarma and Emerich, 2005a). Pyruvate increased nitrogen fixation activity measured as $^{15}N_2$ incorporation into ammonium at rates of more than 5 fold greater than endogenous levels, but that was only ~25% of the rate of succinate (Bergersen and Turner, 1967a; Peterson and Larue, 1981). Aldehyde and alcohols increase nitrogen fixation of *ex planta* bacteroids (Peterson and Larue, 1981) but, like pyurvate, their transport has not been characterized.

Nitrogen Compounds

In 1967, Bergersen and Turner (1967) incubated isolated soybean bacteroids under $^{15}N_2$ and found that ammonium was the labeled product of symbiotic nitrogen fixation. Bacteroids do not express an ammonium transport system (Udvardi and Day, 1997), nor the classical glutamine synthetase/glutamate synthase system. Ammonia was thought to diffuse across the bacteroid membrane (Udvardi and Day, 1997), become ionized in the more acidic symbiosome space and be transported via an ammonium transporter in the symbiosome membrane (White et al., 2007) into the plant cytosol and then assimilated to amino acids, amides and/or ureides.

In 1985, Kahn et al. proposed nutrient exchange models in which the fixed nitrogen may be carried across the bacteroid membrane, for example, as an amine or amide in exchange for dicarboxylates or some other compound(s). Subsequently, evidence began to appear suggesting nutrient exchange occurred during symbiosis (Appels and Haaker, 1991; Rosendahl et al., 1992; Salminen and Streeter, 1990; Waters et al., 1998). Labeling studies have shown that plant metabolites can be used for amino acid biosynthesis in the bacteroid (White et al., 2007). Proteomic and transcriptomic results verify the bacteroid's ability to synthesize amino acids (Becker et al., 2004; Chang et al., 2007; Pessi et al., 2007; Sarma and Emerich, 2005). Aspartate aminotransferase has been shown to be essential for nitrogen fixation in pea (Lodwig et al., 2003) and alfalfa (Rastogi and Watson, 1991) bacteroids. Aspartate excreted from pea bacteroids could be transported from the H^+/aspartate transporter found on the symbiosome membrane (Rosendahl et al., 2001). An alanine dehydrogenase mutant of *R. leguminosarum* inoculated onto pea has shown that although ammonia can serve as the

primary transported species, alanine biosynthesis was necessary to enhance plant mass (Allaway et al., 2000). Inoculation of a double mutant of *R. leguminosarum*, blocked in two ABC-type amino acid transport systems, *aap* and *bra*, resulted in nitrogen deficient pea plants. The bacteroids were reported to have nitrogenase activity equivalent to that of the wild type, implying that the fixed nitrogen could only be provided to the plant if supplied as amino acids (Lodwig et al., 2003).

Prell and Poole (2006) have proposed amino acid cycles, which in their simplest form is the exchange of one amino acid for another, for example, glutamate obtained from the plant and bacteroid-derived alanine or aspartate returned. While the proposed amino acid cycles would explain various anomalies of symbiotic metabolism, neither an amino acid cycle nor a nutrient exchange system have yet to be conclusively demonstrated (White et al., 2007). Intuitively, global nitrogen and carbon metabolism should be inherently integrated in leguminous symbioses. However, this most fundamental aspect of leguminous nodules, manifested in the form of these nutrient exchange/amino acid cycles, are among the least understood interactions of symbiosis.

Bacteroid Metabolism

Nitrogenase

The reduction of atmospheric dinitrogen to ammonium is the primary function of the symbiosis. Nitrogenase catalyzes the MgATP-dependent reduction of N_2 to ammonia: $N_2 + 8e^- + 16\ MgATP + 8H^+ \rightarrow 2NH_3 + H_2 + 16\ MgADP + P_i$.

Hydrogen evolution is an inherent step of the catalytic mechanism of nitrogenase (Simpson and Burris, 1984). A number of strains of the slow-growing rhizobia possess hydrogenases which recycle the hydrogen thereby recapturing some of the lost energy (Albrecht et al., 1979; Emerich et al., 1979).

Although there are several different types of nitrogenases, rhizobia possess only the molybdenum-containing type (Howard and Rees, 2006). The Mo nitrogenases are composed of two proteins: a Mo-Fe protein and a Fe protein. The MoFe protein is a 220 to 240 kDa tetramer, an $(\alpha\beta)_2$ complex, of the *nif*D (α-subunit) and *nif*K (β-subunit) gene products each of which contains complex metalloclusters. Each tetramer of two αβ pairs contains two P-clusters [Fe_8S_7] and two FeMo cofactors. The FeMo cofactor, located within the α-subunit, consists of a $MoFe_3$-S_3 cluster bridged to a Fe_4-S_3 cluster by three sulfur ligands with a homocitrate co-ordinated to the molybdenum (Howard and Rees, 2006). The Fe protein is ~ 60 kDa dimer of the *nif*H gene with a single 4Fe-4S cluster located between the subunits. A MgATP binding site is located on each subunit (Howard and Rees, 2006). During catalysis, electrons are delivered one at a time from the Fe protein to the MoFe protein in a reaction coupled to the hydrolysis of 2 MgATP for each electron transferred (Rees and Howard, 2000). The P-clusters are thought to mediate electron transfer from the Fe protein to the FeMo-cofactor of the MoFe protein, the site for substrate binding and reduction. In addition to performing a catalytic role, the Fe Protein serves as a Mo/homocitrate insertase (Hu et al., 2006).

There are more than 20 genes involved in nitrogenase synthesis and regulation. Oxygen is a primary regulator of nitrogenase expression in all symbiotic bacteria. In *B. japonicum*, two regulatory cascades, FixLJ-$FixK_2$ and RegSR-NifA respond to oxygen

(Lindemann et al., 2007). The FixL protein is the heme-containing sensory partner of a two-component regulatory system which undergoes autophosphorylation as the oxygen concentration declines. Phosphorylated FixL phosphorylates FixJ, which in turn activates *fix*K_2 of *B. japonicum*. In *S. meliloti* phosphorylated FixJ activates *nif*A, *fix*K and *fix*K'. In *B. japonicum*, *fix*K_2 activates *fix*K_1, of which there are no known targets, and *nif*R which mediates the expression of genes for denitrification (Mesa et al., 2006). Sciotti et al. (2003) proposed the two oxygen regulatory cascades control genes required for microaerobic and anaerobic lifestyles, respectively, in *B. japonicum*. During infection the invading bacteria are exposed to a decreasing concentration of oxygen. The induction of the FixLJ-FixK_2 cascade would result in gene expression necessary for preparing the rhizobia for the microaerobic lifestyle, such as expression of the high affinity ccb_3-type oxidase. Once the environment is established, the NifA-dependent genes activate the expression of the *fix* and *nif* genes (Sciotti et al., 2003).

Hexose Metabolism

Bacteroids receive dicarboxylates from the plant based on the selective permeability of both the bacteroid and symbiosome membranes (Udvardi and Day, 1997). Bacteroids are deficient in enzymes of sucrose metabolism, the Embden-Meyerhof pathway, and the Entner-Doudoroff pathway (Copeland et al., 1989c; Vance and Heichel, 1991). However, the efficacy of fructose uptake (Udvardi et al., 1990), the presence of α-mannosidase II in the symbiosome space (Kinnback et al., 1987), the presence of enzymes of glycolysis (Finan et al., 1991), the presenece of the pentose phosphate pathway (Copeland et al., 1989c; Romanov et al., 1994) and the identification of a xylose

isomerase (Djordjevic et al., 2003) permit speculation that hexoses may perform a role in bacteroid metabolism. *B. japonicum* bacteroids are capable of synthesizing trehalose (Salminen and Streeter, 1986), a disaccharide of α,α-1,1 linked glucose, which is present in the bacteroid at greater concentrations than that found in the soybean nodule cytosol (Streeter, 1987). Streeter (1982) reported that soybean nodule bacteroids possessed a greater specific activity of both trehalase and maltase activities than the plant nodule cytosol.

Metabolism of Two- and Three-Carbon Compounds

The three carbon portion of glycolysis has been demonstrated to be required for symbiosis in *S. meliloti* bacteroids, as mutants in glyceraldehyde-3-phosphate dehydrogenase, enolase, and 3-phosphoglycerate kinase were symbiotically defective, resulting in nitrogenase activities less than 5% of the wild-type (Finan et al., 1991). Glyceraldehyde 3-phosphate dehydrogenase and enolase have been identified in the proteome of *B. japonicum* bacteroids (Dainese-Hatt et al., 1999; Sarma and Emerich, 2005) and former enzyme measured in bacteroid extracts (Shah and Emerich, 2006).

Both *S. meliloti* (Irigoyen et al., 1990) and *B. japonicum* (Smith et al., 1994) bacteroids possess pyurvate kinase activity suggesting the production of pyruvate, which could be further metabolized to acetyl-CoA via pyruvate dehydrogenase (Dunn, 1998), or alanine via alanine dehydrogenase (Allaway et al., 2000; Smith and Emerich, 1993a; Smith and Emerich, 1993b). Phosphoenolpyruvate carboxylase (Smith et al., 1994) has been measured in *B. japonicum* bacteroids and correlated with the development of nitrogenase activity. Pyruvate carboxylase mutants of *R. tropici*, *R. etli* (Dunn et al.,

1996), *R. leguminosarum* bv. trifolii (Ronson and Primrose, 1979) and bv. viciae (Arwas et al., 1986) had no symbiotic phenotype suggesting they are not required for nitrogen fixation.

Phosphoenolpyruvate carboxykinase has been measured in *R. tropici* (Romanov et al., 1994) and in *B. japonicum* (Smith et al., 1994) and in the later symbiosis, development of the enzyme activity correlated with the expression of nitrogenase activity. *S. meliloti* mutants of phosphoenolpyurvate carboxykinase formed ineffective nodules in which the nitrogenase activities were ~ 60% of wild type (Finan et al., 1991). Moreover, Finan et al. (1991) were unable to measure phosphoenolpyruvate carboxykinase activity in wild-type *S. meliloti* bacteroids and suggested that gluconeogenesis does not occur.

Pyruvate can also be generated by NAD-dependent malic enzyme which has been shown to be necessary for symbiotic nitrogen fixation in *S. meliloti* bacteroids (Driscoll and Finan, 1993). Soybean, pea, alfalfa, and chickpea bacteroids possess pyruvate dehydrogenase permitting the formation of acetyl-CoA (Dunn, 1998). Acetate kinase, acetyl-CoA synthetase and phosphotransacetylase activities of soybean nodule bacteroids were found to correlate with the development of nitrogen fixation activity (Smith et al., 1994). Acetate was found to be among the most abundant carboxylates in soybean nodules (Jackson and Evans, 1966). The polymeric form of acetate, poly-β-hydroxybutyrate, can accumulate to ~60% of the dry weight of of soybean nodule bacteroids (Karr et al., 1983).

Encarnación et al. (1995) have suggested that bacteroids may adapt a fermentative-like metabolism during symbiosis. Peterson and La Rue (1981;1982)

demonstrated that *B. japonicum* bacteroids could utilize aldehydes and alcohols to support acteylene reduction activity *ex planta*. A wide range of aldehyde and alcohols were able to support nitrogen fixation. Several aldehyde and alcohol dehydrogenases were identified in the proteomes of *B. japonicum* (Sarma and Emerich, 2005) and *S. meliloti* (Natera et al., 2000) bacteroids.

Metabolism of Four-Carbon Compounds

Malate is the most abundant dicarboxylic acid in soybean nodules (Stumpf and Burris, 1979) and can be rapidly accumulated by bacteroids (Udvardi and Day, 1997). The citric acid cycle has been believed to be the primary catabolic pathway for energy production for nitrogenase. In the fast growing rhizobia, mutations in several citric acid cycle genes result in ineffective nodules. Dymov et al. (2004) created a malate dehydrogenase mutant of *S. meliloti* and demonstrated it was essential for symbiotic nitrogen fixation. A citrate synthase mutant of *S. meliloti* formed nodules on alfalfa that were unable to fix nitrogen (Mortimer et al., 1999). An isocitrate dehydrogenase mutant of *S. meliloti* formed nodules, but the bacteroids were ineffective for nitrogen fixation (McDermott and Kahn, 1992). A mutant in the dehydrogenase subunit of α-ketoglutarate dehydrogenase (*suc*A) of *R. leguminosarum* inoculated onto peas did not fix nitrogen (Warshaw et al., 1997).

In contrast, aconitase (Thony-Meyer and Kunzler, 1996), isocitrate dehydrogenase (Shah and Emerich, 2006) and α-ketoglutarate dehydrogenase (*suc*A) (Green and Emerich, 1997a) mutants of *B. japonicum* all formed nodules that reduced atmospheric dinitrogen similar to wild type. The later two mutants of *B. japonicum*

resulted in a delay in nodule formation, but reduced dinitrogen at rates not different from the wild-type (Green and Emerich, 1997a; Shah and Emerich, 2006). Thus, there appears to be a clear difference in the role of the citric acid cycle between the fast- and slow-growing rhizobia.

Green et al. (2000) identified a CoA-independent α-ketoglutarate decarboxylase activity in *B. japonicum* bacteroids that was capable of forming succinic semialdehyde directly from α-ketoglutarate, which if succeeded by succinic semialdehyde dehydrogenase would result in a alternate pathway. However, the source of the α-ketoglutarate would not be the citric acid cycle based on the results of the isocitrate dehydrogenase and α-ketoglutarate dehydrogenase mutants in *B. japonicum*, but rather from glutamate. *B. japonicum* bacteroids have the ability to transport exogenous glutamate (Udvardi et al., 1988), which could be transaminated within the bacteroid to form α-ketoglutarate. Aspartate aminotransferase was found in the symbiosome space of soybean nodules, identified in the *B. japonicum* bacteroid proteome (Sarma and Emerich, 2005) and transcriptome (Chang et al., 2007; Pessi et al., 2007), and has been shown to be essential for nitrogen fixation in pea (Lodwig et al., 2003) and alfalfa (Rastogi and Watson, 1991) bacteroids.

Although the fast-growing rhizobia required a complete citric acid cycle, they do not require the gloxylate cycle. Ramírez-Trujillo et al. (2007) demonstrated that *S. meliloti* mutants of isocitrate lyase and malate synthase formed normal nodules. The glyoxylate cycle does not appear to function in the *B. japonicum* bacteroids (Green et al., 1998).

Metabolism of Poly-β-hydroxybutyrate and Glycogen

Bacteroids and cultured rhizobia can accumulate glycogen and poly-β-hydroxybutyrate (Lodwig et al., 2005), although there are marked differences among the fast- and slow-growing rhizobia in the extent of accumulation and the conditions under which they accumulate. The roles of these polymers during symbiosis are not fully understood.

Poly-β-hydroxybutyrate (PHB), a carbon storage polymer of acetate, can accumulate up to 60% of the dry weight of soybean bacteroids (Karr et al., 1983), but does not accumulate as granules in bacteroids of indeterminant nodules where, for example, it accumulates to <5% of the dry weight of bacteroids of chickpea (Kim and Copeland, 1996). The activities of the acetate metabolic enzymes as a group appeared to correlate more closely with the development of nitrogen fixation activity during soybean nodule development than did the pyruvate metabolic enzymes (Smith et al., 1994). Bergersen and co-workers (1990; 1991) proposed that PHB was a mobilizable energy source that supports nitrogen fixation when sucrose and its metabolites are not available. PHB has been proposed to serves a role in differentiation into the bacteroid state (Aneja and Charles, 1999; Lodwig et al., 2005). Mutations in PHB metabolism showed no detrimental effects in either determinant or indeterminant symbioses (Aneja and Charles, 1999; Cai et al., 2000; Lodwig et al., 2005; Peralta et al., 2004). In fact, mutation of the PHB synthetase gene (*phaC*) of *R. etli* which forms determinant nodules on *P. vulgaris* resulted in enhanced symbiotic functioning (Peralta et al., 2004).

Glycogen has been reported in cultured rhizobia that form either determinant or indeterminant symbioses. Marroqui et al. (2001) isolated a Tn5 mutant of *R. tropici* in

glycogen synthase and reported a 38% increase in plant dry weight in plants inoculated with this mutant. In contrast, Lodwig et al. (2005) reported no significant difference in acetylene reduction activity or plant dry weight when the mutant was used as inoculum onto pea plants. Wang et al. (2007) constructed mutations in each of the two glycogen synthase genes, and a double mutant, of *S. meliloti*. The single and double mutants, and a triple mutant of both glucogen synthases and PHB polymerase, were all able to form nitrogen-fixing nodules on *M. truncatula* and *M. sativa* that were not greatly different from the wild-type (Wang et al., 2007).

Plant Nodule Nitrogen Metabolism

In 1954, Aprison et al. determined the distribution of ^{15}N-labeled compounds in intact soybean nodules after a 2-hr exposure to $^{15}N_2$ and found the greatest concentration was in glutamic acid. The reduced form of dinitrogen from bacteroids was assimilated by the combined activities of glutamine synthase and glutamate synthase, which play a central role in plant metabolism including the nodules of leguminous plants (Miflin and Lea, 1980). In soybean, there was a dramatic increase in glutamine synthetase activity following the onset of nitrogen fixation (Anthon and Emerich, 1990; Temple et al., 1996). In *M. truncatula*, there are three glutamine synthetases, MtGS1a and MtGS1b, which were found in the cytosol, and MtGS2 that was found in the plastids (Stanford et al., 1993). Ammonium assimilation in roots was catalyzed by isoform GS1b and in nodules by isoform GS1a whose expression was enhanced during nodule development (Carvalho et al., 2000). The nodule GS1a isoform was regulated by phosphorylation at

several residues via a calcium-independent kinase, which increased the affinity of the enzyme for glutamate (Lima et al., 2006).

Most temperate legume nodules including *L. japonicus* and *M. truncatula* export the amide amino acids, glutamine and asparagine, to the shoot via the concerted action of glutamine synthetase and glutamate synthase, or aspartate aminotransferase and asparagine synthetase (Vance, 2000). Harrison et al. (2003) used antisense to reduce the activity of glutamine synthetase in nodules of *L. japonicus*. The resulting T1 progeny had decreased levels of glutamine synthetase activity, but increased plant fresh weight and increased amino acid contents, particularly asparagine. The authors claimed their results demonstrate that nodules and plants have the plasticity to assimilate ammonium by alternative pathways when glutamine synthetase was impaired. Carvalho et al. (2003) modulated the activity of glutatmine synthetase activity in *M. truncatula* nodules via anti-sense constructs and noted an inverse correlation between glutamine synthetase and asparagine synthetase. Barsch et al. (2006) using gas chromatography/mass spectrometry metabolite profiling reported that glutamate dehydrogenase in addition to glutamine synthetase/glutamate synthase and aspartate aminotransferase/asparagine synthetase coordinately modulate nitrogen supply to the shoot.

Most tropical legumes including soybean export ureides, allantoin, and allantoic acid, to the shoot (Atkins and Smith, 2000). These two compounds account for up to 90% of the total nitrogen in the xylem sap of plants that form determinant nodules (Schubert, 1986). However, the rhizobial endophyte can influence the portion of ureides and amides transported to the shoots (Silvente et al., 2002). Ureides are derived from the oxidation of *de novo* synthesized purines, and are not the result of a purine salvage pathway. The

enzymes for *de novo* purine biosynthesis are elevated several-fold relative to those found in amide-producing nodules (Reynolds et al., 1982). The purine biosynthesis pathway, composed of 10 enzymatic steps, has not been completely demonstated in plants or nodules. However, many of the enzymes have been assayed and characterized sufficiently to demonstrate a high degree of similarity to organisms in which purine biosynthesis has been unambiguously demonstrated (Atkins and Smith, 2000). Transcripts for several of the enzymes have been identified in plant nodules (Atkins and Smith, 2000; Colebatch et al., 2004; Goggin et al., 2003). Several of the genes of purine biosynthesis have been cloned from soybean and cowpea and their sequences contain localization signals for plastids (Atkins and Smith, 2000; Goggin et al., 2003). Enzymes of purine biosynthesis have been found in both the mitochondria and plastids of infected cells. Goggin et al. (2003) demonstrated that aminoimidazole ribonucleotide synthetase was co-localized to both the mitochondria and plastids of cowpea.

Xanthine dehydrogenase, in uninfected cells, begins the catabolism of purines forming uric acid (Datta et al., 1991). Urate oxidase had been thought to convert uric acid to allantoin (Todd et al., 2006). However, Kahn et al. (1997) have shown that the actual product of urate oxidase is 5-hydroxyisourate (Kahn and Tipton, 1997; Modric et al., 1992). Sarma et al. (1999) isolated a novel enzyme, 5-hydroxyisourate hydrolase, which converts 5-hydroxyisourate to 2-oxo-4-hydroxy-4-carboxy-5-ureidoimidazoline. 5-Hydroxyisourate hydolase, localized to the peroxisomes of the uninfected cells, was detectable by both mRNA and immunodetection 12 days after infection of soybean, increased at 21 days and then declined (Raychaudhuri and Tipton, 2002). Sarma et al. (1999) proposed the presence of a decarboxylase which catalyzes the stererospecific

conversion of 2-oxo-4-hydroxy-4-carboxy-5-ureidoimidazoline to (S)-allantoin. Allantoin and allantoic acid are transported to the shoot where they are degraded and transformed into the needed nitrogenous molecules for plant growth and development and for photosynthetic production of sucrose to be transported to the root nodules for symbiotic nitrogen fixation (Todd et al., 2006).

Summary

The benefits of leguminous crop plants were well known in Greek and Roman agriculture. In 1888, Hellriegel and Wilfarth demonstrated leguminous plants utilized atmospheric dintirogen. In the intervening 120 years, scores of investigators have identified and characterized many key components of nodule function, but much still remains to be discovered. The advent of global technologies has re-emphasized the complexity of the symbiosis and have demonstrated anew the cursory extent of our knowledge. The microaerobic environment of the nodule requires a unique interaction of oxygen, carbon and nitrogen metabolism and an intricate array of regulatory processes to maintain the delicate balance of the symbiosis. Among the goals yet to be accomplished is the complete metabolic map of nodule function, the metabolism of carbon, nitrogen and oxygen, and the qualitative and quantitative exchange of carbon and nitrogen metabolites across symbiotic compartments. The next 120 years will reveal many of the complex interactions of leguminous plant symbioses.

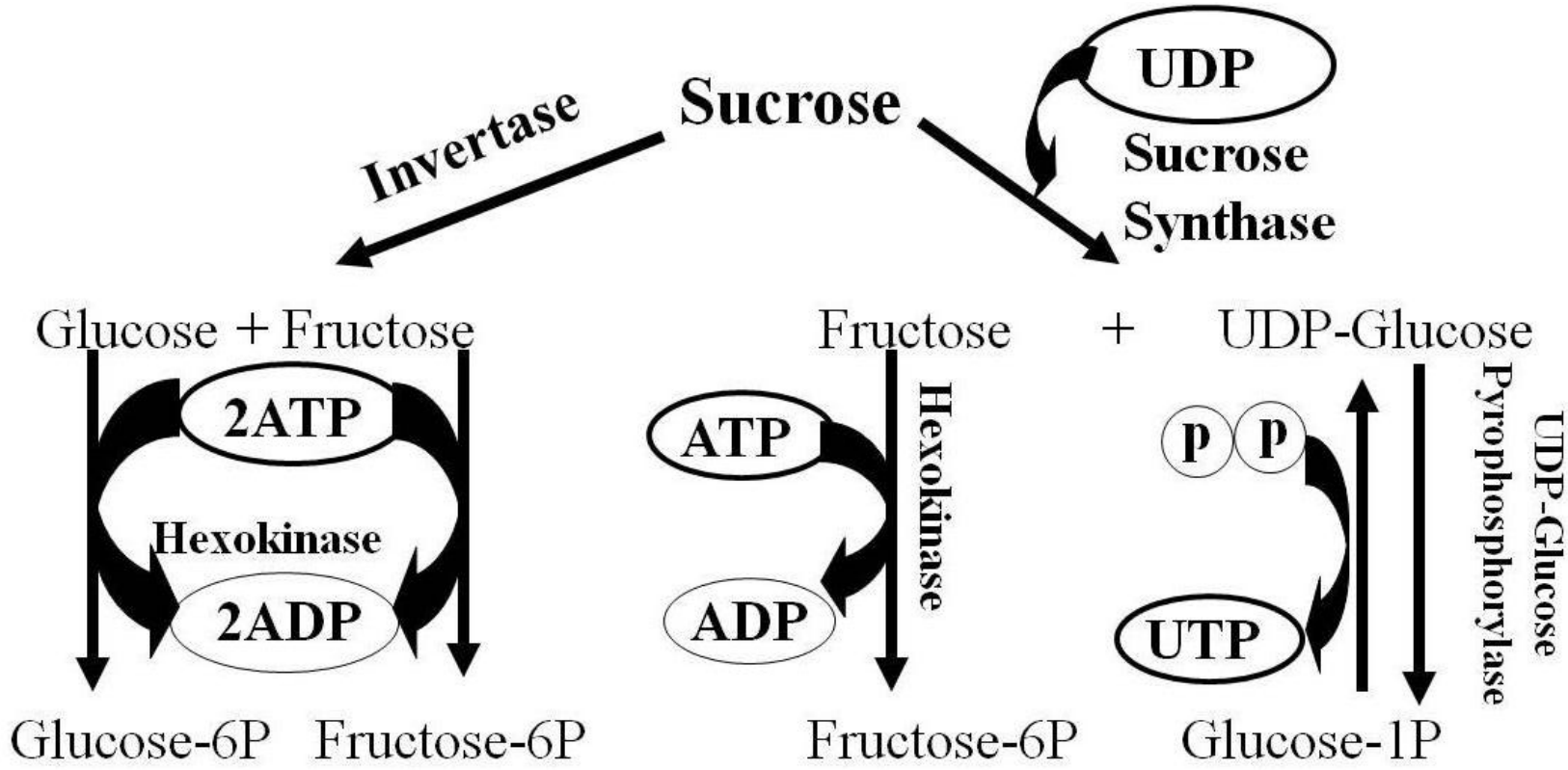

Figure 1. Comparison of the first steps of the Invertase and Sucrose Synthase pathways

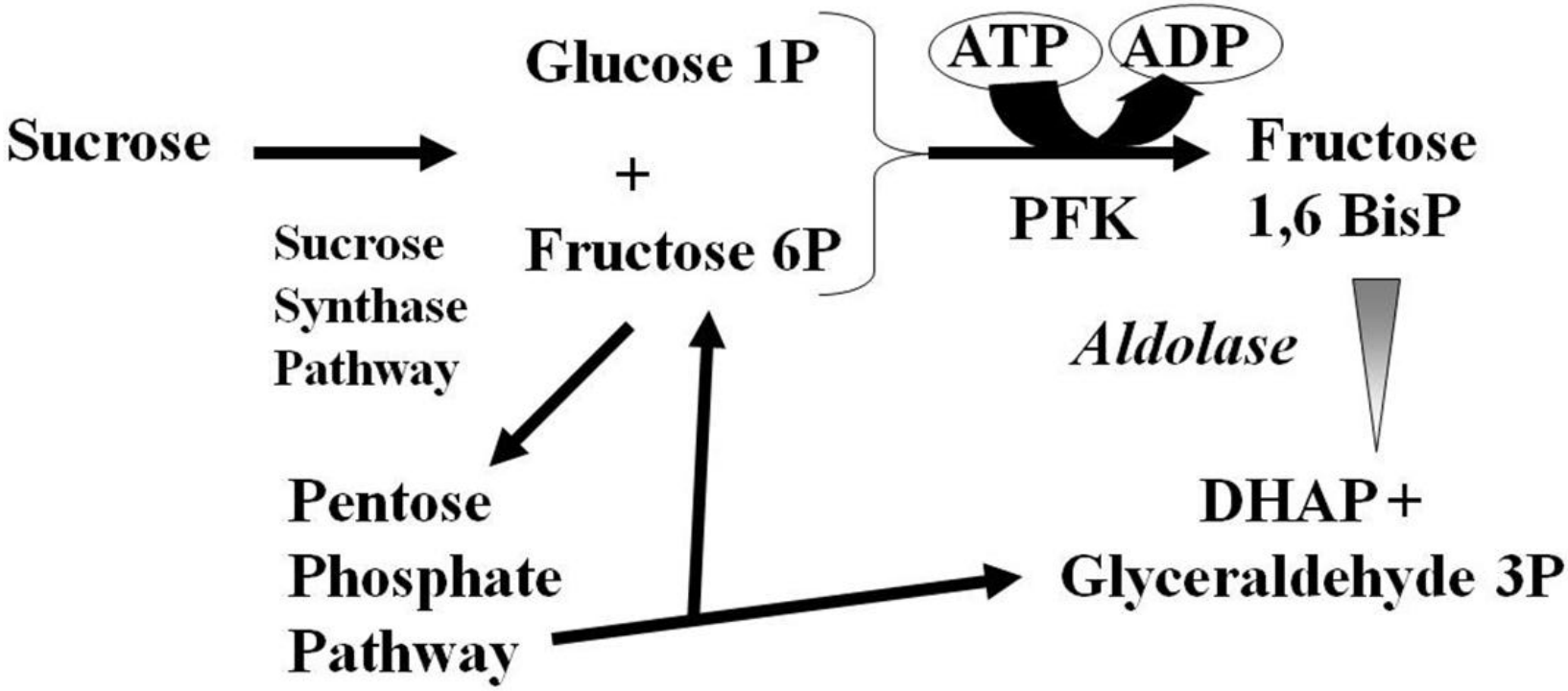

Figure 2. Possible metabolic routes of sucrose to three-carbon intermediates

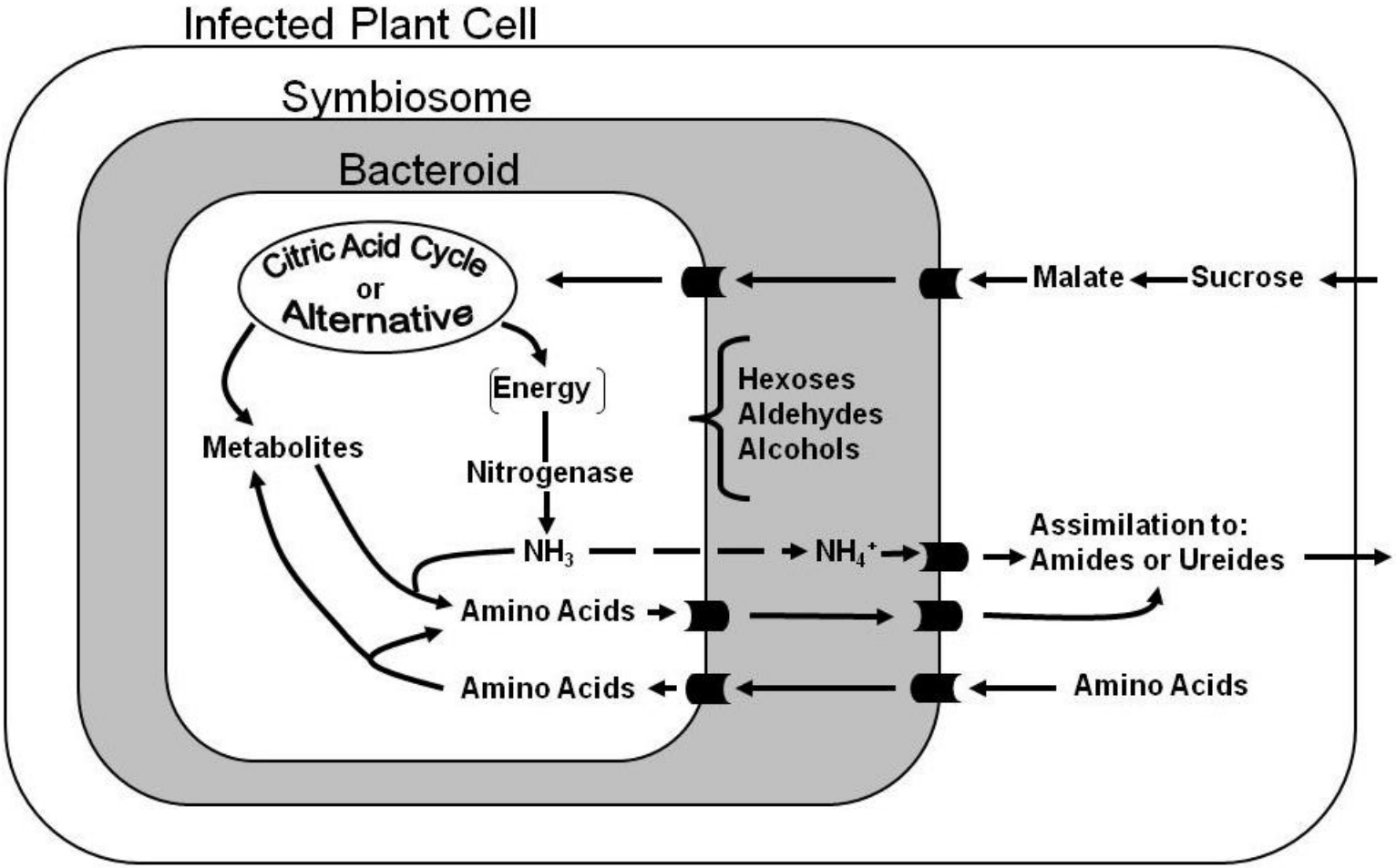

Figure 3. Overview of some of the metabolic activities of infected nodule cells

Chapter II

Comparative Analysis of the Cytoplasmic and Periplasmic Proteome of *Bradyrhizobium japonicum*

Abstract

Proteins were isolated from the periplasm of *Bradyrhizobium japonicum* bacteroids by a modification of the method of Streeter and LeRudilier (1990) and compared to those isolated from the cytoplasm. The modification provides periplasmic protein preparations with minimal contamination of cytoplasmic proteins. The largest groups of identified proteins were in central intermediary metabolism and amino acid metabolism, whereas the smallest were in the categories of DNA replication, recombination, and repair, and purines, pyrimidines, and nucleosides. A theme in the carbon and amino acid metabolism groups of the periplasmic proteins was the production of succinate. A number of plant proteins were found which suggested contamination of the plant portion of the nodule during bacteroid isolation. However, antibodies to two of the identified plant proteins were applied as immunogold labels to soybean nodules sections. The labeling patterns suggested that these two proteins were specifically targeted to the bacteroids.

Introduction

The gram negative, soil bacterium *Bradyrhizobium japonicum* infects soybean (*Glycine max*) roots forming a new plant derived, nitrogen-fixing organ, the nodule. The free-living *B. japonicum* in the nodule tissue transform to a non-growing, non-motile form called a bacteroid that is retained within a plant-derived membrane, the peribacteroid or symbiosome membrane. Inside of the symbiosome membrane and

outside the outer membrane of the bacteroid is the symbiosome space. Between the outer and the inner membrane of gram negative bacteria resides the periplasmic space, which may constitute up to 40% of the total cellular volume. Periplasmic proteins are of considerable interest as they are responsible for sensing the surrounding environment and for transport of selected metabolites into the cytoplasm. Eukaryote-prokaryote communication and metabolite transfer between plant and bacteriod must transit both of these spaces. Further it is not known whether the periplasmic space is a separate compartment or a continuum of the symbiosome space. Identification of the protein/enzyme composition of each of these compartments will help determine how these spaces integrate into nodule function and fate.

Glenn and Dilworth (1979) first demonstrated the ability to separate the periplasmic space from the cytoplasmic space in rhizobia utilizing a lysozyme and EDTA treatment. In 1986 de Maagd and Lugtenberg demonstrated a refinement of the method to fractionate the outer membrane, cytoplasmic membrane, periplasmic space, and cytoplasmic components of *Rhizobium leguminosarium*. They were able to release on average 88% of the total alkaline phosphatase activity, a periplasmic marker enzyme, and only 3-4% of the total activity of the cytoplasmic marker enzyme malate dehydrogenase. Protein patterns based on SDS PAGE confirmed the unique protein contents of each fraction, but no identification of the proteins was performed. Subsequently, Streeter (1989) demonstrated that the periplasmic space of cultured bacteria and bacteroids of *Bradyrhizobium japonicum* and *Rhizobium leguminosarium* biovar *phaseoli* could be enzymatically probed after subjecting them to a dilute Triton X-100 treatment. Incubation at pH 4.0 prior to osmotic shock was found to increase the recovery of

periplasmic marker enzymes while limiting the contamination of the cytoplasmic marker enzyme malate dehydrogenase from *R. leguminosarium* biovar *phaseoli* bacteroids at less than 2% (Streeter and Rudulier, 1990).

An alternative method for identifying periplasmic, secreted, or membrane spanning proteins is the creation of fusions between the putative target gene and *pho*A, the gene encoding the *E. coli* alkaline phosphatase first described by Manoil and Beckwith (1985). The amount of alkaline phosphatase activity is directly correlated with the amount of the fusion protein exported to the periplasm (Manoil and Beckwirth, 1985). Long et al. (1988) used this method to screen 1250 *R. meliloti* mutants, identifying 25 symbiotically defective mutants that formed Fix^- nodules on alfalfa. Thirteen mutants were compromised in synthesizing exopolysaccharides. The remaining twelve mutants consisted of nine membrane proteins, including the gene for *dct*A (dicarboxylic acid transporter), and three periplasmic proteins required for symbiosis. The location of ExoR in the periplasm via PhoA fusions as well as fractionation and western blotting by Wells et al. (2007) suggested that ExoR interacts with the two component system ExoS-Chvl to regulate downstream genes in both the free-living and symbiotic states of *S. meliloti* in a novel manner. The periplasmic localization of ExoR defined it as a novel class of proteins that influences the activity of transcription factors in the cytoplasm (Wells et al., 2007). *B. japonicum* PhoA mutant studies (Muller, 2004; Muller, 1995) have identified genes of signal peptidases, *sipS*, *sipF,*and *sipX*. *B. japonicum sipS* mutants formed ineffective nodules during symbiosis whereas the *sipF* mutants had some biological nitrogen fixation but bacteroids appeared deformed (Muller and Bonnard., 2004). In

contrast, *sip*X mutant bacteroids formed an effective symbiotic interaction (Muller and Bonnard., 2004).

Phage display technology is primarily used for the identification of proteins and peptides with affinity to other molecules (Steiner et al., 2006). However, Rosander et al. (2003) truncated Protein III of the phage, which is directed to the inner membrane by its signal peptide. The truncated form of Protein III lacks a signal peptide, and thus the resulting fusion protein is dependent upon the presence of a signal peptide within the heterologous, fused protein. Fusing the N-terminal portion of *B. japonicum* proteins to Protein III (E-tag) allows for the expression of only those phage display secreted proteins of *B. japonicum* with signal peptides (Muller and Bonnard., 2004). The resulting library was screened symbiotically and a number of proteins were identified including a phosphonate transport protein, and an ATP synthase subunit, FlaD.

There are few reports documenting metabolic events in the periplasmic space of bacteroids or free-living rhizobia. The periplasmic nitrate reductase from free-living *B. japonicum* was recently isolated and characterized (Delgado et al., 2003). The periplasmic nitrate reductase oxidizes quinol via the two-electron reduction of NO_3^- to NO_2^- with the quinol oxidation possibly coupled to proton translocation and conservation of energy. The results of the study suggested that the periplasmic nitrate reductase is the enzyme responsible for anaerobic growth of free-living *B. japonicum* under nitrate respiring conditions (Delgado et al., 2003). *B. japonicum* bacteroids, also, contain the periplasmic nitrate reductase which is responsible for the formation of nitrosylleghaemoglobin from nitric oxide (Meakin, 2007). The nitrosylleghaemoglobin compromises leghaemoglobins ability to effectively bind oxygen. Glucose metabolism

occurs extracellularly as shown by Bernardelli et al. (2001) via a periplasmic PQQ-dependent glucose dehydrogenase that oxidizes glucose to gluconate in *Rhizobium tropici* and *Sinorhizobium meliloti*. Better understanding of metabolic enzymes in the periplasmic space is needed to more fully understand the symbiotic association between the bacteroid and plant.

Recent proteomic studies have greatly expanded the understanding of the symbiosis between *B. japonicum* and *G. max* in looking at secreted proteins, comparison of nodules from the field and growth chamber, and in *in vitro* growth conditions (Batista et al., 2010; Delmotte et al., 2010; Hempel et al., 2009; Sarma and Emerich, 2005; Sarma and Emerich., 2006). Though several studies have utilized protein prediction to determine subcellular localization none has attempted fractionation of periplasmic proteins (Batista et al., 2010; Delmotte et al., 2010).

To date no global examination of the periplasmic proteome of *B. japonicum* bacteroids has been undertaken. This chapter describes the refinement of a previous technique (Streeter and Rudulier, 1990) for isolating periplasmic proteins from *B. japonicum* bacteroids and the identification via LC-MS/MS. A total of 364 proteins were confidently identified in this study with 92 being exclusive to the periplasmic space, 124 proteins in the cytoplasmic space, and 148 proteins in common.

Materials and Methods

Plant Material

Soybean plants (*Glycine max* L. cv Williams 82 derivative Pioneer 93M11) were collected from University of Missouri-Columbia Bradford Farm fields over a ten week

period (56-119 days after planting) between July 1-September 2, 2008. Nodules were removed from the roots and all dirt and root debris was removed with washes in distilled water. Bacteroids were isolated from nodules as previously described (Karr et al., 1984).

Periplasmic Protein Isolation

Bacteroids isolated from thirty grams of nodules were aliquoted into three equal amounts and gently brought up into isolation buffer (50mM Tris-Hcl, pH 7.5 with 2mM EDTA and 20% sucrose) using an artist paint brush. Ready-Lyse Lysozyme Solution (25,000 U, Epicentre-Madison, WI) and Protease Inhibitor Cocktail (10 μL, Calbiochem, Rockland, MA) were added to the suspended bacteroids and mixed gently followed by incubation for 30 minutes at room temperature. The periplasm was collected by centrifugation at 12,000xg for 10 min at 4^{o}C. The resulting bacteroid spheroplasts were suspended in 15 ml of MEP buffer (5mM $MgCl_2$, 1mM EDTA, 50mM K-phosphate buffer, pH 7.0) containing 10 μL of Protease Inhibitor Cocktail and then ruptured in the French Press as previously described (Karr et al., 1984).

Enzyme Assays

The following enzymes were measured spectrophotometrically on a Cary 1Bio spectrophotometer. Background rates were determined by a 2-min preincubation period of the complete reaction mixture minus the indicated substrate.

B-hydroxybutyrate Dehydrogenase. Assays contained 600μM NAD^+, 20mM sodium DL-hydroxybutyrate, 50mM TES, pH 7.9, and enzyme extract (50 μL of periplasmic

fractions; 2.5 µL of bacteroid fractions) in a 1mL final volume. Hydroxybutyrate was added to begin the assay and the rate of NADH formation was measured at 340 nm.

Malate Dehydrogenase. Assays contained 0.20 mM NADH, 0.50mM cis-oxaloacetate, 95 mM K-phsophate, pH 7.4, and enzyme extract (50 µL of periplasmic fractions; 2.5 µL of bacteroid fractions) in a 1mL final volume. Oxaloacetate was added to initiate the assay and the rate of NADH oxidation was measured at 340 nm.

Isocitrate Dehydrogenase. Assays contained 0.5 mM DL-isocitrate, 0.4 mM $NADP^+$, 3.3 mM $MgCl_2$, 10 mM K-phosphate, pH 7.4, enzyme extract (50 µL of periplasmic fractions; 2.5 µL of bacteroid fractions) in a 1mL final volume. Isocitrate was added to initiate the reaction and the rate of $NADP^+$ reduction was measured at 340 nm.

Cyclic phosphodiesterase Assay. Assays contained 68 mM sodium acetate, pH 6.0, 10 mM $MgCl_2$, 2 mM $CoCl_2$, 0.73 mM bis(ρ-nitrophenyl) phosphate, and enzyme extract (50 µL of periplasmic fractions; 2.5 µL of bacteroid fractions) in a 5.0 ml final volume. The reaction was incubated at 30°C with 1 mL aliquots of the assay being stopped with 2.0mL of 0.1 M NaOH at 0, 15, 30, and 60 minutes. Formation of ρ-nitrophenol was measured at 410 nm.

Protein Isolation and Identification

The periplasmic and bacteroid fractions were each precipitated using equal volumes of phenol saturated with 0.1 M Tris-HCl, pH 8.8 and were mixed gently at room temperature for one hour followed by centrifugation at 4,000xg for 10 minutes at 4°C. The phenol phase was collected and four volumes of 100% methanol containing 0.1 M ammonium acetate and 10 mM dithiothreitol were added. Protein was precipitated

overnight at -20°C. Protein precipitate was collected by centrifugation at 4,000xg from 10 min at 4°C. The protein pellet was washed once with the methanol/ammonium acetate/DTT solution. The protein pellet was then washed three times with 90% ethanol containing 10mM DTT and then stored in 90% (v/v) ethanol/DTT at -80°C overnight.

Precipitated proteins were collected by centrifugation at 4,000 g and 4°C. The pellet was dissolved in reconstitution buffer (30 mM Tris-HCl, 7 M urea, 2 M thiourea, 4% (w/v) CHAPS at pH 8.8) by gentle vortexing for one hour. Samples were quantified using the Bradford method. A 20 μg portion of protein from each sample was removed and diluted to 1 μg/μL with reconstitution buffer. As an internal standard, 200 ng of BSA was added to give a protein ratio of 1% (w/w) BSA protein.

Disulfide bonds were reduced with 10 mM DTT (100 mM stock in 50 mM ammonium bicarbonate), at 25°C for 1 hour. Reduced cysteines were alkylated with 40 mM iodoacetamide (200 mM stock in 50 mM ammonium bicarbonate), at 25°C in the dark for 1 hour. Iodoacetamide was quenched by adding additional DTT to 30 mM (100 mM stock in 50 mM ammonium bicarbonate) and incubating at 25°C for 30 minutes. Urea was brought to 1 M by dilution with 50 mM ammonium bicarbonate. Trypsin (Sequencing Grade Modified-Promega, Madison, WI) was reconstituted to 0.02 μg/μL and activated in the provided re-suspension buffer per manufacturer's instructions, then added to samples at a ratio of 1:200 (w/w) (trypsin/sample). Samples were incubated at 37°C for 16 hours. Digests were then lyophilized to dryness.

Mass Spectrometry Analysis

Lyophilized protein samples were reconstituted in 100 µL of 18 MΩ water with 0.1% (v/v) formic acid and 5.0% (v/v) acetonitrile by pipetting and mild vortexing. Samples were spun at 13,000 rpm at 4^{o}C for 10 minutes in a tabletop centrifuge to remove insoluble debris. Twenty µL portions from each sample were aliquoted into a polypropylene 96 v-well plate, covered with adhesive film, and then briefly centrifuged to collect samples at the bottom of the well, and placed in the cooled tray of the LC auto-sampler. For analysis, 10 µL injections were run on a LTQ ProteomeX linear ion trap LC-MS/MS instrument (Thermo Fisher, San Jose, CA). Peptides were concentrated and desalted on in-line C_8 captraps (Michrom Bioresources, Auburn, CA) prior to final separation by C_{18} column using an acetonitrile gradient of 0-90% solvent B (100% acetonitrile with 0.1% (v/v) formic acid), in solvent A (deionized 18 MΩ water with 0.1% (v/v) formic acid for a duration of 110 minutes. The peptide trap and C_{18} column were then re-equilibrated for 25 minutes with 100% solvent A before applying the next sample.

LC separation was performed using fused silica nanospray needles, 26 cm length, (360 µm outer diameter, 150 µm inner diameter; Polymicro Technologies, Phoenix, AZ), that were packed with "Magic C18" (200Å, 5 µm particles, Michrom Bioresources) in 100% methanol. Before sample acquisition, columns were equilibrated for 3-4 hours at 200 nL/min (at the column tip) with a 60:40 mix of solvent B to solvent A. Samples were analyzed in the data-dependent positive acquisition mode on the LC-MS/MS instrument, using normal scan rate for precursor ion analysis, and dynamic exclusion enabled (1 repeat count, 30 s repeat duration, list size of 50, and 30 s exclusion).

Following each full scan (400-2000 *m/z*), a data-dependent triggered MS/MS scan for the three most intense parent ions were acquired. The nanospray column was held at ion sprays of 2.0 kV.

Database Searching and Spectral Analysis

Tandem mass spectra were extracted by BioWorks version 3.3. All MS/MS samples were analyzed using SEQUEST (ThermoFinnigan, San Jose, CA; version 2.7). SEQUEST was set up to search a FASTA formatted protein database of "translated potential coding regions of the *Bradyrhizobium japonicum* genome and viridiplantae genomes (*Arabidopsis thaliana* and *Glycine max*)", provided at the websites (http://genome.kazusa.or.jp/rhizobase/Bradyrhizobium/index.html) and (ftp://ftp.ncbi.nih.gov/genomes/PLANTS/), indexed for trypsin digestion. SEQUEST was searched with fragment ion mass tolerance of 1.0Da and a parent ion tolerance of 2.0 Da. Iodoacetamide derivative of cysteine (+57) was specified in SEQUEST as a fixed modification. RAW files were searched using Bioworks "SEQUEST batch-search". The search results file (.srf) were imported into Scaffold™ (Proteome Software, Portland, OR, release 2.0) and analyzed as described below.

Spectral Counting and Quantitation by Scaffold

Criteria for protein identification-Scaffold was used to validate MS/MS-based peptide and protein identifications. Peptide identifications were accepted if they could be established at greater than 95.0% probability as specified by the Peptide Prophet Algorithm (Keller et al., 2002). Protein identifications were accepted if they could be

established at greater than 99.0% probability and contained at least two identified peptides. Protein probabilities were assigned by the Protein Prophet algorithm (Nesvizhskii et al., 2003).

Immunogold Labeling and Electron Microscopy

Antibodies for histone H2A were purchased from Santa Cruz Bioctechnology (Cat. No.sc-10807) and rabbit polyclonal antibodies against soybean lipoxygenase was a gift from Dr. J.C. Polacco, University of Missouri. Immunogold sample preparation was performed as described by the Electron Microscopy Facility at the University of Missouri (http://www.emc.missouri.edu/) and visualized on a JEOL 1400 transmission electron microscope.

Results and Discussion

Protein Isolation

Periplasmic protein isolation techniques have relied upon high amounts of lysozyme to degrade the peptidoglycan layer making the bacteria or bacteroid more susceptible to rupture of the outer membrane via an osmotic pressure from a hypertonic sucrose solution and release of periplasmic enzymes. This method is not ideal for the recovery and identification of proteins utilizing mass spectrometry due to the high levels of lysozyme (~1mg/mL). This concentration of lysozyme was sufficient to obscure the identity of isolated periplasmic proteins even after two dimensional gel electrophoresis and MALDI-TOF/TOF (data not presented). Utilizing a recombinant Ready-lyse lysozyme from Epicentre and 20% sucrose (w/v) as the osmotic reagent, we were able to

fractionate the *B. japonicum* bacteroid into periplasm and cytoplasm fractions sufficient for protein purification followed by identification with LC-MS/MS (Figure 4).

Fractionation techniques in rhizobia use the enzymes, malate dehydrogenase, (MDH) and β-hydroxybutyrate dehydrogenase (β-HBDH) as cytoplasmic markers (Streeter, 1989). The cytoplasmic enzyme marker (ICDH) was, also, included to verify purity of the periplasmic fraction from the cytoplasmic fraction. Phosphodiesterase is included as the periplasmic marker enzyme. Table 1 includes the specific activities and standard deviation for the marker enzymes measured at two time points, 56 and 64 days after planting. Approximately 8-10% of the total PDE activity was released into the periplasmic fraction. MDH activity was 8-16% of total activity in the periplasm while β-HBDH was 1-4% and ICDH was 1-5%. MDH appeared to be more sensitive than β-HBDH and ICDH to release in the fractionation. As shown previously, commercial preparations of isocitrate contain malate as a contaminant, which overestimates ICDH activity in crude enzyme preparations (Shah and Emerich, 2006). The substrates for the other enzyme activities used here were at best 95% and thus could also overestimate enzyme activity. Thus, the apparent levels of cytosolic comtamination of periplasmic preparations are likely lower than reported in Table 1. This enzyme data suggested that the method of fractionating the bacteroid compartments was suitable for obtaining periplasmic and cytosolic fractions from bacteroids.

Protein Characterization

A total of 364 proteins, 92 in the periplasmic fraction, 124 in the cytosolic fraction and 148 common to both were identified in the combined LC-MS/MS analysis

(Figure 5). The identified proteins were then analyzed using the computational prediction program database, cPSORTdb (http://db.psort.org/), for *B. japonicum* USDA110. Of the 364 proteins identified by LC-MS/MS, cPSORTdb assigned 157 to the cytoplasm, 25 to the periplasm, 5 to the outer membrane, and 126 were not assigned a cellular location. To further analyze the proteins identified for signal peptides the prediction algorithms LipoP (http://www.cbs.dtu.dk/services/LipoP/), TatP (http://www.cbs.dtu.dk/services/TatP/), CELLO (http://cello.life.nctu.edu.tw/), and AdaBoost Learner (http://chemdata.shu.edu.cn/subcell/) were used. Surprisingly 52 proteins were not from *B. japoncium*, but were annotated as plant proteins from soybean (*Glycine max*). Seven of the plant proteins were found in the cytoplasmic fraction, the rest were found in the periplasmic fraction. Proteins identified in the cytoplasmic fraction and then predicted to be cytoplasmic by the prediction algorithms were excluded from further analysis. All proteins that were identified in the periplasmic fraction and then predicted by cPSORTdb to be localized in the periplasm were further analyzed for their cellular functions. Also included in the tables below are those proteins identified in both the cytoplasmic and periplasmic fractions, but with an unknown localization. Proteins found in both locations always yielded a greater number of hits in the cytoplasmic fractions than the periplasmic fractions. The enzymatic data suggest cytoplasmic contamination of the periplasmic fractions to be <10%. Of those peptides found in both fractions, the relative percent of peptide fragments in the periplasm was also ~10%. Note that these percentages are not directly comparable due to differences in the sampling and measurement techniques of each procedure, but they do substantiate the isolation procedure used in this study.

Of the 92 proteins in the periplasmic fraction, only four of them had more than the minimum number of 2 peptide fragments, which was the chosen selection criteria. The average number of peptides identified for all proteins in this study was 3.3. The proteomic analysis, based on peptide hits, indicates fewer proteins are present in the periplasm than the cytoplasm. The greater protein concentration of the cytoplasm coupled with its greater volume compared to the periplasm indicates the inherent difficulty in identifying proteins from the periplasmic space. Assigning a categorical space for proteins is important in determining function, protein-protein interaction partners, and regulation. A number of proteins in this study were found in both the periplasmic and cytoplasmic fraction that were believed to be strictly cytoplasmic, i.e. not having signal peptides or known function outside of the cytoplasm. Given the recent interest in non-classical protein secretion of bacteria and recent studies of the periplasm, new definitions of protein localization must be made (Bendsten et al., 2005b; Bendsten, 2004). An analysis of the *B. japonicum* genome by Hempel et al. 2009 identified 961 proteins (12% of the genome) that contain a signal sequence, of these 95 proteins were identified as using the TAT pathway for export. Surprisingly 391 proteins (5% of the genome) could be exported by non-classical methods as defined by (Bendsten et al., 2005b).

The proteins identified in this study were characterized by their locations, periplasm only, cytoplasm only, or both locations. Each localized group was plotted relative to their positions in the genome to determine whether some of the proteins were localized in clusters. The isolated proteins were grouped into functional categories which are discussed in the following paragraphs.

Protein Folding

Chaperones were noted as the most abundant group of proteins in the *B. japonicum* proteome (Sarma and Emerich, 2005). This is consistent with the decrease in protein synthesis as bacteroids mature in soybean nodules (Karr and Emerich, 1996). The abundance was evident with GroEL3 (bll2059), which had ~18-fold greater number of identified unique peptides (59) in this study than the majority of the other peptides identified (Table 2). The average number of peptides identified for all proteins was 3.3. The 60kDa chaperonin GroEL (blr5626) and GroEs co-chaperonin (bll2060) were also identified at several fold greater than most other peptides.

In this study, several chaperones and a GroEL chaperonin were identified in the periplasmic space of *B. japonicum* bacteroids (Table 2). Notably, the GroEL chaperonin, Blr5227, was identified only in periplasmic space, but was not one of the chaperonins identified previously (Sarma and Emerich, 2005). The corresponding GroES3, which was previously identified as the major GroES in bacteroids (Sarma and Emerich, 2005) was identified in both periplasmic and cytosolic fractions. GroES3 has been shown to be *nif*A regulated (Fischer et al., 1993). Extracellular location of chaperones and chaperonin has been demonstrated in the extracytoplasmic fractions of *B. japonicum* and *R. etli* CE3 (Hempel et al., 2009; Meneses et al., 2010). GroEL of *Haemophilus ducreyi* is associated at the bacterial cell surface and influences the adherence of the bacteria to the eukaryotic cell (Frisk et al., 1998). GroEL and DnaK are involved in colonization, attachment, and invasion by *Legionella pneumophila* and *Helicobacter pylori* (Bumann et al., 2002). Further GroEL and DnaK may function in the extracellular proteome to properly fold accumulated proteins from the type II and IV secretion systems as seen in pathogenic *E.*

coli strains extracellular proteomes (Sandkvist, 2001). The presence of chaperones and a chaperonin in the periplasm suggests the need to maintain the proteins in this space in an active conformation to sustain symbiosis.

Three different GroEL chaperonins were assigned to the cytosolic fraction. GroEL3 (bll2059), which had the greatest number of identified unique peptides in this study, was found to be induced not by heat shock, but by the two-component regulatory system RegR under microoxic conditions (Fischer et al., 1993; Lindemann et al., 2007). RegR also controls the expression of of cytochrome P450 BJ-1 & 4 (blr2144 & blr2147) under microoxic conditions (Fischer et al., 1993). The 60kDa chaperonin encoded by blr7533 was found to be under the control of a CIRCE promoter, as was GroES4 (blr5625) that was strongly derepressed when the repressor, *hrc*A, was partially replaced with a kanamycin cassette (Minder et al., 2000). GroEL5 (blr4635) was found to be under the control of $FixK_2$ in microoxic cultured cells (Mesa et al., 2008). Another heat shock protein DnaK was shown to be inducible after heat shock to a steady state level (Munchbach et al., 1999). The GrpE heat shock protein functions as a nucleotide exchange factor, promoting the exchange of ADP and ATP, for DnaK (Harrison, 2003).

Central Intermediary Metabolism

The proteins responsible for nitrogen fixation were well represented in the data set and the nitrogenase component proteins, in particular, were found in greater abundance (>4-fold) than the majority of peptides in this study (Table 3) A number of *fix* and *nif* genes including (blr1744, blr1769,blr1743,blr2038, blr1744, blr1773, blr1747, & blr1771) have been shown to be controlled by the RegR two component regulatory

system that responds to microoxic conditions during symbiosis (Lindemann et al., 2007; Sciotti et al., 2003).

There were proteins identified for carbohydrate metabolism (amylo-α-1,6-glucosicase, blr2754;a putative sugar hydrolase blr1964; trehalose synthase, blr6767; UDP-glucose 6-phosphate, bll8129 and GDP-mannose 1-phosphate guanylyltransferase, bll5919). The putative sugar hydrolase and a UDP-glucose 6-phosphate dehydrogenase were found in the periplasm (Table 3). The putative sugar hydrolase (*gun*A;blr1964), a possible cell-wall degrading enzyme, was found to not be induced by genistein, and unlike *gun*A2, the *gun*A mutant did not impede symbiosis (Baumberger et al., 2003). Conversely *gun*A was found to be induced upon exposure of *B. japonicum* to soybean seed extract (Wei et al., 2008). Enzymes of the glycolytic, and gluconeogenic pathways and a citric acid cycle were found with most located in both compartments. Phosphoenolpyruvate carboxykinase (*pck*A, bll8141) is the first step of gluconeogenesis, the conversion of oxaloacetate to phosphoenolpyruvate. The *pck*A gene was found to be host dependent on its need for effective symbiotic association in *R. leguminosarum* (McKay et al., 1985; Osteras et al., 1991). Mutants of *S. meliloti pck*A grew poorly with TCA cycle intermediates, but induced a secondary pathway for PEP formation utilizing malic enzyme and pyruvate phosphate dikinase (Osteras et al., 1997). Pyruvate phosphate dikinase (*ppd*K, blr2538) converts pyruvate to phosphoenolpyruvate in a reversible reaction requiring ATP. PPDK is not required in *S. meliloti* to form an effective symbiosis (Osteras et al., 1997). Acetyl-CoA synthetase (blr0573) catalyzes the activation of acetate to acetyl-CoA utilizing ATP and CoA as cofactors and has been characterized in *B. japonicum* bacteroids (Preston et al., 1990).

Citrate synthase (*glt*A, blr4839) was found to be essential in *S. fredii and S. meliloti* for nitrogen fixation though nodules did form on soybean and alfalfa (Krishnan et al., 2003; Mortimer et al., 1999). Dihyrolipoamide succinyl transferase (*sucB*;bll0451) is part of the enzyme complex 2-oxoglutarate dehydrogenase, along with sucA. Mutants of 2-oxoglutarate dehydrogenase in *R. leguminosarum* formed ineffective nodules and excreted large quantities of glutamate and 2-oxoglutarate (Walshaw et al., 1997). Drought conditions caused an increase in the protein profile of *S. meliloti* bacteroids for *suc*B (Larrainzar et al., 2007). Succinate dehydrogenase flavoprotein (*sdh*A) contains the catalytic active site for succinate oxidation and flavin binding. SdhA associates to the inner membrane with SdhB via the membrane spanning proteins SdhC and D and in *B. japonicum* this complex is functionally similar to the mitochondrial succinate dehydrogenase complex (Westenberg and Guerinot, 1999). Malate dehydrogenase (bll0456) was an abundant protein with regard to peptide fragments identified making it a suitable marker protein for both enzymatic and proteomic analysis (Table 3). The extracellular proteomes of *B. japonicum* and *R. etli* were found to have SucB (both), SdhA (*R. etli*), and Mdh (*B. japonicum*) (Hempel et al., 2009; Meneses et al., 2010).

Lactate dehydrogenase (blr4823) was found solely in the periplasm (Table 3). L-lactate dehydrogenase (lldA) was shown in *H. pylori* to directly reduce cytochrome c-553 without the participation of cytochrome c reductase (Tsukita et al., 1999).

Malate synthase (*glc*B, bll1474) condenses glyoxylate with acetylCo-A to produce malate in order to replenish TCA cycle intermediates from the glyoxylate cycle, was found but not isocitrate lyase, which is consistent with the enzymatic analysis of Green et al. (1998). A *S. meliloti* mutant in malate synthase was not impaired in nodulation or

nitrogen fixation (Ramirez-Trujillo, 2007). Malic enzyme (blr4145) which produces pyruvate was found. Dao et al. (2008) reported that an NAD-malic enzyme *B. japonicum* mutant reduces nitrogen fixation activity of soybean nodules.

Several aldehyde dehydrogenases (bll7607, blr2816, blr5873) were identified. They function in a variety of pathways including glycolysis/gluconeogenesis, fatty acid metabolism, and a variety of amino acid metabolism, including branched chain amino acid degradation.

Several proteins were identified in the periplasm catalyzing benzoate and phenyl metabolism (Table 3). Prephenate dehydratase (bll1421) converts chorismate to prephenate leading to phenylacetate synthesis. In *R. etli*, prephenate dehydratase was found to be down-regulated in a mutant for the extracytoplasmic function sigma factor *rpoE4* (Martinez-Salazar et al., 2009). 4-hydroxybenzoate 3-monooxygenase (*pob*A, bll7838) catalyzes the conversion of 4-hydroxybenzoate and molecular oxygen to protocatechuate and water utilizing NADPH as an electron donor and FAD as a cofactor. *B. japonicum* can grow solely on 4-hydroxybenzoate and mutations in the β-ketoadipate pathway can lead to toxic levels of 4-hydroxybenzoate (Lorite et al., 1998). 4-hydroxybenzoate 3-monooxygenase was shown to be necessary in *R. leguminosarum* for the uptake of 4-hydroxybenzoate (Wong et al., 1994). Phenylacetate-CoA ligase (*paa*K, blr2897) gene was found to be regulated by the two-component regulatory system RegSR (Lindemann et al., 2007). Along with the 4-hydroxybenzoate 3-monooxygenase (*pob*A) (bll7838), the phenylacetate-CoA ligase is the beginning of the pathway for degradation of aromatic compounds that ends with the beta-ketoadipyl CoA thiolase (blr0925) yielding succinyl-CoA and acetyl CoA (Nogales et al., 2007). 3-Oxoadipate CoA

transferase (bll7093) is also part of the pathway from aromatic compounds to succinyl-CoA and acetyl-CoA.

Amino Acid Metabolism

A large number of peptides were identified from proteins of amino acid metabolism (Table 4). Only a few yielded greater than 3.3 peptides: an uncharacterized aminotransferase (blr1686), glutamine synthetase I (blr4949), glutamine synthase large subunit (blr7743), N5-methylenetetrahydropteroyltriglutamate-homoserine methyltransferase (blr2068), serine hydroxymethyltransferase (bll5033), and propionyl-CoA carboxylase, alpha subunit (bll5267). Rhizobia contain at least two glutamine synthetases, with glutamine synthetase I being active and regulated by adenylation of its dodecameric subunits while glutamine synthetase II is regulated by the two component system ntrBC (Lopez-Garcia et al., 2001). A *S. meliloti* double mutant in glutamine synthetase I and glutamine synthetase II preferentially metabolized glutamine over succinate, with (^{14}C) succinate unable to be converted to PHB (Encarnacion, 1998).

In addition to glutamine and glutamate, the metabolic pathways for many of the other amino acids are represented. Serine hydroxymethyltransferase (bll5033) assimilates formaldehyde into serine biosynthesis and was proposed to be responsible for detoxification of formaldehyde from the catabolism of vanillate in a mutant of *mxaF* (blr6213) (Sudtachat et al., 2009). O-acetylhomoserine sulfhydrylase (cysD, blr4967) is necessary for the incorporation of sulfate to L-cysteine or L-homocysteine, the precursors for organic molecules that contain sulfur. A *cys*D mutant of *S. meliloti* produced sulfate-free Nod factors and exhibited decreased nitrogen fixation capacity due to rhizobial

growth defects, though nitrogen fixation was restored upon addition of methionine to growth media (Snoeck et al., 2003). S-adenosylmethionine synthetase (*met*K, bll5945) converts methionine to S-adenosyl-L-methionine. The *S. meliloti* LuxR homolog *nesR* controls active methyl cycle genes, including metK (Patankar and Gonzalez, 2009). A *nesR* mutant caused downregulation in these genes including *metK*. L-asparaginase (bll4950) catalyzes the hydrolysis of L-asparagine to L-aspartate and ammonium and an isoform has been characterized in the periplasm of *E. coli* (Cedar and Schwartz, 1967). Asparagine can serve as both the carbon and nitrogen skeleton for *R. etli* (Huerta-Zepeda et al., 1996). *R. etli* bacteroids were found to have the same amount of asparaginase activity in bacteroids as cells grown with asparagine as the sole carbon and nitrogen source (Huerta-Zepeda et al., 1996). 3-hydroxyisobutyrate dehydrogenase (bll3740) converts (reversibly) 3-hydroxyisobutyrate to methylmalonate-semialdehyde in the metabolism of valine, though a mutant in *P. aeruginaosa* was not lethal (Steele et al., 1992). Homospermidine synthase (bll7762) converts two molecules of putrescine to homospermidine. Nodules of plants that export ureides show enrichment for ^{15}N (Shearer et al. 1982) with an enrichment of ^{15}N homospermidine in both the nodule and rhizobia, *B. japonicum* and *R. fredii* (Yoneyama et al., 1998). Aspartate aminotransferase (bll7416) catalyzes the amination of oxaloacetate to L-aspartate. A mutant in aspartate aminotransferase of *S. meliloti* formed symbiotically defective nodules (Rastogi and Watson, 1991). Aspartate aminotransferase activity was characterized previously in the periplasm of *B. japonicum* bacteroids (Streeter and Salminen, 1990).

Several proteins were localized solely to the periplasm: alanine racemase (bll4070), isopropylmalate isomerase large subunit (blr0488), Nif S (blr4342),

propionyl-CoA carboxylase, alpha subunit (bll5267), a probable acetolactate synthase (bll7231) and amidohydrolase (blr5691) (Table 3). The 3-isopropylmalate isomerase large subunit has been shown to be up-regulated during iron repletion in *B. japonicum* (Rudolph et al., 2006) and mutation in the 3-isopropylmalate isomerase small subunit (*leu*D) of *R. leguminosarum* was shown to form 50-80 fewer nodules, but acetylene reduction was comparable to wildtype (Prell et al., 2009). NifS may function as a cysteine desulfarase (Zheng et al., 1993) providing sulfur for the Fe-S center of nitrogenase or a selenocysteine lyase for selenophosphate biosynthesis as characterized in *Azobacter vinelandii* (Lacourciere and Stadtman, 1998). Bedekovics et al. (2011) have shown that leucine biosynthesis, in particular isopropylmalate isomerase, regulates iron-sulfur metabolism. Acetolactate synthase (bll7231) converts pyruvate to acetolactate and is necessary in several pathways, including the formation of branched-chain amino acids, though in *R. leguminosarum* the gene encoding acetolactate synthase is downregulated in bacteroids (Prell et al., 2009). Allaway et al. (2000) have demonstrated that *R. leguminosarum* mutants blocked in the transport of branched chain amino acids results in nitrogen deficient pea plants. Prell and Poole (2006) have proposed that amino acid cycles are necessary for effective nitrogen fixation.

Propiony-CoA carboxylase (bll5267) was found exclusively in the periplasm and displayed the greatest number of peptide fragments of any of the periplasmic-located proteins. Propionyl-CoA carboxylase can participate in a number of metabolic pathways including fatty acid synthesis, odd-chain fatty acid degradation, synthesis of polyketides, and 3-hydroxypropionate cycle (Dunn et al., 2004), but in particular, branch chain amino acid degradation. DeHertogh et al. (1964a,b) identified the enzymes of the pathway

from propionate to succinyl-CoA in *B. japonicum* bacteroids which included propionyl-CoA carboxylase. This is notable for two reasons. The first is the potential participation in an amino acid cycle (Prell and Poole, 2006) and the second is the production of succinyl-CoA. Isocitrate dehydrogenase (Shah and Emerich, 2006) and α-ketoglutarate dehydrogenase (Green and Emerich, 1997a) are not necessary for symbiosis, but succinate is required (Bergersen and Turner, 1967a; el-Din, 1992; Ronson et al., 1981). Thus a non-citric acid cycle source(s) of succinate is required for an effective symbiosis. Since the C_4-dicarboxylate transporter is absolutely required for symbiosis it implicates that succinate is supplied extracellularly. The source of the succinate is not known, but the presence of enzymes in the periplasm that participates in the production of succinate suggests the periplasm is the source of succinate.

Fatty Acid Metabolism

Enoyl-CoA hydratase encoded by blr1160 and bll7821 (Table 5) could be involved in the metabolism of poly-3-hydroxybutyrate (PHB), branched chain amino acids, or fatty acids (Aneja et al., 2002; Kazakov et al., 2009; Yang et al., 1988). 3-hydroxybutyrate dehydrogenase (*bdh*A, blr1488) catalyzes a reversible oxidation of 3-hydroxybutyrate to acetoacetate and is a central enzyme in the PHB cycle (Aneja et al., 2002). A mutant in *S. meliloti* 3-hydroxybutyrate dehydrogenase showed no symbiotic defects and accumulates the same amount of PHB as the wildtype which is characteristic of the indeterminate systems (Aneja and Charles, 1999). Acetyl-CoA acetyltransferase (blr3924 and bll7400) can reversibly yield two-acetyl CoA from acetoacetyl CoA and has been characterized in *B. japonicum (Suzuki et al., 1987)*. This step can be both the

start point for biosynthesis and the metabolic endpoint of PHB. Glcyerol kinase (*glp*K, blr1410) keeps glycerol in the cell by phosphorylation to sn-glycerol 3-phosphate (Voegele et al., 1993). A *S. meliloti* glpK mutant (upstream of *bdh*A) was unable to utilize glycerol as a sole carbon source (Aneja and Charles, 1999).

3-oxoacyl-(ACP) synthase II (bll3808) is involved in long-chain fatty acid biosynthesis (Garwin et al., 1980). *R. leguminosarum* mutants in a putative 3-oxoacyl-(ACP) synthase II gene lacked very long chain fatty acid (VLCFA) modification to its lipid A moiety and was sensitive to dessication and osmotic stress (Vanderlinde et al., 2009). Acyl-CoA dehydrogenase (bll2657) is required for β-oxidation of fatty acids. The acyl-CoA dehydrogenase gene of *Salmonella typhimurium* was found to be up-regulated during carbon starvation while the gene of the denitrifying bacterium strain EbN1 was involved in the anaerobic degradation of ethylbenzene (Rabus et al., 2002; Spector et al., 1999). Enzyme activities for propionyl-CoA carboxylase and acetyl-CoA carboxylase were described in cultured *R. etli* (Dunn et al., 2004).

Energy Metabolism

Quinoprotein ethanol dehydrogenase (bll6220**,** Table 6) was found to have increased expression in *B. japonicum* during dessication stress (Cytryn et al., 2007). The authors suggested that induction of PQQ related orfs may reduce oxidative stress during dessication. Quinoprotein ethanol dehydrogenase (bll6220) was found to be repressed when exposed to soybean seed extract (Wei et al., 2008). $NAD(P)^+$ transhydrogenase (*pnt*A;bll7126) along with *pnt*B forms a membrane bound transhydrogenase that was found to not be needed to maintain NADPH balance in several bacterium including *S.*

meliloti (Fuhrer and Sauer, 2009). The c-type cytochromes are necessary for nitrogen fixation and respiration in bacteroids in *R. leguminosarium* (Delgado et al., 1995) and *B. japonicum* (Ritz et al., 1993; Ritz et al., 1995). The cytochrome c-type biogenesis protein (*cyc*H;blr3125) is a transmembrane protein facing the periplasm that helps coordinate the attachment of the heme to the apocytochrome c along with CycK and CycL (Ritz et al., 1995; Thony-Meyer et al., 1994).

Biosynthesis of Cofactors and Prosthetic Groups

Thioredoxin (*trx*A:bll0751) (Table 7) reduces disulfide bonds of target proteins, for example the biogenesis of c-type cytochromes where it mediates the transfer of electrons from the cytoplasm to the periplasm through DsbD (Fabianek et al., 2000). The operon encoding bll0751 displays synteny to that in *Agrobacterium tumefaciens* where it is near *folC* and DNA helicase (*uvr*D) (Vattanaviboon et al., 2007).

Regulatory Functions

The two component sensor histidine kinase (*rag*B, bll0303, Table 8) has been localized to the outer membrane of *Porphyromonas gingivalis* where it is associated with RagA forming a receptor that is linked functionally to TonB (Nagano et al., 2007). *B. japonicum* bacteroids were capable of protein phosphorylation (Karr and Emerich, 1989).

DNA Replication, Recombination, Repair

Since bacteroids are not dividing, emphasis would be presumed to be on DNA repair rather than replication (Table 9). Two of the three proteins in this category were

localized only to the periplasm. The RecA recombinase protein (bll5755) catalyzes strand exchange between homologous DNAs and acts as a co-protease on the LexA protein resulting from DNA damage (Cox, 1991; Cox, 1993; Little, 1993). RecA has been found to co-localize to the outer membrane fraction of *Escherichia coli* (Lopez-Campistrous et al., 2005). The binding of MutL (blr7493), a DNA mismatch repair protein, to DNA is dependent upon MutS, which activates the MutH endonuclease activity at unmethylated d(GATC) of the synthesized DNA strand (Spampinato and Modrich, 2000). MutL is up-regulated in free living *B. japonicum* during dessication (Cytryn et al., 2007).

Purines, Pyrimidines, and Nucleosides

Three of the six proteins in this category were localized to the periplasm (Table 10). Carbamoyl phosphate synthase (blr7371), uridylate kinase (bll4859), and CTP synthase (bll4805) are proteins in the pathway of CTP synthesis. Carbamoyl phosphate synthase (*car*A) makes the intermediate carbamoylphosphate and is required for effective nitrogen fixation in *R. meliloti* (Kerppola and Kahn, 1988). Uridylate kinase (*pyr*H) phosphorylates UMP to UDP and mutants have been shown to be lethal to several bacteria (Ingraham and Neuhard, 1972; Lee et al., 2007; Smallshaw and Kelln, 1992). CTP synthase (*pry*G) is an amidotransferase that converts UTP, glutamine, and ATP to CTP, glutamate, and ADP (Jorgensen et al., 2003). CTP synthase is necessary for the formation of CMP-Kdo(3-deoxy-D-manno 2-octulosonic acid), a precursor molecule in the core oligosaccharide of lipopolysaccharides of bacteria (King et al., 2009; Price et al., 1994).

Adenylosuccinate lyase (*purB,* blr5690) catalyzes the conversion of 5-phosphoribosyl-5-amino-imidazole-4-N-succinocarboxamide to 5-aminoimidazole-4-carboxamide riboside as well as the conversion of adenylosuccinate to AMP. A mutant of *purB* in *M. loti* was required for infection thread formation and nodule development (Okazaki et al., 2007). Inositol-5-monophosphate dehydrogenase (blr3972) is a step in the biosynthesis of purines. A mutant in *Bradyrhizobium* sp. strain ORS278 was affected in symbiosis forming pseudo nodules (Giraud et al., 2007).

Transcription

Ribonuclease E (bll4305, Table 11) was found to regulate *nifA* gene expression in *R. leguminosarum* at the post-transcriptional level (Zhang and Hong, 2009). Ribonucleases have, also, been found to be excreted by several bacteria and in the smut fungus *Ustilago sphaerogena* extracellular ribonucleases are utilized to breakdown exogenous RNA for metabolism and nitrogen assimilation (Holloman and Dekker, 1971; Lanyi and Lederberg, 1966). The transcription factor *rpoE4* was induced under stress conditions (oxidative, saline, and osmotic shock) and under microaerobic and stationary-phase growth, like that found in a bacteroid (Martinez-Salazar et al., 2009).

Translation

Protein content and the capacity to synthesize proteins decline with bacteroid development (Karr and Emerich, 1996). However, proteomic analysis revealed a large number of proteins correlated with translation (Table 12). A number of the proteins in this category were found in the secretomes of *B. japonicum*, *R. etli*, and *Erwinia*

chrysanthemi including EF-Tu, ribosomal proteins, and tRNA-synthetases (Hempel et al., 2009; Kazemi-Pour et al., 2004; Meneses et al., 2010). Curiously, ribosomal proteins were found in the periplasmic fraction. The presence of ribosomal proteins extracellularly also has been seen in several other bacteria (Bendsten et al., 2005a; Bendsten et al., 2005b; Gallaher, 2006; Tjalsma, 2004). Elongation factor G (fusA, bll5403), elongation factor Tu (bll5402), and 30S ribosomal protein S7 (*rps*G, bll5404), were all found to be induced in *B. japonicum* when induced to oxidative stress by paraquat (Donati et al., 2011). This is significant in that rhizobia must respond to the reactive oxygen species of plant defense to establish the symbiotic partnership and is reviewed in Pauly et al. (2006) . EF-Tu of *Agrobacterium tumefacians* is perceived by *Arabidopsis thaliana* through the perception pathogen-associated molecular patterns via a receptor kinase that is essential for EF-Tu perception and elicitation of associated plant defense response (Zipfel et al., 2006). Several 30S and 50S ribosomal subunits along with aspartyl-tRNA synthetase were found to necessary for nitrogen fixation in the photosynthetic *Bradyrhizobium* Sp. Strain ORS278 (Bonaldi et al., 2010). Several t-RNA synthetases were found in both the cytosol and periplasmic fraction. Though cross-compartment contamination is possible, well documented accounts of secondary activities for t-RNA synthetases have been established in eukaryotes and bacteria beyond protein translation (Guo et al., 2010; Lee et al., 2004). Two genes of *B. japonicum* bll0957 and bll6282 (not identified in this study) that encode atypical-seryl-tRNA synthetases were shown to transfer activated amino acids to phosphopantetheine prosthetic groups of putative carrier proteins (Mocibob et al., 2010).

The serine protease DO or DegP/htrA (blr5428) is a periplasmic endopeptidase/chaperone that is up-regulated under stress conditions in *E. coli* (Jomaa et al., 2009). *Streptococcus mutans* mutants in DegP were found to be deficient in the biogenesis of extracellular proteins necessary for biofilm formation and the extracellular glycolytic enzymes enolase and glyceraldehyde-3-phosphate dehydrogenase (Biswas and Biswas, 2005). DegP is not necessary for the *R. meliloti*-alfalfa symbiosis (Glazebrook et al., 1996). CtpA is a periplasmic protease that is necessary for dessication tolerance in *R. leguminosarum* (Gilbert et al., 2007). Identification of two isomers of Lon protease (bll4942 & blr6174) were found in this study. A *S. meliloti* mutant of Lon protease was found to produce higher levels of expolysaccharide when grown on succinate medium when compared to wildtype and to form psuedonodules on alfalfa that contained few bacteroids and did not fix nitrogen (Summers et al., 2000).

Cell Envelope

The cell envelope is a critical component of the symbiosis as every metabolite must cross this barrier (Table 13). In *Streptococcus pyogenes* the 67 kDa myosin-crossreactive streptococcal antigen gene is only found in the pathogenic streptococcal groups (Kil et al., 1994). The function of the 67 kDa myosin-cross reactive streptococcal antigen homolog (bll0025) in *B. japonicum* is unknown. The *B. japonicum* homolog contains a soybean trypsin inhibitor (Kunitz) protease inhibitor family signature according to PROSITE.

4-hydroxy-3methylbut-2en-l-yl diphosphate synthase (*gcp*E, blr0936) catalyzes the conversion of 2C-methyl-D-erythritol 2,4-cyclodiphosphate to 1-hydroxy-2-methyl-2-

(E)-butenyl-4 diphosphate in the non-mevalonate pathway to terpenes (Altincicek et al., 2001; Hecht et al., 2001). It is of note that the gcpE protein is listed in Rhizobia as a peptidoglycan acetylation protein and could serve in either role.

D-Alanine aminotransferase (bll7596) converts pyruvate to D-alanine utilizing D-glutamate as the source of nitrogen and requiring pyridoxal phosphate as a cofactor. D-Alanine is required to complete the peptide cross links between N-acetylglucosamine and β-(1-4)-N-acetylemuramic acid of the peptidoglycan (Humann and Lenz, 2009).

Transport and Binding Proteins

A large number of ABC transport substrate-binding proteins were found with annotated functions as branched chain amino acid binding proteins (Table 14). With consideration to the role branched chain amino acid play in *R. leguminosarum*, possibly regulating the symbiosis by the plant through the use of branched chain amino acids, this could explain the need for so many branched chain binding proteins (Prell et al., 2009). C^{14} leucine uptake was demonstrated in *B. japonicum* bacteroids where it was metabolized to acetyl-CoA and then PHB (Karr and Emerich, 1996). Possible broad amino acid substrate specificity by substrate binding proteins may indicate amino acid cycling between the bacteroid and plant (Hosie et al., 2002; White et al., 2009). ABC transporter substrate binding protein (blr2442) was found to be induced by both genistein and soybean seed extracts (Wei et al., 2008). Mutations in the gene of the periplasmic protein tolB of *P. putida* reduced outer membrane stability leaking periplasmic proteins into the culture medium (Llamas et al., 2000). Bll0733 and blr1091 (*pst*S) were both predicted to have PhoB regulated promoters (Yuan et al., 2006b). Mutation in the

inorganic phosphate pathway (PstSCAB) of *S. meliloti* indicated that the metabolism of the bacteroid is not limited by inorganic phosphate (Yuan et al., 2006a). *B. japonicum* utilizes a periplasmic mannitol-binding protein (blr4203) to bind and transport mannitol, in contrast to the system of *E. coli* that transports mannitol via phosphoenolpyruvate-dependent phosphotransferase system (Davis and Robb, 1985). Mathis et al. (1986) described a mannitol utlizing strain of USDA 110 that had superior N_2-fixing capabilities when compared to the parent strain USDA 110 in 49-day old, but not in 28-day old soybean. Phosphate transport system regulatory protein (phoU, blr1095) is responsible in *E. coli* for persistent survivors of antibiotic treatment (Li and Zhang, 2007). A mutant in *pho*U was found to have higher susceptibility to antibiotic treatment. The phosphonate binding periplasmic protein, PhoD, has been shown to be necessary for the transport of inorganic phosphate in *R. meliloti* and mutants were found to be unable to fix nitrogen (Bardin et al., 1996).

Other Categories

2-hydroxyhepta-2,4-diene-1,7-dioate isomerase (blr7891, Table 15) has been described in *E. coli* as being *hpcF* where it is a step in the catabolism of homoprotocatechuate to pyruvate and succinate semi-aldehyde (Jenkins and Cooper, 1988). Soybean seed extract was found to increase the expression of bll2063 (*nrg*C) and bll2067 (*nfe*C), though *nrg*C is not essential for symbiosis (Nienaber et al., 2000; Wei et al., 2008). A knockout mutant in the TldD protein of *Gluconobacter oxydans* did not produce detectable amounts of PQQ, and showed low periplasmic dehydrogenase activity due to lack of PQQ (Holscher and Gorisch, 2006). Symbiotic bacteria express a

number of enzymatic antioxidant responses to reactive oxygen species that help establish and maintain the symbiosis (Pauly et al., 2006). Superoxide dismutase converts the radical O_2^- to O_2 and H_2O_2. Catalase then converts the H_2O_2 to O_2 and H_2O. A single mutation in one of three known catalase genes (*kat*G) of *B. japonicum* did not result in a phenotype (Panek and O'Brian, 2004) while double knockouts (*kat*B/C and *katA*/C) in *S. meliloti* are impaired in nodulation formation and nitrogen fixation (Jamet et al., 2003). Proteins for superoxide dismutase and catalase were found in the stationary-phase of the *R. etli* secretome (Meneses et al., 2010). Anti-oxidant protein (blr5308) is in a family of proteins related to alkyl hydroperoxide reductase (AhpC) that may use H_2O_2 as a substrate (Seaver and Imlay, 2001). Carbon monoxide dehydrogenase activity (bll5914) has been described in *B. japonicum* strain 110*spc4* with the strain capable of growing solely on carbon monoxide in an aerobic environment (Lorite et al., 2000).

Plant Proteins

Of particular interest are the 54 plant proteins and one viral protein identified in this study (Table 16). The presence of relatively large numbers of plant proteins in the periplasmic fraction suggested the the bacteroid preparations may be contaminated with soybean nodule proteins. Previously, we had developed a procedure to remove contaminating plant proteins from our bacteroids isolations employing a two step sucrose gradient procedure (Waters et al., 1985). The majority (52/54) of the plant proteins listed recorded the minimum of two peptides identified and the two other proteins recorded only three peptide hits. The low number of peptides suggested plant protein contamination. Curiously, the most abundant protein in the nodule, leghemoglobin, was absent as well as

other abundant proteins and enzymes known to be present via enzymatic and proteomic analysis (Anthon and Emerich, 1990; Copeland et al., 1989b; Kouchi et al., 1988). An alternative explanation is that these proteins were transported to the bacteroid surface. Two plant proteins were chosen for immunogold localization to soybean nodule preparations. Histone H2A was chosen as it was the plant protein which yielded the greatest percent coverage and for which antibodies were available (Figure 6). Soybean lipoxygenase was one of two proteins that yielded three peptide fragments and antibodies were also available (Figure 7). For both antibodies, labeling was found predominately associated with the bacteroid and within the symbiosome space. There was little labeling within the plant cytoplasm in either infected or uninfected cells. Thus, for at least two of the plant proteins identified in the periplasmic fraction, there appears to be a specific localization to the bacteroid or at least within the symbisome space.

Histone H2A and H2B have been previously described in the Pacific white shrimp and Atlantic cod as being excreted and utilized as anti-microbial peptides along with ribosomal proteins (Bergsson et al., 2005b; Patat et al., 2004). Histone H4 as well as lipoxygenase, ATP synthase, and xyloglucan endotransglucosylase have been identified as being excreted from pea root tips (Wen et al., 2007). These proteins could be interacting with the bacteroid in the periplasm or possibly be interacting with proteins in the symbiosome space acting as a means of communication between the plant and rhizobia.

The 19 soybean sequences shown in Table 17 possessed serine/threonine-rich regions with at lease two serine/threonine residues demonstrating a spacing of S/T X_6S/T. The first seven sequences above have arginines between the two serine/threonine residues

which would be cleaved by trypsin prior to MS analysis. Alignment with known soybean sequences places these peptides with serines/threonines near the N-terminals of each respective protein. If each peptide were part of a protein with the S/T X_6S/T alignment and an intervening arginine or lysine residue, the N-terminal serine/threonine would be separated from the C-terminal serine/threonine upon trypsin treatment prior to MS/MS analysis. Twelve peptide fragments were found with a serine/threonine motif near the predicted N-terminal portion a protein with no intervening arginine or lysine residues (last 12 peptides in Table 17).

Obviously, the significance of the enriched serine/threonine regions and serine/threonine spacing are not known at this time. These regions may be sites of *O*-glycosylation. Although there is a consensus sequence for N-glycosylation, *O*-glycosylation sites are not reliably predictable (Christlet and Veluraja, 2001). Proline residues at positions +3 and/or-1 relative to a serine residue favors glycosylation (Christlet and Veluraja, 2001). That preference was found in the stomatal density protein, the putative argininosuccinate synthase, the putative acetylornithine transaminase, the putative kinesin-like protein [but not for a serine/threonine in the S/T X_6S/T motif] and the first of the four Unknown proteins [+3 of the N-terminal serine in the S/T X_6S/T motif]. However, other serines/threonines could be *O*-glycosylated that do not fit the proline consensus spacing. Alternatively, serine residues are frequently the site of phosphorylation. However, none of the sequences possessed the consensus sequence for phosphorylation such as those found in soybean nodulin Nod26 or *Lotus japonicus* LIMP2 (Fortin et al., 1987).

The availability of the soybean genome will permit further analysis of these sequences. The results do permit speculation that these proteins possess sequence information that targets them to the bacteroid periplasm and/or symbiosome space. It is known that soybean nodule thioredoxin (AAS88427) has been reported to be localized within the infected plant cells of the nodule, but its subcellular localization has not been determined (Lee et al., 2005). Soybean thioredoxin, which was identified in the bacteroids periplasmic proteome (Table 7), contains two tandem serine/threonine motifs, one of which contains an intervening arginine (Table 17). Also, in mammals, a serine/threonine–rich motif (LRSVSTGSSRPSK) was demonstrated to be a nuclear localization signal that determines the unidirectional transport of the mineralocorticoid receptor to the nucleus (Walthers et al., 2005). The serine/threonine-rich motif may serve as, or be indicative for, a translocation signal/mechanism to place symbiotically functional plant-derived proteins into the periplasm of the bacteroid and/or symbiosome space.

Summary

A total of 92 proteins were found exclusively in the periplasmic space of *B. japonicum* bacteroids annotated as *B. japonicum* proteins and another 54 proteins were found in the periplasm annotated as plant proteins. The enzymatic analysis of the periplasmic fraction, the lack of the most abundant protein in the soybean nodule, leghemoglobin, and the number of unique peptides identified from cytoplasmic and periplasmic proteins demonstrates that the procedure for obtaining bacteroids and fractionation of periplasm proteins are adequate. The plant proteins identified in the

periplasmic fraction may have been specifically transported to the bacteroids within the symbiosome as shown by immunolocalization of two of the identified plant proteins. The proteins identified in the periplasm grouped in the intermediary carbon metabolism and amino acid metabolism suggest a periplasmic production of succinate, which is supported by the symbiotic requirement of the C_4-dicarboxylate transporter (el-Din, 1992) and that succinate yields the greatest rates of nitrogen fixation activity (Bergersen and Turner, 1967b; Stumpf and Burris, 1979).

Table 1 - Enzyme Activity in Periplasmic and Cytosolic Fractions of Bacteroids Isolated from Soybean Nodules at Two Different Ages

Days After Planting	Fraction	Cyclic-phosphodiesterase nmol/min/ug[a]	Malate Dehydrogenase umol/min/ug[a]	Isocitrate Dehydrogenase nmol/min/ug[a]	β-Hydroxybutyrate Dehydrogenase nmol/min/ug[a]
56	**Periplasm[b]**	**0.96±0.2**	**0.164±0.024**	**2.92±1.89**	**4.6±2.5**
56	**Cytosol[c]**	**11.4±1.0**	**1.98±0.08**	**247.4±25.4**	**359.47±20.32**
64	**Periplasm[b]**	**1.33±0.32**	**.291±0.038**	**8.78±10.48**	**13.93±6.97**
64	**Cytosol[c]**	**11.0±0.7**	**1.52±0.24**	**174±16**	**568±105**

[a]Values are the mean ± standard deviation. [b]Periplasmic values are the result of three biological replicates measured in triplicate.
[c]Cytoplasmic fractions were measured in triplicate with mean and standard deviation then calculated.

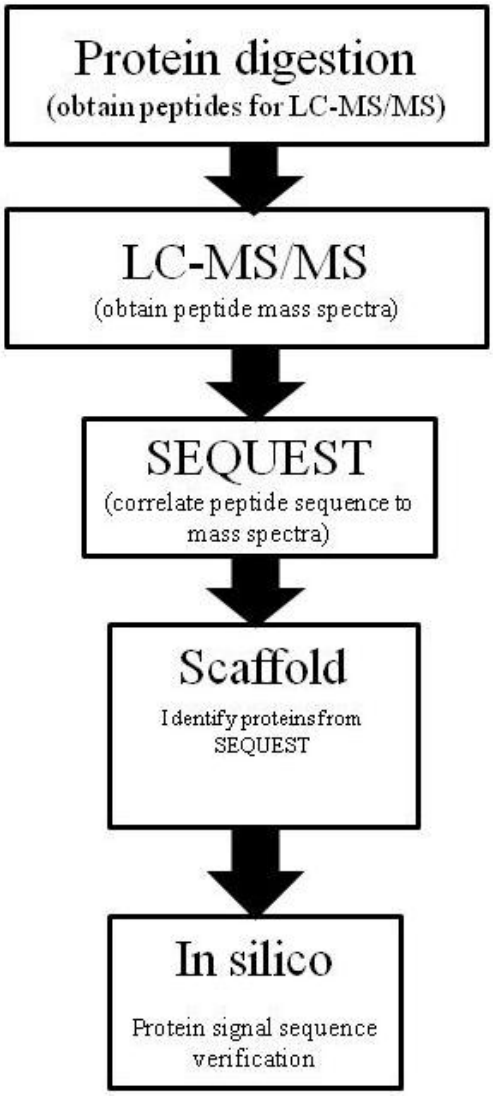

Figure 4. Proteomics workflow for protein identification during *B. japonicum* bacteroid fractionation study.

Figure 5- Venn diagram of proteins identified via LC-MS/MS in the periplasmic and/or cytosolic fractions of bacteroids from soybean nodules

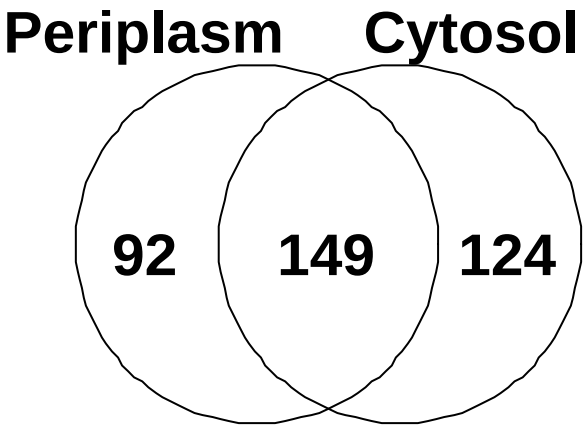

Table 2. Protein Folding

Protein Identified	Rhizobase #	Acc. #	Localization	Predicted Localization	# of hits	% coverage
60kDa chaperonin	blr7533	NP_774173	both		3	14
60kDa chaperonin GroEL	blr5626	NP_772266	both		13	35
GroEL chaperonin	blr5227	NP_771867	PP		3	7.6
GroEL3 chaperonin	bll2059	NP_768699	both		59	82
GroEL5 chaperonin	blr4635	NP_771275	cyt		2	6
GroES4	blr5625	NP_772265	cyt/pp		2	32
GroES co-chaperonin	bll2060	NP_768700	both	LipoP	9	54
heat shock protein (grpE)	blr0676	NP_767316	cyt	Cello	2	19
cold shock protein	bsl3986	NP_770626	cyt	Cello, Adaboost	2	64
DnaK	blr0678	NP_767319	both		3	11
trigger factor	bll4945	NP_771585	both		3	7
Cytochrome P-450 BJ-1	blr2144	NP_768784	both		3	16
Cytochrome P-450 BJ-4	blr2147	NP_768787	cyt		2	10
Cytochrome P-450 family protein	blr1853	NP_768493	cyt		3	14
competence-damage associated protein (*cin*A)	bll5611	NP_772251	cyt		2	16

Table 3. Central Intermediary Metabolism

Protein Identifed	Rhizobase #	Acc. #	Localization	Predicted Localization	# of hits	% coverage
nitrogenase molybdenum-iron protein beta chain (*nif*K)	blr1744	NP_768384	both		16	45
nitrogenase reductase (*nif*H)	blr1769	NP_768409	both		17	66
nitrogenase molybdenum-iron protein alpha chain (*nif*D)	blr1743	NP_768383	both		13	41
nitrogenase stabilizing/protective protein (*nif*W)	blr1771	NP_768411	cyt		2	21
iron-molibdenum cofactor processing protein (*nif*X)	blr1747	NP_768387	cyt		2	25
Flavoprotein (*fix*C)	blr1774	NP_768414	both		3	19
amylo-alpha-1,6-glucosidase (GDE_C family)	blr2754	NP_769394	cyt		2	3.3
putative sugar hydrolase	blr1964	NP_768604	PP	TatP, LipoP	2	7
trehalose synthase	blr6767	NP_773407	cyt		2	5
UDP-glucose 6-dehydrogenase	bll8129	NP_774769	PP		2	11
GDP-mannose 1-phosphate guanylyltransferase	bll5919	NP_772559	both		2	11
bifunctional transaldolase/phosoglucose isomerase	blr6758	NP_773398	both		4	8
putative transketolase alpha subunit protein	blr2168	NP_768808	cyt		2	14
putative transketolase beta subunit protein	blr2169	NP_768809	cyt	TatP	2	11
fructose bisphosphate aldolase	bll1520	NP_768160	both		2	13
fructose 1,6-bisphosphatase II	blr4363	NP_771003	both		4	27
D-3-phosphoglycerate dehydrogenase (*ser*A)	bll7401	NP_774041	both		3	14
glyceraldehyde-3-phosphate dehydrogenase	bll1523	NP_768163	both		5	25
D-3-phosphoglycerate dehydrogenase	bll7965	NP_774605	both		2	7

glycerate dehydrogenase	bll2918	NP_769558	cyt		2	11
enolase	bll4794	NP_771434	both		4	21
phosphoenolpyruvate carboxykinase	bll8141	NP_774781	both	Cello, Adaboost	3	6
pyruvate dehydrogenase subunit beta	bll4782	NP_771422	both		4	14
pyruvate phosphate dikinase	blr2538	NP_769178	both	TatP	6	14
L-lactate dehydrogenase	blr4823	NP_771463	PP		2	13
acetyl-CoA synthetase	blr0573	NP_767213	cyt	Cello	2	6
aldehyde dehydrogenase	blr2816	NP_769456	both	Cello	5	23
putative aldehyde dehydrogenase	bll7607	NP_774247	both	TatP	4	14
putative alcohol dehydrogenase precursor	bll6220	NP_772860	cyt	TatP, LipoP, cPSORTdb	2	6
type II citrate synthase	blr4839	NP_771479	both	Cello	5	18
isocitrate dehydrogenase	blr5747	NP_772387	both		3	13
dihydrolipoamide dehydrogenase	bll0449	NP_767089	both		2	12
dihydrolipoamide succinyl transferase (sucB)	bll0451	NP_767091	both	Cello	5	17
alpha-ketoglutarate decarboxylase	bll0452	NP_767092	cyt		4	9
succinyl-CoA synthetase alpha chain	bll0453	NP_767093	cyt		2	10
succinyl-CoA synthetase subunit beta	bll0455	NP_767095	cyt		4	15
succinate dehydrogenase flavoprotein subunit (sdhA)	blr0514	NP_767154	cyt	cPSORtdb	3	11
succinate-semialdehyde dehydrogenase	blr0807	NP_767447	both		5	21
fumarate hydratase class I	bll5796	NP_772436	both	Cello	6	17
malate dehydrogenase	bll0456	NP_767096	both		10	52
malic enzyme	blr4145	NP_770785	cyt		2	6
malate synthase G	bll1474	NP_768114	both	Cello	4	11
prephenate dehydratase (*phe*A)	bll1421	NP_768061	PP		2	14
4-hydroxybenzoate 3-monooxygenase (*pob*A)	bll7838	NP_774478	PP		2	14

3-oxoadipate CoA-transferase subunit A	bll7093	NP_773733	both		3	24
phenylacetate-coenzyme A ligase	blr2897	NP_769537	PP		2	25
benzoyl-CoA oxygenase component	blr1081	NP_767721	both		5	22
phenolhydroxylase-like protein	bll2063	NP_768703	both	TatP	8	33

Table 4. Amino Acid Metabolism

Protein Identified	Rhizobase #	Acc. #	Localization	Predicted Localization	# of hits	% coverage
alanine dehydrogenase oxidoreductase protein	blr3179	NP_769819	both		3	16
alanine racemase	bll4070	NP_770710	PP		2	4
aspartate aminotransferase	bll7416	NP_774056	cyt	Cello	2	8
aspartate-semialdehyde dehydrogenase	bll0501	NP_767141	both		2	14
L-asparaginase	bll4950	NP_771590	cyt	TatP, LipoP	2	11
Cysteine desulfurase (nifS)	blr4342	NP_770982	PP		2	9.2
glutamine synthetase I	blr4949	NP_771589	both	Cello	8	31
glutamate synthase large subunit	blr7743	NP_774383	both		5	8
isopropylmalate isomerase small subunit	blr0495	NP_767135	both		3	31
3-Hydroxyisobutyrate dehydrogenase	bll3740	NP_770380				
3-isopropylmalate dehydrogenase	bll0504	NP_767143	both		3	18
isopropylmalate isomerase large subunit	blr0488	NP_767128	PP		2	5.3
N5-methylenetetrahydropteroyltriglutamate-homocysteine methyltransferase	blr2068	NP_768708	Both		6	14
serine hydroxymethyltransferase	bll5033	NP_771673	both		5	22
O-acetylhomoserine aminocarboxypropyl transferase	blr4967	NP_771607	both	LipoP	3	13
propionyl-coenzyme A carboxylase alpha polypeptide	bll5267	NP_771907	PP		4	13
methylmalonate-semialdehyde dehydrogenase	blr3954	NP_770594	both		3	14
fumarylacetoacetate hydrolase superfamily	blr3199	NP_769839	both	Adaboost, Cello	2	8
anthranilate phosphoribosyltransferase	bll2049	NP_768689	both		2	15

tryptophan synthase subunit beta	blr0745	NP_767385	cyt		3	13
succinyl-diaminopimelate desuccinylase (*dapE*)	blr3064	NP_769704	cyt		2	12
glutaryl-CoA dehydrogenase	blr2616	NP_769256	both		3	16
possible lysine decarboxylase	bll3794	NP_770434	cyt		2	26
S-adenosyl-L-homocysteine hydrolase	bll5944	NP_772584	cyt/PP		3	16
S-adenosylmethionine synthetase	bll5945	NP_772585	PP		2	12
methionine sulfoxide reductase A	bll6260	NP_772900	cyt		2	19
S-adenosyl-L-methionine-dependent methyltransferases family	blr2372	NP_769012	both		3	20
ketol-acid reductoisomerase	bll6497	NP_773137	cyt		2	9
probable acetolactate synthase I	bll7231	NP_773871	PP		2	7
Propionyl-CoA Carboxylase, alpha subunit	bll5267	NP_77190	PP		4	13
homospermidine synthase	blr7762	NP_774402	both	Cello	2	5
amidohydrolase	blr3021	NP_769661	cyt		2	13
aminotransferase	blr1686	NP_768326	both		21	49
aminotransferase	blr4134	NP_770774	cyt		2	8
putative aminotransferase	blr2136	NP_768776	cyt	LipoP	2	12
amidohydrolase	blr5691	NP_772331	PP		2	10
ornithine aminotransferase	blr3010	NP_769650	cyt		2	7
probable arginine/lysine/ornithine decarboxylases	bll3177	NP_769817	cyt		2	4

Table 5. Fatty acid, phospohlipids, and sterols

Protein Identified	Rhizobase #	Acc. #	Localization	Predicted Localization	# of hits	% coverage
acetyl-CoA carboxylase carboxyltransferase subunit alpha	blr0191	NP_766831	PP	cPSORTdb	2	18
acyl-CoA dehydrogenase	bll2657	NP_769297	cyt		2	6
acyl-CoA dehydrogenase	blr1158	NP_767798	cyt	TatP	2	7
enoyl-CoA hydratase	bll6081	NP_772721	cyt		3	22
enoyl-CoA hydratase	blr1160	NP_767800	both	Cello	4	12
enoyl CoA hydratase	bll3036	NP_769676	cyt		2	11
enoyl Co-A hydratase/isomerase family	blr1080	NP_767720	cyt		2	8
fatty oxidation complex alpha subunit	bll7821	NP_774461	PP		2	8
3-oxoacyl-(acyl carrier protein) synthase II	bll3808	NP_770448	both	Cello, LipoP	2	12
3-oxoacyl-(acyl carrier protein) synthase II	bll3809	NP_770449	both		4	23
glycerol kinase	blr1410	NP_768050	PP		2	8
3-hydroxybutyrate dehydrogenase	blr1488	NP_768128	both	TatP, LipoP	3	21
acetyl-CoA acetyltransferase	bll7400	NP_774040	cyt	TatP	2	11
acetyl-CoA acetyltransferase	blr1159	NP_767799	both		2	14
acetyl-CoA acetyltransferase	blr3924	NP_770564	PP	Cello	2	11
acetoacetate decarboxylase family	blr0028	NP_766668	both	cytoplasmic membrane	6	32
Phosphlipase/carboxylesterase	bll1566	NP_768206	PP	LipoP	2	13

Table 6. Energy Metabolism

Protein Identification	Rhizobase #	Acc. #	Localization	Predicted Localization	# of hits	% coverage
F0F1 ATP synthase subunit alpha	bll0442	NP_767082	both		5	15
F0F1 ATP synthase subunit beta	bll0440	NP_767080	cyt		7	29
electron transfer flavoprotein alpha chain (fixB)	blr1773	NP_768413	cyt/PP blank		5	20
electron transfer flavoprotein beta subunit	blr1377	NP_768017	both		3	18
quinone oxidoreductase	bll1503	NP_768143	both		2	13
NAD(P)+ transhydrogenase	bll7126	NP_773766	PP	Cello	2	12
quinone oxidoreductase	bll6137	NP_772777	both		3	19
electron transfer flavoprotein beta chain (fixA, nifX)	blr2038	NP_768678	both		6	30
cytochrome C-type biogenesis protein (cycH)	blr3125	NP_768765	cyt	Cello, Adaboost, LipoP	2	11
Quinoprotein ethanol dehydrogenase	bll6220	NP_772860	cyt	Cello, Adaboost, TatP, LipoP, cPSORTdb	2	6

Table 7. Biosynthesis of cofactors and prosthetic groups

Proteins Identified	Rhizobase #	Acc. #	Localization	Predicted Localization	# of hits	% coverage
beta alanine--pyruvate transaminase	blr2221	NP_768861	both		3	13
thioredoxin C-1 (trxA)	bll0751	NP_767391	cyt	Cello, Adaboost	5	53
glutathione S-transferase	bll6702	NP_773342	cyt		2	13
lactoylglutathione lyase	bll4399	NP_771039	cyt		2	27
4-hydroxybenzoate 3-monooxygenase (pobA)	bll7838	NP_774478	PP		2	14

Table 8. Regulatory Functions

Protein Identified	Rhizobase #	Acc. #	Localization	Predicted Localization	# of hits	% coverage
extragenic suppressor protein	bll1517	NP_768157	cyt		2	14
MoxR family protein	bll2465	NP_769105	both		3	21
two-component response regulator	bll7795	NP_774435	both		4	32
two-component response regulator	blr8144	NP_774784	both		4	19
transcriptional regulator	bll2785	NP_769425	both	Cello	2	28
two-component response regulator	blr3131	NP_769771	both		2	18
two-component hybrid sensor and regulator	bll2599	NP_769239	cyt	cytoplasmic membrane	2	2
two-component sensor histidine kinase	bll0303	NP_766943	PP	LipoP	2	9
phosphate regulon, two-component response regulator	blr1096	NP_767736	cyt		2	11
transcriptional regulatory protein	blr7380	NP_774021	both		3	20
PrkA serine protein kinase C-terminal domain	bll6756	NP_773396	both		4	9.7

Table 9. DNA replication, recombination, and repair

Protein Identified	Rhizobase #	Acc. #	Localization	Predicted Localization	# of hits	% coverage
recombinase A	bll5755	NP_772395	PP		2	15
DNA gyrase subunit B	bll0823	NP_767463	both		2	5.5
DNA mismatch repair protein	blr7493	NP_774133	PP		2	3.3

Table 10. Purines, pyrimidines, and nucelosides

Protein Identified	Rhizobase #	Acc. #	Localization	Predicted Localization	# of hits	% coverage
adenylosuccinate lyase (purB)	blr5690	NP_772330	both		3	14
nucleoside diphosphate kinase	blr4119	NP_770759	cyt		4	62
uridylate kinase (pyrH)	bll4859	NP_771499	PP		2	18
CTP synthetase (pyrG)	bll4805	NP_771445	PP	LipoP	2	9.4
ribosome recycling factor	bll4858	NP_771498	cyt		2	27
carbamoyl phosphate synthase small subunit (carA)	blr7371	NP_774011	PP	Cello, Adaboost	2	7.3

Table 11. Transcription

Protein Identification	Rhizobase #	Acc. #	Localization	Predicted Localization	# of hits	% coverage
DNA-directed RNA polymerase subunit alpha	bll5376	NP_772016	cyt		2	10
DNA-directed RNA polymerase subunit beta	bll5410	NP_772050	both		13	18
polynucleotide phosphorylase/polyadenylase	bll0779	NP_767419	both		4	12
transcription elongation factor NusA	bll0785	NP_767425	both		2	6
DNA-directed RNA polymerase subunit beta'	bll5409	NP_772049	both		6	7
transcription antitermination protein NusG	bll5416	NP_772056	both		2	23
ribonuclease E	bll4305	NP_770945	PP		2	4
transcription termination factor Rho	bll0635	NP_767275	both		3	9

Table 12. Translation

Protein Identification	Rhizobase #	Acc. #	Localization	Predicted Localization	# of hits	% coverage
translation initiation factor IF-2	bll0783	NP_767423	cyt		2	5
elongation factor G	bll7414	NP_774054	both		3	11
elongation factor G (fusA)	bll5403	NP_772043	both		10	30
elongation factor Tu (tuf)	bll5402	NP_772042	both		8	28
30S ribosomal protein S1	blr0740	NP_767380	both		7	21
30S ribosomal protein S5	bll5383	NP_772023	both		4	22
30S ribosomal protein S6	bll4079	NP_770719	both	Cello	2	14
30S ribosomal protein S7 (rpsG)	bll5404	NP_772044	both		3	34
30S ribosomal protein S8	bll5386	NP_772026	both		3	43
30S ribosomal protein S18	bsl4078	NP_770718	both		2	15
30S ribosomal protein S19	bsl5396	NP_772036	cyt	Cello, Adaboost	2	22
50S ribosomal protein L4	bll5399	NP_772039	cyt		2	12
50S ribosomal protein L5	bll5388	NP_772028	both		2	22
50S ribosomal protein L28	blr0162	NP_766802	cyt	Adaboost	2	18
ATP-dependent protease ATP-binding subunit (clpB)	blr1404	NP_768044	both		5	9
ATP-dependent protease LA (lon)	blr6174	NP_772814	both		4	8
ATP-dependent protease LA (lon)	bll4942	NP_771582	both		6	16
ATP-dependent protease ATP-binding subunit	bll4943	NP_771583	both		4	25
elongation factor Ts	bll4860	NP_771500	both		3	21
ATP-dependent Clp protease proteolytic subunit	bll4944	NP_771584	cyt		2	27
alanyl-tRNA synthetase	bll5750	NP_772390	cyt		2	4
aspartyl-tRNA synthetase	blr4143	NP_770783	PP		2	9
lysyl-tRNA synthetase	blr1133	NP_767773	cyt	Cello, Adaboost	3	9
phenylalanyl-tRNA synthetase subunit alpha	bll0706	NP_767346	cyt		3	14
phenylalanyl-tRNA	bll0705	NP_767345	both		3	8

synthetase subunit beta						
prolyl-tRNA synthetase	bll4877	NP_771517	both		3	14
tryptophanyl-tRNA synthetase	bll0802	NP_767442	cyt		2	15
putative glutamyl-tRNA(Gln) amidotransferase	bll7917	NP_774557	PP	Cello	2	7
peptidyl prolyl cis-trans isomerase	bll4690	NP_771330	cyt		2	16
ribosome recycling factor	bll4858	NP_771498	cyt		2	27
translation-associated GTPase	bll7439	NP_774079	cyt		2	6

Table 13. Cell Envelope

Proteins Identified	Rhizobase #	Acc. #	Localization	Predicted Localization	# of hits	% coverage
67 kDa Myosin-crossreactive streptococcal antigen-like protein	bll0025	NP_766665	both		4	12
4-hydroxy-3-methylbut-2-en-1-yl diphosphate synthase (gcpE)	blr0936	NP_767576	both		2	10
D-alanine aminotransferase	bll7596	NP_774236	cyt		2	7.7

Table 14. Transport and Binding Proteins

Protein Identified	Rhizobase #	Acc. #	Localization	Predicted Localization	# of hits	% coverage
ABC transporter substrate-binding protein	bll0887	NP_767527	both	Cello, Adaboost, LipoP, cPSORTdb	9	33
ABC transporter substrate-binding protein	blr1424	NP_768064	both	Cello, cPSORTdb, LipoP, TatP	3	11
ABC transporter substrate-binding protein	blr1448	NP_768088	both	Cello, Adaboost	2	10
ABC transporter substrate-binding protein	bll2304	NP_768944	cyt	Cello, Adaboost, LipoP	2	8
ABC transporter substrate-binding protein	blr2442	NP_769082	cyt	Cello, Adaboost, cPSORTdb, LipoP, TatP	2	8
ABC transporter substrate-binding protein	blr3234	NP_769874	cyt	Cello, Adaboost, cPSORTdb, LipoP, TatP	2	8
ABC transporter substrate-binding protein	blr3341	NP_769981	both	Cello, Adaboost, cPSORTdb, LipoP, TatP	3	10
ABC transporter substrate-binding protein	blr4039	NP_770679	both	Cello, Adaboost, LipoP	6	30
ABC transporter substrate-binding protein	blr4511	NP_771151	cyt	Cello, Adaboost, cPSORTdb, LipoP, TatP	2	8
ABC transporter substrate-binding protein	blr4884	NP_771524	cyt	Cello, Adaboost, cPSORTdb, LipoP, TatP	2	10
ABC transporter substrate-binding protein	blr5574	NP_772214	cyt/pp	Cello, Adaboost, LipoP, TatP	2	12
ABC transporter substrate-binding protein	bll5596	NP_772236	both	Cello, Adaboost, cPSORTdb, LipoP, TatP	3	12
ABC transporter substrate-binding protein	blr5675	NP_772315	both	Cello, Adaboost, cPSORTdb, LipoP	7	26
ABC transporter substrate-binding protein	blr6158	NP_772798	cyt	Cello, Adaboost, LipoP	2	9
ABC transporter substrate-binding protein	blr6246	NP_772886	both	Cello, Adaboost, LipoP	3	21

ABC transporter substrate-binding protein	blr7099	NP_773739	both	Cello, Adaboost, LipoP	2	11
ABC transporter substrate-binding protein	bll7769	NP_774409	cyt	Cello, LipoP	2	10
ABC transporter substrate-binding protein	bll7921	NP_774561	both	Cello, Adaboost, cPSORTdb	10	32
ABC transporter substrate-binding protein	blr7922	NP_774562	both	Cello, Adaboost	4	17
ABC transporter substrate-binding protein	blr8117	NP_774757	both	cPSORTdb	2	19
ABC transporter amino acid-binding protein	blr4446	NP_771086	both	Cello, Adaboost, cPSORTdb, LipoP	4	22
ABC transporter amino-acid-binding protein	bll7600	NP_774240	cyt/pp	Cello, Adaboost, cPSORTdb, LipoP	2	15
ABC transporter glycerol-3-phosphate-binding protein	bll0733	NP_767373	both	Cello, Adaboost, cPSORTdb, LipoP, TatP	4	16
ABC transporter phosphate-binding protein	blr1091	NP_767731	both	Cello, Adaboost, cPSORTdb, LipoP, TatP	4	18
periplasmic substrate binding protein	blr0998	NP_767638	PP	Cello, Adaboost, LipoP	2	7
periplasmic mannitol-binding protein	blr3743	NP_770383	cyt/pp	Cello, Adaboost, LipoP, TatP	4	23
amino acid binding protein	bll2909	NP_769549	both	Cello, Adaboost, LipoP, cPSORTdb	8	42
phosphonates-binding periplasmic precursor	bll7946	NP_774586	both	Cello, Adaboost, cPSORTdb, LipoP	4	21
phosphate transport system regulatory protein (phoU)	blr1095	NP_767735	both		2	16
Periplasmic binding protein-like II superfamily	bll6093	NP_772733	cyt	Adaboost, Cello, TatP	2	10
Preprotein translocase subunit SecA	bll0204	NP_766844	cyt		3	6.9
preprotein translocase SecB	bll0641	NP_767281	cyt	Cello, Adaboost	2	17

translocation protein TolB	bll7152	NP_773792	both	Cello, Adaboost, cPSORTdb	3	14
bacterioferritin	bll6680	NP_773320	both		8	69
periplasmic mannitol-binding protein	blr4203	NP_770843	cyt	Cello, Adaboost, TatP, LipoP	3	22

Table 15. Other Categories

Protein Identified	Rhizobase #	Acc. #	Localization	Predicted Localization	# of hits	% coverage
alkyl hydroperoxide reductase	bll1777	NP_768417	both		7	56
1-aminocyclopropane-1-carboxylate deaminase	blr0241	NP_766881	both		8	37
aminopeptidase	bll7941	NP_774581	PP		2	11
anit-oxidant protein	blr5308	NP_771948	cyt	Cello, Adaboost	6	46
ATP-binding protein	blr4340	NP_770980	cyt		2	20
carboxy-terminal protease	blr0434	NP_767074	both	Cello, TatP, LipoP	2	10
carbon monoxide dehydrogenase large chain	bll5914	NP_772554	cyt		3	7.2
catalase	blr0778	NP_767418	both	Cello, Adaboost	8	18
dehydrogenase	blr2146	NP_768786	both		5	36
dehydrogenase	bll3740	NP_770380	both	Cello, Adaboost, LipoP	3	17
dioxygenase	bll2125	NP_768765	cyt		2	12
dehydrogenase	blr5873	NP_772513	PP		2	6
DNA-binding protein HU 1	bll6175	NP_772815	PP	Cello	2	30
putative N-methylhydantoinase B	bll7179	NP_773819	both	Cello	4	11
histone-like protein	blr4404	NP_771044	cyt	Cello, Adaboost, TatP	2	30
2-hydroxyhepta-2,4-diene-1,7-dioate isomerase	blr7891	NP_774531	both	Cello, Adaboost	2	16
methyltransferase	bll4939	NP_771579	cyt	Cello	2	12
NADP-dependent oxidoreductase	blr3973	NP_770613	cyt	cytoplasmic membrane	2	9
nodulate formation efficiency C protein	bll2067	NP_768707	both	Cello, LipoP	3	18
oxidoreductase	blr2609	NP_769249	cyt		2	16
oxidoreductase	blr2928	NP_769568	cyt	Cello, Adaboost, LipoP	2	13
peptidyl-dipeptidase (dcp)	bll7756	NP_774396	both		3	10
PmbA/TldD related protein	bll7519	NP_774159	both		2	12
putative acetyltransferase	bll0009	NP_766649	cyt	Cello	2	12
putative decarboxylase	blr6729	NP_773369	cyt		2	10

putative GMC-oxidoreductase	bll5055	NP_771695	cyt		2	9
putative haloacid dehalogenase	blr4364	NP_771004	cyt	LipoP	2	12
putative pilus assembly protein	blr3492	NP_770132	PP	Cello, LipoP	2	16
putative hydrolase serine protease transmembrane protein	bll6508	NP_773148	cyt	Cello, LipoP	2	6.4
putative monooxygenase	blr7602	NP_774242	PP	Cello	2	7
putative oligosaccharide deacetylase	bll4148	NP_770788	cyt	Cello, Adaboost, TatP, LipoP	2	9
putative oxidoreductase protein	blr5618	NP_772258	PP	Cello, Adaboost, LipoP	2	13
putative oxidoreductase	bll5442	NP_772082	cyt	Adaboost	2	10
putative 3-oxoacyl-[acyl-carrier-protein] reductase	blr7888	NP_774528	cyt		3	14
putative peptidase	blr1971	NP_768611	cyt	Cello, LipoP	2	7
serine protease DO-like precursor	blr3130	NP_769770	both	Cello, Adaboost, LipoP, cPSORTdb	3	13
Superoxide dismutase	bll7774	NP_774414	both	Cello	14	23
TldD protein	bll1168	NP_767808	cyt	Cello	2	9
zinc protease	bll1795	NP_768435	cyt	cPSORTdb	2	11
zinc protease	blr7484	NP_774124	cyt	Cello, TatP, LipoP, cPSORTdb,	2	9
zinc protease	blr7485	NP_774125	both	Cello	9	31

Table 16. Plant Proteins

Protein Identified	Acc. #	Localization	# of hits	% coverage
histone H2B, putative [Arabidopsis thaliana]	gi|15231854|ref|NP_190933.1|	PP	2	18
P49 [Indian peanut clump virus D]	gi|27462596|gb|AAO15494.1| AF447396_3	PP	2	9.3
histone H2A, putative [Arabidopsis thaliana]	gi|15241857|ref|NP_195876.1|	PP	2	22
60 kDa chaperonin (Protein Cpn60) (groEL protein)	gi|6225132|sp|O66212|CH60_KLEPL	both	2	5.9
histone H2A, putative [Arabidopsis thaliana]	gi|15237024|ref|NP_194453.1|	PP	2	25
Chain A, Complex Of The Second Kunitz Domain Of Tissue Factor Pathway Inhibitor With Porcine Trypsin	gi|2914482|pdb|1TFX|A	PP	2	13
glycine-rich protein GRP17 [Arabidopsis thaliana]	gi|15081223|gb|AAK83835.1|	PP	2	12
histone H2B, putative [Arabidopsis thaliana]	gi|15237148|ref|NP_197679.1|	PP	2	21
Seed lipoxygenase, gi|18746|emb|CAA39604.1| lipoxygenase [Glycine max]	gi|126411|sp|P24095|LOXX_SOYBN	PP	3	5.1
Uricase-2 isozyme 1 (Uricase II isozyme 1) (Urate oxidase) (Nodulin 35) (N-35) (Nodule-specific uricase)	gi|549169|sp|P04670|URIC1_SOYBN	PP	2	18
pentatricopeptide (PPR) repeat-containing protein [Arabidopsis thaliana]	gi|15217470|ref|NP_177298.1|	PP	2	7.2
histone H2A, putative [Arabidopsis thaliana]	gi|15221875|ref|NP_175868.1|	PP	2	23
ATP synthase subunit alpha, mitochondrial, gi|22739|emb|CAA78407.1| atpA [Glycine max]	gi|231585|sp|Q01915|ATPAM_SOYBN	PP	2	8.9
protein transport protein Sec24, putative [Arabidopsis thaliana]	gi|30680129|ref|NP_187366.2|	PP	2	3.6
ATGSL12 (GLUCAN SYNTHASE-LIKE 12); 1,3-beta-glucan synthase/ transferase, transferring glycosyl groups [Arabidopsis thaliana]	gi|30684210|ref|NP_196804.2|	cyt	2	2.4
unknown protein [Arabidopsis thaliana]	gi|15229172|ref|NP_190528.1|	PP	2	8
ATMRP7 (Arabidopsis thaliana multidrug resistance-associated protein 7)	gi|30682486|ref|NP_187917.3|	PP	2	2
FAT domain-containing protein /	gi|22329206|ref|NP_680770.1|	PP	2	2

phosphatidylinositol 3- and 4-kinase family protein [Arabidopsis thaliana]				
protein kinase family protein [Arabidopsis thaliana]	gi|15242791|ref|NP_200569.1|	PP	3	6
protein kinase family protein [Arabidopsis thaliana]	gi|42569078|ref|NP_179266.2|	cyt	2	5
unknown protein [Arabidopsis thaliana]	gi|26451927|dbj|BAC43056.1|	cyt	2	8
band 7 family protein [Arabidopsis thaliana]	gi|15241939|ref|NP_201080.1|	PP	2	9.8
kinesin like protein [Arabidopsis thaliana]	gi|2244790|emb|CAB10212.1|	cyt	2	4
copia-like retrotransposable element [Arabidopsis thaliana]	gi|9294121|dbj|BAB01972.1|	cyt	2	2.9
Preprotein translocase subunit secA, chloroplast precursor	gi|17369638|sp|Q9SYI0|SECA_ARATH	PP	2	5
Ferredoxin-dependent glutamate synthase 2, chloroplast precursor (Fd-GOGAT 2)	gi|12643859|sp|Q9T0P4|GLTB2_ARATH	PP	2	3
RPP13 (RECOGNITION OF PERONOSPORA PARASITICA 13); ATP binding [Arabidopsis thaliana]	gi|15231449|ref|NP_190237.1|	cyt	2	5
arginosuccinate synthase family [Arabidopsis thaliana]	gi|22328910|ref|NP_194214.2|	PP	2	9.3
hypothetical protein [Arabidopsis thaliana]	gi|5262196|emb|CAB45793.1|	PP	2	29
chaperonin, putative [Arabidopsis thaliana]	gi|30685604|ref|NP_850203.1|	PP	2	6
probable aminopeptidase F24D7.4 [imported] - Arabidopsis thaliana	gi|25289686|pir||G96662	PP	2	5
Unknown protein [Arabidopsis thaliana]	gi|17065080|gb|AAL32694.1|	PP	2	6
EFR (EF-TU RECEPTOR); ATP binding / kinase/ protein serine/threonine kinase [Arabidopsis thaliana]	gi|15241369|ref|NP_197548.1|	PP	2	5.2
RPM1 (RESISTANCE TO P. SYRINGAE PV MACULICOLA 1) [Arabidopsis thaliana]	gi|15231371|ref|NP_187360.1|	PP	2	5.6
retrovirus-related like polyprotein [Arabidopsis thaliana]	gi|2244802|emb|CAB10225.1|	PP	2	3
Ulp1 protease family protein [Arabidopsis thaliana]	gi|15233485|ref|NP_192348.1|	PP	2	3
integral membrane protein, putative [Arabidopsis	gi|22331867|ref|NP_191491.2|	PP	2	13

thaliana]				
terpene synthase [Arabidopsis thaliana]	gi|29468412|gb|AAO85540.1|	PP	2	6
unnamed protein product [Arabidopsis thaliana]	gi|10178025|dbj|BAB11477.1|	PP	2	6
ATPU1 (PULLULANASE 1); alpha-amylase/ limit dextrinase [Arabidopsis thaliana]	gi|30680478|ref|NP_196056.2|	PP	2	4
unnamed protein product [Arabidopsis thaliana]	gi|9293869|dbj|BAB01772.1|	PP	2	8
chromomethylase 2 (CMT2) [Arabidopsis thaliana]	gi|42566945|ref|NP_193637.2|	PP	2	3
disease resistance protein (TIR-NBS-LRR class), putative [Arabidopsis thaliana]	gi|42563187|ref|NP_177429.2|	PP	2	5
S-locus protein kinase, putative [Arabidopsis thaliana]	gi|18407211|ref|NP_564777.1|	PP	2	6
XTR6 (XYLOGLUCAN ENDOTRANSGLYCOSYLASE 6); hydrolase, acting on glycosyl bonds [Arabidopsis thaliana]	gi|15235997|ref|NP_194311.1|	PP	2	17
TTL1 (TETRATRICOPETIDE-REPEAT THIOREDOXIN-LIKE 1); binding [Arabidopsis thaliana]	gi|15219271|ref|NP_175737.1|	cyt	2	8
seed maturation family protein [Arabidopsis thaliana]	gi|15238703|ref|NP_200139.1|	PP	2	36
SDD1 (STOMATAL DENSITY AND DISTRIBUTION); subtilase [Arabidopsis thaliana]	gi|18379242|ref|NP_563701.1|	PP	2	6
kinesin-like protein [Arabidopsis thaliana]	gi|9294524|dbj|BAB02786.1|	PP	2	4
eukaryotic translation initiation factor 2 subunit 3, putative / eIF2S3, putative / eIF-2-gamma, putative [Arabidopsis thaliana]	gi|15224215|ref|NP_179462.1|	PP	2	6
putative Athila-like protein [Arabidopsis thaliana]	gi|4309705|gb|AAD15489.1|	PP	2	14
resistance protein PLTR [Arachis hypogaea]	gi|62361110|gb|AAX81234.1|	PP	2	21
Unknown protein [Arabidopsis thaliana]	gi|5903077|gb|AAD55635.1|AC008017_8	PP	2	10

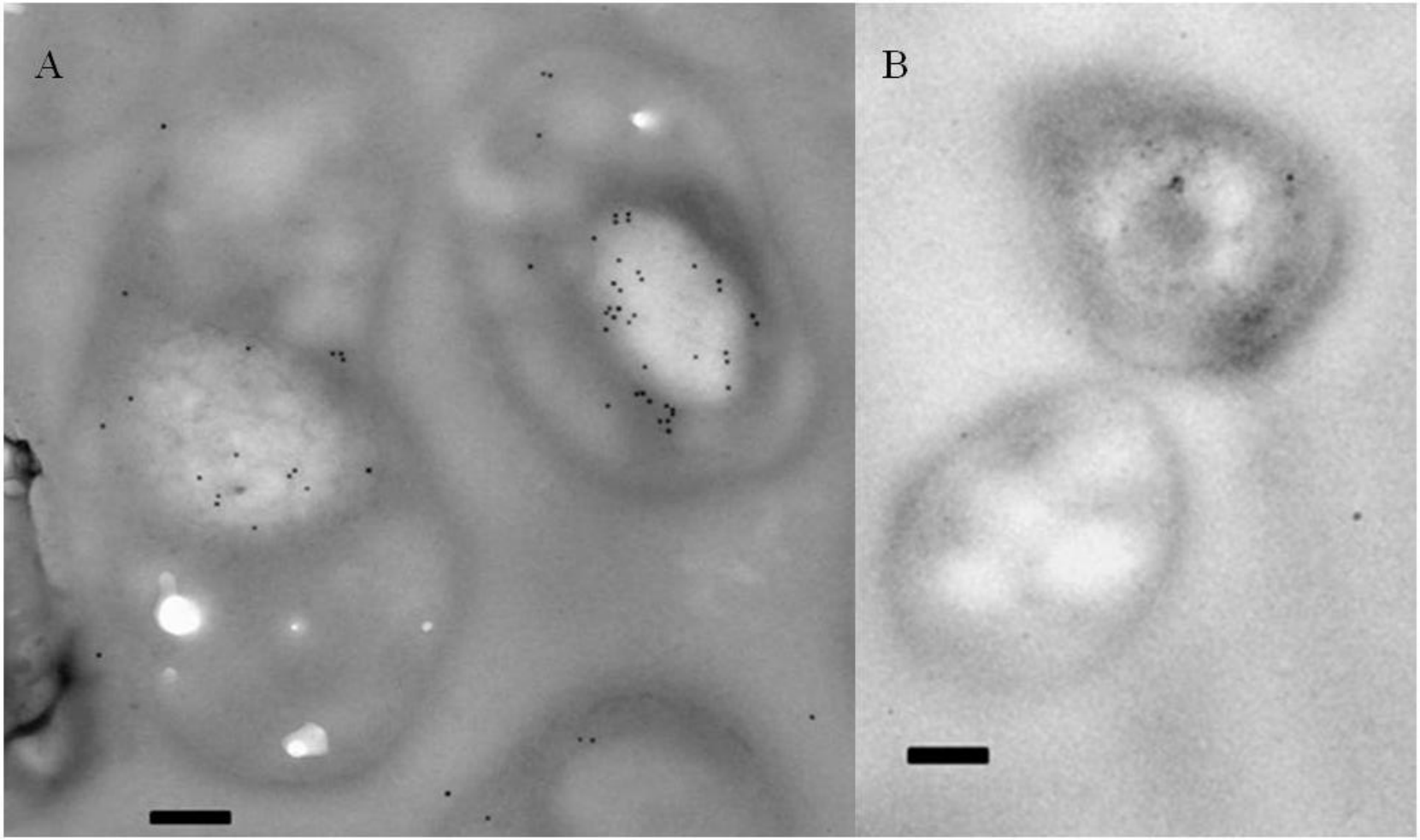

Figure 6. Transmission electron micrographs of histone H2A immunogold labeled (A) and control (B) 56 day old soybean nodule sections showing labeling restricted to the bacteroids. Scale bar = 0.2 µM.

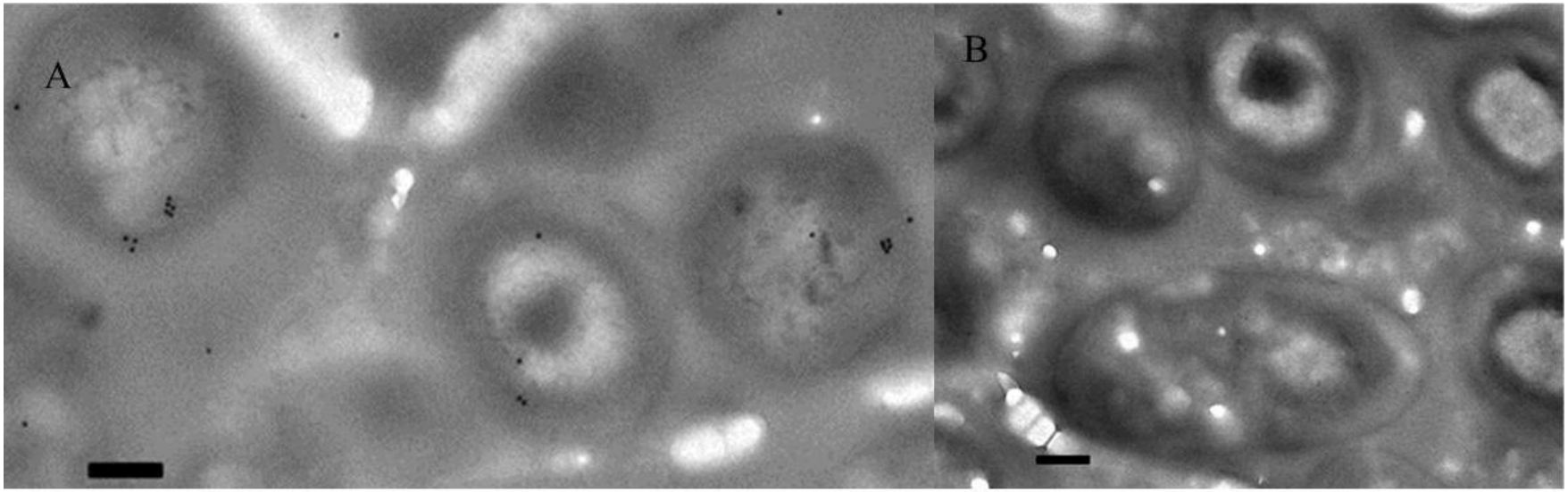

Figure 7. Transmission electron micrographs of lipoxygenase immunogold labeled (A) and control (B) 56 day old soybean nodule sections showing labeling restricted to the bacteroids. Scale bar = 0.2 μM.

Table 17. N-terminal sequence alignments of proteins found in the *B. japonicum* bacteroid periplasm. The first seven proteins were identified and full-length sequences found in protein databases. These sequences were analyzed by PSORT and the predicted leader sequence removed. The resulting sequences displaying the S/T X_6S/T are presented. Portions of each of these sequences were found during proteomic analyses. Complete sequences of those shown were not found due to the presence of internal arginine and lysine which permit cleavage by trypsin. The sequences for the last twelve proteins were those found via proteomic analysis. Homology to other plant proteins predicted these sequences to be near the N-terminal portion of each protein.

Protein	**Proximal N-terminal Sequence**
Histone H2B	KKISKEGG**S**EKKKKR**T**KKSVET
Lipoxygenase [CAA39604]	IDTAT**S**FLGRNI**S**MQLI**S**ATQTDG**S**GNGK
Thioredoxin [AAS88427]	AT**S**SPE**S**SA**S**RVQ**S**FH**S**SAR
ATP synthase subunit α [Q2PMS8]	MV**T**IRADEI**S**KIIRER
Stomatal density protein	WD**S**DPSGTK**T**CIDTK
Putative Fd-dep. glutamine synthase	GASS**S**VSRLLS**S**AK
Putative Chaperonin CPN60-like	CT**S**QIGSRLN**S**TR
Putative Arginiosuccinate synthase	AT**S**FPSSS**SS**ALVIRS**S**HNGSLK
Putative Xyloglucan endotransglycosylase	ISYS**T**DVVALLA**S**FMICSV**S**ANFQR
Putative Protein kinase	SG**S**VNS**S**VT**S**LVS**S**LNDEPHR
Putative acetylornithine transaminase	ASLSQI**T**LPHAPS**S**EIGLLR
Putative kinesin-like protein	APTP**S**S**S**HSNQ**T**Q**T**LIR
Putative ET-TU Receptor	LSF**S**LVHNAL**T**LLLQVCIFAQAR
Putative Glutathione S-transp. ATPase	LLE**S**NYFHMF**S**IFFNLLLLLVMFR
Putative protein	EAITA**T**LTATLT**T**NMAK
Putative protein	A**S**TGHFS**SS**LCDLGS**S**INLMPK
Unknown protein	PPH**S**AHPISV**T**HNDNLL**S**PIR
Unknown protein	LIS**S**DNDTEW**S**PVLAPLIR
Unknown protein	VET**S**IDMEEG**T**LEIGME**T**R
Unknown protein	LIS**S**DNDTEW**S**PVLAPDLIR

Chapter III
Characterization of the Post-Symbiotic Form of *Bradyrhizobium japonicum*

Abstract

The form and physiology of *Bradyrhizobium japonicum* after the decline of symbiotic nitrogen fixation has been characterized. Proteomic analyses showed that the post-symbiotic *B. japonicum* undergoes metabolic remodeling, as well defined groups of proteins declined, increased, or remained unchanged from 56 to 119 days after planting. Enzymatic analysis also showed distinct patterns in both the cytoplasm and the periplasm. Similar to the bacteroid, the post-symbiotic bacteria rely on a non-citric acid cycle supply of succinate and although viable, they did not demonstrate the ability to grow.

Introduction

In 1879, the German mycologist Heinrich Anton de Bary, defined symbiosis as "the living together of unlike organisms" (Douglas, 1994; Douglas, 2010). Nitrogen-fixing symbioses between rhizobia and legumes have been studied since 1888 (Hellriegel and Wilfarth, 1888) with the vast number of investigations describing the infection events and the mature nitrogen-fixing nodule. During nodule formation the rhizobia transform into a non-growing form, called the bacteroid, capable of reducing atmospheric dinitrogen. The plant receives reduced nitrogen compounds in exchange for photosynthetically-derived substrates. In determinant nodules, such as those formed between *B. japonicum* and soybean, the nitrogen fixation activity of the nodule increases in parallel with nodule development and then declines as the plant portion of the nodule senesces. Bacteroids obtained from senescing, determinant nodules are able to de-differentiate into free living bacteria and thus remain viable (Cermola et al., 2000; Groten

et al., 2006; Muller et al., 2001; Puppo et al., 2005; Vasse et al., 1990). Thus, the bacteroids within the decaying nodule would also have the potential to differentiate to necrotrophs to take advantage of the abundant supply of metabolites from the decaying plant nodule. According to the original definition by Heinrich Anton de Bary, the senescing nodule is no longer a symbiosis since the unlike organisms are no longer living together, but rather one is surviving on the remains of the other. This post-symbiotic lifestyle of bradyrhizobia has received scant attention, but has significant ecological relevance as it may be the primary mechanism by which the bacteria are perpetuated in the rhizosphere. The rhizosphere supports a far greater number of bacteria than the bulk soil (Hiltner, 1904) because up to 20% of the entire carbon fixed photosynthetically by the plant may be excreted from the roots (Marschner, 1995). Unlike the symbiotic state in which the symbiotic bacteroids are provided a defined diet of substrates dictated by the plant, the post-symbiotic bacteria are presented with a diverse mileux of metabolites derived from the entire cellular content of plant nodule cells. In contrast to the rhizosphere where bacteria must compete for excreted materials, the bradyrhiobia are imbedded within a rich metabolic matrix for which they do not need to compete. Elucidating the genes and molecular events for survival and perpetuation of applied strains beyond symbiosis in the soil would be of agricultural and financial benefit to farmers in third world countries who lack the resources for annual fertilizer applications.

Proteomic and transcriptomic analysis of *B. japonicum* bacteroids has been undertaken to better understand the symbiosis between *B. japonicum* and its obligate legume soybean (*Glycine max*) host to improve crop production (Delmotte et al., 2010; Sarma and Emerich, 2005). However, the majority of this work has only focused on the

early stages of infection to the peak of symbiotic nitrogen fixation. Though much is known about the process of nodule senescence in regards to the plant, little is known about the determinate bacteroid and its process of post-symbiotic redifferentiation (Evans et al., 1999; Pladys and Vance, 1993; Puppo et al., 2005; Sarath et al., 1986). Only one published proteomics report has looked at the bacteroid past the peak of nitrogen fixation and utilized soybean root nodules grown under field conditions (Delmotte et al., 2010). This leaves a glaring omission in the critical stage of the natural cycle where the bradyrhizobia return to the soil. This study was undertaken to provide a global proteomic analysis of the post-symbiotic form of *B. japonicum*. Purified bacteroids were fractionated into their periplasmic and cytoplasmic compartments and marker enzymes were followed over a period of 10 weeks. The fractionated proteins were prepared for analysis via LC-MS/MS. Three general patterns were chosen for functional identification: proteins decreasing in abundance, constitutive proteins, and proteins increasing in abundance.

The results of this study should increase the understanding how *B. japonicum* persists after the symbiosis to provide greater insight into how the association could be better exploited to increase crop production.

Materials and Methods

Source of Nodules and Bacteroid Preparations

Soybean plants were obtained from the Bradford Research Farm of the University of Missouri in the summer of 2008 over a ten week period (56-119 days after planting; add dates). *B. japonicum* strains were commercial and the seeds were not inoculated prior to planting. Soybean plants were harvested from the same, un-irrigated field

between 8 and 9 a.m. Intact roots and nodules attached to the tap root were placed in ice water and then harvested at 4°C. Bacteroids were isolated as described previously (Karr et al., 1984) and enzyme activities were performed on the same day. Cytoplasmic and periplasmic fractions were prepared as described in Chapter II.

Enzymatic, Leghemoglobin, and PHB Analysis

To ascertain the level of purity of the bacteroid periplasmic fraction several enzymes known to be cytoplasmic were measured in both fractions as well as cyclic phophodiesterase, a known periplasmic marker, to assay the amount of the periplasmic release as previously outlined for rhizobia and bradyrhizobia bacteroids (Streeter and Rudulier, 1990). Also, measured for activity was the possible periplasmic enzyme protocatechuate 3,4-dioxygnease. Procedures for measurement of enzymes can be found in Chapter II. Leghemoglobin concentration was measured using Drabkin's reagent (Drabkin and Austin, 1935). PHB was measured as described by Karr et al. (1983).

Protein Isolation and Identification

The periplasmic and cytoplasmic fractions were each precipitated using equal volumes of phenol. The fractions were mixed at room temperature for one hour. Phases were then separated by centrifugation at 4,000xg for 10 minutes at 4°C. The phenol phase was collected and four volumes of 100% methanol containing 0.1M ammonium acetate and 10 mM dithiothreitol added. Protein was precipitated overnight at -20°C. Protein precipitate was collected by centrifugation at 4000xg from 10 min at 4°C. The protein pellet was washed once with the methanol/ammonium acetate/DTT solution. The

protein pellet was then washed three times with 90% ethanol containing 10mM DTT and then stored in 90% (v/v) ethanol/DTT at -80^{o}C.

Precipitated protein in 90% (v/v) ethanol/DTT was collected by centrifugation at 4000xg and 4^{o}C. The pellet was dissolved in reconstitution buffer (30 mM Tris-HCl, 7 M urea, 2 M thiourea, at pH 8.8) by gentle vortexing for one hour. Samples were quantified using the Bradford method. A 20 μg portion of protein from each sample was removed and diluted to 1 ug/uL with reconstitution buffer. As an internal standard, 200 ng of BSA was added to give a protein percent of 1% (w/w) BSA protein.

Disulfide bonds were reduced with 10 mM DTT (100 mM stock in 50 mM AmBic), at 25^{o}C for 1 hour. Reduced cysteines were alkylated with 40 mM iodoacetamide (200 mM stock in 50 mM AmBic), at 25^{o}C in the dark for 1 hour. Iodoacetamide was quenched by adding additional DTT to 30 mM (100 mM stock in 50 mM AmBic) and incubating at 25^{o}C for 30 minutes. Urea was brought to 1 M by dilution with 50 mM AmBic. Trypsin (Sequencing Grade Modified-Promega, Madison, WI) was reconstituted to 0.02 ug/uL and activated in the provided re-suspension buffer per manufacturer's instructions, then added to samples at a ratio of 1:200 (w/w) (trypsin:sample). Samples were incubated at 37^{o}C for 16 hours. Digests were then lyophilized to dryness.

Mass Spectrometry Analysis

Lyophilized protein samples were reconstituted in 100 uL of 18 MΩ water with 0.1% (v/v) formic acid and 5.0% (v/v) acetonitrile by pipetting and mild vortexing. Samples were spun at 13,000 rpm at 4^{o}C for 10 minutes in a tabletop centrifuge to

remove insoluble debris. Twenty uL portions from each sample were aliquoted into a polypropylene 96 v-well plate, covered with adhesive film, briefly centrifuged to collect samples at the bottom of the well, and placed in the cooled tray of the LC auto-sampler. For analysis, 10 uL injections were run on a LTQ ProteomeX linear ion trap LC-MS/MS instrument (Thermo Fisher, San Jose, CA). Peptides were concentrated and desalted on in-line C_8 captraps (Michrom Bioresources, Auburn, CA) prior to final separation by C_{18} column using an acetonitrile gradient of 0-90% solvent B (100% acetonitrile with 0.1% (v/v) formic acid), in solvent A (deionized 18 MΩ water with 0.1% (v/v) formic acid for a duration of 110 minutes. The peptide trap and C_{18} column were then re-equilibrated for 25 minutes with 100% solvent A before applying the next sample.

LC separation was performed using fused silica nanospray needles, 26 cm length, (360 μm outer diameter, 150 μm inner diameter; Polymicro Technologies, Phoenix, AZ), that were packed with "Magic C18" (200Å, 5 μm particles, Michrom Bioresources) in 100% methanol. Before sample acquisition, columns were equilibrated for 3-4 hours at 200 nL/min (at the column tip) with a 60:40 mix of solvent B to solvent A. Samples were analyzed in the data-dependent positive acquisition mode on the LC-MS/MS instrument, using normal scan rate for precursor ion analysis, and dynamic exclusion enabled (1 repeat count, 30 s repeat duration, list size of 50, and 30 s exclusion). Following each full scan (400-2000 *m/z*), a data-dependent triggered MS/MS scan for the three most intense parent ions were acquired. The nanospray column was held at ion sprays of 2.0 kV.

Database Searching

Tandem mass spectra were extracted by BioWorks version 3.3 (Figure 8). All MS/MS samples were analyzed using SEQUEST (ThermoFinnigan, San Jose, CA; version 2.7). SEQUEST was set up to search a FASTA file containing translated coding regions for both *B. japonicum* and *G. max* with a concatenated random database (Kaneko et al., 2002a; Schmutz et al., 2010). These protein sequence files, named "brady.p.aa.gz" "Gmax_109_peptide.fa.gz" were provided at the websites (ftp://ftp.kazusa.or.jp/pub/RhizoBase/Bradyrhizobium/) and (ftp://ftp.jgi-psf.org/pub/JGI_data/phytozome/v7.0/Gmax/annotation/) repectively. The random concatenated database was generated using the tool "DecoyDBCreateor" found at (http://p3db.org/tools/DecoyDBCreator/). SEQUEST was searched with fragment ion mass tolerance of 1.0 Da and a parent ion tolerance of 2.0 Da. Iodoacetamide derivative of cysteine (+57.0) was specified in SEQUEST as a fixed modification, and oxidation of methionines (+15.9) was specified as a variable modification. RAW files were searched using Bioworks "SEQUEST batch-search" with 10 matches reported without redundancy reporting. SEQUEST results were saved as .srf files.

Peptide Match Filtering

In order to filter the SEQUEST matches for non-random hits, first the files were converted to .SQT file formats using John Prince's Srf2sqt converter (Prince and Marcotte, 2008). Filtering of the SEQUEST matches (in SQT file format) by %FDR (% false discovery rate) was performed using SEPro (Paolo C. Carvalho, unpublished) with

the following settings: Spectral FDR: 5%, Peptide FDR: 3% and final filtering of protein hits at: 1%. All filtered data was saved as SEPro file outputs (.sepr).

Protein Expression Trends

Spectral count data associated with the filtered protein IDs provided by SEPro were used for trend analysis via the proteomic analysis software PatternLab (Carvalho et al., 2008). As per the software workflows, PatternLab input files were created using the Regrouper software (SparseMatrix and index files). Folders for each time point in the timecourse were created, and the selected SEPro files for each timepoint were placed into the folders. Regrouper was pointed to these folders, and the SparseMatrix and index files were created. These files were provided to PatternLab in the TrendQuest module. Trends were created using the parameters:

Periplasmic and cytosolic proteins were assigned a minimum average signal of two, with minimum data points of two, minimum items per cluster of three, and a health of 0.800. Protein information associated with each trend cluster (protein name, accession number) was exported as a text file. This protein information was used to obtain the original peptide sequences from the SePro files. In order to verify possible redundancy associated with each protein match by SEQUEST (no redundant matches reported, see above) text mining software (in-house) was used to check for other protein entries containing identical peptide sequences. Only proteins with non-redundant peptide matches were reported

Results

Nodule Mass and Leghemoglobin Content

Soybean root nodules were measured for mass per nodule and leghemoglobin content over the 10 week (56-119 days after planting; add dates) post-symbiotic period (Figure 9). Nodule mass fluctuated , but the leghemoglobin content was consistently between 8-9 mg of leghemoglobin per g fresh weight of nodules until day 112 when leghemoglobin concentration started to decline with a final concentration of 3 mg per g nodule by day 119 (Figure 10). To place these results in context of the nitrogen fixing portion of the association, the maximal acetylene reduction activity was observed on day 43 and by day 55 had declined to 25% and by day 95 had become negligible (Strodtman et al., 2011).

Bacteroid Protein and PHB Content and Enzymes Activities in the Post-Symbiotic Period

Total bacteroid protein fluctuated with a pattern similar to but not identical with that of nodule mass (Figure 11). The PHB content remained relatively unchanged until day 104-112 when it increased nearly 3 fold (Figure 12).

Isolated bacteroids were fractionated into periplasmic and cytoplasmic fractions. The periplasm is at the interface between the bacteria and the plant and thus would be assumed to respond to changes caused by the post-symbiotic environment.

The periplasmic marker enzyme cyclic phosphodiesterase was found in both periplasmic and cytoplasmic fractions but displayed different patterns (Figure 13). The cytoplasmic activity displayed a bi-modal pattern while the periplasmic activity increased

from day 55 to 91 and then remained constant (Figure 13**).** β-hydroxybutyrate dehydrogenase, a cytoplasmic enzyme marker necessary for the production of polyhydroxybutyrate in the bacteroid, displayed patterns similar to those of cyclic phosphodiesterase with the cytoplasmic activity remaining relatively constant and the periplasmic activity increasing to 91 days and remaining relatively constant until it declined at 112 and 119 days (Figure 14). Isocitrate dehydrogenase, another cytosoplasmic marker enzyme, has been previously shown to decline over the first five weeks of symbiosis (Karr et al., 1984; Shah and Emerich, 2006) and Figure 15 shows it continues to decline and became undetectable at 112 and 119 days. Cytoplasmic malate dehydrogenase activity showed a bi-modal trend similar to cyclic phosphodiesterase activity and the periplasmic malate dehydrogenase activity showed a gradual increase through 78 days and then a more pronounced increase to 91 days and a decrease at 112 and 119 days (Figure 16). Protocatechuate 3,4-dioxygenase activity in both fractions showed a bi-modal activity profile (Figure 17).

Proteomics Time Course

LC-MS/MS analysis was performed on the proteins of the cytosolic and periplasmic fractions of bacteroids isolated from soybean plants over the ten week time course. Periplasmic protein samples covered the entirety of the time course while cytoplasmic analysis covered the seven time points of days 63, 70, 91-119. (Tables 18-20) There were 4718 peptides identified in both fractions and 1869 unique cytoplasmic peptides and 2849 unique periplasmic peptides via SePro. Trend Quest from Pattern Lab for Proteomics identified three unambiguous progressions of peptide frequencies:

proteins that declined following symbiosis, proteins that increased following symbiosis, and constitutive proteins. The other patterns reported displayed significant fluctuations at various sampling times that are difficult to interpret and determine their physiological role in context of the post-symbiotic period. These proteins may be more responsive to climatic or soil conditions than those of the three unambiguous patterns.

Proteins that Declined Following Symbiosis

The rate of protein synthesis and protein turnover have been shown to decline during nodule development due to the diversion of cellular energy to nitrogen fixation (Karr and Emerich, 1996), and as expected in the post-symbiotic period, proteins directly associated with nitrogen fixation nifD, nifK, and fixC (blr1743, blr1744, blr1774) were found to decrease over the ten week time course (Table 18). All three proteins are regulated by RegR under microoxic conditions (Lindemann et al., 2007; Sciotti et al., 2003). The ability to assimilate fixed nitrogen into transferable amino acids was also seen to decrease over time as aminotransferase proteins (blr1686, blr4134), glutamate synthase (blr7743), and glutamine synthethase I (blr4949). *B. japonicum* has been shown through C^{14} glutamate labeling experiments to have aspartate aminotransferase activity in the periplasmic fraction and that up 30% of the label is converted to alpha-ketoglutarate after 30 minutes (Streeter and Salminen, 1990).

Branched chain amino acid production via *leuB* and *leuC* (bll0504, blr0488) appears to decrease as well over the time course. Succinate semi-aldehyde dehydrogenase (blr0807) is necessary for the breakdown of glutmate and phenylalanine to succinate (Green et al., 2000) also declined.

Glycolysis and gluconeogensis were well represented in the decreasing data set with pyruvate dehydrogenase (bll4782), phosphoenolpyruvate carboxykinase (bll8141;pckA), fructose bisphosphate aldolase (bll1520), and enolase (bll4794). TCA cycle enzymes succinyl-CoA synthetase (bll0455), malate dehydrodgenase (bll0456), and succinate dehydrogenase (blr0514) were found to decrease over time as well indicating the decreases in cellular energy needs for nitrogen fixation and the need for carbon backbones for the production of amino acids. Pyruvate dehydrogenase (bll4782) provides a link between glycolysis and the TCA cycle to branched chain amino acid biosynthesis.

A large number of proteins associated with the ribosome were found to decline. The symbiotic specific GroEL/S3 (blr2059, blr2060) is notable as it serves as a marker of the decline of the symbiotic state of the bacteroid as GroEL/S3 are induced during the symbiotic state and are *nif*A regulated (Fischer et al., 1993; Hauser et al., 2007) and GroEL1 (blr5626) has a sigma 32-dependent promoter (Babst et al., 1996; Narberhaus et al., 1996). The decline of several proteases, LA protease (bll4942), serine transmembrane protease (bll6508), and a zinc protease (blr7485), may suggest a physiological adaptation following symbiosis.

Proteins that Increased Following Symbiosis

The number of proteins found to be increasing over the time course was much lower (16 vs. 71) than what was found for the proteins in decline. Of the proteins associated with this pattern, half were unknown or hypothetical proteins. Annotated proteins in this pattern include fatty acid metabolism proteins (enoyl-CoA hydratase

(blr1160), acetyl-CoA carboxylase (blr0191), acyl-CoA thiolase (blr1159), and enoyl-CoA hydratase (bll7821)), CheY (bll7795) a two-component transcriptional regulator which was found to be expressed during times of desiccation stress (Cytryn et al., 2007), the carboxy terminal protease (blr0434), and the peptidyl cis-trans isomerase (bll4690), which is required for proper protein folding. Among the proteins without annotation, bll2012 and blr1830 were found to be induced by soybean seed extracts (Wei et al., 2008).

Constitutive Proteins

The proteins in this group include a set involved in nitrogen metabolism: an ABC transporter substrate binding protein for oligopeptides (bll2909, bll5596, bll7921), a peptidyl-dipeptidase (bll7756), a glycine hydroxymethyltransferase (bll5033), a probable amino acid binding protein (bll2909), a glu/leu/phe/val dehydrogenase (blr2146), which causes the reversible oxidative deamination of the substrate to its coordinated α-keto acid, an ATP dependent protease ClpB (blr1404), and N- utilization substance protein (bll0785). A glycine hydroxymethyltransferase, involving C1 metabolism can be coupled to the degradation of vanillate which would be further metabolized via the β-ketoadipate pathway with final cleavage to acetyl-CoA and succinyl-CoA via β-ketoadipyl CoA thiolase (blr0925) (Sudtachat et al., 2009) which is known the be constitutively expressed in *B. japonicum* (Parke and Ornston, 1986). In addition to β-ketoadipyl CoA thiolase, the proteins involved in carbon metabolism include the pentose phosphate enzymes transketolase (bll1524) and transaldolase (blr6758), which provides a range of metabolites and a mechanism for redox cofactor balancing (Falcone and Tabita, 1991;

Gourion et al., 2011; Hillmer and Gest, 1977; McKinlay and Harwood, 2010; Richardson et al., 1988) , methymalonate-semialdehyde dehydrogenase (blr3954), which participates in active turnover of branched chain amino acids and propanoate metabolism leading to a source of acetyl-CoA and propanoyl-CoA, a putative alcohol dehydrogenase precursor (bll6220) and carbonic anhydrase (bll2065).

Proteins involved in reactive oxygen metabolism were found: superoxide dismutase (bll7774) and alkyl hydroperoxide reductase (bll1777).

Several soybean proteins, histone H4, histone H3, glu/leu/phe/val dehydrogenase (Glyma02g38920.1, Glyma06g32880.1, Glyma16g04560.1) are found throughout the period of study.

Discussion

Bacteroid is the term that refers to the symbiotic, nitrogen-fixing form of rhizobia. The data collected over the period of time from 56 to 119 days after planting clearly demonstrate metabolic activity of the bacteria that reside within the decaying plant nodule. The bacteria although possessing enzyme activity do not possess nitrogenase activity, the central metabolic activity of the symbiosis and furthermore, the symbiosis no longer occurs as per the definition of Heinrich Anton de Bary, who defined symbiosis as "the living together of unlike organisms." Thus, the post-symbiotic form should not be called ‘bacteroid’ as they no longer possess two of the key features of the symbiosis, nitrogenase and a living host partner. However, like bacteroids, the post-symbiotic form(s) of the bacteroid do not display any of the proteins or processes consistent with

cellular growth and division, but they can be extracted from senescing nodules and grown on artificial medium.

Studies during the developmental time course of *B. japonicum* bacteroids through symbiosis have followed several enzymes during the symbiosis including nitrogenase, TCA cycle enzymes, and the carbon storage compound poly-β-hydroxybutyrate (Karr et al., 1984; Wong and Evans, 1971). These enzymes constitute the fixing of atmospheric dinitrogen, the energy metabolism for nitrogen fixation, and the storage of carbon metabolites in the determinate nodule system. Other studies have looked at the effects of mutations in hydrogenase systems on nitrogen fixation, leghemoglobin content, and nodule physiology out to 71 days after emergence (Rodrigues et al., 1998). Beyond these studies there is no knowledge at present for the changes that the *B. japonicum* bacteroid experiences during its redifferentiation to a bacterium in the post-symbiotic state. The enzymatic and proteomic analysis provide insight into the physiological nature of the post-symbiotic form of *B. japonicum*.

A number enzymatic and transport activities were identified suggesting the post-symbiotic form of *B. japonicum* was accumulating and hydrolyzing peptides from the decaying plant nodule cells. These proteins were grouped with those which showed no change during the post-symbiotic period suggesting these activities may have been induced prior to the sampling period or are processes that occur throughout symbiosis and continue. The senescing nodule would be a metabolite rich environment with active proteases from the plant cells providing amino acids and peptides as metabolites. In contrast, the branched chain amino acid pathways have been shown to be highly regulated in the symbiosis between *Rhizobium leguminosarum* and pea (Prell et al.,

2009), indicating a cycling of amino acids between the host and the bacteroid. The decline of their metabolism further supports their role during symbiosis. Transcriptomic analysis of nodules from *Medicago truncatula* indicated that more than 50% of the nodule-specific genes are secretory proteins or peptides and could thus be targeted to the symbiosome (Maunoury et al., 2010), which could provide a source of metabolites for the post-symbiotic bacteria. The bacteroids of winged bean appear to be protected from degradation via a 21 kDa nodulin that is homologous to a plant Kunitz trypsin inhibitor (Manen et al., 1991). This raises the issue that not only is the senescing nodule a source of nutrients, but also a source of potentially harmful hydrolases. The PQQ-dependent alcohol dehydrogenase (bll6220) further supports a role in bacterial protection as it was previously found to be one of three PQQ-dependent dehydrogenases induced during osmotic stress (Cytryn et al., 2007). The presence of CheY suggests the post-symbiotic bacteria are able to respond to the changing conditions within the senescing nodule. The presence of enzymes in reactive oxygen metabolism suggests the bacteria are attempting to protect against reactive oxygen species generated during plant nodule senescence.

A previous study of 28 day old, green house grown *B. japonicum* bacteroids, at the period of maximal nitrogenase activity, indicated no defined fatty acid metabolism (Sarma and Emerich, 2005). Fatty acid metabolism was markedly increased in the post-symbiotic period (Table 18). Almost 30 times more membrane is generated in the form of symbiosome membrane than the plasma membrane in soybean root nodules during nodule development (Winzer et al., 1999). The turnover of membrane lipids derived from the senescing plant cell (both symbiosome and plasma membrane) could provide a rich source of energy. Repair and maintenance of the symbiosome membrane may serve to

protect the plant nodule cytosol from hydrolytic activities and continue to serve as a selective transporter of nutrients to the post-symbiotic bacteria. Symbiosome membranes appeared to remain intact in nodules up to 105 days (Chapter V).

The proteomic analysis provides a broad perspective of metabolic processes, which require further measurement of specific enzyme activities and metabolic processes. Nitrogenase activity during nodule developmental profile provides the metric for symbiosis by which enzymes of the citric acid cycle and poly-β-hydroxybutyrate accumulation have been compared (Karr et al., 1984; Wong and Evans, 1971). Isocitrate dehydrogenase activity was shown to decline over the first 35 days of symbiosis (Karr et al., 1984) and it was found to continue to decline from 56 to 119 days (Figure 15). Isocitrate and α-ketoglutarate dehydrogenases (Green and Emerich, 1997a; Shah and Emerich, 2006) have been shown not to be necessary for symbiosis, but the dicarboxylates of the citric acid cycle components are required (Dymov et al., 2004; Ronson et al., 1981). Proteomic analyses suggest several pathways for production of succinyl-CoA from β-ketoadipyl thiolase, which would bypass the two decarboxylation steps of the citric acid cycle and provide succinate. Protocatechuate 3,4-dioxygenase funnels several benzoate precursors toward β-ketoadipyl thiolase. Protocatechuate 3,4-dioxygenase encoded by blr2333-2334 was not essential for acetylene reduction activity although a mutation in these genes resulted in a delay in maximal activity (Chapter IV). The isozyme expressed by blr0927-0928 was essential for the development of acetylene reduction activity (Chapter IV). Protocatechuate 3,4-dioxygenase enzyme activity was present from 56 to 119 days, but it is not known which isozyme yielded the measured

activity. β-ketoadipyl CoA thiolase was present in each proteomic sample indicating that the β-ketoadipate pathway is active over the entirety of the post-symbiotic period.

The majority of the activity for protocatechuate 3,4-dioxygenase was found in the periplasmic fraction. It was found only in the periplasmic fraction on day 56. The protocatechuate 3,4-dioxygenase and cyclic phosphodiesterase activities of the periplasm parallel each other as do their activities in the cytoplasm. Protocatechuate 3,4-dioxygenase activity is of great interest in field grown soybeans as the application of glyphosphate causes an accumulation of hydroxybenzoic acids and specifically protocatechuic acid in the bacteorid (Hernandez et al., 1999; Moorman et al., 1992). Enzyme activity requires diatomic oxygen which impacts its role during symbiosis, but would not necessarily be a limitation during the post-symbiotic period.

The presence of malate dehydrogenase could indicate an active malate-aspartate shuttle as shown in pea root nodules (Appels and Haaker, 1991). Soybean bacteroids that have been incubated with malate and/or glutamate export large amounts of aspartate and/or alanine from the bacteroid (Kouchi et al., 1991).

Depending upon the integrity of the symbiosome membrane and symbiosome space the periplasm may have to undertake an additional role in nutrient procurement and protection from the changing environment. Curiously, the protocatechuate 3,4-dioxygenase and malate dehydrogenase activities display inverse patterns between 56 and 119 days in both the periplasmic and cytoplasmic fraction. This could be interpreted to mean that the two metabolic sources of dicarboxylates, represented by protocatechuate dioxygenase and malate dehydrogense, are inversely regulated to maintain a constant source of dicarboxylates. β-ketoadipyl CoA thiolase was constitutively present over the

post-symbiotic period. This result is consistent with that seen in the free living form of *B. japonicum* (Parke and Ornston, 1986).

The β-hydroxybutyrate dehydrogenase activity in the cytoplasm remains relatively constant over the time course while the activity in the periplasm is negligible until 78 days. Levels of poly-β-hydroxybutyrate, the major carbon storage molecule in determinate nodules, but not indeterminate nodules (Kereszt et al., 2011), were stable over the majority of the time course and then surprisingly increased nearly 3 fold between days 104-112 (Figure 12), without a corresponding change in β-hydroxybutyrate dehydrogenase activity (Figure 14).

Combined the activity profiles of the enzymes of the post-symbiotic bacteria each demonstrate unique patterns suggesting the post-symbiotic bacteria are actively and purposely expressing metabolic responses to its changing environments. The presence of heat shock (blr0678), cold shock (bsl1386) and peptidyl prolyl cis-trans isomerase (bll4690) suggest the bacteria have the means for the remodeling of the bacteroid as it transitions to the post-symbiotic bacteria.

Three soybean proteins were found throughout the time course in the periplasm. Histone H2A was immunolocalized to the bacteroid surface (Chapter II) suggesting these proteins perform a role in the physiology of the post-symbiotic bacteria. Regulation of microbial communities has been explored previously with regards to histones excreted by Pacific white shrimp and Atlantic cod and the excretion of histone H4 from pea root tips has been documented (Bergsson et al., 2005a; Patat et al., 2004; Wen et al., 2007).

In summary, the post-symbiotic form of the bacteroid possesses many active metabolic processes, except growth, as it exits symbiosis.

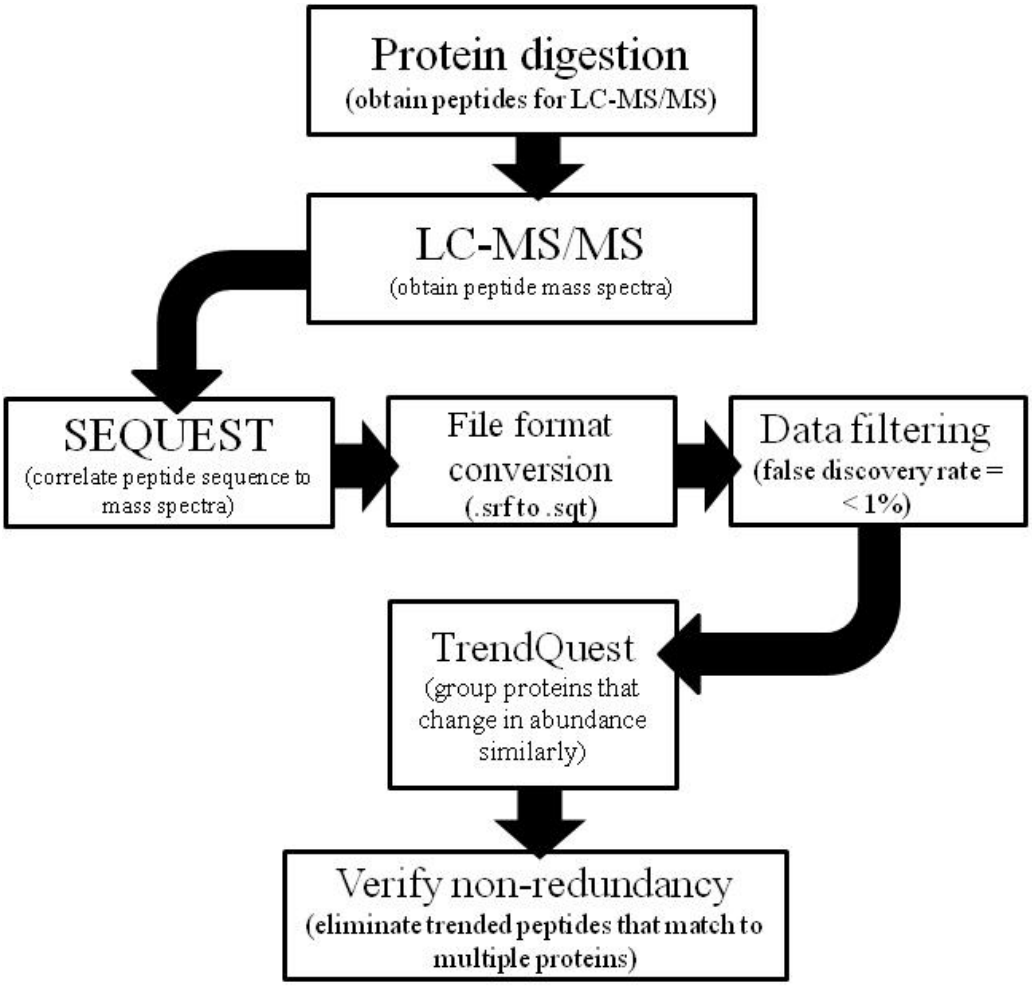

Figure 8. Proteomics workflow for protein identification during *B. japonicum* bacteroid time course study.

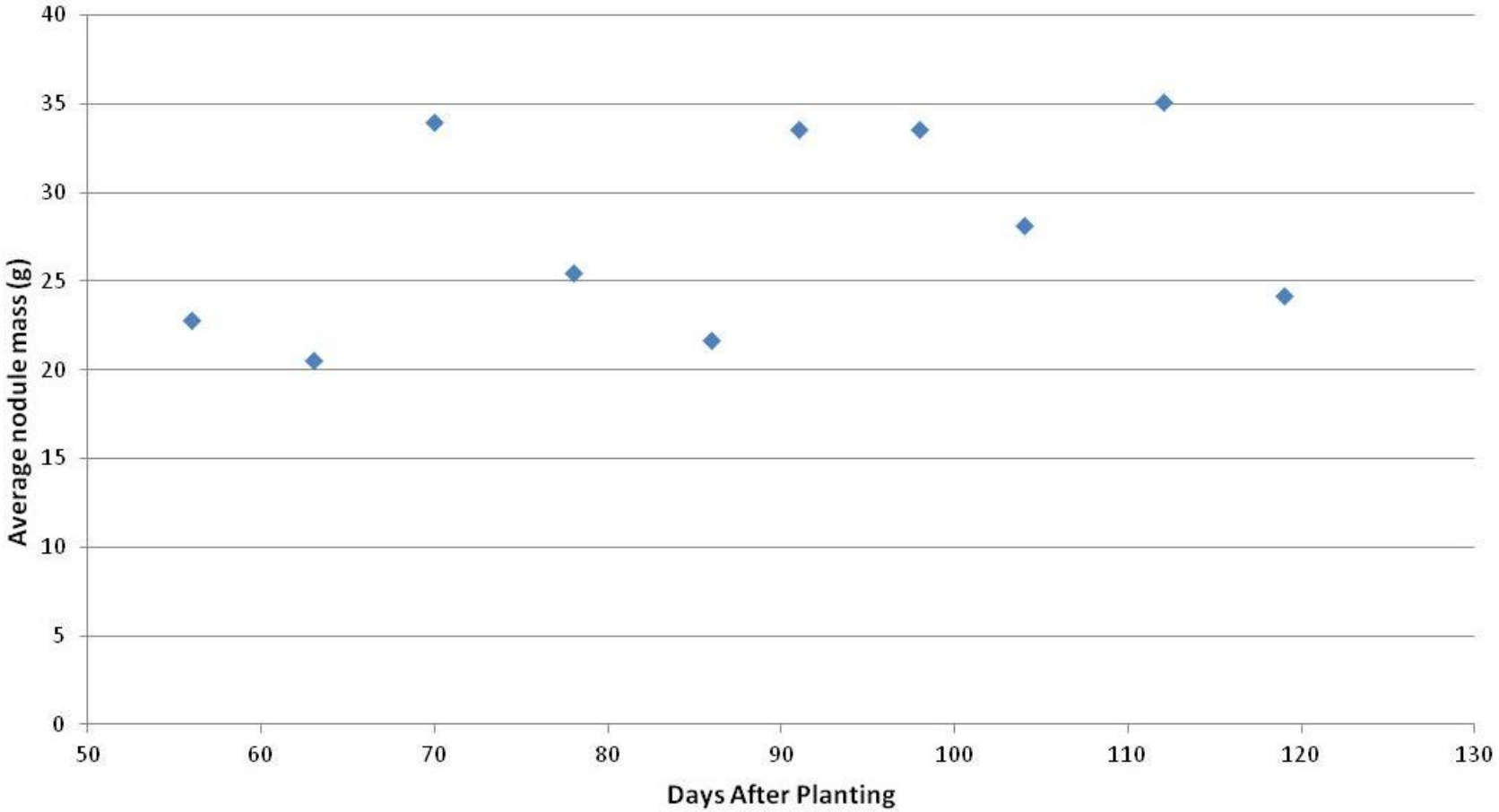

Figure 9. Average soybean nodule mass over the time course.

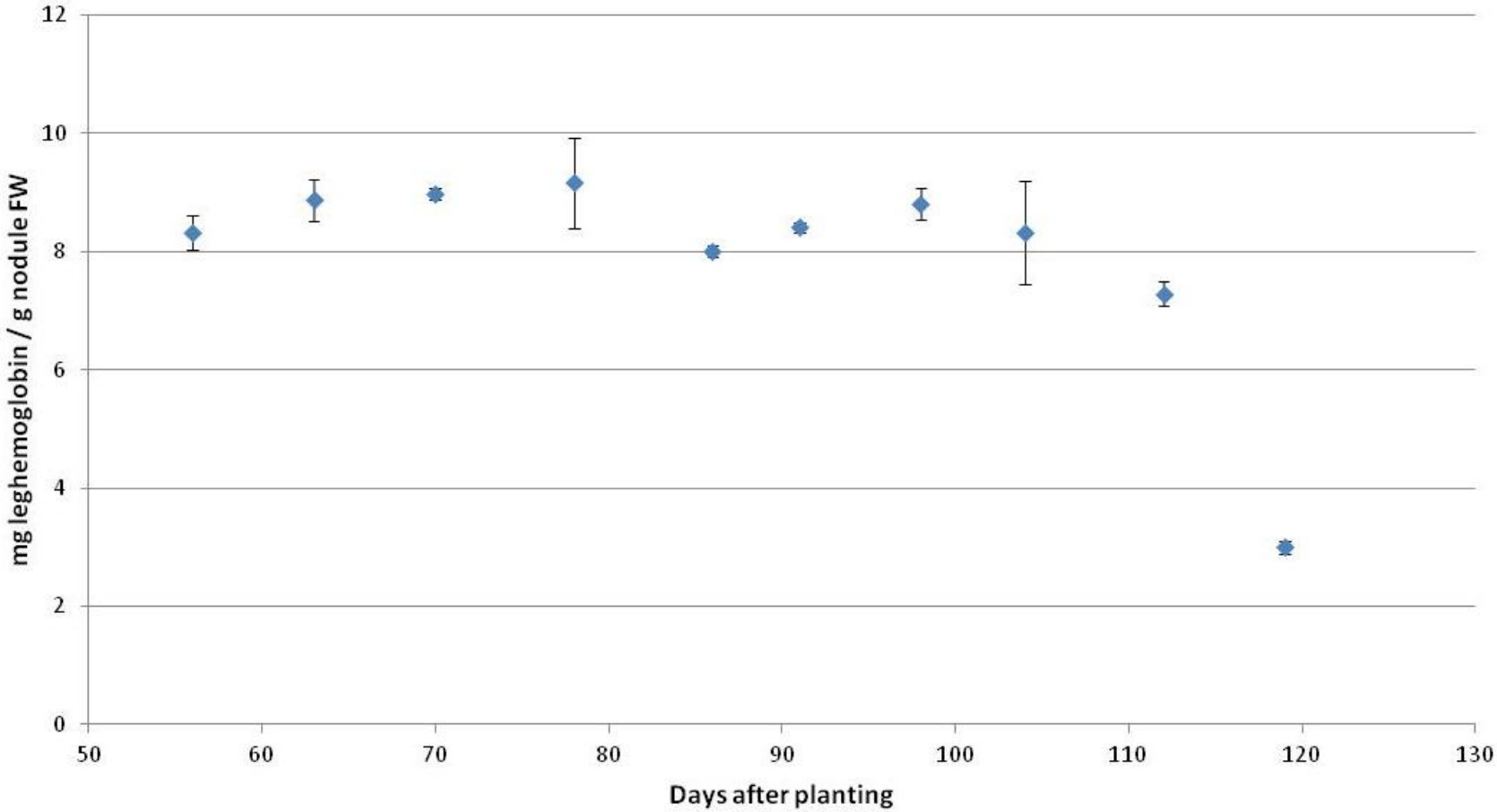

Figure 10. Leghemoblobin (mg) content per gram soybean nodule during the time course.

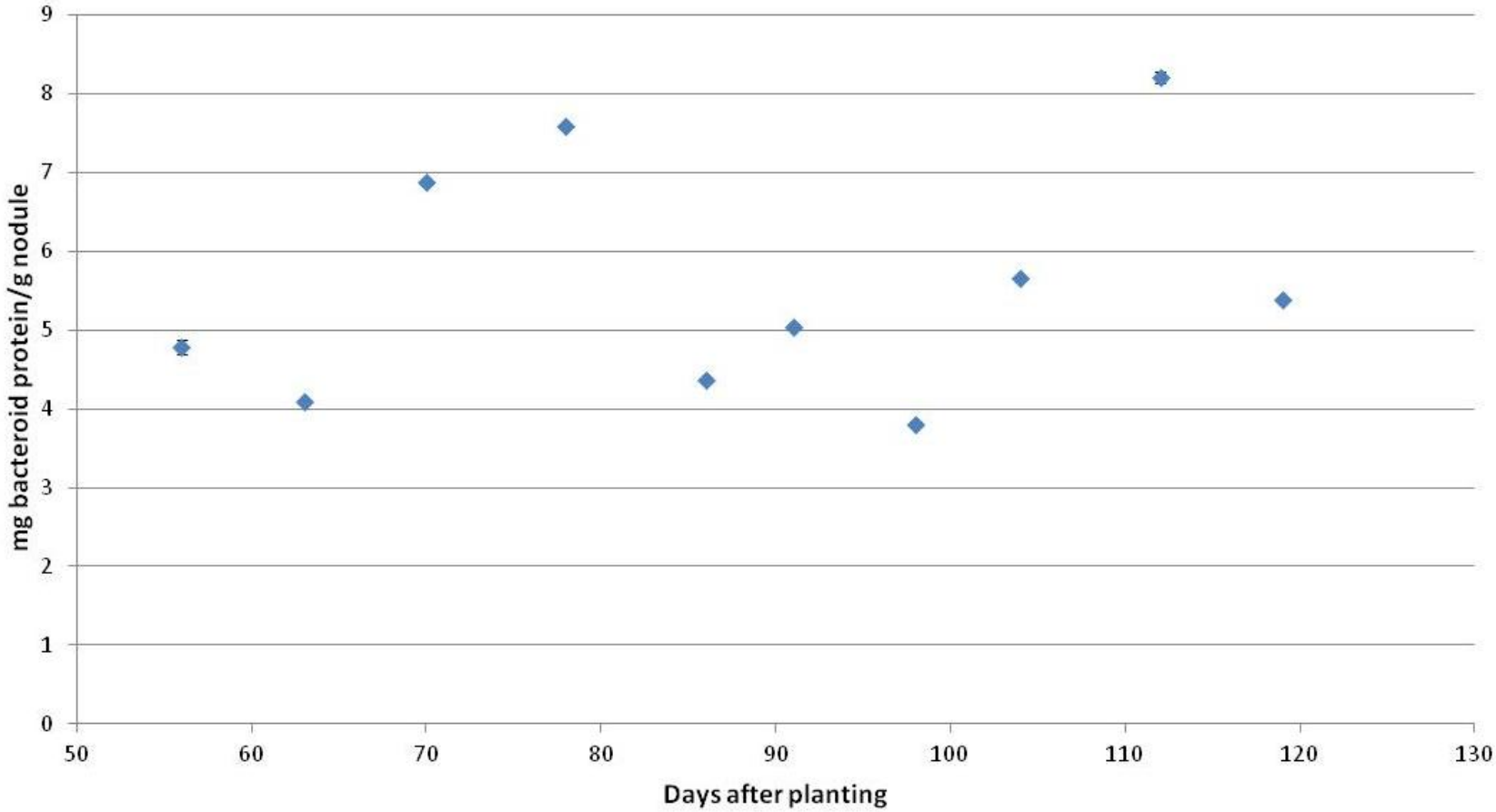

Figure 11. Bacteroid protein (mg) per gram soybean nodule during the time course.

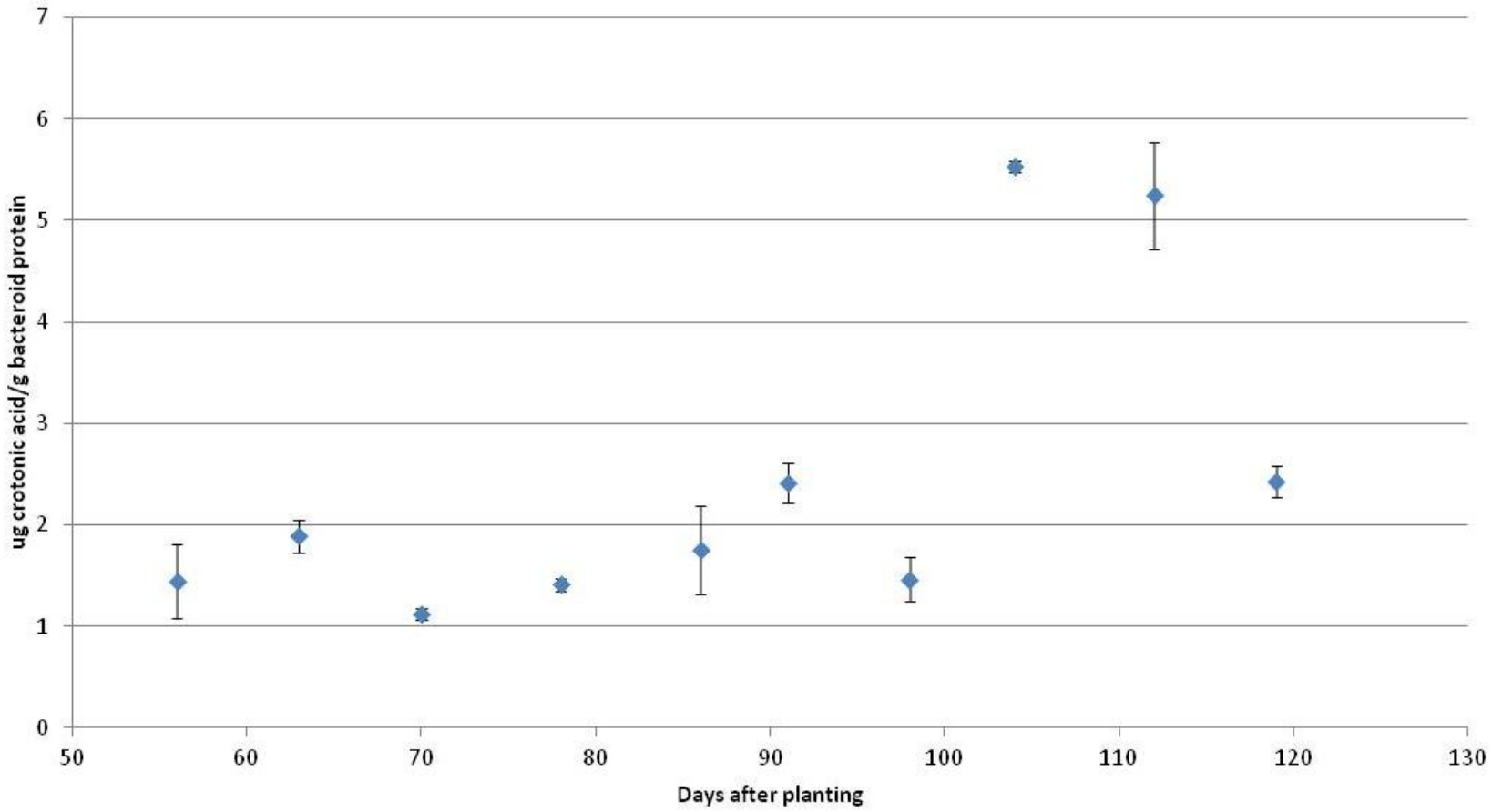

Figure 12. Accumualation of poly-hydroxybutyrate in bacteroids from field nodules collected during time course study. Crotonic acid evolution was measured at 208 nm.

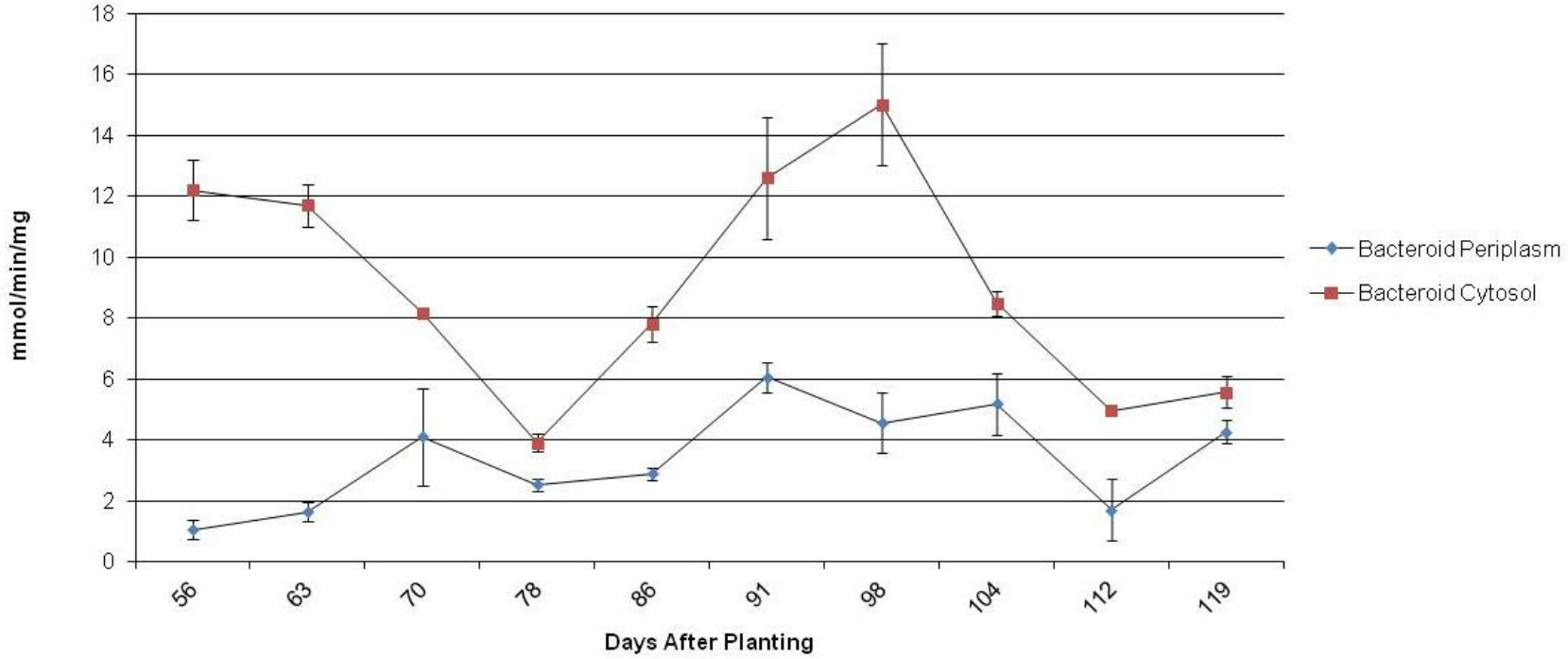

Figure 13. Cyclic-phosphodiesterase activity assayed as described in the 'Materials and Methods' of *B. japonicum* bacteroids recovered from soybean nodules and fractionated into cytosolic and periplasmic fractions. Activity is expressed in mmol formation of ρ-nitrophenol 410 nm/min/mg protein.

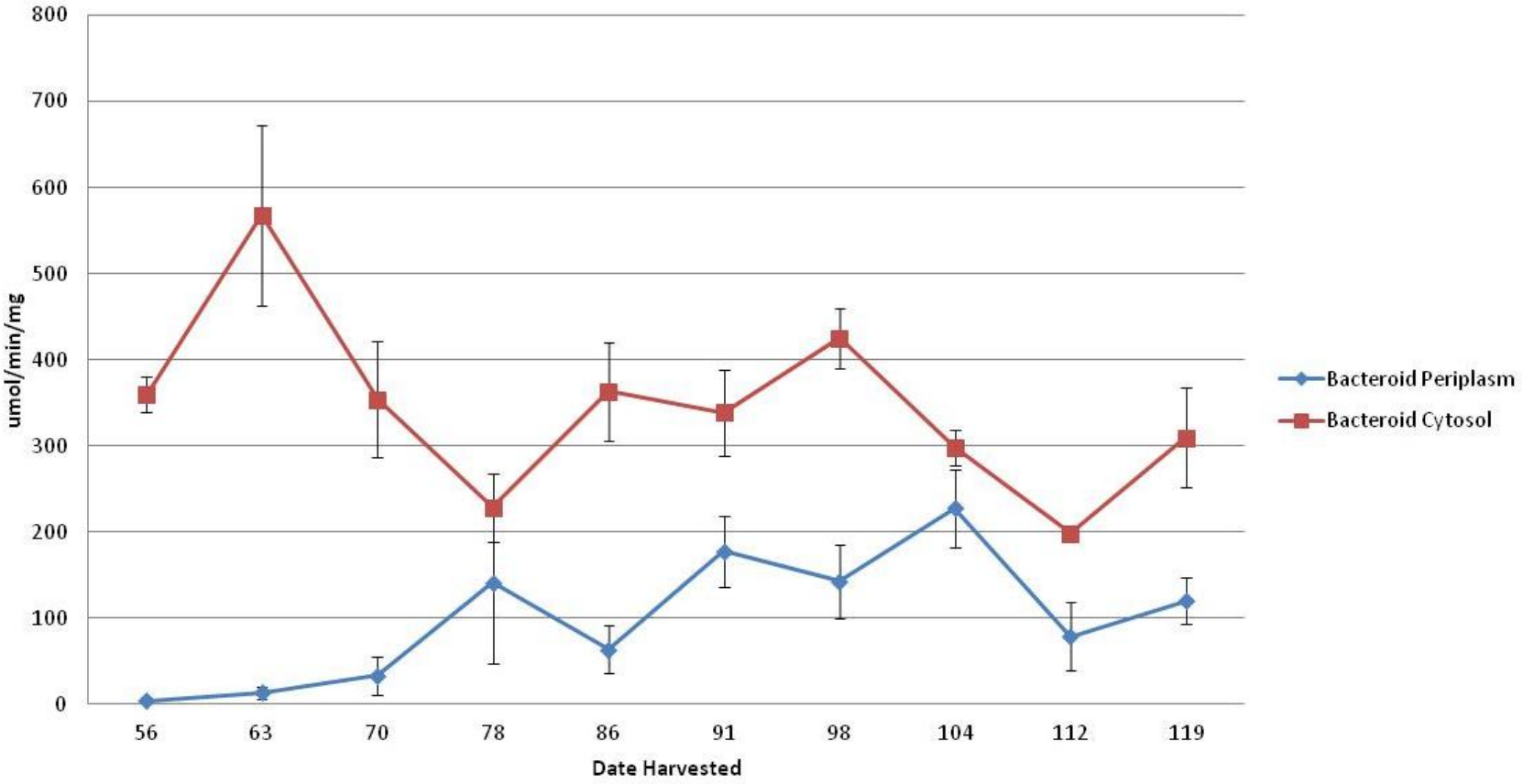

Figure 14. β-hydroxybutyrate dehydrogenase activity assayed as described in the 'Materials and Methods' of *B. japonicum* bacteroids recovered from soybean nodules and fractionated into cytosolic and periplasmic fractions. Activity is expressed in umol NADH consumed at 340 nm/min/mg protein.

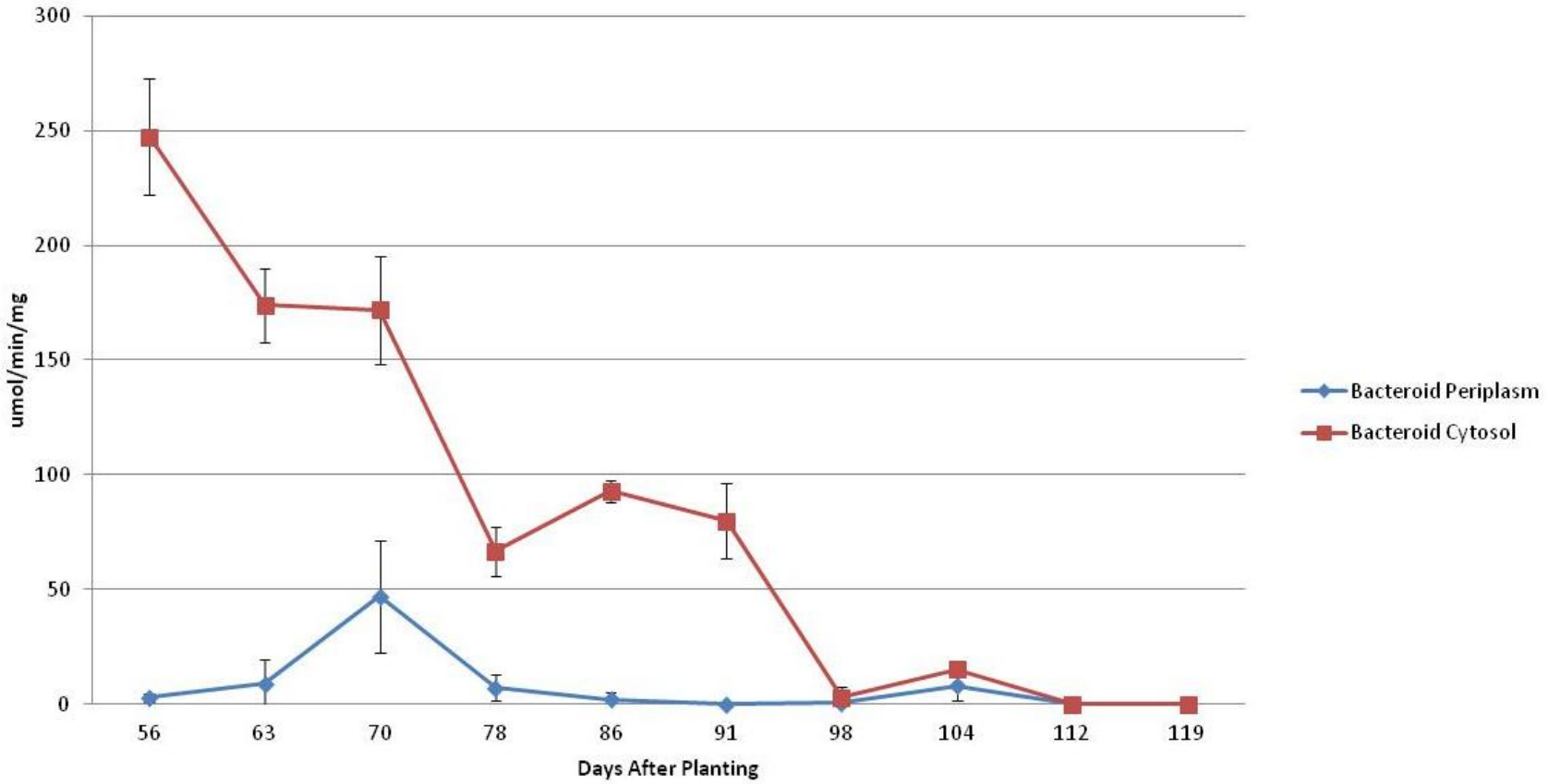

Figure 15. Isocitrate dehydrogenase activity assayed as described in the 'Materials and Methods' of *B. japonicum* bacteroids recovered from soybean nodules and fractionated into cytosolic and periplasmic fractions. Activity is expressed in umol NADH consumed at 340 nm/min/mg protein.

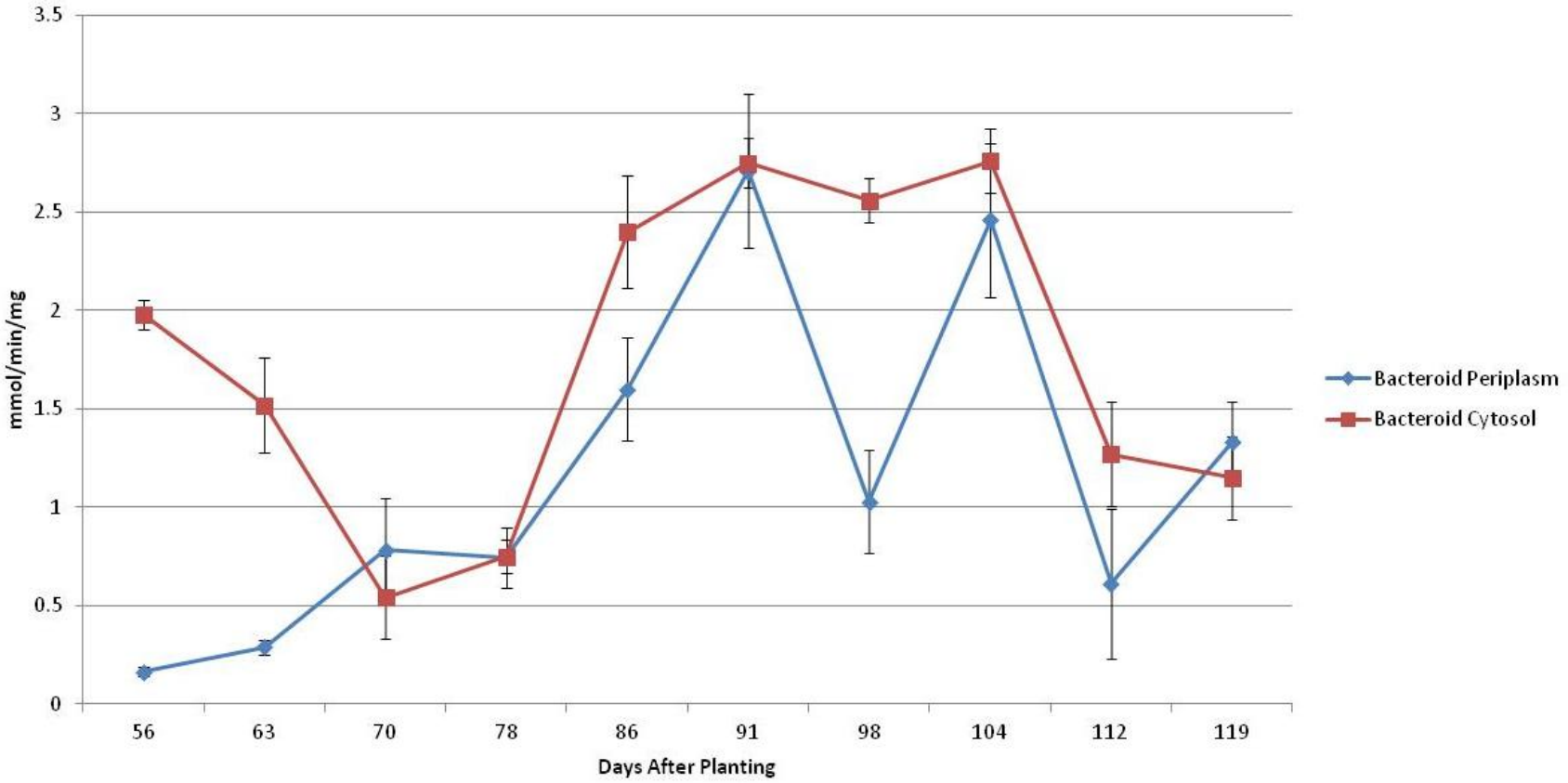

Figure 16. Malate dehydrogenase activity assayed as described in the 'Materials and Methods' of *B. japonicum* bacteroids recovered from soybean nodules and fractionated into cytosolic and periplasmic fractions. Activity is expressed in mmol NADH consumed at 340 nm/min/mg protein.

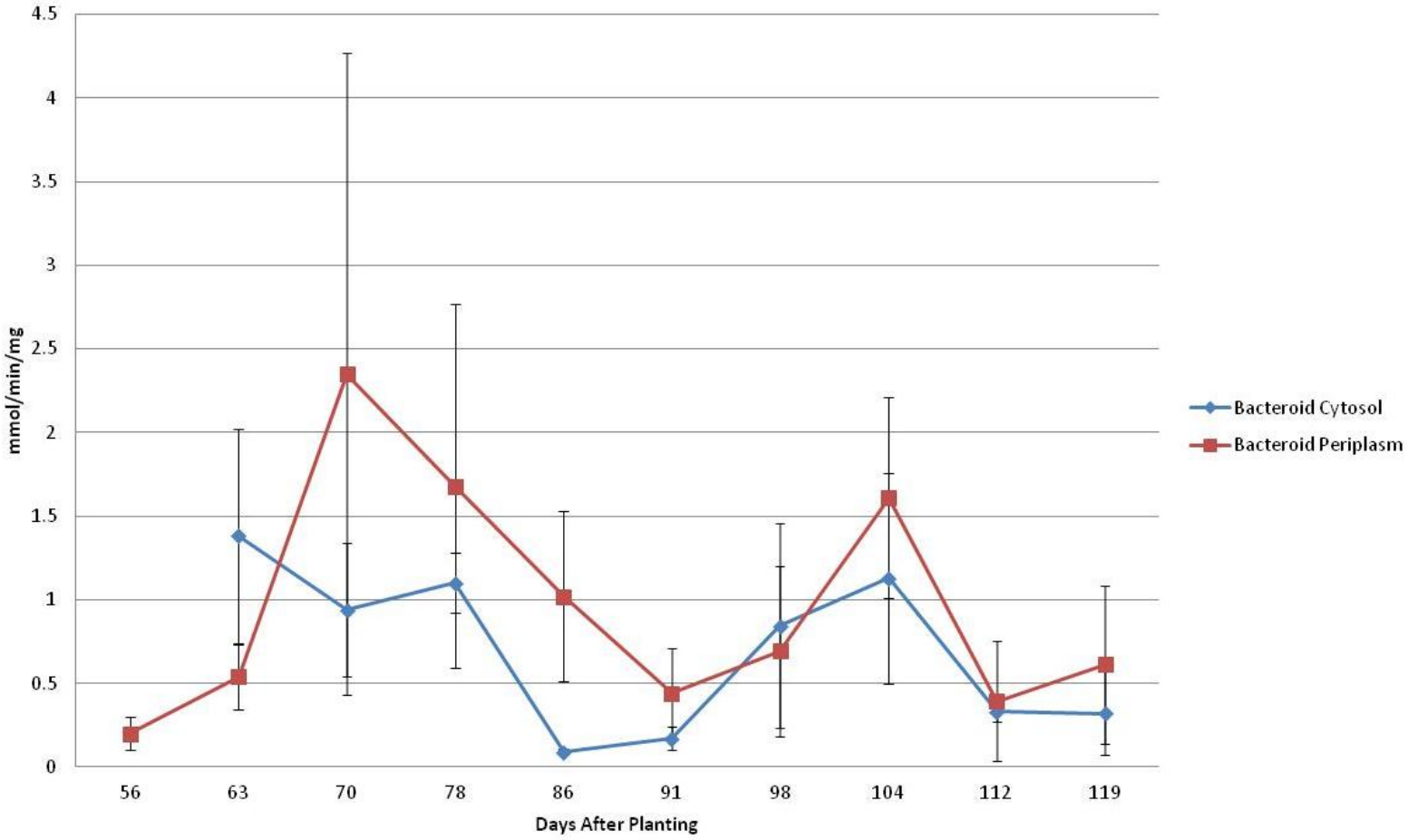

Figure 17. Protocatechuate 3,4-dioxygenase activity assayed as described in the 'Materials and Methods' of *B. japonicum* bacteroids recovered from soybean nodules and fractionated into cytosolic and periplasmic fractions. Activity is expressed in mmol protocatechuate consumed at 290 nm/min/mg protein.

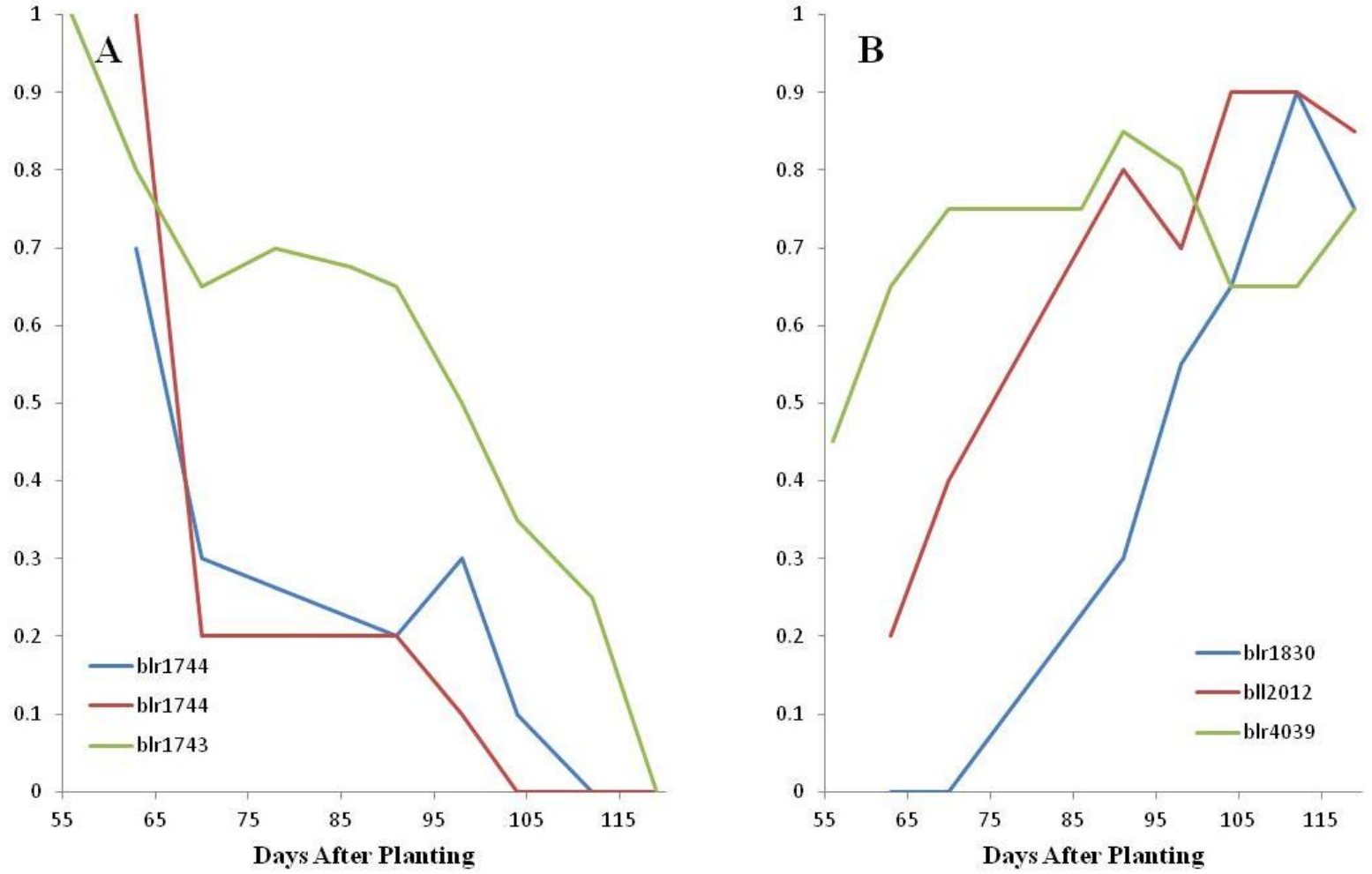

Figure 18. Examples of decreasing (A) and increasing (B) protein profiles as modeled in Proteome Lab. The Y axis is an arbitrary signal intensity value.

Table 18. Peptide profiles that decreased over the proteomics time course

Accession Number	Description	Fraction
bll0025	67 kDa Myosin-crossreactive streptococcal antigen homolog	Cyt
bll0449	dihydrolipoamide dehydrogenase	Cyt
bll0455	succinyl-CoA synthetase beta chain	Cyt
bll0456	malate dehydrogenase	Cyt
bll0504	3-isopropylmalate dehydrogenase	Cyt
bll0641	protein-export protein	Cyt
bll0733	ABC transporter glycerol-3-phosphate-binding protein	Cyt
bll0779	polyribonucleotide nucleotidyltransferase	Cyt
bll0887	ABC transporter substrate-binding protein	Cyt
bll1520	fructose bisphosphate aldolase	Cyt
bll1875	hypothetical protein	Cyt
bll2059	GroEL3 chaperonin	Both
bll2060	GroES3 chaperonin	Cyt
bll2063	phenolhydroxylase homolog	Both
bll2465	MoxR family protein	Cyt
bll2909	probable amino acid binding protein	Cyt
bll4445	cystathionine beta lyase	Cyt
bll4781	hypothetical protein	Cyt
bll4782	pyruvate dehydrogenase beta subunit	Cyt
bll4794	enolase	Cyt
bll4860	translation elongation factor Ts	PP
bll4877	prolyl-tRNA synthetase	Cyt
bll4942	ATP-dependent protease LA	Cyt
bll4945	trigger factor	Cyt
bll5390	50S ribosomal protein L14	Cyt
bll5402	elongation factor TU	Cyt
bll5403	translation elongation factor G	Cyt
bll5404	30S ribosomal protein S7	Cyt
bll5409	DNA-directed RNA polymerase beta' chain	Cyt
bll5410	DNA-directed RNA polymerase beta chain	Cyt
bll5914	carbon monoxide dehydrogenase large chain	Cyt
bll6508	putative hydrolase serine protease transmembrane protein	Cyt
bll7093	3-oxoadipate CoA-transferase subunit A	Cyt
bll7374	DNA-binding stress response protein, Dps family	Cyt
bll7795	two-component response regulator	Cyt
bll8141	phosphoenolpyruvate carboxykinase	Cyt

bll8309	unknown protein	PP
blr0028	hypothetical protein	Cyt
blr0488	3-isopropylmalate dehydratase large subunit	Cyt
blr0514	succinate dehydrogenase flavoprotein subunit	Cyt
blr0740	30S ribosomal protein S1	Cyt
blr0778	catalase	Cyt
blr0807	succinate-semialdehyde dehydrogenase	Cyt
blr1160	enoyl-CoA hydratase	Cyt
blr1686	putative aminotransferase protein	Both
blr1743	nitrogenase molybdenum-iron protein alpha chain (nifD)	Both
blr1744	nitrogenase molybdenum-iron protein beta chain (nifK)	Both
blr1774	flavoprotein (fixC)	Both
blr1852	similar to pantoate--beta-alanine ligase	Cyt
blr2068	5-methyltetrahydropteroyltriglutamate-homocysteine S-methyltransferase	Cyt
blr2146	dehydrogenase	Cyt
blr2372	unknown protein	Cyt
blr2616	glutaryl-CoA dehydrogenase	Cyt
blr2816	aldehyde dehydrogenase	Cyt
blr4039	ABC transporter substrate-binding protein	Cyt
blr4119	nucleoside diphosphate kinase	Cyt
blr4134	aminotransferase	Cyt
blr4145	NAD-dependent malic enzyme	Cyt
blr4839	citrate synthase	Both
blr4949	glutamine synthetase I	Cyt
blr5308	anti-oxidant protein	Cyt
blr5626	60 KDA chaperonin	Both
blr5690	adenylosuccinate lyase	Cyt
blr5706	30S ribosomal protein S4	Cyt
blr6718	hypothetical protein	Cyt
blr7070	hypothetical protein	Cyt
blr7485	hypothetical zinc protease	Cyt
blr7743	glutamate synthase large subunit	Cyt
blr8117	ABC transporter substrate-binding protein	Cyt
blr8144	two-component response regulator	Cyt
bsl4078	30S ribosomal protein S18	Cyt

Table 19. Peptide profiles that increased over the proteomics time course

Accession Number	Description	Fraction
bll2012	hypothetical protein	Cyt
bll4278	unknown protein	Cyt
bll4690	peptidyl prolyl cis-trans isomerase	Cyt
bll5155	hypothetical protein	Cyt
bll7395	hypothetical protein	Cyt
bll7795	two-component response regulator	PP
bll7821	probable fatty oxidation complex, alpha subunit	PP
blr0191	acetyl-CoA carboxylase carboxyl transferase alpha subunit	Cyt
blr0434	carboxy-terminal protease	PP
blr1159	acyl-CoA thiolase	PP
blr1160	enoyl-CoA hydratase	PP
blr1830	unknown protein	Cyt
blr3804	hypothetical protein	Cyt
blr4039	ABC transporter substrate-binding protein	PP
blr5502	hypothetical protein	Cyt
bsl3986	cold shock protein	Cyt

Table 20. Peptide profiles that were constitutive over the proteomics time course

Accession Number	Description	Fraction
bll0785	N-utilization substance protein A	PP
bll1524	transketolase	PP
bll1777	alkyl hydroperoxide reductase	Cyt
bll2065	carbonic anhydrase	Cyt
bll2067	nodulate formation efficiency C protein	PP
bll2909	probable amino acid binding protein	Both
bll5033	glycine hydroxymethyltransferase	PP
bll5403	translation elongation factor G	PP
bll5596	ABC transporter substrate-binding protein	Cyt
bll5755	RecA protein	PP
bll6069	hypothetical protein	PP
bll6220	putative alcohol dehydrogenase precursor(PQQ-dependent dehydrogenase)	Cyt
bll7756	peptidyl-dipeptidase	PP
bll7774	superoxide dismutase	Cyt
bll7921	ABC transporter substrate-binding protein (Putative oligopeptide binding protein)	Both
bll8229	hypothetical protein	PP
blr0678	heat shock protein 70	PP
blr0925	beta-ketoadipyl CoA thiolase	PP
blr0936	peptidoglycan acetylation protein	PP
blr1404	ATP-dependent protease, ATP-binding subunit	PP
blr2146	dehydrogenase	PP
blr3954	methylmalonate-semialdehyde dehydrogenase	PP
blr6758	probable transaldolase	PP
Glyma02g38920.1	Histone H3	PP
Glyma06g32880.1	Histone H4	PP
Glyma16g04560.1	glu/leu/phe/val dehydrogenase	PP

Chapter IV

Protocatechuate Dioxygenase Genes of *Bradyrhizobium japonicum* Affect Symbiotic Nitrogen Fixation with Soybean.

Abstract

Protocatechuate 3,4-dioxygenase catalyzes the ring cleavage of 3,4-dihydroxybenzoate to 2-hydroxy-5-carboxymethymuconate semialdehyde and subsequently to succinyl-CoA which could be further metabolized via the partial citric acid cycle of *Bradyrhizobium japonicum* bacteroids. Mutants of each of the two paralogs of the enzyme at positions blr0927-0928 and blr2333-2334 were created by insertion of a streptomycin resistance cassette. The enzyme encoded by loci blr2333-34 is not necessary for nitrogen fixation activity, but does perform a role in the temporal development of the root nodule. In contrast, enzyme encoded by loci blr0927-28 was necessary for an effective nitrogen fixing symbiosis with soybean.

Introduction

The symbiotic, nitrogen-fixing soil bacterium, *Bradyrhizobium japonicum* forms a symbiotic relationship with the legume soybean (*Glycine max*). Symbiotic nitrogen fixation between leguminous host plants and rhizobia require large inputs of energy which is derived from the photosynthetic carbon compounds from the plants own metabolism. One such source could be phenolic compounds, such as phytoalexins, that are excreted by the roots of soybean for host defense and signaling to other plants or microbes living in rhizosphere. Phenolic compounds would be available to the differentiated symbiotic associated bacteria known as bacteroids living in the nodule

during symbiosis. The metabolism of phenolics in the bacteroid has been infrequently examined to date which is in contrast to the free living form of rhizobia. A more complete review of plant and rhizobial signaling involving phenolic compounds can be found in Hirsch et al. (2003).

Phenolic compounds, such as vanillate, are found in the soil where they are released from lignin by oxidative cleavage (Martinez et al., 2005; Nardi et al., 2003). Lignin is the second most abundant organic material in the biosphere and the most abundant renewable source of aromatic polymers in nature (Parke, 1992; Wong, 2009). Another source of phenolic compounds is plant tannins that are released to the rhizosphere by host plants. Tannins, such as catechol, can interact with proteins and polysaccharides to inhibit the growth of microbes (Waheeta and Mahadevan, 1997). Other plant phenolic compounds are released as isoflavones during seed germination and from the roots in to the rhizosphere. The isoflavones act as signal molecules to initiate the symbiosis between host legume and the rhizobia (Long, 1989; Peters and Verma, 1990). The flavonoids genistein and daidzen from soybean cause the induction of *nod* genes in *B. japonicum* (Kosslak et al., 1987).

The ability of *B.japonicum* and other rhizosphere organisms, both symbiotic and pathogenic, to metabolize phenolic compounds via the β-ketoadipate pathway for energy has been well studied (Ito et al., 2006; Parke and Ornston, 1986). *B. japonicum* has been shown to have positive chemotactic response to phenolic compounds such as hydroxycinnamic acids and protocatechuate (Kape et al., 1991; Parke et al., 1985). The conservation of the β-ketoadipate pathway in rhizosphere microbes indicates that the

pathway performs essential roles in rhizosphere ecology and plant-microbe interactions (Peters and Verma, 1990).

Particular interest has been given to the degradation of protocatechuate by the enzyme protocatechuate 3,4-dioxygenase (*pcaHG)* (Ito et al., 2006; Parke and Ornston, 1986; Parke et al., 1985; Podila et al., 1993). *B. japonicum* has a fully annotated β-ketoadipate pathway for the degradation of protocatechuate as well as two paralogs of *pcaHG*, encoded by the genes blr0927-28 and blr2333-34. A mutant in the β-carboxy-cis,cis-muconate cycloisomerase (*pcaB*) of *B. japonicum* was unable to grow on the the phenolic metabolites 4-hydroxybenzoate and protocatechuate indicating these compounds were catabolized by the β-ketoadipate pathway (Lorite et al., 1998). Further a mutant in blr2333-34 was unable to catabolize and grow when protocatechuate, or its precursor vanillate, were provided as the sole carbon source (Sudtachat et al., 2009). The function of the *pcaHG* gene cluster blr0927-28 has not been elucidated and was found to be not markedly induced during a transcriptomic study where *B. japonicum* was grown on various carbon sources, including several phenolic compounds (Ito et al., 2006).

These studies have documented the degradative capacity of *B. japonicum* for protocatechuate and its derivatives in the free living form. Agriculturally, the application of glyphosphate to transgenic-glyphosphate resistant soybean has been shown to cause an accumulation of hydroxybenzoic acids, particularly protocatechuic acid, within the bacteroid nodule population of *B. japonicum* causing reduction in nitrogenase activity in green house grown plants (Hernandez et al., 1999; Moorman et al., 1992).

Although protocatchuate metabolism has been studied in cultured rhizobia, to date no study has been reported on the relationship between protocatechuate metabolism and

the symbiotic, nitrogen fixation capacity of *B. japonicum.* Phenolic compounds that are excreted by the roots of soybean can serve roles in host defense, and thus protocatechuate may have a role in infection of root hairs of soybean. *B. japonicum* bacteroids have been found to have the ability to degrade protocatechuate over the lifetime of the symbiosis (Chapter III), and thus may have a role in maintenance of the symbiotic state and toward the reduction of atmospheric dinitrogen (Brechenmacher et al., 2010). A mutant in each paralog of *pcaHG* in *B. japonicum* USDA 110 was constructed and tested for their ability to create an effective nitrogen fixing symbiosis with soybean.

Material and Methods

Bacterial Strains and Growth Conditions

B. japonicum and *E. coli* strains used as hosts for cloning and donors in conjugation, and the vectors and plasmids used in the research are listed in Table 21.

Bradyrhizobium japonicum USDA110 was routinely cultured at 28^{o}C in AG (Arabinose-Gluconate) medium (per liter): 1 g Arabinose, 1 g yeast extract, 1g gluconic acid, 1.1 g MES, 1.3 g HEPES, 0.125 g Na_2HPO_4, 0.25 g Na_2SO_4, 0.18 g $MgSO_4$ $7H_2O$, 0.004 g $FeCl_3$, 0.013 g $CaCl_2$, at pH 6.8 with shaking at 28^{o}C.

Growth on selected carbon sources was carried out on Tully's defined medium (per liter): 1.98 g $(NH_4)_2SO_4$, 0.17 g $MgSO_4$ 7 H_2O, 0.06 g $CaCl_2$ $2H_2O$, 1.17 g NaCl, 0.4 g K_2HPO_4, 8.3 g MOPS, plus vitamins, plus minerals, with 2 mM selected phenolic carbon substrate and 20 mM of L-malate or succinate at pH 6.8 with shaking at 28^{o}C. Cells were checked for ABS at 630 nm and were then diluted in phosphate buffered saline and 0.02% Tween 20 to ~100 colonies per plate. Growth was monitored for 14 days after inoculation at 28^{o}C.

Antibiotic concentrations used were 100 μg/ml streptomycin, 100 μg/ml kanamycin, 20 μg/ml nystatin, 30 μg/ml chloramphenicol, and 90 μg/ml tetracycline. Agar at 1.5% (w/v) was used to solidify media.

Biparental matings were performed on AG plates supplemented with 300 μM di-amino pimelic acid (DAP) and no antibiotic at 28^{o}C.

Escherichia coli cultures were grown at 37^{o}C at pH 7.5 in LB medium (10 g tryptone, 5 g yeast extract, 10 g NaCl). Antibiotic concentrations used for *E. coli* were 30 μg/ml streptomycin, 50 μg/ml kanamycin, 50 μg/ml ampicillin, 30 μg/ml chloramphenicol, and 30 μg/ml tetracycline.

DNA Manipulations

The Fermentas Genomic DNA Isolation Kit was used to isolate genomic DNA from *B. japonicum* per the manufacturer's instruction (Fermentas, Waltham, MA). The isolated genomic DNA was resuspended in TE (10mM Tris, pH 8.0, 1mM EDTA) and stored at -20^{o}C.

Plasmids were isolated utilizing the Fermentas Gene Jet Plasmid Purification Kit according the manufacturer's instructions. Restriction enzyme digests were performed according to the manufacturer's instruction. Fragments were analyzed by agarose gel electrophoresis in 0.8% agarose in 40 mM Tris acetate, 2 mM EDTA buffer with 0.5 ug/mL ethidium bromide for visualization of nucleic acid with ultraviolet light. PCR products and restriction digest fragments were purified using the Fermentas PCR isolation kit per the manufacturer's instructions. Nucleic acid fragments (dsDNA) isolated from agarose gels were purified via the Fermentas Gel Isolation Kit per the

manufacturer's instructions. Ligations were performed using 5-15 units of T4 DNA Ligase (New England Biolabs, Ipswich, MA). All ligation reactions were incubated on ice for 12-18 hours. *E. coli* strains were transformed either by electroporation (WM3064) or by heat shock (BL21 DE3) as outlined in Short Protocols in Molecular Biology (Ausubel et al., 2002) or as outlined by the manufacturer (Xl-1 Blue Supercompetent Cells, Stratagene). Electroporations were performed on a Gene-Pulser (Bio-Rad, Hercules, CA) at 2.0 V at 25 μFD and 200 ohms in a 0.2 cm gap width pulse cuvette.

Cloning of Protocatechuate 3,4-Dioxygenase *pcaHG* Paralogs

B. japonicum contains two paralogs, blr0927-28 and blr2333-34, encoding the two subunits of the enzyme protocatechuate dioxygenase (*pcaHG*). Both subunits of each gene cluster were cloned from genomic DNA utilizing PCR. Oligonucletide primers for the amplification of blr0927-28 were KS143 and KS144. blr2333-34 was amplified using KS141 and KS142. After an initial denaturation at 94^{o}C for 3 minutes, 35 cycles of 94^{o}C for 30 seconds, annealing at 55^{o}C for 30 seconds followed by elongation at 68^{o}C for 2 minutes 30 seconds were performed. Reactions contained 1U Taq DNA polymerase (New England Biolabs, Ipswich, MA), 0.5 mM each dNTP, 3 mM $MgSO_4$, 10 pmol each primer, 5% DMSO, 1μg genomic DNA, and 1X Thermopol Reaction Buffer in a 50 μL reaction. Amplification was performed on an Eppendorf Mastercycler Thermocycler. After amplification, the 2.5 kb DNA fragments of blr0927-28 and blr2333-34 were TA cloned into the XcmI site of pKOTCII giving plasmids pKNS115 and pKNS114. Plasmids were verified via PCR of purified plasmid and sequencing of plasmid.

Sequence Analysis

All constructs were sequenced through the University of Missouri DNA Core Facility utilizing ABI Big Dye Terminator cycle sequencing chemistry on the ABI 3730 96-capillary DNA Analyzer (Applied Biosystem Inc., Foster City, CA). Resulting sequences were aligned using CLUSTALW multiple sequence alignment program in SDSC Biology Workbench (San Diego Supercomputer Center, UCSD, La Jolla, CA, www.workbench.sdsc.edu).

Construction of *B. japonicum* Protocatechuate Dioxygenase (*pcaHG*) Knock-Out Mutants

Blr0927-28 was interrupted with a streptomycin cassestte via the following procedure: pKNS115 was double digested with XbaI and SalI that resulted in a 2.5 kb fragment that was then ligated into pBluescript SK II (+) (Fermentas, Waltham, MA) digested with XbaI and SalI. The resulting plasmid pKNS127 was then digested with BglII that removed an ~630 bp fragment that was ~320 bp from the start codon of blr0927 and ~390 bp from the stop codon of blr0928. The 2.0 kb omega cassette encoding resistance for streptomycin and spectinomycin was then removed from pHP45Ω (Prentki and Krisch, 1984) via digestion with BamHI and ligated into the BglII digested pKNS127. The resulting plasmid, pKNS128, was then double digested with XbaI and SalI and the resultant 3.9 kb fragment ligated into pLOI (Lenz et al., 1994) (mobilization suicide vector that carries kanamycin resistance gene cassette) that had been double digested with XbaI and SalI. The resultant plasmid pKNS129 was then electroporated into the *E. coli* mating strain WM3064 (Saltikov and Newman, 2003).

Blr2333-34 was interrupted with a streptomycin cassette via the following procedure: pKNS114 was double digested with XbaI and XhoI that resulted in a 2.5 kb fragment that was then ligated into pBluescript SK II (+) (Fermentas, Waltham, MA) that had been digested with XbaI and XhoI. The resultant plasmid, pKNS132, was then digested with AgeI removing ~750 bp that was ~200 bp from the start codon of blr2333 and ~440 bp from the stop codon of blr2334. The 2.0 kb omega cassette was removed from pHP45Ω by digestion with XmaI and ligated into the AgeI cut pKNS132 resulting in pKNS133. pKNS133 was then double digested with XbaI and XhoI with the resultant 3.8 kb fragment being ligated into the XbaI and XhoI sites of pLOI. Plasmid pKNS134 was then electroporated into *E. coli* mating strain WM3064.

Construction of *B. japonicum* Complementation Constructs

The open reading frame of blr0927-28 plus 100 bp upstream of the start codon of blr0927 encoding the promoter and ribosome binding site were amplified via PCR utilizing primers KS155 and KS156. The resultant 1.5 kb fragment was then used as a template to place HindIII sites on the 5′ and 3′ via primers KS157 and KS158. This 1.5 kb fragment was then digested with HindIII and ligated into the HindIII site of pRK311 (Ditta et al., 1985). The resultant plasmid pKNS137 was then electroporated into the *E. coli* mating strain WM3064.

The open reading frame of blr2333-34 plus 100 bp upstream of the start codon of blr2333 encoding the promoter and ribosome binding site were amplified via PCR utilizing primers KS160 and KS161. The resultant 1.5 kb fragment was then used as a template to place HindIII site on the 5′ and 3′ via primers KS162 and KS163. The PCR

product was then digested with HindIII and ligated into the HindIII site of pRK311 resulting in plasmid pKNS138. Plasmid pKNS138 was then electroporated into the *E. coli* mating strain WM3064.

Biparental Matings

Recipient *B. japonicum* USDA 110 strain (or in the case of complementation KNS1 and KNS2) were grown to mid-log phase on AG medium, *E. coli* donor strain WM3064 was grown to mid-log phase in LB supplemented with 300 μM diaminopimelic acid and the appropriate antibiotics. Five milliliters of each culture was centrifuged at 5,000 x g and washed twice in sterile water. Cultures were then mixed in a 1:1 ratio and resuspended in no more than 0.5 mL of sterile water. After mating for 3 days on a 0.45 μm pore sized filter (Millipore, Billerica, MA) the bacterial mixture was resuspended in PBS-0.02% Tween 20 and cultured in AG with the appropriate antibiotic until mid-log phase had been reached. One milliliter of culture was then transferred to a fresh AG flask with appropriate antibiotic and grown to mid-log phase. The cell culture was then diluted in PBS-0.02% Tween 20 and plated on AG plates with appropriate antibiotics to single colonies. Presumptive mutant colonies were transferred to duplicate AG Strep 100 and AG Kan 100 plates where both contained nystatin and chloramphenicol. Colonies exhibiting growth on AG Strep 100, but not on AG Kan 100 were then selected as putative double recombinants ($Strep^{r}Kan^{s}$). These colonies were then analyzed via colony PCR. The 5' of KNS1 (Δblr2333-34) was screened via PCR with primers KS170 which is 600 bp upstream of the start codon of blr2333 and KS 173 (strep rev) resulting in a 2.16 kb PCR product. The 3' was probed with KS171 which is 600 bp downstream

of the stop codon of blr2334 and KS 172 (strep for) resulting in a 2.11kb PCR product. Resultant PCR products were sequenced to verify double recombinant events. The 5' end of KNS2 (Δblr0927-28) was screened via PCR with primers KS168 which is 600 bp upstream of the start codon of blr0927 and KS173 (strep rev) resulting in a 2.2 kb PCR product. The 3'end of KNS2 was amplified utilizing KS169 which is 600 bp downstream of the stop codon forbBlr0928 and KS172 (strep for) resulting in a 1.99 kb PCR product. PCR products were sequenced to verify double recombinant events.

Complementation constructs pKNS137 and pKNS138 in *E. coli* conjugation strain WM3064 were mated with KNS2 and KNS1 respectively as described above yielding KNS3 and KNS4. Selection was performed in AG medium with streptomycin, nystatin, chloramphenicol, and tetracycline and grown to mid-log phase and then subcultured. The subcultured cells at mid-log phase were diluted in PBS-0.02% Tween 20 and plated on AG streptomycin, tetracycline, nystatin, and chloramphenicol. Single colonies were then picked and assayed for activity.

Plant Studies

Soybean seeds (*Glycine max* Merrill cv. Williams 82) were surface sterilized by soaking them in 95% (v/v) ethanol for 4 minutes, then soaking them in 6% sodium hypochlorite for 1 minute followed by rinsing with sterile distilled water. Seeds were then germinated in the dark at 28^{o}C for 48 hours on 1% water agar containing 20 μg/mL nystatin and 500 μg/mL penicillin G. After 48 hours, seedlings were inoculated with *B. japonicum* USDA 110, mutants KNS1 or KNS2, or complemented transconjugates KNS 3 or KNS 4 for 30 minutes and then planted in autoclaved Leonard jars (Karr et al.,

1984). Sterile nutrient solution was added to the lower reservoir as needed during growth. Plants were grown in a growth chamber with day night temperature of 27/24^{o}C and 16 hour photoperiod. Nodules were harvested from the root crown area of the tap root 14-40 days after planting and used for further analysis.

Acetylene Reduction Assays

Nitrogenase enzyme activity of intact root crown nodules was estimated by the rate of production of ethylene using the acetylene reduction method (Schwinghamer et al., 1970). The reaction was started by injecting two mL of acetylene, freshly generated from distilled water and calcium carbide, to 22.4 mL bottles containing intact nodules on the root crown. 0.2 mL samples of the gas phase were taken every two minutes for 10 minutes and analyzed on a Varian 3800 FID gas chromatograph. A Thermo Scientific (Waltham, MA) TG-BOND Alumina (KCl Deactivation) 30m x 0.53mmx10µm column was used with 11 psi of He as carrier gas; column temperature was set at 40^{o}C for one minute followed by ramping to 120^{o}C at 20^{o}C/min and a hold at 120^{o}C for one minute, the injector temperature was set at 180^{o}C, while the FID was set at 200^{o}C with hydrogen gas at 55 psi and compressed air at 33 psi. Ethylene production rate was determined with a minimum of three plants at each time point and values were normalized to the fresh weight of nodules.

Light Microscopy

Root hair curling and foci pictures were taken using an Olympus SZ-60 Dissecting Microscope with a PixelLINK Digital Camera (Secaucus, NJ). Pictures were then viewed and analyzed with PixelLINK Capture SE photoimaging software. Soybean root nodules were fixed in 2.5% (v/v) glutaraldehyde and 0.1M sodium phosphate buffer, pH 7.0, dehydrated through an ethanol chloroform series and embedded in paraffin. Section were mounted on glass slides and stained with Toluidine Blue by the University of Missouri Electron Microscopy core facility (http://www.emc.missouri.edu/). Images were taken with an Olympus Vanox microscope utilizing a Leica DFC295 camera and Leica Application Suite Software at the University of Missouri Cytology Core (http://biotech.missouri.edu/mcc/).

Transmission Electron Microscopy

Soybean root nodules were prepared for transmission electron microscopy (TEM) at the University of Missouri Electron Microscopy core facility (http://www.emc.missouri.edu/). Briefly, sliced nodule sections were treated with primary fixative (2% glutaraldehyde, 2% paraformaldehyde) rinsed with 0.1 M sodium cacodylate, 0.01 M 2-mercaptoethanol, 0.13 M sucrose buffer (2-ME buffer). Secondary fixation was 1% buffered osmium tetroxide, rinsed with 2-ME buffer and then ultra pure Milli-Q water. An acetone dehydration series (20, 50, 70, 90, 3 x 100%) was followed by infiltration of Epon-Spurr's resin and polymerization. Ultrathin sections (85 nm) were collected using a Lecia Ultracut UCT microtome fitted with a 45^{o} Diatome diamond knife, and placed on 200 mesh copper thin bar grids and double post stained with 5%

uranyl acetate (UA) and Sato's triple lead stain (Pb) (3 min Pb, 18 min UA, 8 min Pb). Samples were viewed with a JEM-1400 JEOL TEM.

Methylene Blue Staining

The methylene blue staining protocol described by (Green and Emerich, 1999) was used to identify curled root hairs on three and five day old soybean seedlings. Root segments approximately 3 cm long, starting 0.5 cm above the root tip, were cut from pouch grown seedlings. Root segments were then soaked in 2% (w/v) sodium hypchlorite (a 1:3 dilution of commercial bleach, Clorox, in water) for 1 -2 hours. Roots were rinsed in deionized water and then stained with 0.01% (w/v) methylene blue in water for 12-16 hours. Root segments were then destained in 35% (v/v) ethanol in water for 2 hours followed by destaining with 70% (v/v) ethanol in water for 2 hours or overnight. Root segments were then observed using a dissecting microscope under bright field illumination.

Hematoxylin Staining of Nodule Primordia

Soybean root segments were harvested as described for methylene blue staining and were stained with hematoxylin using a method described by (Green and Emerich, 1999). Root segments were boiled for 1-2 minutes in lactophenol (32% glycerol, 16% lactic acid, 20% phenol, by volume in water). Root segments were then blotted on paper towels and rinsed in water for 2-3 minutes. The water was decanted and hematoxylin solution, Harris type, (Sigma, St. Louis, MO) was added to cover the roots. Staining

proceeded overnight in the dark. Root segments were destained for 2-4 hours in water and then observed under a dissecting microscope using dark field illumination.

Leghemoglobin Concentration

Approximately 200-300 mg of nodules were homogenized in MEP buffer (5mM $MgCl_2$, 1 mM EDTA, 50 mM potassium phosphate, pH 7.0) in 1.5 mL microcentrifuge tubes with a pestle. The preparation was then spun at 2,000 x g for 3 minutes to remove the heavy plant debris. The supernatant containing the leghemoglobin and bacteroids was then removed and placed over sucrose gradients of 42% and 60 % and spun at 5,000 x g for 10 minutes. The supernatant containing the leghemoglobin was extracted and then assayed for leghemoglobin content with Drabkins solution (Sigma, St. Louis, MO) and the 42% layer containing the bacteroids was extracted, diluted with MEP 1:3, and spun at 13,000 x g for 5 minutes to pellet the bacteroids. Purified bacteroids were then characterized for their poly-β-hydroxybuyryate content and PCA 3,4-dioxygenase enzyme activity. The content of the fully oxidized leghemoglobin in the solution was determined photometrically at 540 nm with the cyanmethemoglobin method as determined by Wilson and Reisenauer (1963). Horse heart myoglobin was used as the standard.

Poly-β-Hydroxybutyrate Measurment

Poly-β-hydroxybuyryate (PHB) analysis was performed on bacteroids isolated from soybean root nodules. The purified bacteroid cell pellets were digested in concentrated sulfuric acid and then diluted with 0.014N H_2SO_4 (0.3-12 μg of sample per

mL final concentration). Samples were then assayed at 208 nm. A standard curve was constructed using crotonic acid as the standard (Karr et al., 1984).

Protocatechuate 3,4-Dioxygenase Activity

Bacteroids purified from soybean root nodules were ruptured using Bacterial Protein Extraction Reagent Phosphate Buffered (Pierce, Waltham, MA). The cells were pipette up and down several times until a homogenous suspension was achieved. The suspension was then analyzed for protein content utilizing Bradford Reagent (Bio-Rad, Hercules, CA) and compared to a standard curve using BSA. A total of 50 uL of the suspension was then placed into a quartz cuvette with 900 uL of 50 mM CHES, pH 9.3 buffer, and 50 uL of 40 mM protocatechuic acid. The cuvette was quickly inverted to mix and the decomposition of protocatechuic acid was measured at 290 nm. Activities were computed using the molar abosorptivity constant of protocatechuic acid at 290 nm, 3.8 mM^{-1} cm^{-1} (Fujisawa and Hayaishi, 1968).

Results

Cloning and Construction of Protocatechuate 3,4-Dioxygenase (*pcaHG*) Mutants

B. japonicum contains two gene sets that encode protocatechuate 3,4-dioxygenase, blr0927-28 and blr2333-34. Both gene sets were cloned as described in the Materials and Methods section utilizing PCR beginning 500 bp upstream of the start codon of the pcaH subunit and 500 bp downstream of the pcaG subunits, respectively, resulting in the expected 2.4kb fragment containing blr0927-28 and the 2.5kb fragment containing blr2333-34. Both fragments were cloned into the suicide vector pKOTcII's

XcmI site (creating pKNS114 and 115, respectively) and then sequenced at the University of Missouri DNA Core Facility.

Both pcaHG gene sets were transferred from pKOTcII to pBlueScript SK (+). The 2.0kb omega cassette encoding both streptomycin and spectinomycin resistance of pHP45Ω (Prenti & Krisch 1984) was digested with BamHI and transferred into pKNS127 cut with BglI that removed ~630 bp fragment ~320 bp downstream from the start codon of blr0927 and ~390 bp upstream from the stop codon of blr0928 creating pKNS128. This fragment was of sufficient size to remove the majority of both genes and the start codon of blr0928. After digestion with XbaI and SalI a 3.8 kb fragment was transferred to the same restriction sites in the suicide vector pLOI creating pKNS129.

The knockout construct for blr2333-34 was made in a similar fashion with pKNS114 being double digested with XbaI and XhoI that resulted in a 2.5 kb fragment that was then ligated into pBluescript SK II (+) that had been digested with XbaI and XhoI. The resultant plasmid, pKNS132, was then digested with AgeI removing ~750 bp that was ~200 bp from the start codon of blr2333 and ~440 bp from the stop codon of blr2334. The 2.0 kb omega cassette was removed from pHP45Ω by digestion with XmaI and ligated into the AgeI cut pKNS132 resulting in pKNS133. pKNS133 was then double digested with XbaI and XhoI with resultant 3.8 kb fragment being ligated into the XbaI and XhoI sites of pLOI.

Both pKNS129 and pKNS134 were then transformed into the *E.coli* mating strain WM3064 which is deficient in the ability to synthesize diaminopimelic acid (DAP), a necessary metabolite in lysine biosynthesis. Transformants were selected for resistance to streptomycin, chloramphenicol in liquid AG medium with DAP omitted to select

against the *E. coli* donor strain WM3064. After growth to mid-log phase, one mL was then subcultured in the above media, grown to mid-log phase and plated on streptomycin, chloramphenicol, nystatin AG agar plates. Single colonies were then picked to duplicate streptomycin, chloramphenicol and kanamycin, chloramphenicol AG plates to select for double homologous (full integration of the disrupted pcaHG alleles into the *B. japonicum* chromosome) or single homologous (mutagenic plasmid incorporation into the chromosome) recombinant events. Plates exhibiting both single and double recombinants were then screened via colony PCR. The 5' end of both putative mutants was probed first, with subsequent positively identified clones being then probed on the 3' end via PCR as described in the Materials and Methods. Figure 20 shows the results for KNS2 (Δblr0927-28) and Figure X the results for KNS1 (Δblr2333-34). Resultant PCR products were then sequenced at the University of Missouri DNA Core to verify the intended marker exchange. Sequencing results confirmed that both marker exchanges occurred as intended by sequencing from genomic regions outside the construct sequences amplified in pKNS114 and pKNS115 (Figure 19).

Growth on Carbon Substrates

The growth of the wild-type and mutant strains was compared on solid media with a number of different carbon substrates (Table 23). Mutant KNS2 (Δblr0927-28) was able to grow at comparable rates on the same carbon substrates as wild-type: malate, succinate, 2,4-dihydroxybenzoic acid, 4-hydroxybenzoic acid, vanillic acid, and 3-hydroxybenzoic acid. Mutant KNS1 (Δblr2333-34) was able to grow at comparable rates as wild-type on malate, succinate, and 2,4-dihydroxybenzoic acid. However, it was

unable to grow on 4-hydroxybenzoic acid, vanillic acid, or 3-hydroxybenzoic acid, which is consistent with the results for a previously constructed Δblr2333-34 mutant (Sudtachat et al., 2009). KNS4 (KNS1 carrying the complementation plasmid pKNS138) however was able to grow on 2mM 4-hydroxybenzoate. The complement to KNS2, KNS3 showed no difference in growth on AG media or on a variety of phenolic carbon substrates. Both pcaHG mutants as well as the wild-type USDA110 were unable to metabolize 2,5-dihydroxybenzoate and showed no growth suggesting that USDA110 lacks the capability to metabolize this phenolic compound.

Symbiotic Phenotype

Symbiotic properties of the two protocatechuate 3,4-dioxygenase mutants, KNS1 and KNS2, were investigated to determine their abilities to form nodules and fix nitrogen in symbiosis with soybean plants. Nodules formed by KNS1 and KNS2 were similar in size and shape when compared to the control at 19 days after inoculation as seen in Figure 21. KNS1 formed nodules similar to the control in that they occurred on the taproot and in similar number and size. KNS2 however formed nodules mostly on the lateral roots and none were found at the root crown after growing five repetitions of five pots with 3-5 plants per pot. There were no nodules on the un-inoculated controls.

Both mutants had lower nodule mass relative to the wild type at ages later than 22 days. Nodules formed with mutant KNS1, because of its delayed phenotype, did accumulate sufficient nodule mass by 30 days to not be statistically different from the control. KNS2 was unable to gain nodule mass past 22 days after infection and appeared to display early senescence. Nodule size was, also, consistently smaller and mass did not

increase significantly over time (Figure 21**)**. The complementation construct KNS3 for mutant KNS2 was able to recover the phenotype of root crown nodules and partially restore the nitrogenase activity at 28 days after inoculation (Figure 24).

Leghemoglobin content for nodules formed by USDA110 was approximately 8 mg leghemoglobin/g nodule fresh weight at day 20 and declined by 35 days to approximately 6.75 mg leghemoglobin/ g nodule fresh weight (Figure 22). Leghemoglobin contents for both mutants increased from approximately 5 mg leghemoglobin/g nodule fresh weight at day 20 to approximately 8 mg leghemoglobin/g nodule fresh weight at days 30-35.

Bacteroids recovered from a random sampling of nodules from soybean plants infected with KNS1 and KNS2 were found to be resistant to streptomycin indicating retention of the antibiotic marker used to construct the two mutants (Data not shown). Bacteroids recovered from KNS3 and KNS4 were found to be resistant to streptomycin and tetracycline.

Acetylene Reduction Assay

Nitrogenase enzyme activity was determined for soybean root nodules infected with the mutant strains KNS1 and KNS2 as well as the wild type USDA110 using the acetylene reduction assay (Figure 23 and 24**).** The development of acetylene reduction activity of the wild type and mutant KNS1 were similar in both the initiation of activity and the initial rate of increase. At approximately 19 days after inoculation, the rate of increase of acetylene reduction activity notably decreased for KNS1 relative to the wild type. Nodules formed by inoculation of the wild type and mutant KNS1 achieved similar

maximum acetylene reduction rates, but the maximal activity observed for nodules formed by mutant KNS1 were delayed nearly seven days (Figure 23).

The wild type and mutant KNS2 showed the same initiation of activity, but the mutant had a lower rate of increase and reached its maximal rate of activity earlier. The acetylene reduction activity of nodules formed by mutant KNS2 was less than 20% of that of the wild type strain (Figure 24).

The nitrogen fixation capacity of the complement strains KNS3 and KNS4 was assayed at 28 days after inoculation. KNS3, the complement of mutant KNS2, increased the nitrogen fixation capacity approximately twice that of the mutant strain and half that of the control indicating a partial restoration of wild-type phenotype (Figure 24). Loss of the complementation plasmid over time could explain the lower than wild-type levels of acetylene reduction at 28 days after inoculation though the increase in activity is in line with the restoration of blr0927-28 to the mutant KNS2. KNS4 surprisingly dropped the level of acetylene reduction that was found in KNS1 at 28 days by nearly threefold and to that of the wild-type USDA110 by more than two fold (Figure 23).

Nodule Development

Changes in the morphology following inoculation were studied using histochemical and structural stains. Staining of soybean seedlings two to five days after inoculation with methylene blue monitors the formation of curled root hairs, one of the earliest responses of soybean plants in the infection process of *B. japonicum* (Green and Emerich, 1999). Both mutants, KNS1 and KNS2 induced root hair curling that was

indistinguishable from wild-type USDA 110 at two and five days after infection (Figure 25).

Hematoxylin staining detects formation of nodule primordial foci, on soybean seedlings as early as two days after inoculation by chelating the abundance of Fe(III) in newly synthesized leghemoglobin. Foci are defined as patches of darkly stained, newly divided cells that have not yet begun to protrude from the surface of the root (Green et al., 1998). Hematoxylin staining for both mutants, KNS1 and KNS2, was not significantly different from what was seen in the wild type USDA110 control with dark, foci patches (Figure 26).

Nodule Morphology

Light microscopy of Toluidine Blue stained nodule cross sections and transmission electron microscopy (TEM) were used to observe changes in the morphology of mutants KNS1 and KNS2 when compared to the control USDA110 at 19 days and 35 days for KNS1 and 30 days for KNS2 (Figure 27). Light micrographs of soybean root nodules at 19 days after inoculation indicated that KNS1 had slightly fewer infected cells than the control with less differentiation in size than the control when compared to the uninfected cells. At 35 days after inoculation there were no apparent differences between KNS1 and the control. KNS2 exhibited smaller infected cells at both 19 and 30 days after infection than the control and more uninfected cells than the control. The location of infected cells in the central portion of the root nodule was the same as that seen in control. The ratio of uninfected cells to infected cells appeared to be greater in nodules formed by KNS2.

TEM images of both mutants showed no obvious difference in bacteroid number per infected cell of the plant nodule when compared to the control (Figure 28). Nodules formed by KNS1 exhibited no discernable difference in the number, size, spacing, or morphology of the infected cells from the control at 19 and 35 days after infection. KNS2, however, clearly had fewer infected cells than the wild-type control at 19 days after infection with larger air spaces between the cells. Additionally cells did not appear as smooth and rounded as in the control, but had irregular edges.

Bacteroid Poly- β-hydroxybutyrate Accumulation

Poly- β-hydroxybutyrate content increased over the time course as expected for the USDA 110 control (Karr et al., 1984) with values reaching approximately 3 ug PHB/ ug protein by 32 days (Figure 29). Nodules formed by KNS1 increased over time as well with 3.5 ug PHB/ ug protein peaking at 35 days after inoculation. Nodules formed by KNS2 peaked at 2.75 ug PHB/ ug protein at 30 days after inoculation, which was slightly lower than the control and KNS1, and unlike the other two strains then displayed a decrease in PHB by 34 days after inoculation.

Bacteroid Protocatechuate 3,4-Dioxygenase Activity

B. japonicum USDA 110 bacteroids had appreciable levels of PCA 3,4-dioxygenase activity over the time course (Figure 30). The level of activity declined from day 20 to 32 with an increase in activity at day 35 indicating a possible change over between the two PCA 3,4-dioxygenase homologs of *B. japonicum*. Nodules formed by KNS1 had similar maximum levels of activity as the wildtype with a shift in this activity

occurring several days after maximum activity of the control. This pattern follows with observed acetylene reduction pattern between KNS1 and the wildtype USDA110. Nodules formed by KNS2 surprisingly had a large increase in activity at 23 days after inoculation that was almost double the amount seen in the control and KNS1 (Figure 30).

Discussion

Phenolic compounds serve important roles in plant defense and signaling for soil microbes as well as being utilized for metabolic energy sources. Protocatechuate 3,4-dioxygenase is positioned at a metabolic conjunction where several phenolic metabolites are funneled into the β-ketoadipate pathway, which yields the TCA cycle intermediates, succinyl CoA and acetyl-CoA. Succinate has been demonstrated to provide the greatest rates of nitrogen fixation activity of isolated bacterods (Bergersen and Turner, 1967b; Stumpf and Burris, 1979) and which is compatible with the modified TCA cycle model that has been elucidated in *B. japonicum* bacteroids by biochemical and genetic means (Green and Emerich, 1997a; Shah and Emerich, 2006; Streeter and Salminen, 1993; Udvardi et al., 1989), and acetyl-CoA is the metabolic unit of poly- β-hydroxybutyrate, which can accumulate to greater than 60% of the bacteroid dry weight. Although the metabolism of phenolic compounds has been studied in cultured *B. japonicum*, the symbiotic relationship between phenolic metabolism and the symbiosis of *B. japonicum* bacteroids and soybean has not been well elucidated (Ito et al., 2006; Lorite et al., 1998; Parke and Ornston, 1986; Parke et al., 1985; Podila et al., 1993; Sudtachat et al., 2009; Waheeta and Mahadevan, 1997). To this end, each of the two *B. japonicum* protocatechuate 3,4-dioxygenases (PCAD) (blr0927-28;blr2333-34) open reading frames

were interrupted by insertion of streptomycin resistance cassettes creating mutants (KNS1;KNS2) to better understand the roles that phenolic compounds perform in bacteroids during symbiosis. Previously, blr2333-34 has been shown to be active in free living cells induced by a variety of phenolic metabolites (Ito et al., 2006; Sudtachat et al., 2009). In contrast, blr0927-28 has not been identified in proteomic or transcriptomic studies as being induced in the free living state or during symbiosis. This is surprising as blr0927-28 is part of a small cluster of genes that includes catechol 1,2-dioxygenase (blr0926) and the β-ketoadipate pathway terminal enzyme β-ketoadipate Co-A thiolase (blr0925), that are well represented in the proteomics of *B. japonicum* bacteroids (Delmotte et al., 2010; Sarma and Emerich, 2005).

Results from growth on a variety of carbon substrates are consistent with the known metabolic pathways in which several phenolic metabolites are channeled through protacatechuate 3,4 dioxygenase encoded by blr2333-34 (Ito et al., 2006; Sudtachat et al., 2009). In contrast, a physiological role for blr0927-28 has not been identified based upon the metabolites screened in culture. These results provide yet more evidence that in the free living form of pcaHG, encoded by blr2333-34 (KNS1), and not blr0927-28 (KNS2) is used in the aerobic degradation of protocatechuate and its derivative compounds for metabolic energy and growth.

There was no difference in the ability of KNS1 to cause root hair curling and no deficiency in the ability of KNS1 to invade cortical cells and initiate the formation of nodule primordial (Figure 26). The mitotic phase of soybean nodule development (Newcomb, 1981) appeared to be unaffected, but the expansion phase proceeded more slowly than the wild type. The light micrographs and TEM images of nodules formed by

KNS1 at 19 and 35 days appear to have the same number of infected cells and uninfected cells as that seen in the control (Figures 25 and 26). The most notable features of the nodules formed by KNS1 were the delays in accumulation of nodule mass and in maximum acetylene reduction activity by 6-8 days when compared to the wild type control. However, the amount of total nitrogen fixation by KNS1 could be greater than control when integrating the area under the curve for acetylene reduction activity.

The delay in maximal nitrogen fixation is similar to that observed with *B. japonicum* mutants of isocitrate dehydrogenase (Shah and Emerich, 2006), α-ketoglutarte dehydrogenase (Green and Emerich, 1997a), genes involved in production of acidic exopolysaccharides, lipopolysaccharides, and capsular polysaccharide surface components (*exo, exp, lps*) (Parniske et al., 1993; Parniske et al., 1994), the *ndvC* (nodule development) gene (Bhagwat and Keister, 1995),and the nodule formation efficiency gene (*nfe*) (Deshmane and Stacey, 1989). The light and electron micrographs of KNS1 nodules and those of the isocitrate and α-ketoglutarte dehydrogenase show a delay in proper infected cell population/colonization, but not in bacteroid maturation, that is the ability to reduce atmospheric dinitrogen. The isocitrate and α-ketoglutarte dehydrogenase mutants produced fewer bacteroids than the wild type, but each bacteroid yielded the same *ex planta* acetylene reduction activity suggesting a limitation in a population/colonization step, which if completed effectively allowed the bacteria to develop to the functional bacteroid state. The similar phenotype of the nodules formed by KNS1 suggests a similar limitation in a population/colonization step.

Complementation of KNS1 had restored the growth on 4-hydroxybenzoic acid confirming its role in aerobic phenolic degradation (Sudtachat et al., 2009). This

indicates that the function of blr0927-28 in protocatechuate metabolism is necessary for a fully functional nitrogen fixing symbiosis.

Symbiotically, complementation of KNS1 resulted in a decrease in acetylene reduction activity at 28 days (Figure 23). At 28 days the acetylene reduction activity of nodules formed by KNS1 was approximately 70% of that of the wild type. The acetylene reduction of nodules formed by KNS4 was 25% of that of nodules formed by KNS1 and 36% of that formed by wild type nodules. The loss of expression of blr2333-2334 resulted in an increase in acetylene reduction activity at 28 days, but complementation of KNS1, presumable through multiple copies of blr2333-2334 resulted in reduced acetylene reduction activity, suggesting this particular isozyme of protocatechuate 3,4-dioxygenase influences the temporal expression of nitrogen fixation.

Consistent with the delay in the mass of nodules formed by inoculation with KNS1 was the delay in the accumulation of leghemoglobin present in the nodules (Figure 22). The need to sequester the bacteroids from exogenous levels of free oxygen is crucial to maintaining active levels of nitrogen fixation (Bergersen, 1997; Bergersen et al., 1982; Layzell et al., 1990). The reduced leghemoglobin contents is notable considering that protocatechuate dioxygenase requires molecular oxygen for activity. Leghemoglobin resides in the infected cell but not within the symbiosome in which the bacteroids are located. Thus, the bacteroids are not in contact with leghemoglobin, which raises the question about how molecular oxygen is transported to the bacteroid surface. Protocatechuate may not only perform a role in supplying succinyl-CoA, but also in maintaining low oxygen concentrations within the symbiosome space.

The number, size, and shape of the KNS1 bacteroids present in the infected nodules qualitatively appeared to be the same as the control. KNS1 bacteroids had similar levels of PHB per ug protein as the wild type control (Figure 29). KNS1 bacteroids had comparable levels of protocatechuate 3,4-dioxygenase activity suggesting blr2333-2334 contributes little to the overall activity found within bacteroids or that blr0927-0928, or another cryptic dioxygenase compensates for the loss of blr2333-blr2334.

The interruption of blr0927-28 did not significantly affect the growth of free-living bacteria when cultured on protocatechuate precursors (Ito et al., 2006). Complementation of KNS2 had no effect on the growth of cultured bacteria on various phenolic compounds (Table 23).

The ability of KNS2 to curl root hairs and form nodule primordial was the same as the wild type control (Figures 25 and 26). However, the symbiotic phenotype of KNS2 was markedly different from that of KNS1. No nodules were found on the tap root of plants inoculated with KNS2. All nodules were formed on the lateral roots with nodules for acetylene reduction assays being taken from the first lateral roots around the tap root. Inoculation of soybeans with the complemented strain, KNS3, resulted in nodulation on the crown of the tap root, indicating the mutant phenotype was due to blr0929 and not to a downstream polar effect.

The ontogeny of KNS2 nodule development showed the failure to progress from the mitotic phase of nodule development to the expansion phase . Light micrographs and TEM images of KNS2 clearly indicate that the mutant strain was unable to infect cells at the same rate as the control (Figures 27 and 28). The number of uninfected cells were approximately double that of the control with larger air-spaces between the nodule cells.

The uninfected cells were considerable smaller consistent with the inability to progress to the expansion phase of nodule development. Nodules formed by KNS2 displayed a similar nodule phenotype to the α-ketoglutarate dehydrogenase mutant with many uninfected cells and large spaces between the infected and uninfected cells (Green and Emerich, 1997b).

Detectable acetylene reduction activity of nodules inoculated with KNS2, KNS1 and USDA 110 occurred on the same day, also suggesting the infection and early events are not affected significantly by the mutations (Figures 23 and 24). Acetylene reduction values for nodules inoculated with KNS2 were considerably lower through the time course and were 5 fold lower compared to the maximal activity of the wild type control (Figure 24). Acetylene reduction activity and nodule mass accumulation followed the same pattern (Figure 21). The nitrogen fixation profile of KNS2 was similar to a α-ketoglutarate dehydrogenase mutant of *B. japonicum* that had similar reduced fixation capacity (Green and Emerich, 1997b). The commonality between the *pcaHG* mutant KNS2 and the α-ketoglutarate dehydrogenase mutant are their roles in providing succinyl-CoA to the TCA cycle of the bacteroid. These mutants suggest that disruption of succinyl-CoA flux to the bacteroid negatively impacts the ability of the bacteroid to fix atmospheric nitrogen.

Acetylene reduction activity was partially restored in the complementation strain KNS3, doubling the activity of the mutant KNS2, and being approximately half that of the wild-type control (Figure 24). Full restoration of activities during symbiosis is difficult in *B. japonicum* as the complementation plasmid is likely to be lost from the bacteria if not kept under selective antibiotic selection. The partial restoration of activity

lends support to the contention that the phenotype of KNS2 is based solely on the mutation of blr0927-28and not a polar event on a downstream gene. This indicates that the function of blr0929 downstream of the insertion was not likely affected by the insertion of the streptomycin cassette as normal root crown nodules were formed.

Leghemoglobin levels of nodules from KNS2 were similar to that seen in KNS1 with a steady increase in concentration over time, which is in contrast to the wild type control that had steady state levels of leghemoglobin from 20 days to 35 days (Figure 22). These results support the contention that the function of Blr0927-28 in protocatechuate metabolism is necessary for a fully functional nitrogen fixing symbiosis.

Surprisingly, the levels of protocatechuate 3,4-dioxygenase activity of bacteroid extracts of KNS2 were nearly double that of the wild type control at 23 days, the day of maximal acetylene reduction activity, and continued through day 30 (Figure 30). These results suggest that the bacteroid was attempting to restore functional symbiosis by inducing protocatechuate dioxygenase activity, perhaps blr2333-34.

The accumulation of PHB by KNS2 bacteroids was greater that the wild type or KNS1 at 20 and 23 days, but less at 34 days (Figure 29). The reduction of PHB content at 34 days suggests the bacteroids are mobilizing this storage compound.

In summary, the results indicate that protocatechuate 3,4-dioxygenase formed by Blr2333-34 was not necessary for nitrogen fixation activity, but does perform a role in the early development of the root nodule. In contrast, blr0927-28 was necessary for an effective nitrogen fixing symbiosis with *B. japonicum*. Although the functional role of each protocatechuate dioxygenase remains to be identified, these enzymes serve as a

metabolic conjunction to provide protocatehcuate catabolites, particularly succinyl-CoA to the partial citric acid cycle of the bacteroid.

Table 21. Strains and Plasmids used in this study

Strain or Plasmid	Genotype or Markers	Source or Reference
E. coli		
Xl-1 Blue Supercompetent Cells	*recA1 endA1 gyrA96 thi-1 hsdR17 supE44 relA1 lac* [F´ *proAB lacI*q*ZΔM15* Tn*10* Tet^R]	Stratagene
WM3064	Donor strain for conjugation:*thrB1004*, *pro*, *thi*, *rpsL*, *hsdS*, *lacZ*ΔM15, RP4-1360, Δ(*araBAD*)567, Δ*dapA*1341::[*erm pir*(wt)]	Saltikov & Newman 2003
B. japonicum		
USDA 110	Cm^R (wild type)	
KNS1	110 (Blr2333-34::str), Cm^R, Str^R	This study
KNS2	110 (Blr0927-28::str), Cm^R, Str^R	This study
KNS3 (pKNS137)	KNS2, Cm^R, Str^R, Tet^R	This study
KNS4 (pKNS138)	KNS2, Cm^R, Str^R, Tet^R	This study
Vectors		
pKOTcII	Suicide vector, Tet^R	Stacey Lab
pBlueScript SK II (+)	Amp^R, *lacZ*, f1 ori, MCS, Mob^-	Fermentas
pLOI	Km^R, *sacB*, RP4 *oriT*, ColE1 *ori*	Lenz et al. 1994
pHP45Ω	Amp^R, Str^R/$Spec^R$ in Ω cassette	Prentki and Krisch 1984
pRK311	RK2 origin, Tra^+, Mob^-, Tet^R, λ cos *lacZ(α)*	Ditta et al. 1985
pKNS114	Tet^R, 2.5 kb fragment of Blr2333-34 in the XcmI site of pKOTCII	This study
pKNS115	Tet^R, 2.5 kb fragment of Blr0927-28in the XcmI site of pKOTCII	This study
pKNS127	Amp^R, XbaI/SalI 2.5 kb fragment of pKNS115 ligated into XbaI/SalI sites of pBluescriptSKII(+)	This study
pKNS128	Amp^R,Str^R, pKNS127 with a ~630 bp BglII deletion in Blr0927-28 and a 2.0 kb BamHI Ω insertion	This study
pKNS129	Str^R, Kan^R, XbaI/SalI fragment of pKNS128 inserted into the XbaI/SalI site of the suicide vector pLOI	This study
pKNS132	Amp^R, XbaI/XhoI 2.5 kb fragment of pKNS114 ligated into XbaI/XhoI sites of pBluescriptSKII(+)	This study
PKNS133	Amp^R,Str^R, pKNS132 with a ~750 bp AgeI deletion in Blr2333-34and a 2.0 kb XmaI Ω insertion	This study
pKNS134	Str^R, Kan^R, XbaI/XhoI fragment of pKNS128 inserted into the XbaI/XhoI site of the suicide vector pLOI	This study
pKNS137	Tet^R, pcr amplified region of Blr0927-28 in the HindIII site of	This study

	pRK311	
pKNS138	Tet^R, pcr amplified region of Blr2333-34 in the HindIII site of pRK311	This study

Table 22. Primers used in this study

Name	Description	Sequence
KS141	500 bp upstream of the N terminal of Blr2333 Forward	5'-cag gtg cag gct ctt cac ct -3'
KS142	500 bp downstream of the C terminal of Blr2334 Reverse	5'-tct act aca cga ccc tca tc-3'
KS143	500 bp upstream of the N terminal of Blr0927 Forward	5'-aga acc agg acc ccg agc aa-3'
KS144	500 bp downstream of the C terminal of Blr0928 Reverse	5'-ctg atc cgg ctc gcg cat gg-3'
KS155	100 bp upstream of the N terminal of Blr0927 Forward	5'-tgg tact cg ctc gac cac acc tac c-3'
KS156	Reverse of the C terminal Blr0928	5'-tca cac gtc gaa gaa cac cgt ctc gtt-3'
KS157	HindIII flank for the N terminal of Blr0927-28 Forward	5'-aag ctt aag ctt aag ctt tgg tact cg ctc gac cac acc tac c-3'
KS158	HindIII flank for the C terminal Blr0927-28 Reverse	5'-aag ctt aag ctt aag ctt tca cac gtc gaa gaa cac cgt ctc gtt-3'
KS160	100 bp upstream of the N terminal of Blr2333 Forward	5'-ctt ctt cca gca cgg cga gga a-3'
KS161	Reverse of the C terminal Blr2334	5'-tca gac gtc gaa gaa cac ggt ctc ct-3'
KS162	HindIII flank for the N terminal of Blr2333-34 Forward	5'aag ctt aag ctt aag ctt ctt ctt cca gca cgg cga gga a-3'
KS163	HindIII flank for the C terminal Blr2333-34 Reverse	5'-aag ctt aag ctt aag ctt tca gac gtc gaa gaa cac ggt ctc ct-3'
KS168	600 bp upstream of the N terminal of Blr0927 for genomic screening Forward	5'-gtg gac aag gat ggc cgt c-3'
KS169	600 bp downstream of the C terminal of Blr0928 for genomic screening Reverse	5'-cgt aat cct tgc gga gct gg-3'
KS170	600 bp upstream of the N terminal of Blr2333 for genomic screening Forward	5'-cgt gat cat gag atc gca ccg-3'
KS171	600 bp downstream of the C terminal of Blr2334 for genomic screening Reverse	5'-cga cat cga cta cag gcg tct-3'
KS172	N terminal forward for streptomycin	5'-aca ttt gta cgg ctc cgc a-3'
KS173	C terminal Reverse for streptomycin	5'-tta aag ttt cat tta gcg cct caa ata ga-3'

Table 23. Growth phenotype on selected carbon substrates for *B. japonicum* strains. *B. japonicum* USDA110, mutant strains KNS1 and KNS2, and their complements KNS3 and KNS4 were grown on defined Tully's medium with selected carbon sources as outlined in the materials method. Positive (+) growth indicates that colonies formed after two-four weeks after plating. Negative (-) indicates no discernable colony growth after two-four weeks after plating.

Carbon Substrate	USDA 110	KNS1	KNS2	KNS3	KNS4
Malate (20 mM)	+	+	+	+	+
Succinate (20 mM)	+	+	+	+	+
4-Hydroxybenzoic Acid (2 mM)	+	–	+	+	+
Vanillic Acid (2 mM)	+	–	+	+	+
3-Hydroxybenzoic Acid (2mM)	+	–	+	+	+
2,5-Dihydroxybenzoic Acid (2 mM)	–	–	–	–	–

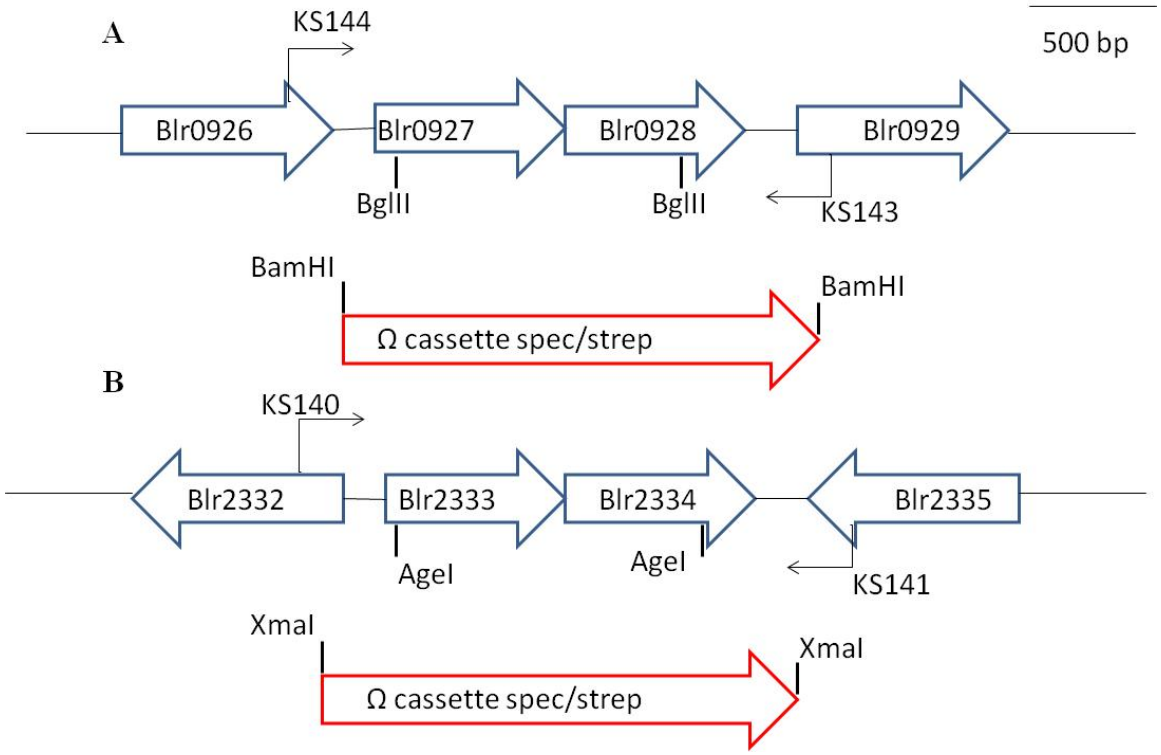

Figure 19. Physical map of the *B. japonicum pcaHG* mutants KNS1(B) and KNS2(A) from the genes blr2333-34 and blr0927-28 interrupted with the Ω cassette (red). Relevent restriction enzymes are shown.

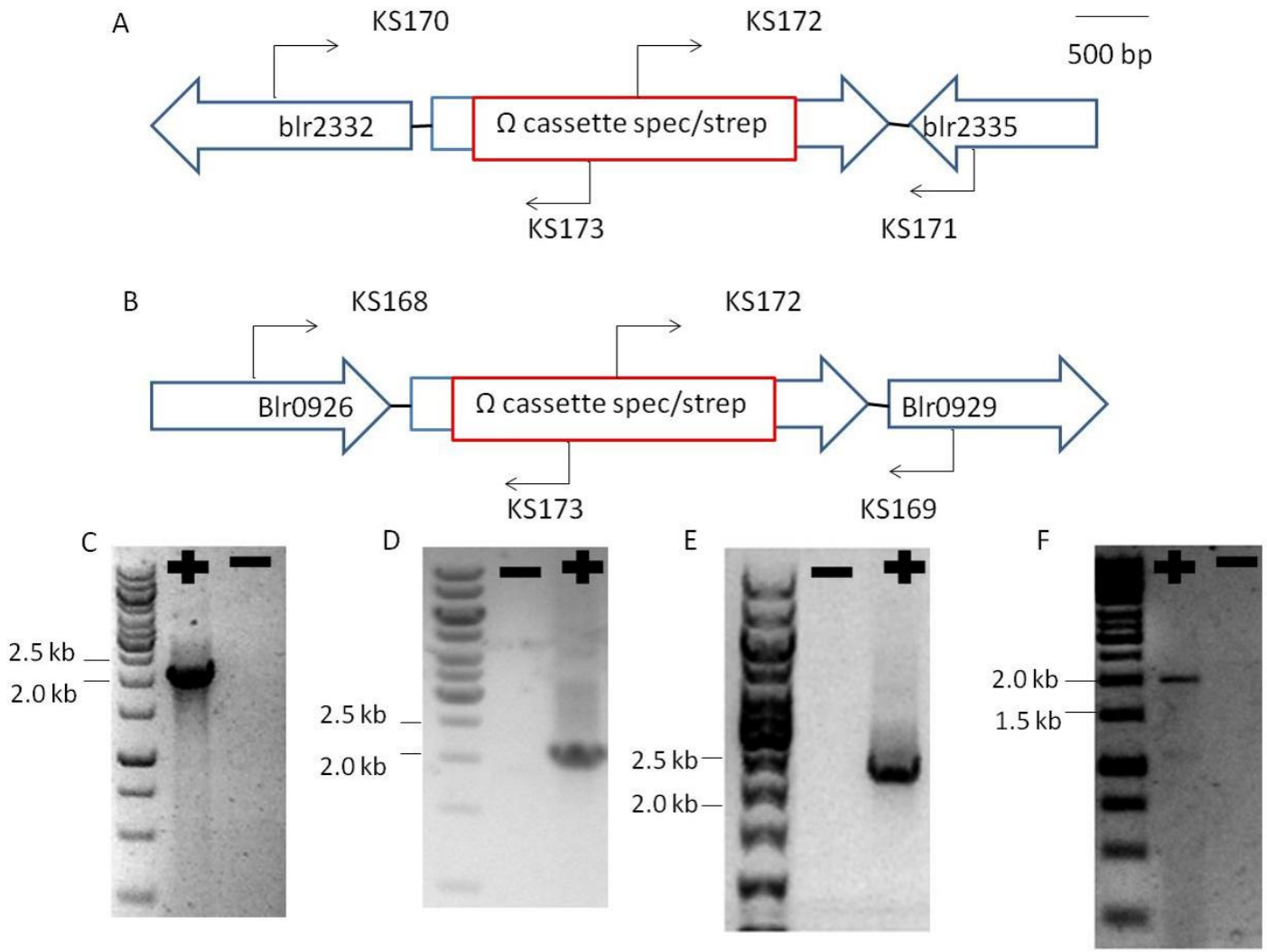

Figure 20. Physical map of mutant KNS1 (A), KNS2 (B), 5' PCR product of KNS1 made with primers KS170/KS173-2,160 bp (C), 3' PCR product of KNS2 from primers KNS172/KS171-2,110 bp, (D), 5' PCR product of KNS2 made with primers KS168/KS172-2200 bp (E), 3' PCR product KNS2 from primers KS172/KS169-1990 bp (F). (+) indicates PCR product of expected size. (-) indicates control PCR reaction with wild type template DNA.

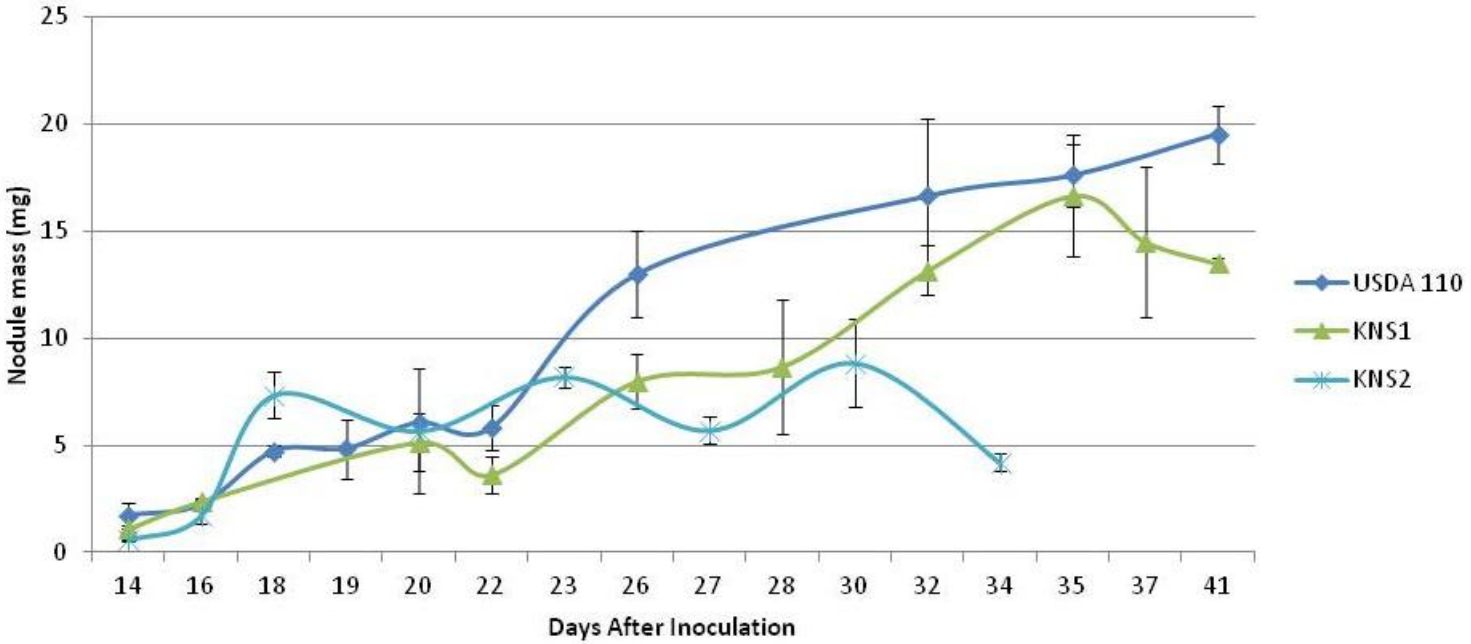

Figure 21. Average nodule fresh mass as a function of time of soybean plants inoculated with *B. japonicum* strains USDA110, KNS1, and KNS2.

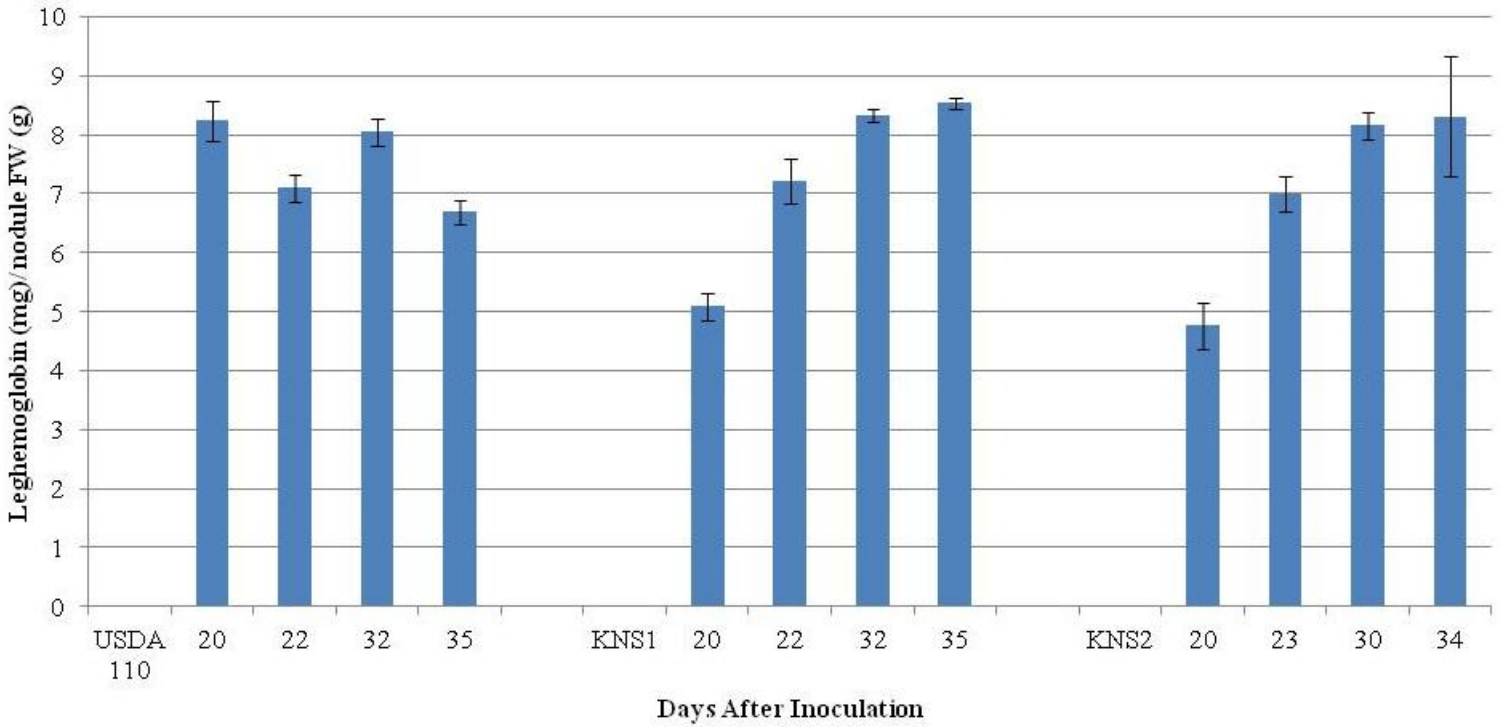

Figure 22. Average leghemoglobin concentration (mg) per gram nodule for *B. japonicum* strains USDA110, KNS1, and KNS2.

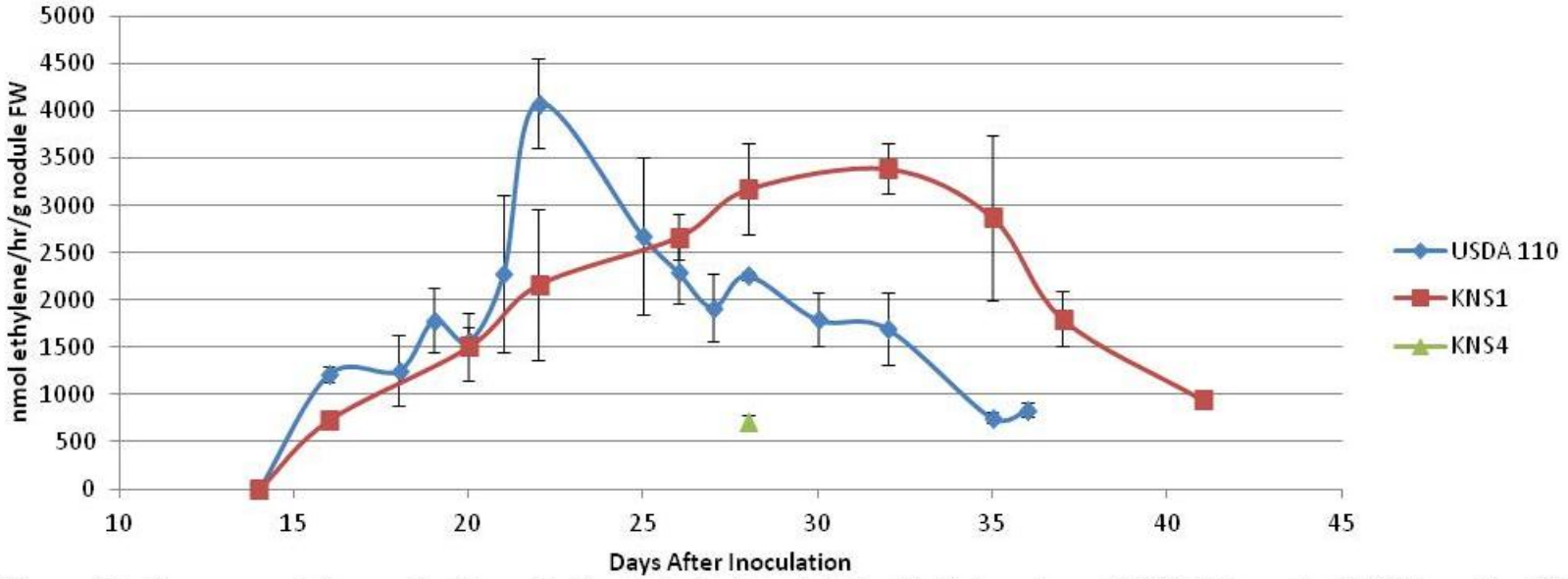

Figure 23. Average acetylene reduction activity of plants inoculated with *B. japonicum* USDA110, mutant KNS1, or the KNS1 compliment, KNS4.

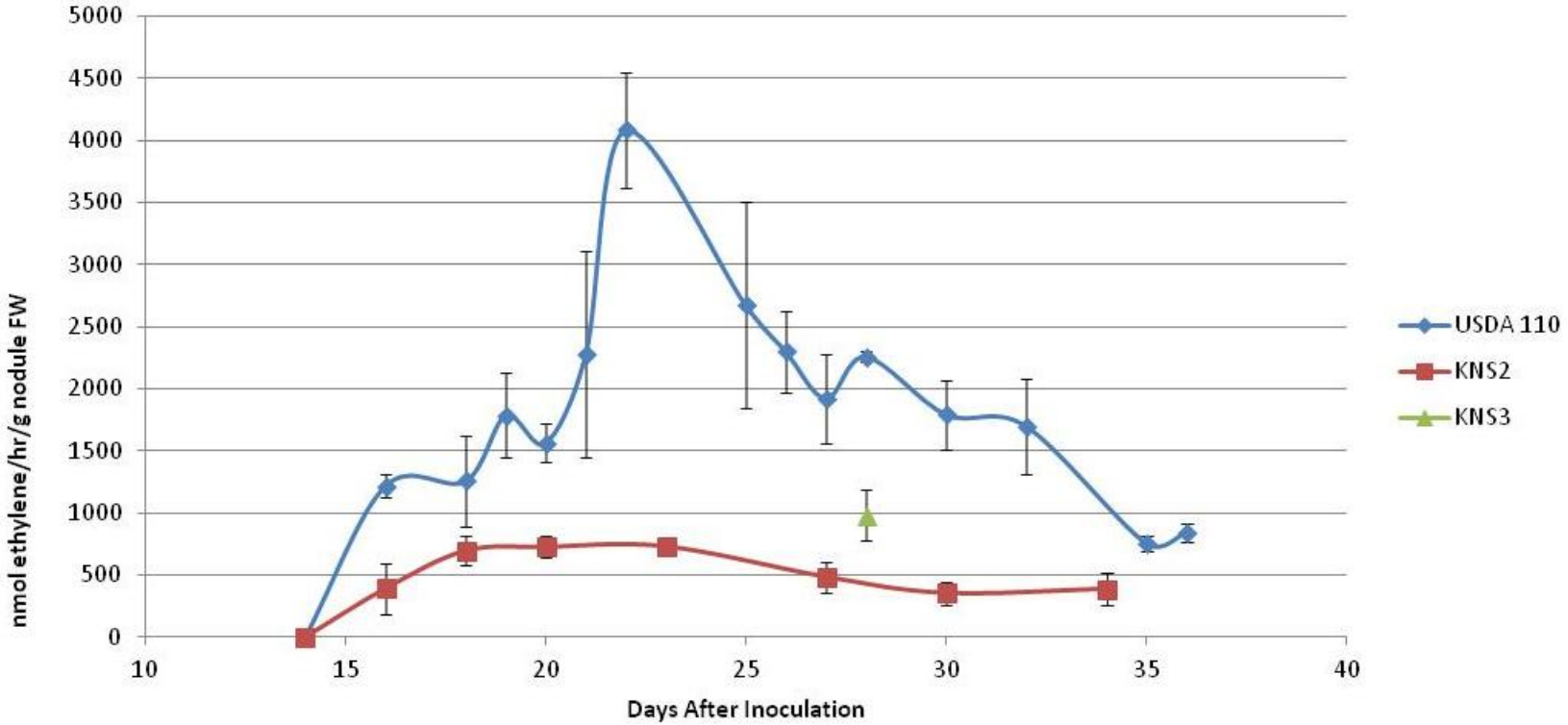

Figure 24. Average acetylene reduction activity of plants inoculated with *B. japonicum* USDA110, mutant KNS2, and the KNS2 compliment, KNS3.

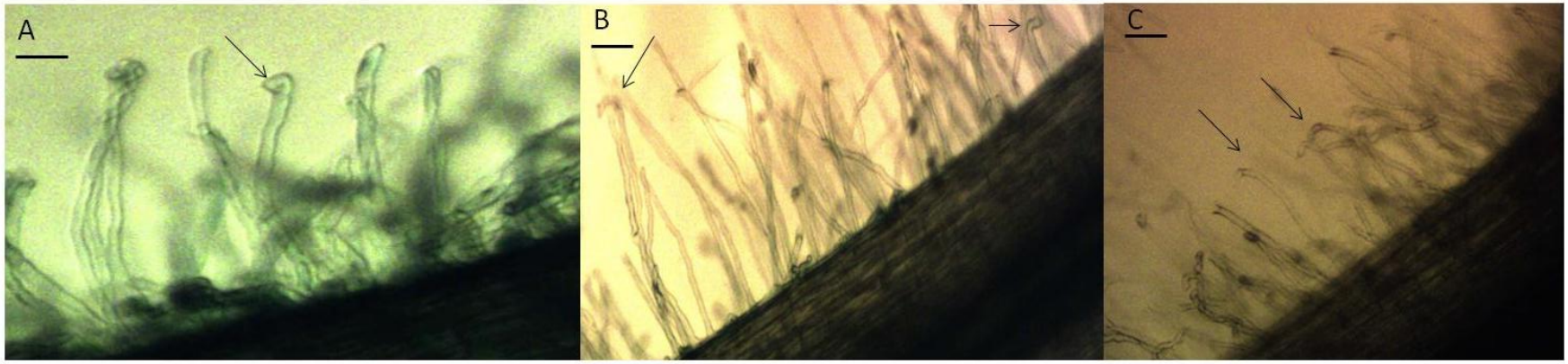

Figure 25. Methylene blue stained root hairs showing root hair curling. Soybean seedlings were harvested 5 days after inoculation with the *B. japonicum* strains USDA110(A), KNS1(B), and KNS2(C) and were stained with methylene blue and visualized as outlined in the Materials and Methods. Scale bars = 0.25mm.

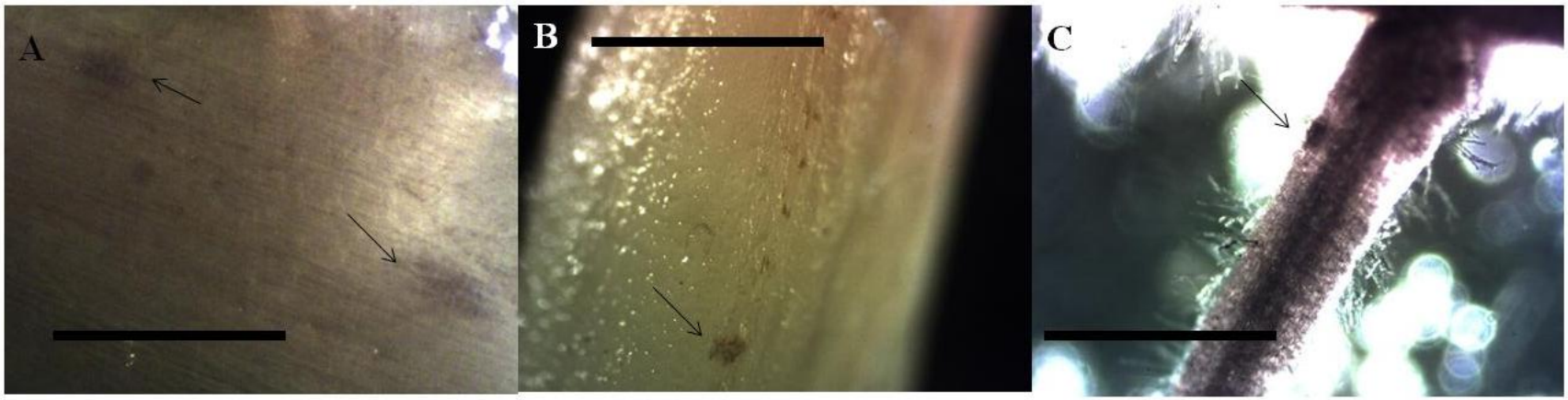

Figure 26. Haematoxylin-stained soybean root segments indicating staining of nodule primordia foci. Soybean roots were stained with haemalatoxylin at 5, 2, and 8 days after inoculation with *B. japonicum* strains KNS1 (A), KNS2 (B), and USDA 110 (C). Scale bars = 1mm.

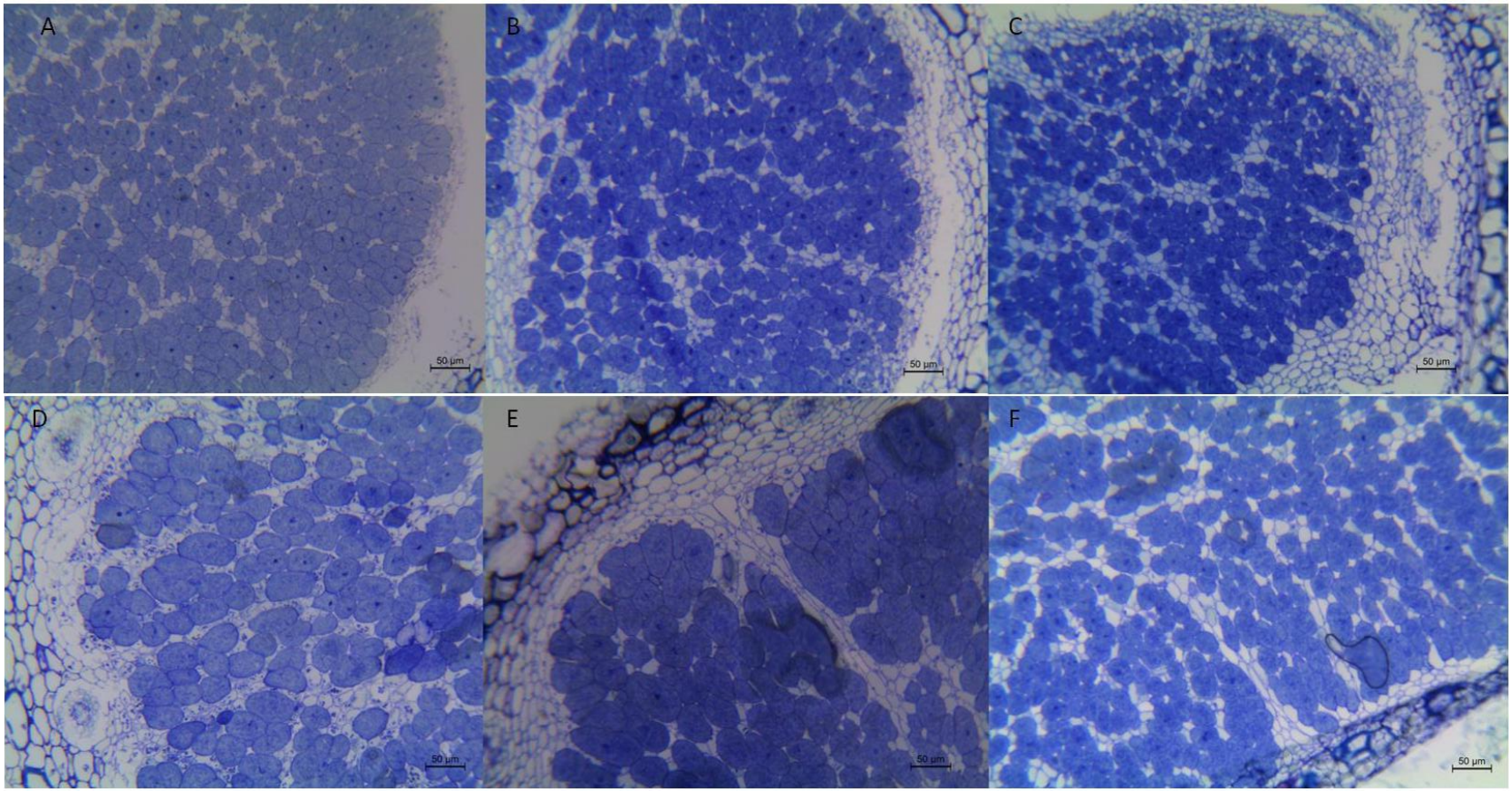

Figure 27. Light micrographs of nodules formed by USDA 110 19 (A) and 35 (D) , KNS1 19 (B) and 35 (E), KNS2 19 (C) and 30 (F) day old nodule cross sections stained with toluidine blue. Scale bars = 50 µm.

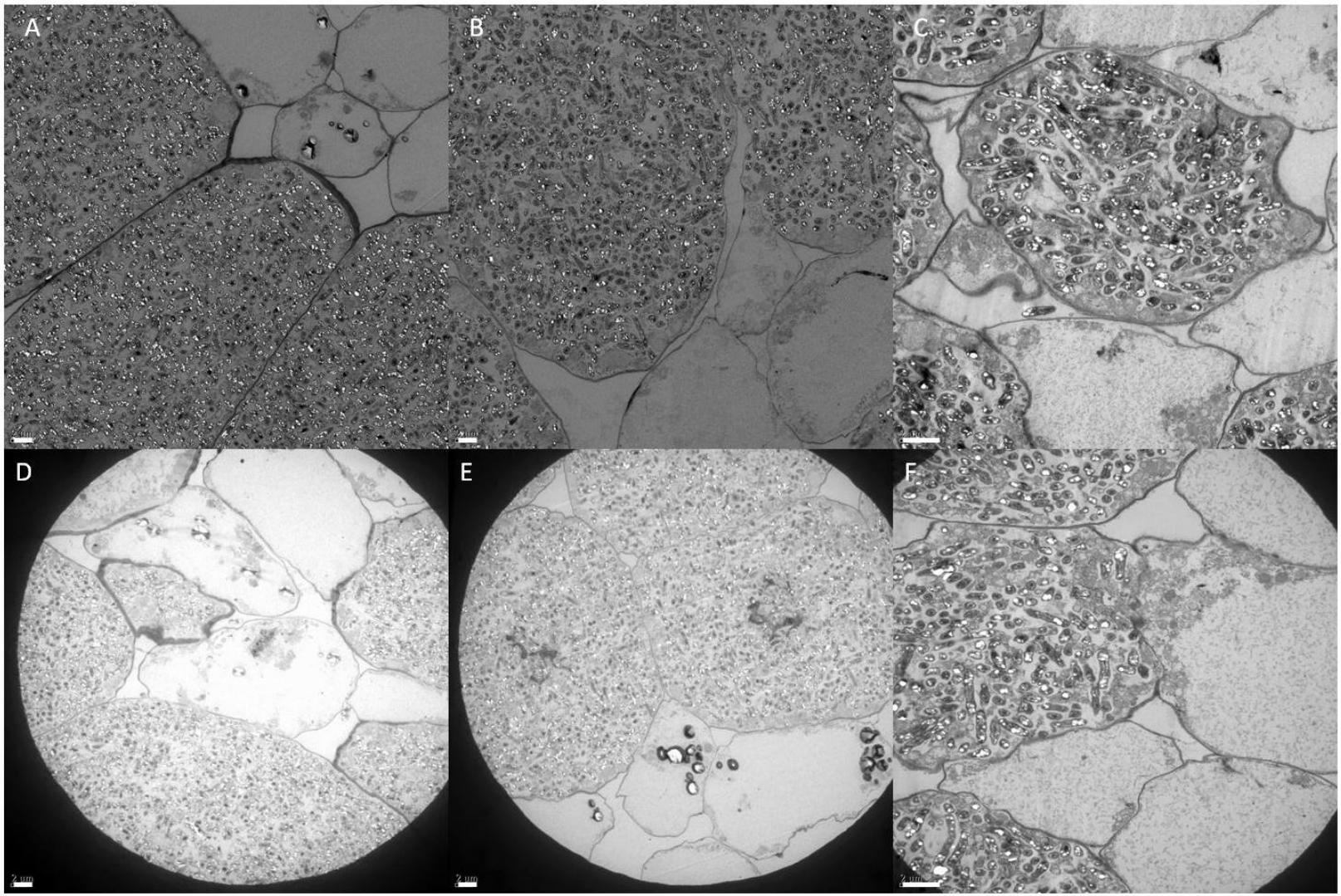

Figure 28. Transmission electron micrographs of nodules formed by USDA 110 19 (A) and 35 (D) , KNS1 19 (B) and 35 (E), KNS2 19 (C) and 30 (F) day old nodule cross sections. Scale bars = 2 µm.

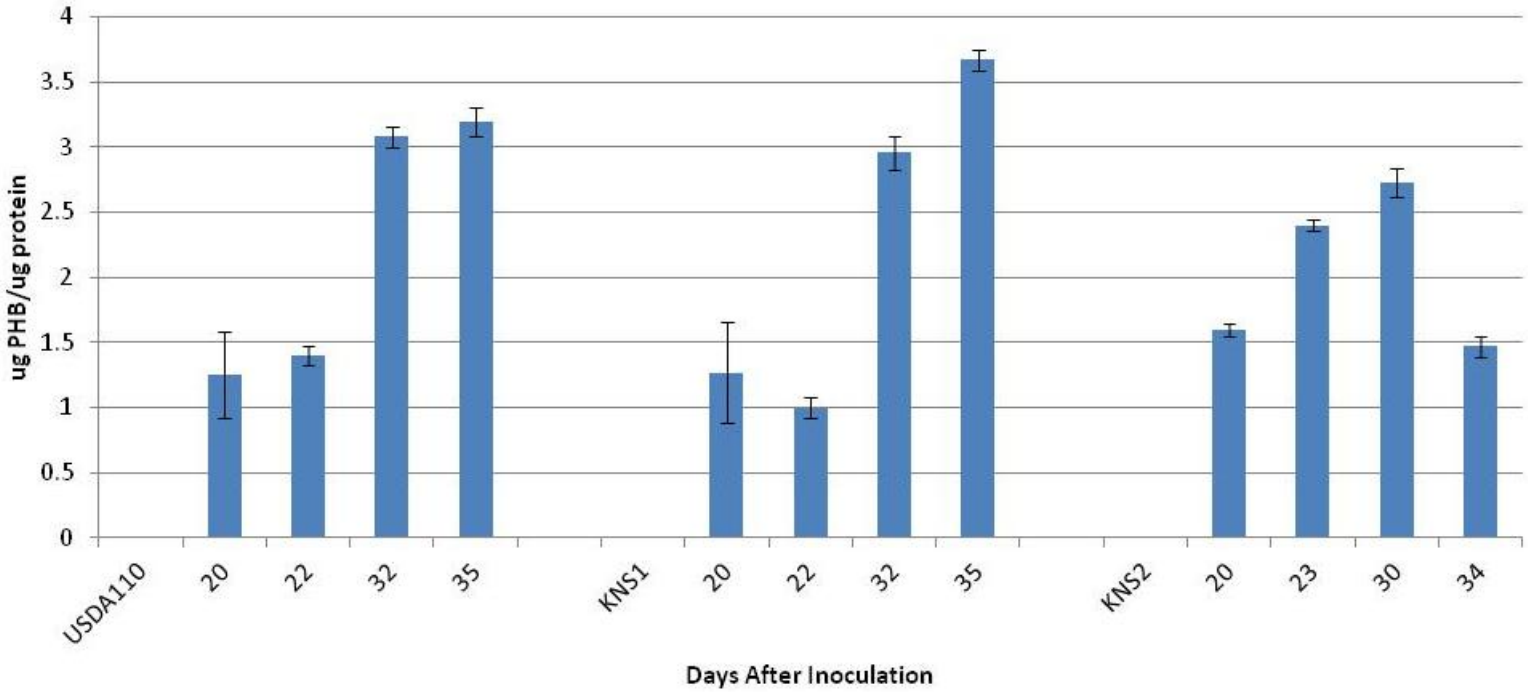

Figure 29. Average poly-hydroxybutyrate concentration (ug of crotonic acid) per ug bacteroid protein in *B. japonicum* strains USDA110, KNS1, and KNS2.

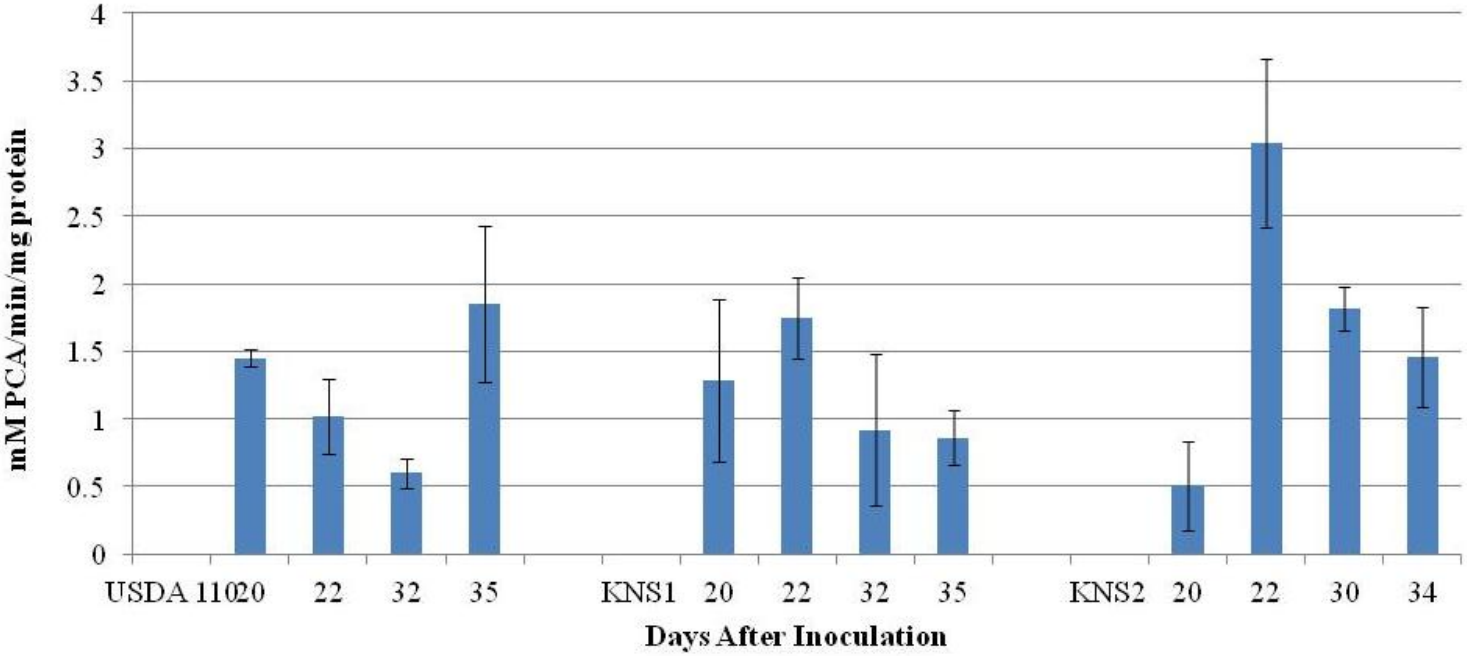

Figure 30. Average protocatechuate 3,4-dioxygenase activity of bacteroids recovered from soybean root nodules infected by *B. japonicum* strains USDA110, KNS1, and KNS2.

Chapter V

Bradyrhizobium japonicum bacteroid appendages expressed in senescing and argon-treated soybean nodules

Symbiosis **(2011) 54:95-100**

Abstract

Bradyrhizobium japonicum bacteroids in soybean nodules expressed fibrillar appendages during senescence. In both scanning and transmission electron microscopy (SEM and TEM), these structures were observed to connect adjacent bacteroids, and bacteroids to symbiotic membranes. They were 20–25 nm in diameter, 100–2,500 nm in length and were linear, branched, or part of a web-like matrix. Bacteroids expressing appendages were not uniformly distributed, but were abundant within localized regions in the senescing nodule. The root systems of nodulated greenhouse-grown plants flushed with argon induced the appendages at earlier plant ages, and they were more prolific and wide spread than those in untreated nodules. *Bradyrhizobium japonicum* symbiotic appendages appear to be a response to an environmental niche within senescing nodules.

Introduction

Bacteria produce several types of fibrillar appendages each with unique functions; flagella, pili or fimbriae, and nanowires. A typical flagellum of a Gram negative eubacterium is a helically wound hollow cylinder with a diameter between 15 and 20 nm made up of protein subunits (flagellin), a hook and a complex basal body, which mediates insertion of the flagellum into the cell envelope. Its rotation relative to the cell body

provides cellular motility. More than 10 separate proteins are required for flagella, which can achieve lengths of 8 μm.

The terms pili and fimbriae are often used interchangeably, but some researchers employ the term pilus exclusively for the structure required for bacterial conjugation. Pili and fimbriae are like flagella in that they are cytoplasmic protrusions through the cell membrane and penetrate through the peptidoglycan layers of the cell wall. The best characterized pili are Type I (Duguid and Campbell, 1969; Martinez et al., 2000), Type IV (Freitag et al., 1995; Gibiansky et al., 2010; Koga et al., 1993), and curli pili (Kikuchi et al., 2005; Olsen et al., 1989). Pili and fimbriae are hollow structures composed of a single protein. Sex pili number 1–4 per cell, common pili or Type 1 fimbriae are 100–200 per cell. Typical pili and fimbriae are 2–8 nm in diameter and can vary from 0.5 to 10 μm in length. Curli pili are thin aggregate amyloid fibers, 1–2 nm in diameter, that perform roles in cell adhesion and long term survival (Wang and Chapman, 2008).

Nanowires are bacterial appendages, 50 nm to >150 nm in diameter, that have been reported in several bacterial species, and are believed to function in conducting electrons from bacteria in reduced oxygen environments toward those bacteria located in regions in which oxygen is more abundant to promote the continuance of metabolism in anoxic environments (Gorby et al., 2006; Nielsen et al., 2010; Reguera et al., 2005). In *Shewanella oneidensis*, redox-active cytochrome c is proposed to occupy the core of the nanowire with the iron atoms of the heme promoting electron flow (Gorby et al., 2006). However, the actual mechanism of transport within these structures remains to be demonstrated.

Bradyrhizobium japonicum is a dimorphic soil microorganism that forms a symbiotic association with soybean resulting in a new organ on the root of the plant called a nodule. The cultured form of *B. japonicum* is unusual in that it has two types of subpolar flagella, one thick flagellum (22 nm) and several thin flagella (12 nm) (Kanbe et al., 2007). The *B. japonicum* genome possesses two sets of flagellar gene clusters and several small operons containing a few flagellar genes (Kaneko et al., 2002b). Kanbe et al. (2007) demonstrated that the thick flagellum is encoded by the gene cluster beginning at 6,375 kbp and the thin flagella at 7,545 kbp. Krishnan et al. (2011) reported that the flagella of two strains of *Sinorhizobium fredii* were similar in structure, but their pili were different, indicating variability among strains grown in culture.

The symbiotic forms of *B. japonicum*, called bacteroids, which reduce atmospheric dinitrogen within the plant-derived microaerophilic environment of the nodule, are devoid of flagella (Bisset and Hale, 1951). As nodules senescence, *B. japonicum* bacteroids have the genetic ability to transform to a saprophytic lifestyle and express chemotactic mobility which would require flagella. Here we report on the appearance of inter-bacteroid and intra-bacteroid-plant membrane appendages during soybean nodule senescence.

Materials and Methods

Nodules were obtained from soybean (Pioneer 93 M11) plants, grown at the Bradford Research and Extension Center of the University of Missouri, harvested at intervals (34, 43, 49, 55, 71 and 95 days after planting) over the entire growing period, and from soybean (Williams 82) plants, inoculated with *B. japonicum* USDA 110, grown

in a greenhouse of the Sears Plant Growth Facility at the University of Missouri. The nodulated roots of greenhouse grown plants were either untreated or flushed continuously with argon (Ar) for 7 days beginning at 28 days after planting. Acetylene reduction on nodulated tap root segments were performed as described by (Karr et al., 1984).

For scanning electron microscopy (SEM), nodules were freed of soil, cleaned and fixed in 2% glutaraldehyde/2% paraformaldehyde in 0.1 M cacodylate buffer, followed by buffer rinses. Secondary fixation was in aqueous 1% osmium tetroxide, followed by water rinses and dehydration in a graduated ethanol series to 90% ethanol. Nodules were then frozen in liquid nitrogen, fractured, processed through 100% ethanol and critical point dried, mounted on aluminum stubs, sputter-coated with platinum and examined with a Hitachi S-4700 Scanning Electron Microscope. The soybean nodules for transmission electron microscopy (TEM) were prepared at the University of Missouri Electron Microscopy core facility (http://www.emc.missouri.edu/). Briefly sliced nodule sections were treated with primary fixative (2% glutaradedhye, 2% paraformaldehyde) rinsed with 0.1 M sodium cacodylate, 0.01 M 2-mercaptoethanol, 0.13 M sucrose buffer (2-ME buffer). Secondary fixation was 1% buffered osmium tetroxide, rinsed with 2-ME buffer and then ultra pure Milli-Q water. An acetone dehydration series (20, 50, 70, 90, & 3 x 100%) was followed by infiltration of Epon-Spurr's resin and polymerization. Ultrathin sections (85 nm), collected using a Leica Ultracut UCT microtome fitted with a 45° Diatome diamond knife, were placed on 200 mesh copper thin bar grids and double post stained with 5% uranyl acetate (UA) and Sato's triple lead stain (Pb) (3 min Pb, 18 min UA, 8 min Pb). Samples were viewed with a JEM-1400 JEOL TEM.

Bacteroids were isolated from nodules immediately after harvest and kept at 4°C for proteomic and transcriptomic analysis (Chang et al., 2007; Sarma and Emerich, 2005). Proteomic analyses were performed as described previously Sarma and Emerich (2005), and transcriptomic analyses were performed as described by Chang et al. (2007) with mid-log phase arabinose-cultured *B. japonicum* as comparative control.

Results & Discussion

Nodules harvested from the root crown of field-grown soybean plants at 34, 43, 49, 55, 71 and 95 days after planting were examined by acetylene reduction activity and SEM. At 55 days after planting, the acetylene reduction activity of the plants had markedly declined and continued to decline to negligible activity at day 95 (Fig. 31). When observed under the SEM, prior to 55 days after planting, bacteroids appear as rod-shaped cells frequently in physical contact with other bacteriods and with no obvious protruding appendages (Fig. 32a). There appeared to be little, if any, morphological change of the bacteroids during senescence even at 95 days after planting as they retained their normal size and shape (Fig. 32b, c). At 55 days after planting, fibrils were first observed occasionally connecting two adjacent bacteroids. By day 95, these fibrils were more apparent throughout the bacteroid population, and became highly abundant within specific locales, which accounted for 15–20% of the entire bacteroid population (Fig. 32b, c, and e). Beyond 95 days it was not possible to physically remove the older nodules as they disintegrated upon removal from the soil. These fibers were observed in frozen nodules of similar ages collected in two previous years (data not shown). We were unable to locate any previous reports of electron micrographs of soybean nodules at similar stages of senescence for comparison.

Bradyrhizobium japonicum bacteroid fibrillar appendages were ~20–25 nm in diameter and up to 2,500 nm in length. The diameter was similar to those of flagella of other organisms, but smaller than those of nanowires and larger than those of pili and fimbriae (Gorby et al., 2006; Kanbe et al., 2007; Reguera et al., 2005). These structures could be linear, branched, or form web-like networks among adjacent bacteroids (Fig. 32b, c, d, and f). The fibrillar appendages were also found to connect to (Fig. 32c) and possibly transect (Fig. 32e) symbiosome membranes.

Transmission electron micrographs of 95, but not 49, day old nodules showed fibrillar structures within symbiosomes in the space surrounding the bacteroids (Fig. 33a). The symbiotic fibrils appeared as linear, branched and web-like structures like the appendages observed in the SEMs. In contrast, the surface appendages of cultured *S. fredii* were only linear (Krishnan et al., 2011). The symbiotic fibrils appeared to attach, or integrate into the symbiosome and bacteroid membranes (Fig. 33b, c, d, e, f). The fibrillar network appeared to connect symbiosome membranes to bacteroid membranes (Fig. 33b, c), and between bacteroid membranes (Fig. 33d, e, f), similar to the patterns observed in the scanning electron micrographs. The TEMs, like the SEMs, showed fibrils that appeared to transect the symbiosome membrane (Figs. 32e and 33b). The maximal observed width of the fibrils is consistent with the diameters of the appendages observed in the SEMs.

Transcriptomic (Fig. 34) and proteomic (data not shown) analyses were performed on bacteroids from nodules harvested at each time point. None of the annotated pili or flagellar genes of *B. japonicum* showed positive increases in expression over the entire interval from 34 to 95 days after planting that correlated with the

appearance of bacteroid appendages. Only bll5826, a flagellar synthesis protein, *fliM*, in the thick flagella cluster, showed significant fold increase in expression in this interval (Fig. 4), but still remained well below the cultured cell control. As only a portion of bacteroids expressed appendages in abundance, the size of this population may preclude identification of the responsible genes via transcriptomic analysis. Proteomic analysis failed to identify a single annotated pilar or flagellar protein during this time interval (data not shown).

There are relatively few reports on legume nodule senescence to put the observations reported here into a physiological context (Puppo et al., 2005), and none which microscopically examined nodule structure during late senescence. Evans et al. (1999) have shown that oxidative stress occurs during soybean nodule senescence in green-house grown plants. A plant nodule-specific heme protein, leghemoglobin (Lb), provides oxygen to the bacteroids during the period of symbiotic functioning. The advent of senescence is noted by the degradation of Lb leaving the bacteria without an oxygen transport mechanism. Evans et al. (1999) have measured the traits associated with oxidative stress during a 10.5 week period in nodules of green house grown plants. The appearance of bacteroid appendages, in localized regions of field-grown soybean nodules began to appear at ~8 weeks and proliferated through 13.5 weeks. The inherent differences in green-house and field nodules do not permit a temporal alignment, and the localized occurrences of the appendages imply an environmental or nutritional influence that is not uniform throughout the senescing nodule.

The correlation of the appearance of the appendages as Lb degrades suggested they were expressed as a function of available oxygen. To test this hypothesis, the root

systems of 4 week old greenhouse grown soybean (Williams 82) plants were flushed with argon for 7 days after which the nodules at the crown were examined for bacteroid appendages (Fig. 32f). The nodules of untreated plants were devoid of bacteroid appendages. The argon treatment resulted in a greater frequency of the structures relative to that observed in 95 day old field nodules.

Apparent in the Ar-treated nodules were clusters of bacteroids similar to those found within symbiosomes (Fig. 32d). Clusters of ~10–20 bacteroids exist within symbiosomes and are bounded by a plant-derived, symbiosome membrane. These clusters were observed only in the Ar-treated nodules. The expression of the appendages in both field and greenhouse-inoculated plants demonstrates that they are not dependent on the strain of *B. japonicum* or the cultivar of soybean.

The viability of bacteroids during senescence has been debated (Karr and Emerich, 1988; Tsien et al., 1977). The expression of the bacteroid appendages requires appreciable transcriptional and translational activity by bacteroids during late nodule senescence demonstrating that at least a portion of the bacteroid population is metabolically active during the later stages of senescence. The activity could be in response to the changing oxygen and nutrient status or a systematic transformation to a saprophytic lifestyle.

The senescing nodule may present a variety of microenvironments, some of which are suitable for the expression of the bacteroid appendages. The role of the symbiotic appendages is not known, but the localized occurrence within nodules and their increased expression in Ar-treated nodulated root systems suggests they are produced in response to

an environmental niche that develops in senescing nodules, perhaps in response to variations in oxygen supply to groups of bacteroids.

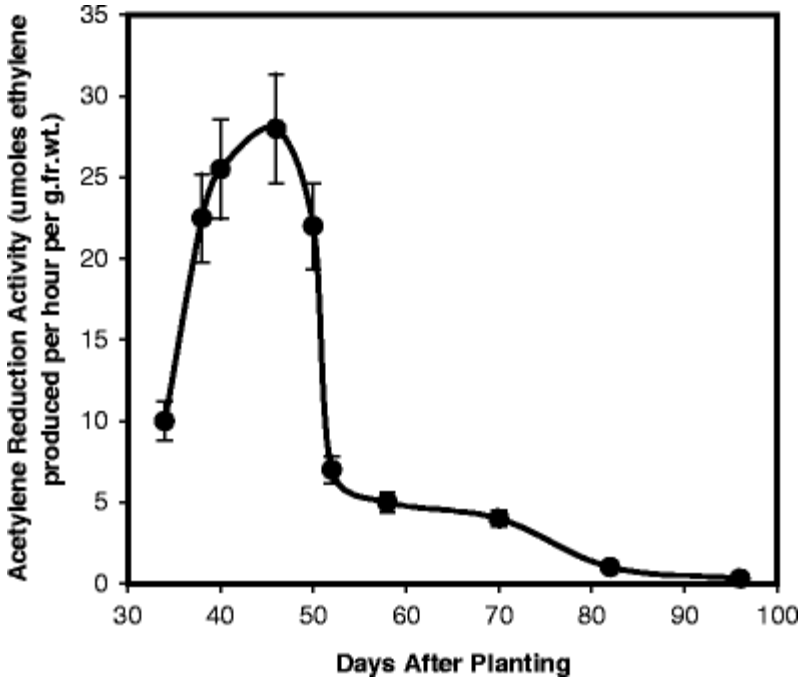

Figure 31. Acetylene reduction of field-grown soybean plants. Pioneer 93 M11 soybean plants, grown at the Bradford Experimental Station, were removed from the soil and the nodulated taproot was cut quickly and fitted into 20 mL glass serum bottles, capped and acetylene was added to 10% of the total volume. One mL gas samples were removed at 4 min intervals, sealed and returned to the laboratory for analysis as described by Karr et al. (1984)

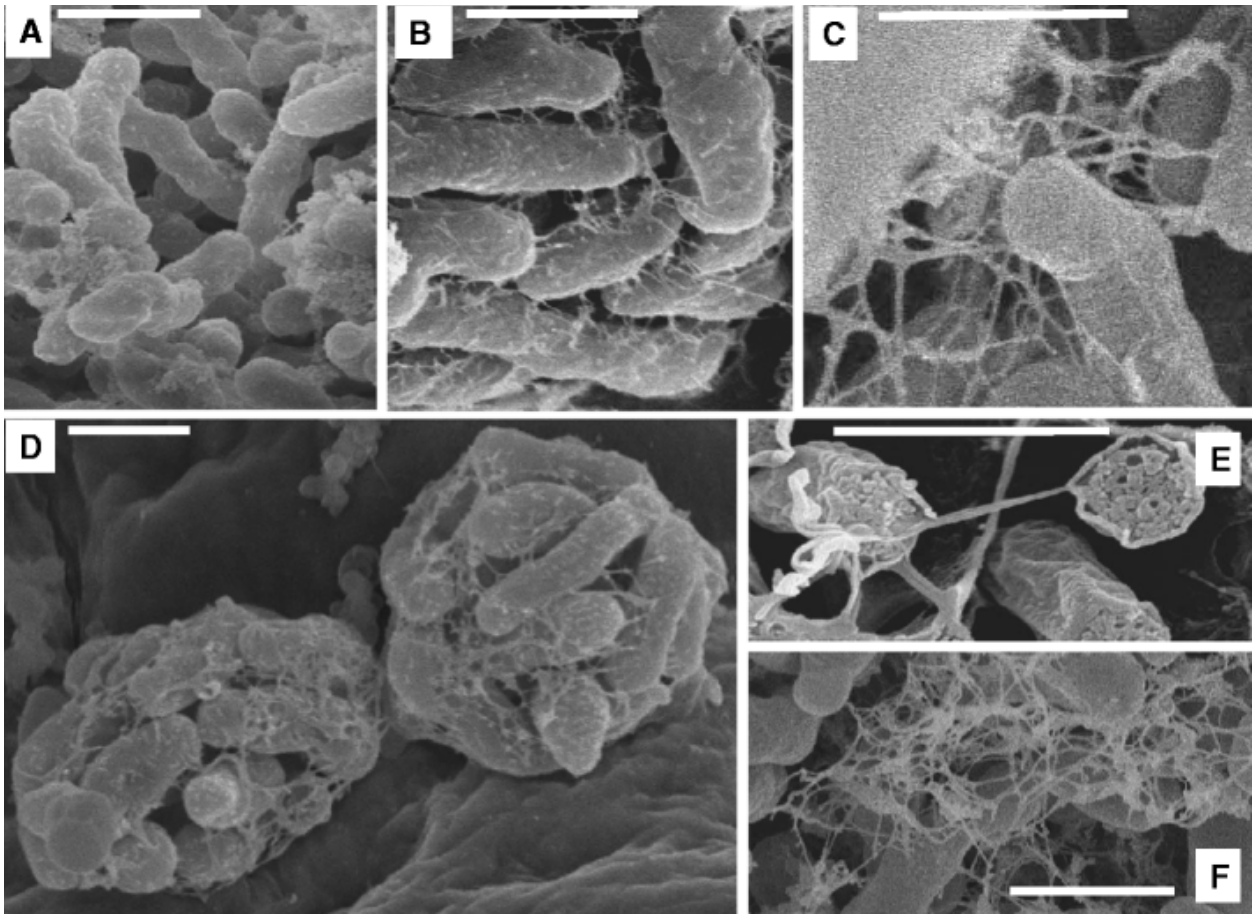

Figure 32. Scanning electron micrographs of bacteroids within soybean nodules. Bacteroids from field grown nodules at (**a**) 43 days after planting; (**b**, **c**) 95 days after planting; (**e**) 71 days after planting, and (**d**, **f**) bacteroids from 35 day old greenhouse-grown nodules flushed with argon for 7 days prior to harvest. The bar on each figure represents 1 μm

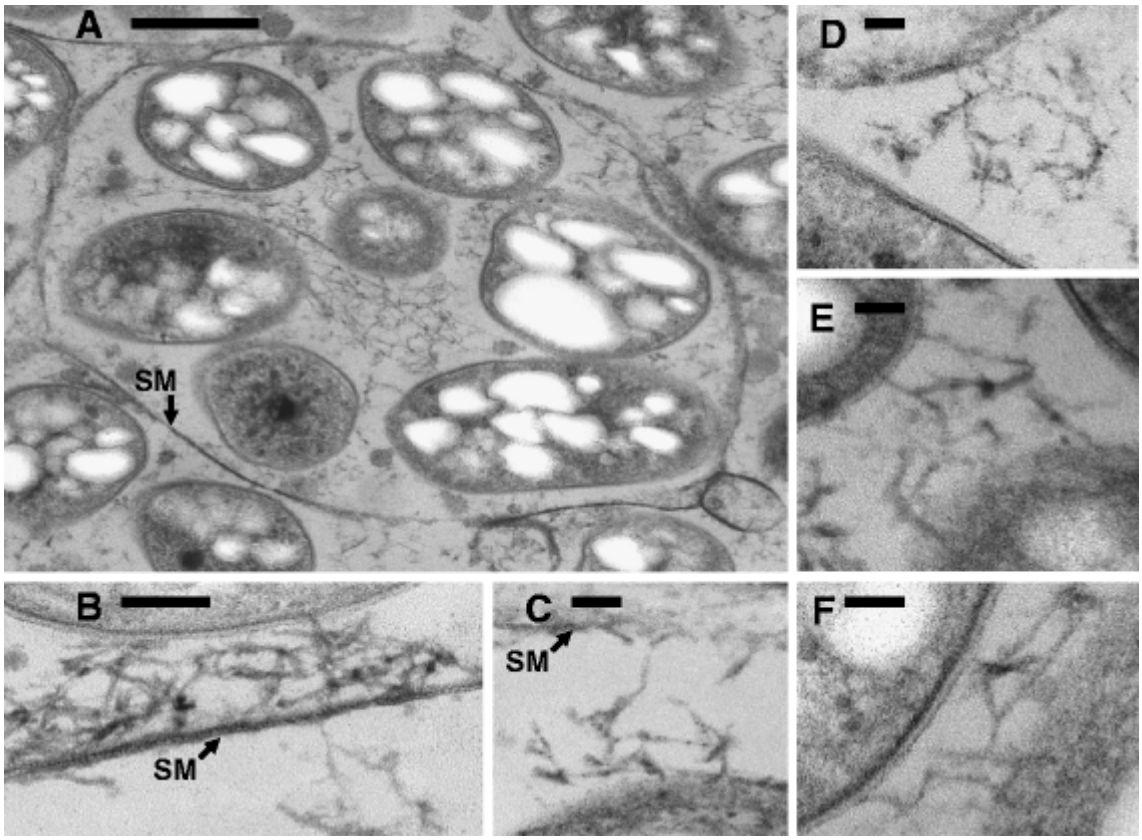

Figure 33. Transmission electron micrographs of 95 day old soybean nodules. A symbiosome containing 7 bacteroids in the plane of the micrograph with appendages within the symbiosome space (**a**). Appendages connecting bacteroids to the symbiosome membrane (**b**) and (**c**) and to other bacteroids (**d**–**f**). The bar on figure (**a**) represents 400 nm and on figures (**b**–**f**) represents 50 nm. SM refers to the symbiosome membrane

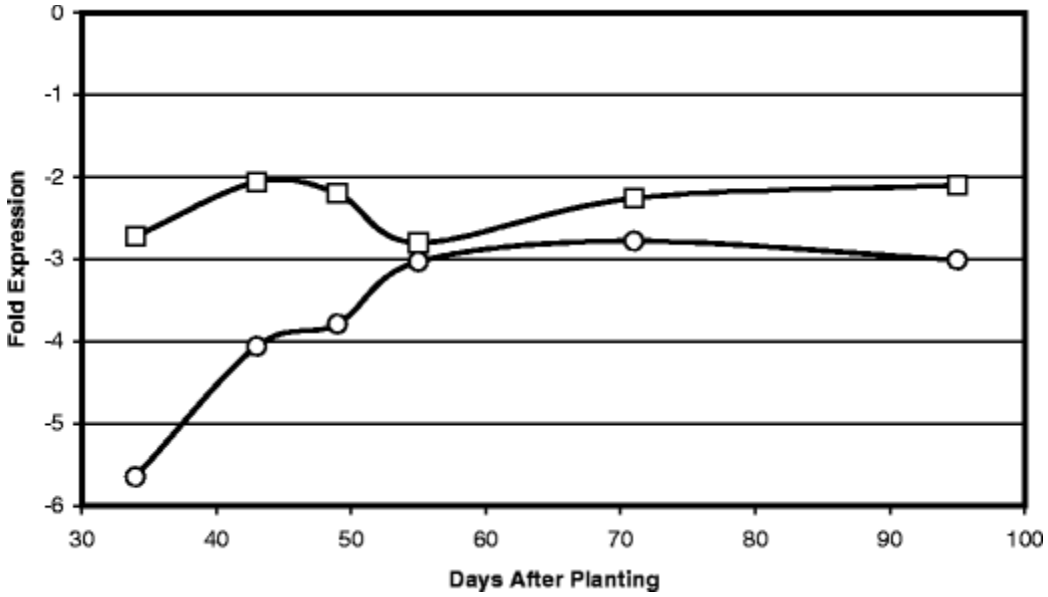

Figure 34. Transcriptomic analysis of bacteroids isolated from nodules of different ages. Pioneer 93 M11 soybean plants, grown at the Bradford Experimental Station, were removed from the soil, immediately placed in ice and transported back to the lab where bacteroids were isolated at 4°C. RNA isolation, cDNA preparation and transcriptomic analysis were performed as described by Chang et al. (2007). The transcriptomic analysis of bll5814 (□) and bll5826 (○) are shown. The pattern of bll5814 is representative of the annotated flagella and pili genes of *B. japonicum* bacteroids (Chang et al. 2007)

Bibliography

Albrecht S.L., Maier R.J., Hanus F.J., Russell S.A., Emerich D.W., Evans H.J. (1979) Hydrogenase in Rhizobium japonicum Increases Nitrogen Fixation by Nodulated Soybeans. Science 203:1255-7. DOI: 203/4386/1255 [pii] 10.1126/science.203.4386.1255.

Allaway D., Lodwig E.M., Crompton L.A., Wood M., Parsons R., Wheeler T.R., Poole P.S. (2000) Identification of alanine dehydrogenase and its role in mixed secretion of ammonium and alanine by pea bacteroids. Mol Microbiol 36:508-15. DOI: mmi1884 [pii].

Altincicek B., Kollas A.K., Sanderbrand S., Wiesner J., Hintz M., Beck E., Jomaa H. (2001) GcpE is involved in the 2-C-methyl-D-erythritol 4-phosphate pathway of isoprenoid biosynthesis in Escherichia coli. J Bacteriol 183:2411-6. DOI: 10.1128/JB.183.8.2411-2416.2001.

Ames G.F.L. (1988) Structure and mechanism of bacterial periplasm transport systems. J. Bioenerg. Biomembr. 20:1-18.

Aneja P., Charles T.C. (1999) Poly-3-hydroxybutyrate degradation in Rhizobium (Sinorhizobium) meliloti: isolation and characterization of a gene encoding 3-hydroxybutyrate dehydrogenase. J Bacteriol 181:849-57.

Aneja P., Dziak R., Cai G.Q., Charles T.C. (2002) Identification of an acetoacetyl coenzyme A synthetase-dependent pathway for utilization of L-(+)-3-hydroxybutyrate in Sinorhizobium meliloti. J Bacteriol 184:1571-7.

Anthon G.E., Emerich D.W. (1990) Developmental regulation of enzymes of sucrose and hexose metabolism in effective and ineffective soybean nodules. Plant Physiol 92:346-51.

Appels M.A., Haaker H. (1988) Identification of cytoplasmic nodule-associated forms of malate dehydrogenase involved in the symbiosis between Rhizobium leguminosarum and Pisum sativum. Eur J Biochem 171:515-22.

Appels M.A., Haaker H. (1991) Glutamate Oxaloacetate Transaminase in Pea Root Nodules : Participation in a Malate/Aspartate Shuttle between Plant and Bacteroid. Plant Physiol 95:740-7.

Aprison M.H., Magee W.E., Burris R.H. (1954) Nitrogen fixation by excised soy bean root nodules. J Biol Chem 208:29-39.

Ardissone S., Frendo P., Laurenti E., Jantschko W., Obinger C., Puppo A., Ferrari R.P. (2004) Purification and physical-chemical characterization of the three

hydroperoxidases from the symbiotic bacterium Sinorhizobium meliloti. Biochemistry 43:12692-9. DOI: 10.1021/bi048836s.

Arwas R., Glenn A.R., McKay I.A., Dilworth M.J. (1986) Properties of double mutants of Rhizobium leguminosarum which are defective in the utilization of dicarboxylic acids and sugars. J. Gen. Microbiol. 132:2743-2747.

Atkins C.A., Smith P. (2000) Uriede synthesis in legume nodules Horizon Scientific Press, Wymondham, UK.

Ausubel F.M., Brent R., Kingston R.E., Moore D.D., Seidman J.G., Smith J.A., Struhl K. (2002) Short Protocols in Molecular Biology Wiley.

Babst M., Hennecke H., Fischer H.M. (1996) Two different mechanisms are involved in the heat-shock regulation of chaperonin gene expression in Bradyrhizobium japonicum. Mol Microbiol 19:827-39.

Bardin S., Dan S., Osteras M., Finan T.M. (1996) A phosphate transport system is required for symbiotic nitrogen fixation by Rhizobium meliloti. J Bacteriol 178:4540-7.

Barnett M.J., Toman C.J., Fisher R.F., Long S.R. (2004) A dual-genome Symbiosis Chip for coordinate study of signal exchange and development in a prokaryote-host interaction. Proc Natl Acad Sci U S A 101:16636-41. DOI: 10.1073/pnas.0407269101.

Barsch A., Carvalho H.G., Cullimore J.V., Niehaus K. (2006) GC-MS based metabolite profiling implies three interdependent ways of ammonium assimilation in Medicago truncatula root nodules. J Biotechnol 127:79-83. DOI: S0168-1656(06)00503-7 [pii]10.1016/j.jbiotec.2006.06.007.

Bassarab S., Schenk S.U., Werner D. (1989) Fatty acid composition of the peribacteroid membrand and the ER in nodules of *Glycine max* varies after infection by different strains of the microsymbiont. Bot. Acta. 102:196-201.

Batista J.S., Torres A.R., Hungria M. (2010) Towards a two-dimensional proteomic reference map of Bradyrhizobium japonicum CPAC 15: spotlighting "hypothetical proteins". Proteomics 10:3176-89. DOI: 10.1002/pmic.201000092.

Baumberger I.C., Fraefel N., Gottfert M., Hennecke H. (2003) New NodW- or NifA-regulated Bradyrhizobium japonicum genes. Mol Plant Microbe Interact 16:342-51. DOI: 10.1094/MPMI.2003.16.4.342.

Becana M., Dalton D.A., Moran J.F., Iturbe-Ormaetxe I., Matamoros M.A., Rubio M.C. (2000) Reactive oxygen species and antioxidants in legume nodules. Physiologia Plantarum 109:372-381.

Becana M., Klucas R.V. (1990) Enzymatic and nonenzymatic mechanisms for ferric leghemoglobin reduction in legume root nodules. Proc Natl Acad Sci U S A 87:7295-9.

Becana M., Paris F.J., Sandalio L.M., Del Rio L.A. (1989) Isoenzymes of Superoxide Dismutase in Nodules of Phaseolus vulgaris L., Pisum sativum L., and Vigna unguiculata (L.) Walp. Plant Physiol 90:1286-92.

Becker A., Berges H., Krol E., Bruand C., Ruberg S., Capela D., Lauber E., Meilhoc E., Ampe F., de Bruijn F.J., Fourment J., Francez-Charlot A., Kahn D., Kuster H., Liebe C., Puhler A., Weidner S., Batut J. (2004) Global changes in gene expression in Sinorhizobium meliloti 1021 under microoxic and symbiotic conditions. Mol Plant Microbe Interact 17:292-303. DOI: 10.1094/MPMI.2004.17.3.292.

Bedekovics T., Li H., Gajdos G.B., Isaya G. (2011) Leucine Biosynthesis Regulates Cytoplasmic Iron-Sulfur Enzyme Biogenesis in an Atm1p-independent Manner. J Biol Chem 286:40878-88. DOI: 10.1074/jbc.M111.270082.

Bendsten J.D., Binnewies T.T., Hallin P.F., Sicheritz-Ponten T., Ussery D.W. (2005a) Genome Update: Prediction of Secreted Proteins in 225 Bacterial Proteomes. Microbiology Comment 151:1725-1727.

Bendsten J.D., Kiemer L., Fausboll A., Brunak S. (2005b) Non-classical Protein Secretion in Bacteria. BMC Microbiology 5:58-71.

Bendsten J.D., L.J. Jensen, N. Blom, G. von Heijne, S. Brunak. (2004) Feature-based Prediction of Non-Classical and Leaderless Protein Secretion. protein Engineering, Design, & Selection 17:349-356.

Bergersen F.J. (1997) Regulation of nitrogen fixation in infected cells of leguminous root nodules in relation to O_2 supply. Plant Soil 191:189-203.

Bergersen F.J., Kennedy C., Hill S. (1982) Influence of low oxygen concentration on derepression of nitrogenase in Klebsiella pneumoniae. J Gen Microbiol 128:909-15.

Bergersen F.J., Peoples M.B., Turner G.L. (1991) A role for poly-β-hydroxybutyrate in bacteroids of soybean nodules. Proc. R. Soc. Lond. B 245:59-64.

Bergersen F.J., Turner G.L. (1967a) Nitrogen fixation by the bacteroid fraction of breis of soybean root nodules. Biochimica et Biophysica Acta 141:507-515.

Bergersen F.J., Turner G.L. (1990) Bacteroids from soybean root nodules:accumulation of poly-β-hydroxybutyrate during supply of malate and succinate in relation to N2 fixation in flow-chamber reactions. Proc. R. Soc. Lond. B 240:39-59.

Bergersen J.F., Turner G.L. (1967b) Nitrogen fixation by the bacteroid fraction of breis of soybean root nodules. Biochim Biophys Acta 141:507-15.

Bergsson G., Agerberth B., Jornvall H., Gudmundsson G.H. (2005a) Isolation and identification of antimicrobial components from the epidermal mucus of Atlantic cod (Gadus morhua). FEBS J 272:4960-9. DOI: EJB4906 [pii]10.1111/j.1742-4658.2005.04906.x.

Bergsson G., Agerberth B., Jornvall H., Gudmundsson G.H. (2005b) Isolation and Identification of Antimicrobial Components from the Epidermal Mucus of Atlantic Cod (*Gadus morhua*). FEBS Journal 272:4960-4969.

Bernardelli C.E., M.F. Luna, M.L. Galar, and J.L. Boiardi. (2001) Periplasmic PQQ-dependent glucose oxidation in free-living and symbiotic rhizobia. Curr. Microbiol. 42:310-315.

Bestel-Corre G., Dumas-Gaudot E., Poinsot V., Dieu M., Dierick J.F., van T.D., Remacle J., Gianinazzi-Pearson V., Gianinazzi S. (2002) Proteome analysis and identification of symbiosis-related proteins from Medicago truncatula Gaertn. by two-dimensional electrophoresis and mass spectrometry. Electrophoresis 23:122-37. DOI: 10.1002/1522-2683(200201)23:1<122::AID-ELPS122>3.0.CO;2-4.

Bhagwat A., Keister D.L. (1995) Site-directed mutagenesis of the β-(1-3), β-(1-6)-D-glucan synthesis locus in *Bradyrhizobium japonicum*. Mol Plant Microbe Interact 8:366-370.

Bisset K.A., Hale C.M. (1951) The production of swarmers in Rhizobium spp. J Gen Microbiol 5:592-5.

Biswas S., Biswas I. (2005) Role of HtrA in surface protein expression and biofilm formation by Streptococcus mutans. Infect Immun 73:6923-34. DOI: 73/10/6923 [pii]10.1128/IAI.73.10.6923-6934.2005.

Bonaldi K., Gourion B., Fardoux J., Hannibal L., Cartieaux F., Boursot M., Vallenet D., Chaintreuil C., Prin Y., Nouwen N., Giraud E. (2010) Large-scale transposon mutagenesis of photosynthetic Bradyrhizobium sp. strain ORS278 reveals new genetic loci putatively important for nod-independent symbiosis with Aeschynomene indica. Mol Plant Microbe Interact 23:760-70. DOI: 10.1094/MPMI-23-6-0760.

Brechenmacher L., Lei Z., Libault M., Findley S., Sugawara M., Sadowsky M.J., Sumner L.W., Stacey G. (2010) Soybean metabolites regulated in root hairs in response to the symbiotic bacterium Bradyrhizobium japonicum. Plant Physiol 153:1808-22. DOI: 10.1104/pp.110.157800.

Bumann D., Aksu S., Wendland M., Janek K., Zimny-Arndt U., Sabarth N., Meyer T.F., Jungblut P.R. (2002) Proteome analysis of secreted proteins of the gastric pathogen Helicobacter pylori. Infect Immun 70:3396-403.

Cai G.Q., Driscoll B.T., Charles T.C. (2000) Requirement for the enzymes acetoacetyl coenzyme A synthetase and poly-3-hydroxybutyrate (PHB) synthase for growth of Sinorhizobium meliloti on PHB cycle intermediates. J Bacteriol 182:2113-8.

Carvalho H., Lima L., Lescure N., Camut S., Salema R., Cullimore J. (2000) Differential expression of the two cytosolic glutamine synthetase genes in various organs of Medicago truncatula. Plant Sci 159:301-312. DOI: S0168945200003605 [pii].

Carvalho H.G., Lopes-Cardoso I.A., Lima L.M., Melo P.M., Cullimore J.V. (2003) Nodule-specific modulation of glutamine synthetase in transgenic Medicago truncatula leads to inverse alterations in asparagine synthetase expression. Plant Physiol 133:243-52.

Carvalho P., Fischer J., Chen E., Yates J., Barbosa V. (2008) PatternLab for proteomics: a tool for differential shotgun proteomics. BMC Bioinformatics 9:316.

Catalano C.M., Czymmek K.J., Gann J.G., Sherrier D.J. (2007) Medicago truncatula syntaxin SYP132 defines the symbiosome membrane and infection droplet membrane in root nodules. Planta 225:541-50. DOI: 10.1007/s00425-006-0369-y.

Catalano C.M., Lane W.S., Sherrier D.J. (2004) Biochemical characterization of symbiosome membrane proteins from Medicago truncatula root nodules. Electrophoresis 25:519-31. DOI: 10.1002/elps.200305711.

Cedar H., Schwartz J.H. (1967) Localization of the two-L-asparaginases in anaerobically grown Escherichia coli. J Biol Chem 242:3753-5.

Cermola M., Fedorova E., Tate R., Riccio A., Favre R., Patriarca E.J. (2000) Nodule invasion and symbiosome differentiation during Rhizobium etli-Phaseolus vulgaris symbiosis. Mol Plant Microbe Interact 13:733-41. DOI: 10.1094/MPMI.2000.13.7.733.

Chang W.S., Franck W.L., Cytryn E., Jeong S., Joshi T., Emerich D.W., Sadowsky M.J., Xu D., Stacey G. (2007) An oligonucleotide microarray resource for transcriptional profiling of Bradyrhizobium japonicum. Mol Plant Microbe Interact 20:1298-307. DOI: 10.1094/MPMI-20-10-1298.

Choptra J., Kaur N., Gupta A.K. (2002) A comparative developmental pattern of enzymes in carbon metabolism and the pentose phospahte pahtway in mungbean and lentil nodules. Act. Physiol. Plant. 24:67-72.

Christlet T.H.T., Veluraja K. (2001) Database analysis of O-glycosylation sites in proteins. Biophys. J. 80:952-960.

Colebatch G., Desbrosses G., Ott T., Krusell L., Montanari O., Kloska S., Kopka J., Udvardi M.K. (2004) Global changes in transcription orchestrate metabolic differentiation during symbiotic nitrogen fixation in Lotus japonicus. Plant J 39:487-512. DOI: 10.1111/j.1365-313X.2004.02150.x.

Copeland L., Lee H.-S., Cowlishaw N. (1995) Carbon metabolism in chickpea nodules. Soil Biol. Biochem. 27:381-385.

Copeland L., Quinnel R.G., Day D.A. (1989a) Malic enzyme activity in bacteroids from soybean nodules. Journal of General Microbiology 135:2005-2012.

Copeland L., Vella J., Hong Z. (1989b) Enzymes of carbohydrate metabolism in soybean nodules. Phytochem 28:57-61.

Copeland L., Vella J., Hong Z.Q. (1989c) Enzymes of carbohydrate metabolism in soybean nodules. Phytochemistry 28:57-61.

Cox M.M. (1991) The RecA protein as a recombinational repair system. Mol Microbiol 5:1295-9.

Cox M.M. (1993) Relating biochemistry to biology: how the recombinational repair function of RecA protein is manifested in its molecular properties. Bioessays 15:617-23. DOI: 10.1002/bies.950150908.

Cytryn E.J., Sangurdekar D.P., Streeter J.G., Franck W.L., Chang W.S., Stacey G., Emerich D.W., Joshi T., Xu D., Sadowsky M.J. (2007) Transcriptional and physiological responses of Bradyrhizobium japonicum to desiccation-induced stress. J Bacteriol 189:6751-62. DOI: JB.00533-07 [pii]10.1128/JB.00533-07.

Dainese-Hatt P., Fischer H.M., Hennecke H., James P. (1999) Classifying symbiotic proteins from Bradyrhizobium japonicum into functional groups by proteome analysis of altered gene expression levels. Electrophoresis 20:3514-20. DOI: 10.1002/(SICI)1522-2683(19991201)20:18<3514::AID-ELPS3514>3.0.CO;2-T.

Dalton D.A. (1995) Antioxidative defences of plants and fungi Chapman Hall, New York.

Dalton D.A., Baird L.M., Langeberg L., Taugher C.Y., Anyan W.R., Vance C.P., Sarath G. (1993) Subcellular Localization of Oxygen Defense Enzymes in Soybean (Glycine max [L.] Merr.) Root Nodules. Plant Physiol 102:481-489.

Dalton D.A., Russell S.A., Hanus F.J., Pascoe G.A., Evans H.J. (1986) Enzymatic reactions of ascorbate and glutathione that prevent peroxide damage in soybean root nodules. Proc Natl Acad Sci U S A 83:3811-5.

Dao T.V., Nomura M., Hamaguchi R., Kato K., Itakura M., Minamisawa K., Sinsuwongwat S., Le H.T., Kaneko T., Tabata S., Tajima S. (2008) NAD-Malic Enzyme Affects Nitrogen Fixing Activity of Bradyrhizobium japonicum USDA 110 Bacteroids in Soybean Nodules. Microbes Environ 23:215-20.

Datta D.B., Triplett E.W., Newcomb E.H. (1991) Localization of xanthine dehydrogenase in cowpea root nodules: implications for the interaction between cellular compartments during ureide biogenesis. Proc Natl Acad Sci U S A 88:4700-2.

Davis C.L., Robb F.T. (1985) Maintenance of Different Mannitol Uptake Systems during Starvation in Oxidative and Fermentative Marine Bacteria. Appl Environ Microbiol 50:743-748.

Day D.A., Poole P.S., Tyerman S.D., Rosendahl L. (2001) Ammonia and amino acid transport across symbiotic membranes in nitrogen-fixing legume nodules. Cell Mol Life Sci 58:61-71.

de Maagd R.A., Lugtenberg B. (1986) Fractionation of *Rhizobium leguminosarium* Cells into Outer Membrane, Cytoplasmic Membrane, Periplasmic, and Cytoplasmic Components. . J. Bac. 167:1083-1085.

Dehertogh A.A., Mayeux P.A., Evans H.J. (1964a) Effect of Cobalt on the Oxidation of Propionate by Rhizobium Meliloti. J Bacteriol 87:746-7.

Dehertogh A.A., Mayeux P.A., Evans H.J. (1964b) The Relationship of Cobalt Requirement to Propionate Metabolism in Rhizobium. J Biol Chem 239:2446-53.

Delgado M.J., Bonnard N., Tresierra-Ayala A., Bedmar E.J., Muller. P. (2003) The *Bradyrhizobium japonicum napEDABC* genes encoding the periplasmic nitrate reductase are essential for nitrate respiration. . Microbiology 149:3395-3403.

Delgado M.J., Yeoman K.H., Wu G., Vargas C., Davies A.E., Poole R.K., Johnston A.W., Downie J.A. (1995) Characterization of the cycHJKL genes involved in cytochrome c biogenesis and symbiotic nitrogen fixation in Rhizobium leguminosarum. J Bacteriol 177:4927-34.

Delmotte N., Ahrens C.H., Knief C., Qeli E., Koch M., Fischer H.M., Vorholt J.A., Hennecke H., Pessi G. (2010) An integrated proteomics and transcriptomics reference data set provides new insights into the Bradyrhizobium japonicum bacteroid metabolism in soybean root nodules. Proteomics 10:1391-400. DOI: 10.1002/pmic.200900710.

Deshmane N., Stacey G. (1989) Identification of Bradyrhizobium nod genes involved in host-specific nodulation. J Bacteriol 171:3324-30.

Ditta G., Schmidhauser T., Yakobson E., Lu P., Liang X.W., Finlay D.R., Guiney D., Helinski D.R. (1985) Plasmids related to the broad host range vector, pRK290, useful for gene cloning and for monitoring gene expression. Plasmid 13:149-53. DOI: 0147-619X(85)90068-X [pii].

Djordjevic M.A. (2004) Sinorhizobium meliloti metabolism in the root nodule: a proteomic perspective. Proteomics 4:1859-72. DOI: 10.1002/pmic.200300802.

Djordjevic M.A., Chen H.C., Natera S., Van Noorden G., Menzel C., Taylor S., Renard C., Geiger O., Weiller G.F. (2003) A global analysis of protein expression profiles in Sinorhizobium meliloti: discovery of new genes for nodule occupancy and stress adaptation. Mol Plant Microbe Interact 16:508-24. DOI: 10.1094/MPMI.2003.16.6.508.

Donati A.J., Jeon J.M., Sangurdekar D., So J.S., Chang W.S. (2011) Genome-wide transcriptional and physiological responses of Bradyrhizobium japonicum to paraquat-mediated oxidative stress. Appl Environ Microbiol 77:3633-43. DOI: AEM.00047-11 [pii]10.1128/AEM.00047-11.

Douglas A.E. (1994) Symbiotic Interactions Oxford University Press, Oxford.

Douglas A.E. (2010) The Symbiotic Habit Princeton University Press, Princeton.

Drabkin D.L., Austin J. (1935) Spectrophotometric studies: II. Preparations from washed red blood cells, nitric oxide hemoglobin and sulfhemoglobin. J. Biol. Chem. 115:51-65.

Driscoll B.T., Finan T.M. (1993) NAD(+)-dependent malic enzyme of Rhizobium meliloti is required for symbiotic nitrogen fixation. Mol Microbiol 7:865-73.

Duguid J.P., Campbell I. (1969) Antigens of the type-1 fimbriae of salmonellae and other enterobacteria. J Med Microbiol 2:535-53.

Dunn M.F. (1998) Tricarboxylic acid cycle and anaplerotic enzymes in rhizobia. FEMS Microbiol Rev 22:105-23. DOI: S0168-6445(98)00010-2 [pii].

Dunn M.F., Araiza G., Mora J. (2004) Biochemical characterization of a Rhizobium etli monovalent cation-stimulated acyl-coenzyme A carboxylase with a high substrate specificity constant for propionyl-coenzyme A. Microbiology 150:399-406.

Dunn M.F., Encarnacion S., Araiza G., Vargas M.C., Davalos A., Peralta H., Mora Y., Mora J. (1996) Pyruvate carboxylase from Rhizobium etli: mutant

characterization, nucleotide sequence, and physiological role. J Bacteriol 178:5960-70.

Dymov S.I., Meek D.J., Steven B., Driscoll B.T. (2004) Insertion of transposon Tn5tac1 in the Sinorhizobium meliloti malate dehydrogenase (mdh) gene results in conditional polar effects on downstream TCA cycle genes. Mol Plant Microbe Interact 17:1318-27. DOI: 10.1094/MPMI.2004.17.12.1318.

el-Din A.K. (1992) A succinate transport mutant of Bradyrhizobium japonicum forms ineffective nodules on soybeans. Can J Microbiol 38:230-4.

El Yahyaoui F., Kuster H., Ben Amor B., Hohnjec N., Puhler A., Becker A., Gouzy J., Vernie T., Gough C., Niebel A., Godiard L., Gamas P. (2004) Expression profiling in Medicago truncatula identifies more than 750 genes differentially expressed during nodulation, including many potential regulators of the symbiotic program. Plant Physiol 136:3159-76. DOI: 10.1104/pp.104.043612.

Emerich D.W., Ruiz-Argueso T., Ching T.M., Evans H.J. (1979) Hydrogen-dependent nitrogenase activity and ATP formation in Rhizobium japonicum bacteroids. J Bacteriol 137:153-60.

Encarnacion S., Dunn M., Willms K., Mora J. (1995) Fermentative and aerobic metabolism in Rhizobium etli. J Bacteriol 177:3058-66.

Encarnacion S., J. Calderon, A.S. Gelbard, A.J.L. Cooper, & J. Mora. (1998) Glutamine Biosynthesis and the Utilization of Succinate and Glutamine by *Rhizobium etli* and *Sinorhizbium meliloti*. Microbiology 144:2629.

Evans P.J., Gallesi D., Mathieu C., Hernandez M.J., de Felipe M.R., Halliwell B., al. e. (1999) Oxidative stress occurs during soybean nodule senescence. Planta 208:73-79.

Fabianek R.A., Hennecke H., Thony-Meyer L. (2000) Periplasmic protein thiol:disulfide oxidoreductases of Escherichia coli. FEMS Microbiol Rev 24:303-16. DOI: S0168-6445(00)00028-0 [pii].

Falcone D.L., Tabita F.R. (1991) Expression of endogenous and foreign ribulose 1,5-bisphosphate carboxylase-oxygenase (RubisCO) genes in a RubisCO deletion mutant of Rhodobacter sphaeroides. J Bacteriol 173:2099-108.

Fedorova M., I.A. T., Vance C.P. (1999) Expression of C-assimilating enzymes in pea (*Pisum sativum* L.) root ndoules: *in situ* lociatlzation in effective nodules. Plant Cell Environ. 22:1249-1262.

Finan T.M., McWhinnie E., Driscoll B., Watson R.J. (1991) Complex symbiotic phenotypes result from gluconeogenic mutations in *Rhizobium melilioti*. Mol. Plant Micr. Inter. 4:386-392.

Fischer H.M., Babst M., Kaspar T., Acuna G., Arigoni F., Hennecke H. (1993) One member of a gro-ESL-like chaperonin multigene family in Bradyrhizobium japonicum is co-regulated with symbiotic nitrogen fixation genes. EMBO J 12:2901-12.

Flemetakis E., Efrose R.C., Ott T., Stedel C., Aivalakis G., Udvardi M.K., Katinakis P. (2006) Spatial and temporal organization of sucrose metabolism in Lotus japonicus nitrogen-fixing nodules suggests a role for the elusive alkaline/neutral invertase. Plant Mol Biol 62:53-69. DOI: 10.1007/s11103-006-9003-4.

Fortin M.G., Morrison N.A., Verma D.P. (1987) Nodulin-26, a peribacteroid membrane nodulin is expressed independently of the development of the peribacteroid compartment. Nucleic Acids Res 15:813-24.

Freitag N.E., Seifert H.S., Koomey M. (1995) Characterization of the *pilF-pilD* pilus-assembly locus of *Neisseria gonorrhoeae*. Mol Microbiol 16:575-586.

Frendo P., Harrison J., Norman C., Hernandez Jimenez M.J., Van de Sype G., Gilabert A., Puppo A. (2005) Glutathione and homoglutathione play a critical role in the nodulation process of Medicago truncatula. Mol Plant Microbe Interact 18:254-9. DOI: 10.1094/MPMI-18-0254.

Frisk A., Ison C.A., Lagergard T. (1998) GroEL heat shock protein of Haemophilus ducreyi: association with cell surface and capacity to bind to eukaryotic cells. Infect Immun 66:1252-7.

Fuhrer T., Sauer U. (2009) Different biochemical mechanisms ensure network-wide balancing of reducing equivalents in microbial metabolism. J Bacteriol 191:2112-21. DOI: JB.01523-08 [pii]10.1128/JB.01523-08.

Fujisawa H., Hayaishi O. (1968) Protocatechuate 3,4-dioxygenase. I. Crystallization and characterization. J Biol Chem 243:2673-81.

Gallaher T.K., S. Wu, P. Webster, & R. Aguilera. (2006) Identification of Biofilm Proteins in Non-Typeable *Haemophilus influenza*. BMC Microbiology 6:65-73.

Galvez S., Hirsch A.M., Wycoff K.L., Hunt S., Layzell D.B., Kondorosi A., Crespi M. (2000) Oxygen regulation of a nodule-located carbonic anhydrase in alfalfa. Plant Physiol 124:1059-68.

Garrocho-Villegas V., Gopalasubramaniam S.K., Arredondo-Peter R. (2007) Plant hemoglobins: what we know six decades after their discovery. Gene 398:78-85. DOI: 10.1016/j.gene.2007.01.035.

Garwin J.L., Klages A.L., Cronan J.E., Jr. (1980) Beta-ketoacyl-acyl carrier protein synthase II of Escherichia coli. Evidence for function in the thermal regulation of fatty acid synthesis. J Biol Chem 255:3263-5.

Gibiansky M.L., Conrad J.C., Jin F., Gordon V.D., Motto D.A., Mathewson M.A., Stopka W.G., Zelasko D.C., Shrout J.D., Wong G.C. (2010) Bacteria use type IV pili to walk upright and detach from surfaces. Science 330:197. DOI: 10.1126/science.1194238.

Gilbert K.B., Vanderlinde E.M., Yost C.K. (2007) Mutagenesis of the carboxy terminal protease CtpA decreases desiccation tolerance in Rhizobium leguminosarum. FEMS Microbiol Lett 272:65-74. DOI: FML735 [pii]10.1111/j.1574-6968.2007.00735.x.

Giraud E., Moulin L., Vallenet D., Barbe V., Cytryn E., Avarre J.C., Jaubert M., Simon D., Cartieaux F., Prin Y., Bena G., Hannibal L., Fardoux J., Kojadinovic M., Vuillet L., Lajus A., Cruveiller S., Rouy Z., Mangenot S., Segurens B., Dossat C., Franck W.L., Chang W.S., Saunders E., Bruce D., Richardson P., Normand P., Dreyfus B., Pignol D., Stacey G., Emerich D., Vermeglio A., Medigue C., Sadowsky M. (2007) Legumes symbioses: absence of Nod genes in photosynthetic bradyrhizobia. Science 316:1307-12. DOI: 316/5829/1307 [pii]10.1126/science.1139548.

Glazebrook J., Ichige A., Walker G.C. (1996) Genetic analysis of Rhizobium meliloti bacA-phoA fusion results in identification of degP: two loci required for symbiosis are closely linked to degP. J Bacteriol 178:745-52.

Glenn A.R.M.J.D. (1979) An examination of *Rhizobium leguminosarium* for the production of extracellular and periplasmic proteins. J. Gen. Microbiol. 112:405-409.

Goggin D.E., Lipscombe R., Fedorova E., Millar A.H., Mann A., Atkins C.A., Smith P.M. (2003) Dual intracellular localization and targeting of aminoimidazole ribonucleotide synthetase in cowpea. Plant Physiol 131:1033-41. DOI: 10.1104/pp.102.015081.

Gorby Y.A., Yanina S., McLean J.S., Rosso K.M., Moyles D., Dohnalkova A., Beveridge T.J., Chang I.S., Kim B.H., Kim K.S., Culley D.E., Reed S.B., Romine M.F., Saffarini D.A., Hill E.A., Shi L., Elias D.A., Kennedy D.W., Pinchuk G., Watanabe K., Ishii S., Logan B., Nealson K.H., Fredrickson J.K. (2006) Electrically conductive bacterial nanowires produced by Shewanella oneidensis

strain MR-1 and other microorganisms. Proc Natl Acad Sci U S A 103:11358-63. DOI: 10.1073/pnas.0604517103.

Gordon A.J., James C.L. (1997) Enyzmes of carbohydrate and amino acid metabolism in developing and mature nodules of white clover. J. Exp. Bot. 48:895-903.

Gordon A.J., Minchin F.R., James C.L., Komina O. (1999) Sucrose synthase in legume nodules is essential for nitrogen fixation. Plant Physiol 120:867-78.

Gourion B., Delmotte N., Bonaldi K., Nouwen N., Vorholt J.A., Giraud E. (2011) Bacterial RuBisCO is required for efficient Bradyrhizobium/Aeschynomene symbiosis. PLoS One 6:e21900. DOI: 10.1371/journal.pone.0021900PONE-D-11-06893 [pii].

Green L.S., Emerich D.W. (1997a) Bradyrhizobium japonicum does not require alpha-ketoglutarate dehydrogenase for growth on succinate or malate. J Bacteriol 179:194-201.

Green L.S., Emerich D.W. (1997b) The Formation of Nitrogen-Fixing Bacteroids Is Delayed but Not Abolished in Soybean Infected by an [alpha]-Ketoglutarate Dehydrogenase-Deficient Mutant of Bradyrhizobium japonicum. Plant Physiol 114:1359-1368.

Green L.S., Emerich D.W. (1999) Light Microscopy of early stages in the symbiosis of soybean with a delayed-nodulation mutant of *Bradyrhizobium japonicum*. Journal of Experimental Botany 50:1577-1585.

Green L.S., Karr D.B., Emerich D.W. (1998) Isocitrate dehydrogenase and glyoxylate cycle enzyme activities in Bradyrhizobium japonicum under various growth conditions. Arch Microbiol 169:445-51.

Green L.S., Li Y., Emerich D.W., Bergersen F.J., Day D.A. (2000) Catabolism of alpha-ketoglutarate by a sucA mutant of Bradyrhizobium japonicum: evidence for an alternative tricarboxylic acid cycle. J Bacteriol 182:2838-44.

Groten K., Dutilleul C., van Heerden P.D., Vanacker H., Bernard S., Finkemeier I., Dietz K.J., Foyer C.H. (2006) Redox regulation of peroxiredoxin and proteinases by ascorbate and thiols during pea root nodule senescence. FEBS Lett 580:1269-76. DOI: S0014-5793(06)00083-4 [pii]10.1016/j.febslet.2006.01.043.

Guo M., Yang X.L., Schimmel P. (2010) New functions of aminoacyl-tRNA synthetases beyond translation. Nat Rev Mol Cell Biol 11:668-74. DOI: nrm2956 [pii]10.1038/nrm2956.

Harrison C. (2003) GrpE, a nucleotide exchange factor for DnaK. Cell Stress Chaperones 8:218-24.

Harrison J., Jamet A., Muglia C.I., Van de Sype G., Aguilar O.M., Puppo A., Frendo P. (2005) Glutathione plays a fundamental role in growth and symbiotic capacity of Sinorhizobium meliloti. J Bacteriol 187:168-74. DOI: 187/1/168 [pii]10.1128/JB.187.1.168-174.2005.

Harrison J., Pou de Crescenzo M.A., Sene O., Hirel B. (2003) Does lowering glutamine synthetase activity in nodules modify nitrogen metabolism and growth of Lotus japonicus? Plant Physiol 133:253-62.

Haser A., Robinson D.L., Duc G., Vance C.P. (1992) A mutation in Vicia faba results in ineffetive nodules with imparied bacteroid differnetiation and reduced synthesis of late nodulins. J. Exp. Bot. 43:1397-1407.

Hauser F., Pessi G., Friberg M., Weber C., Rusca N., Lindemann A., Fischer H.M., Hennecke H. (2007) Dissection of the Bradyrhizobium japonicum NifA+sigma54 regulon, and identification of a ferredoxin gene (fdxN) for symbiotic nitrogen fixation. Mol Genet Genomics 278:255-71. DOI: 10.1007/s00438-007-0246-9.

Hecht S., Eisenreich W., Adam P., Amslinger S., Kis K., Bacher A., Arigoni D., Rohdich F. (2001) Studies on the nonmevalonate pathway to terpenes: the role of the GcpE (IspG) protein. Proc Natl Acad Sci U S A 98:14837-42. DOI: 10.1073/pnas.20139929898/26/14837 [pii].

Hellriegel H., Wilfarth H. (1888) Untersuchungen uber die Stickstoffnahrung der Gramineon und Leguminosen Beilageheft zu der Ztschr. Ver. Ru¨ benzucker-IndustrieDeutschen Reichs

Hempel J., Zehner S., Gottfert M., Patschkowski T. (2009) Analysis of the secretome of the soybean symbiont Bradyrhizobium japonicum. J Biotechnol 140:51-8. DOI: S0168-1656(08)02440-1 [pii]10.1016/j.jbiotec.2008.11.002.

Henson C.A., Collins M., Duke S.H. (1982) Subcellular localization of enzymes of carbon and nitrogen metabolism in nodules of *Medicago sativa* cultivar vernal. Plant Cell Physiol. 23:227-235.

Hernandez A., Garcia-Plazaola J.I., Becerril J.M. (1999) Glyphosphate effects on phenolic metabolism of nodulated soybean (*Glycine max* L. Merr.). Journal of Agricultural Food Chemistry 47:2920-2925.

Herold S., Puppo A. (2005a) Kinetics and mechanistic studies of the reactions of metleghemoglobin, ferrylleghemoglobin, and nitrosylleghemoglobin with reactive nitrogen species. J Biol Inorg Chem 10:946-57. DOI: 10.1007/s00775-005-0047-8.

Herold S., Puppo A. (2005b) Oxyleghemoglobin scavenges nitrogen monoxide and peroxynitrite: a possible role in functioning nodules? J Biol Inorg Chem 10:935-45. DOI: 10.1007/s00775-005-0046-9.

Herrada G., Puppo A., Rigaud J. (1989) Uptake of metabolites by bacteroid-containing vesicles and by free bacteroids from french bean nodules. J. Gen. Microbiol. 135:3165-3177.

Hillmer P., Gest H. (1977) H2 metabolism in the photosynthetic bacterium Rhodopseudomonas capsulata: production and utilization of H2 by resting cells. J Bacteriol 129:732-9.

Hiltner L. (1904) Über neuere Erfahrungen und Probleme auf dem Gebiete der Bodenbakteriologie unter bessonderer Berücksichtigung der Gründung und Brache. Arb. Dtsch. Landwirtsch. Ges. Berl. 98:59-78.

Hirsch A.M., Bauer W.D., Bird D.M., Cullimore J., Tyler B., Yoder J.I. (2003) Molecular signals and receptors: Controlling rhizosphere interactions between plants and other organisms. Ecology 84:858-868.

Hoa L.T.-P., Nomura M., Kajiwara H., Day D.A., Tajima S. (2004) Proteomic analysis on symbiotic differentiation of mitochondria in soybean nodules. Plant Cell. Physiol. 45:300-308.

Hohnjec N., Becker J.D., Puhler A., Perlick A.M., Kuster H. (1999) Genomic organization and expression properties of the MtSucS1 gene, which encodes a nodule-enhanced sucrose synthase in the model legume *Medicago truncatula*. Mol. Gen. Genet. 261:514-522.

Holloman W.K., Dekker C.A. (1971) Control by cesium and intermediates of the citric acid cycle of extracellular ribonuclease and other enzymes involved in the assimilation of nitrogen. Proc Natl Acad Sci U S A 68:2241-5.

Holscher T., Gorisch H. (2006) Knockout and overexpression of pyrroloquinoline quinone biosynthetic genes in Gluconobacter oxydans 621H. J Bacteriol 188:7668-76. DOI: JB.01009-06 [pii]10.1128/JB.01009-06.

Hong Z.Q., Copeland L. (1990) Pentose phosphate pathway enzymes in nitrogen-fixing leguminous root nodules. Phytochem 29:2437-2440.

Hosie A.H., Allaway D., Galloway C.S., Dunsby H.A., Poole P.S. (2002) Rhizobium leguminosarum has a second general amino acid permease with unusually broad substrate specificity and high similarity to branched-chain amino acid transporters (Bra/LIV) of the ABC family. J Bacteriol 184:4071-80.

Howard J.B., Rees D.C. (2006) How many metals does it take to fix N2? A mechanistic overview of biological nitrogen fixation. Proc Natl Acad Sci U S A 103:17088-93. DOI: 0603978103 [pii]10.1073/pnas.0603978103.

Hu Y., Corbett M.C., Fay A.W., Webber J.A., Hodgson K.O., Hedman B., Ribbe M.W. (2006) Nitrogenase Fe protein: A molybdate/homocitrate insertase. Proc Natl Acad Sci U S A 103:17125-30. DOI: 0602651103 [pii]10.1073/pnas.0602651103.

Huerta-Zepeda A., Duran S., Du Pont G., Calderon J. (1996) Asparagine Degradation in *Rhizobium etli*. Microbiology 142:1071-1076.

Humann J., Lenz L.L. (2009) Bacterial peptidoglycan degrading enzymes and their impact on host muropeptide detection. J Innate Immun 1:88-97. DOI: 10.1159/000181181.

Hunt S., King B.J., Layzell D.B. (1989) Effects of gradual increases in o(2) concentration on nodule activity in soybean. Plant Physiol 91:315-21.

Hunt S., Layzell D.B. (1993) Gas exchange of legume nodules and the regulation of nitrogenase activity. Annu. Rev. Plant Physiol. Plant Mol. Biol. 44:483-511.

Ingraham J.L., Neuhard J. (1972) Cold-sensitive mutants of Salmonella typhimurium defective in uridine monophosphate kinase (pyrH). J Biol Chem 247:6259-65.

Irigoyen J.J., Sanchez-Diaz M., Emerich D.W. (1990) Carbon Metabolism Enzymes of Rhizobium meliloti Cultures and Bacteroids and Their Distribution within Alfalfa Nodules. Appl Environ Microbiol 56:2587-2589.

Ito N., Itakura M., Eda S., Saeki K., Oomori H., Yokoyama T., Kaneko T., Tabata S., Ohwada T., Tajima S., Uchiumi T., Masai E., Tsuda M., Mitsui H., Minamisawa K. (2006) Global Gene Expression *Bradyrhizobium japonicum* Cultured with Vanillin, Vanillate, 4-Hydroxybenzoate, and Protocatechuate. Microbes and Environments 21:240-250.

Jackson E.K., Evans H.J. (1966) Propionate in heme biosynthesis in soybean nodules. Plant Physiol 41:1673-80.

Jamet A., Sigaud S., Van de Sype B., Puppo A., Hérouart D. (2003) Expression of the bacterial catalase genes during *Sinorhizobium meliloti-Medicago sativa* symbiosis and their crucial role during the infection process. . Mol. Plant-Microbe Interactions 16:217-225.

Jenkins J.R., Cooper R.A. (1988) Molecular cloning, expression, and analysis of the genes of the homoprotocatechuate catabolic pathway of Escherichia coli C. J Bacteriol 170:5317-24.

Jomaa A., Iwanczyk J., Tran J., Ortega J. (2009) Characterization of the autocleavage process of the Escherichia coli HtrA protein: implications for its physiological role. J Bacteriol 191:1924-32. DOI: JB.01187-08 [pii]10.1128/JB.01187-08.

Jorgensen C.M., Hammer K., Martinussen J. (2003) CTP limitation increases expression of CTP synthase in Lactococcus lactis. J Bacteriol 185:6562-74.

Kahn K., Tipton P.A. (1997) Kinetic mechanism and cofactor content of soybean root nodule urate oxidase. Biochemistry 36:4731-8. DOI: 10.1021/bi963184wbi963184w [pii].

Kahn M., Kraus J., Sommerville J.E. (1985) A model of nutrient exchange in the Rhizobium-legume symbiosis M. Nijhoff, Dordrecht.

Kaiser B.N., Finnegan P.M., Tyerman S.D., Whitehead L.F., Bergersen F.J., Day D.A., Udvardi M.K. (1998) Characterization of an ammonium transport protein from the peribacteroid membrane of soybean nodules. Science 281:1202-6.

Kanbe M., Yagasaki J., Zehner S., Gottfert M., Aizawa S. (2007) Characterization of two sets of subpolar flagella in Bradyrhizobium japonicum. J Bacteriol 189:1083-9. DOI: 10.1128/JB.01405-06.

Kaneko T., Nakamura Y., Sato S., Minamisawa K., Uchiumi T., Sasamoto S., Watanabe A., Idesawa K., Iriguchi M., Kawashima K., Kohara M., Matsumoto M., Shimpo S., Tsuruoka H., Wada T., Yamada M., Tabata S. (2002a) Complete genomic sequence of nitrogen-fixing symbiotic bacterium Bradyrhizobium japonicum USDA110. DNA Res 9:189-97.

Kaneko T., Nakamura Y., Sato S., Minamisawa K., Uchiumi T., Sasamoto S., Watanabe A., Idesawa K., Iriguchi M., Kawashima K., Kohara M., Matsumoto M., Shimpo S., Tsuruoka H., Wada T., Yamada M., Tabata S. (2002b) Complete genomic sequence of nitrogen-fixing symbiotic bacterium Bradyrhizobium japonicum USDA110 (supplement). DNA Res 9:225-56.

Kape R., Parniske M., Werner D. (1991) Chemotaxis and nod Gene Activity of Bradyrhizobium japonicum in Response to Hydroxycinnamic Acids and Isoflavonoids. Appl Environ Microbiol 57:316-9.

Karr D.B., Emerich D.W. (1988) Uniformity of the microsymbiont population from soybean nodules with respect to buoyant density. Plant Physiol 86:693-9.

Karr D.B., Emerich D.W. (1989) Protein phosphorylation in Bradyrhizobium japonicum bacteroids and cultures. J Bacteriol 171:3420-6.

Karr D.B., Emerich D.W. (1996) Protein Synthesis by Bradyrhizobium japonicum Bacteroids Declines as a Function of Nodule Age. Appl Environ Microbiol 62:3757-61.

Karr D.B., Waters J.K., Emerich D.W. (1983) Analysis of Poly-beta-Hydroxybutyrate in Rhizobium japonicum Bacteroids by Ion-Exclusion High-Pressure Liquid Chromatography and UV Detection. Appl Environ Microbiol 46:1339-44.

Karr D.B., Waters J.K., Suzuki F., Emerich D.W. (1984) Enzymes of the Poly-beta-Hydroxybutyrate and Citric Acid Cycles of Rhizobium japonicum Bacteroids. Plant Physiol 75:1158-62.

Kavroulakis N., Flemetakis E., Aivalakis G., Katinakis P. (2000) Carbon metabolism in developing soybean root nodules: the role of carbonic anhydrase. Mol Plant Microbe Interact 13:14-22. DOI: 10.1094/MPMI.2000.13.1.14.

Kazakov A.E., Rodionov D.A., Alm E., Arkin A.P., Dubchak I., Gelfand M.S. (2009) Comparative genomics of regulation of fatty acid and branched-chain amino acid utilization in proteobacteria. J Bacteriol 191:52-64. DOI: JB.01175-08 [pii]10.1128/JB.01175-08.

Kazemi-Pour N., Condemine G., Hugouvieux-Cotte-Pattat N. (2004) The secretome of the plant pathogenic bacterium Erwinia chrysanthemi. Proteomics 4:3177-86. DOI: 10.1002/pmic.200300814.

Keller A., Nesvizhskii A.I., Kolker E., Aebersold R. (2002) Empirical statistical model to estimate the accuracy of peptide identifications made by MS/MS and database search. Anal Chem 74:5383-92.

Kereszt A., Mergaert P., Kondorosi E. (2011) Bacteroid development in legume nodules: evolution of mutual benefit or of sacrificial victims? Mol Plant Microbe Interact 24:1300-9. DOI: 10.1094/MPMI-06-11-0152.

Kerppola T.K., Kahn M.L. (1988) Genetic analysis of carbamoylphosphate synthesis in Rhizobium meliloti 104A14. J Gen Microbiol 134:921-9.

Kikuchi T., Mizunoe Y., Takade A., Naito S., Yoshida S. (2005) Curli fibers are required for development of biofilm architecture in Escherichia coli K-12 and enhance bacterial adherence to human uroepithelial cells. Microbiol Immunol 49:875-84.

Kil K.S., Cunningham M.W., Barnett L.A. (1994) Cloning and sequence analysis of a gene encoding a 67-kilodalton myosin-cross-reactive antigen of Streptococcus pyogenes reveals its similarity with class II major histocompatibility antigens. Infect Immun 62:2440-9.

Kim S.A., Copeland L. (1996) Enzymes of poly-β-hydroxybutyrate metabolism in soybean and chickpea bacteroids. Applied and Environmental Microbiology 62:4186-4190.

King J.D., Kocincova D., Westman E.L., Lam J.S. (2009) Review: Lipopolysaccharide biosynthesis in Pseudomonas aeruginosa. Innate Immun 15:261-312. DOI: 1753425909106436 [pii]10.1177/1753425909106436.

Kinnback A., Mellor R., Werner D. (1987) α-Mannosidase II isoenzyme in the peribacteroid space of *Glycine max* root nodules. J. Exp. Bot. 38:1373-1377.

Koga T., Ishimoto K., Lory S. (1993) Genetic and functional characterization of the gene cluster specifying expression of Pseudomonas aeruginosa pili. Infect Immun 61:1371-7.

Kosslak R.M., Bookland R., Barkei J., Paaren H.E., Appelbaum E.R. (1987) Induction of Bradyrhizobium japonicum common nod genes by isoflavones isolated from Glycine max. Proc Natl Acad Sci U S A 84:7428-32.

Kouchi H., Fukai K., Katagiri H., Minamisawa K., Tajima S. (1988) Isolation and enzymological characterization of infected and unifected cell protoplasts from root nodules of *Glycine max*. Physiol. Plant 73:327-334.

Kouchi H., Fukai K., Kihara A. (1991) Metabolism of glutamate and aspartate in bacteroids from soybean root nodules. J. Gen. Microbiol. 137:2901-2910.

Kouchi H., Shimomura K., Hata S., Hirota A., Wu G.J., Kumagai H., Tajima S., Suganuma N., Suzuki A., Aoki T., Hayashi M., Yokoyama T., Ohyama T., Asamizu E., Kuwata C., Shibata D., Tabata S. (2004) Large-scale analysis of gene expression profiles during early stages of root nodule formation in a model legume, Lotus japonicus. DNA Res 11:263-74.

Krishnan H.B., Kim W.S., Sun-Hyung J., Kim K.Y., Jiang G. (2003) Citrate synthase mutants of Sinorhizobium fredii USDA257 form ineffective nodules with aberrant ultrastructure. Appl Environ Microbiol 69:3561-8.

Krishnan H.B., Natarajan S.S., Kim W.S. (2011) Distinct Cell Surface Appendages Produced by Sinorhizobium fredii USDA257 and S. fredii USDA191, Cultivar-Specific and Nonspecific Symbionts of Soybean. Appl Environ Microbiol 77:6240-8. DOI: AEM.05366-11 [pii]10.1128/AEM.05366-11.

Kuster H., Fruhling M., Perlick A.M., Puhler A. (1993) The sucrose synthase gene is predominantly expressed in the root nodule tissue of Vicia faba. Mol Plant Microbe Interact 6:507-14.

Kuzma M.M., Winter H., Storer P., Oresnik I.I., Atkins C.A., Layzell D.B. (1999) The site of oxygen limitation in soybean nodules. Plant Physiol 119:399-408.

Lacourciere G.M., Stadtman T.C. (1998) The NIFS protein can function as a selenide delivery protein in the biosynthesis of selenophosphate. J Biol Chem 273:30921-6.

Lanyi J.K., Lederberg J. (1966) Fluorescent method for the detection of excreted ribonuclease around bacterial colonies. J Bacteriol 92:1469-72.

Larrainzar E., Wienkoop S., Weckwerth W., Ladrera R., Arrese-Igor C., Gonzalez E.M. (2007) Medicago truncatula root nodule proteome analysis reveals differential plant and bacteroid responses to drought stress. Plant Physiol 144:1495-507. DOI: pp.107.101618 [pii]10.1104/pp.107.101618.

Layzell D.B., Hunt S., Palmer G.R. (1990) Mechanism of Nitrogenase Inhibition in Soybean Nodules : Pulse-Modulated Spectroscopy Indicates that Nitrogenase Activity Is Limited by O(2). Plant Physiol 92:1101-7.

Lee M.Y., Shin K.H., Kim Y.K., Suh J.Y., Gu Y.Y., Kim M.R., Hur Y.S., Son O., Kim J.S., Song E., Lee M.S., Nam K.H., Hwang K.H., Sung M.K., Kim H.J., Chun J.Y., Park M., Ahn T.I., Hong C.B., Lee S.H., Park H.J., Park J.S., Verma D.P., Cheon C.I. (2005) Induction of thioredoxin is required for nodule development to reduce reactive oxygen species levels in soybean roots. Plant Physiol 139:1881-9. DOI: 10.1104/pp.105.067884.

Lee S., Flores-Encarnacion M., Contreras-Zentella M., Garcia-Flores L., Escamilla J.E., Kennedy C. (2004) Indole-3-acetic acid biosynthesis is deficient in Gluconacetobacter diazotrophicus strains with mutations in cytochrome c biogenesis genes. J Bacteriol 186:5384-91. DOI: 10.1128/JB.186.16.5384-5391.2004186/16/5384 [pii].

Lee S.E., Kim S.Y., Kim C.M., Kim M.K., Kim Y.R., Jeong K., Ryu H.J., Lee Y.S., Chung S.S., Choy H.E., Rhee J.H. (2007) The pyrH gene of Vibrio vulnificus is an essential in vivo survival factor. Infect Immun 75:2795-801. DOI: IAI.01499-06 [pii]10.1128/IAI.01499-06.

Lenz O., Schwartz E., Dernedde J., Eitinger M., Friedrich B. (1994) The Alcaligenes eutrophus H16 hoxX gene participates in hydrogenase regulation. J Bacteriol 176:4385-93.

Li Y., Zhang Y. (2007) PhoU is a persistence switch involved in persister formation and tolerance to multiple antibiotics and stresses in Escherichia coli. Antimicrob Agents Chemother 51:2092-9. DOI: AAC.00052-07 [pii]10.1128/AAC.00052-07.

Lima L., Seabra A., Melo P., Cullimore J., Carvalho H. (2006) Post-translational regulation of cytosolic glutamine synthetase of Medicago truncatula. J Exp Bot 57:2751-61. DOI: erl036 [pii]10.1093/jxb/erl036.

Lindemann A., Moser A., Pessi G., Hauser F., Friberg M., Hennecke H., Fischer H.M. (2007) New target genes controlled by the Bradyrhizobium japonicum two-component regulatory system RegSR. J Bacteriol 189:8928-43. DOI: JB.01088-07 [pii]10.1128/JB.01088-07.

Little J.W. (1993) LexA cleavage and other self-processing reactions. J Bacteriol 175:4943-50.

Llamas M.A., Ramos J.L., Rodriguez-Herva J.J. (2000) Mutations in each of the tol genes of Pseudomonas putida reveal that they are critical for maintenance of outer membrane stability. J Bacteriol 182:4764-72.

Lodwig E.M., Hosie A.H., Bourdes A., Findlay K., Allaway D., Karunakaran R., Downie J.A., Poole P.S. (2003) Amino-acid cycling drives nitrogen fixation in the legume-Rhizobium symbiosis. Nature 422:722-6. DOI: 10.1038/nature01527.

Lodwig E.M., Leonard M., Marroqui S., Wheeler T.R., Findlay K., Downie J.A., Poole P.S. (2005) Role of polyhydroxybutyrate and glycogen as carbon storage compounds in pea and bean bacteroids. Mol Plant Microbe Interact 18:67-74. DOI: 10.1094/MPMI-18-0067.

Long S., S. McCune, and G.C. Walker. . (1988) Symbiotic loci of *Rhizobium meliloti* identified by random TnphoA mutagenesis. . J. Bac. 170:4257-4265.

Long S.R. (1989) Rhizobium-legume nodulation: life together in the underground. Cell 56:203-14.

Lopez-Campistrous A., Semchuk P., Burke L., Palmer-Stone T., Brokx S.J., Broderick G., Bottorff D., Bolch S., Weiner J.H., Ellison M.J. (2005) Localization, annotation, and comparison of the Escherichia coli K-12 proteome under two states of growth. Mol Cell Proteomics 4:1205-9. DOI: D500006-MCP200 [pii]10.1074/mcp.D500006-MCP200.

Lopez-Garcia S.L., Vazquez T.E.E., Favelukes G., Lodeiro A.R. (2001) Improved Soybean Root Association of N-Starved *Bradyrhizobium japonicum*. Journal of Bacteriology 183:7241-7252.

Lorite M.J., Sanjuan J., Velasco L., Olivares J., Bedmar E.J. (1998) Characterization of *Bradyrhizobium japonicum pcaBDC* genes involved in 4-hydroxybenzoate degradation. Biochemica et Biophysica Acta 1397:257-261.

Lorite M.J., Tachil J., Sanjuan J., Meyer O., Bedmar E.J. (2000) Carbon monoxide dehydrogenase activity in Bradyrhizobium japonicum. Appl Environ Microbiol 66:1871-6.

Manen J.F., Simon P., Van Slooten J.C., Osteras M., Frutiger S., Hughes G.J. (1991) A nodulin specifically expressed in senescent nodules of winged bean is a protease inhibitor. Plant Cell 3:259-70. DOI: 10.1105/tpc.3.3.2593/3/259 [pii].

Manoil C., Beckwirth J. (1985) TnphoA: a transposon probe for protein export signals. PNAS USA 82:8129-8133.

Marino D., Gonzalez E.M., Frendo P., Puppo A., Arrese-Igor C. (2007) NADPH recycling systems in oxidative stressed pea nodules: a key role for the NADP+ -dependent isocitrate dehydrogenase. Planta 225:413-21. DOI: 10.1007/s00425-006-0354-5.

Marroqui S., Zorreguieta A., Santamaria C., Temprano F., Soberon M., Megias M., Downie J.A. (2001) Enhanced symbiotic performance by Rhizobium tropici glycogen synthase mutants. J Bacteriol 183:854-64. DOI: 10.1128/JB.183.3.854-864.2001.

Marschner H. (1995) Mineral Nutrition of Higher Plants. Second ed. Academic Press, London.

Martinez-Salazar J.M., Salazar E., Encarnacion S., Ramirez-Romero M.A., Rivera J. (2009) Role of the extracytoplasmic function sigma factor RpoE4 in oxidative and osmotic stress responses in Rhizobium etli. J Bacteriol 191:4122-32. DOI: JB.01626-08 [pii]10.1128/JB.01626-08.

Martinez A.T., Speranza M., Ruiz-Duenas F.J., Ferreira P., Camarero S., Guillen F., Martinez M.J., Gutierrez A., del Rio J.C. (2005) Biodegradation of lignocellulosics: microbial, chemical, and enzymatic aspects of the fungal attack of lignin. Int Microbiol 8:195-204.

Martinez J.J., Mulvey M.A., Schilling J.D., Pinkner J.S., Hultgren S.J. (2000) Type 1 pilus-mediated bacterial invasion of bladder epithelial cells. EMBO J 19:2803-12. DOI: 10.1093/emboj/19.12.2803.

Matamoros M.A., Loscos J., Coronado M.J., Ramos J., Sato S., Testillano P.S., Tabata S., Becana M. (2006) Biosynthesis of ascorbic acid in legume root nodules. Plant Physiol 141:1068-77. DOI: 10.1104/pp.106.081463.

Mathis J.N., Barbour W.M., Miller T.B., Israel D.W., Elkan G.H. (1986) Characterization of a Mannitol-Utilizing, Nitrogen-Fixing Bradyrhizobium japonicum USDA 110 Derivative. Appl Environ Microbiol 52:81-85.

Maunoury N., Redondo-Nieto M., Bourcy M., Van de Velde W., Alunni B., Laporte P., Durand P., Agier N., Marisa L., Vaubert D., Delacroix H., Duc G., Ratet P., Aggerbeck L., Kondorosi E., Mergaert P. (2010) Differentiation of symbiotic cells and endosymbionts in Medicago truncatula nodulation are coupled to two transcriptome-switches. PLoS One 5:e9519. DOI: 10.1371/journal.pone.0009519.

McCloud S.A., Smith R.G., Schuller K.A. (2001) Partial purification and characterization of pyruvate kinase from the plant fraction of soybean root nodules. Physiol Plant 111:283-290. DOI: ppl1110304 [pii].

McDermott T.R., Kahn M.L. (1992) Cloning and mutagenesis of the Rhizobium meliloti isocitrate dehydrogenase gene. J Bacteriol 174:4790-7.

McKay I.A., Glenn A.R., Dilworth M.J. (1985) Gluconeogenesis in *Rhizobium leguminosarum* MNF3841. Journal of General Microbiology 131:2067-2073.

McKinlay J.B., Harwood C.S. (2010) Carbon dioxide fixation as a central redox cofactor recycling mechanism in bacteria. Proc Natl Acad Sci U S A 107:11669-75. DOI: 1006175107 [pii]10.1073/pnas.1006175107.

Meakin G.E., E. Bueno, B. Jepson, E.J. Bedmar, D.J. Richardson, and M.J. Delgado. . (2007) The contribution of bacteroidal nitrate and nitrite reduction to the formation of nitrosyllegheamoglobin complexes in soybean root nodules. Microbiology 153:411-419.

Mellor R.B. (1989) Bacteroids in the *Rhizobium*-legume symbiosis inhabit a plant internal lytic compartment: Implications for other microbial endosymbioses. J. Exp. Bot. 40:831-839.

Meneses N., Mendoza-Hernandez G., Encarnacion S. (2010) The extracellular proteome of Rhizobium etli CE3 in exponential and stationary growth phase. Proteome Sci 8:51. DOI: 1477-5956-8-51 [pii]10.1186/1477-5956-8-51.

Mesa S., Hauser F., Friberg M., Malaguti E., Fischer H.M., Hennecke H. (2008) Comprehensive assessment of the regulons controlled by the FixLJ-FixK2-FixK1 cascade in Bradyrhizobium japonicum. J Bacteriol 190:6568-79. DOI: 10.1128/JB.00748-08.

Mesa S., Hennecke H., Fischer H.M. (2006) A multitude of CRP/FNR-like transcription proteins in Bradyrhizobium japonicum. Biochem Soc Trans 34:156-9. DOI: BST0340156 [pii]10.1042/BST0340156.

Miflin B.J., Lea P.J. (1980) Ammonium assimilation Academic Press, New York.

Miller S.S., Boylan K.L.M., Vance C.P. (1987) Alfalfa root nodule carbon-dioxide fixation. 3. Immunological studies of nodule phosphoenolpyruvate carboxylase. Plant Physiol 84:501-508.

Miller S.S., Driscoll B.T., Gregerson R.G., Gantt J.S., Vance C.P. (1998) Alfalfa malate dehydrogenase (MDH): molecular cloning and characterization of five different forms reveals a unique nodule-enhanced MDH. Plant J 15:173-84.

Minder A.C., Fischer H.M., Hennecke H., Narberhaus F. (2000) Role of HrcA and CIRCE in the heat shock regulatory network of Bradyrhizobium japonicum. J Bacteriol 182:14-22.

Mocibob M., Ivic N., Bilokapic S., Maier T., Luic M., Ban N., Weygand-Durasevic I. (2010) Homologs of aminoacyl-tRNA synthetases acylate carrier proteins and provide a link between ribosomal and nonribosomal peptide synthesis. Proc Natl Acad Sci U S A 107:14585-90. DOI: 1007470107 [pii]10.1073/pnas.1007470107.

Modric N., Derome A.E., Ashcroft S.J.H., Poje M. (1992) Tracing and identification of uricase reaction intermediates. Tetrahedron Lett. 33:6691-6694.

Moorman T.B., Becerril J.M., Lydon J., Duke S.O. (1992) Production of hydroxybenzoic acids by *Bradyrhizobium japonicum* strains after treatment with glyphosphate. Journal of Agricultural Food Chemistry 40:289-293.

Morrell M., Copeland L. (1985) Sucrose synthase of soybean nodules. Plant Physiol 78:149-154.

Mortimer M.W., McDermott T.R., York G.M., Walker G.C., Kahn M.L. (1999) Citrate synthase mutants of Sinorhizobium meliloti are ineffective and have altered cell surface polysaccharides. J Bacteriol 181:7608-13.

Mouritzen P., Rosendahl L. (1997) Identification of a Transport Mechanism for NH4+ in the Symbiosome Membrane of Pea Root Nodules. Plant Physiol 115:519-526. DOI: 115/2/519 [pii].

Muller J., Wiemken A., Boller T. (2001) Redifferentiation of bacteria isolated from Lotus japonicus root nodules colonized by Rhizobium sp. NGR234. J Exp Bot 52:2181-6.

Muller P. (2004) Use of the multipurpose transposon Tn KPK2 for the mutational analysis of chromosomal regions upstream and downstream of the *sipF* gene in *Bradyrhizobium japonicum*. Mol. Gen. Genomics 271:359-366.

Muller P., Bonnard. N. (2004) Studying extracytoplasmic proteins of *Bradyrhizobium japonicum* by E-tag fusion clones obtained from phage display. . Endocytobiosis Cell Res. 15:527-537.

Muller P., K. Ahrens, T. Keller, and A. Klaucke. . (1995) A TnphoA insertion within the *Bradyrhizobium japonicum sipS* gene, homologous to prokaryotic signal peptidases, results in extensive changes in the expression of PBM-specific nodulins of infected soybean (*Glycine max*) cells. . Mol. Microbiol. 18:831-840.

Munchbach M., Dainese P., Staudenmann W., Narberhaus F., James P. (1999) Proteome analysis of heat shock protein expression in Bradyrhizobium japonicum. Eur J Biochem 264:39-48.

Nagano K., Murakami Y., Nishikawa K., Sakakibara J., Shimozato K., Yoshimura F. (2007) Characterization of RagA and RagB in Porphyromonas gingivalis: study using gene-deletion mutants. J Med Microbiol 56:1536-48. DOI: 56/11/1536 [pii]10.1099/jmm.0.47289-0.

Narberhaus F., Weiglhofer W., Fischer H.M., Hennecke H. (1996) The Bradyrhizobium japonicum rpoH1 gene encoding a sigma 32-like protein is part of a unique heat shock gene cluster together with groESL1 and three small heat shock genes. J Bacteriol 178:5337-46.

Nardi S., Pizzeghello D., Bragazza L., Gerdol R. (2003) Low-molecular-weight organic acids and hormone-like activity of dissolved organic matter in two forest soils in N Italy. J Chem Ecol 29:1549-64.

Natera S.H., Guerreiro N., Djordjevic M.A. (2000) Proteome analysis of differentially displayed proteins as a tool for the investigation of symbiosis. Mol Plant Microbe Interact 13:995-1009. DOI: 10.1094/MPMI.2000.13.9.995.

Nesvizhskii A.I., Keller A., Kolker E., Aebersold R. (2003) A statistical model for identifying proteins by tandem mass spectrometry. Anal Chem 75:4646-58.

Newcomb E.H. (1981) Nodule morphogenesis and differentiation. Int. Rev. Cytol. Suppl. 13:247-297.

Nielsen L.P., Risgaard-Petersen N., Fossing H., Christensen P.B., Sayama M. (2010) Electric currents couple spatially separated biogeochemical processes in marine sediment. Nature 463:1071-4. DOI: 10.1038/nature08790.

Nienaber A., Huber A., Gottfert M., Hennecke H., Fischer H.M. (2000) Three new NifA-regulated genes in the Bradyrhizobium japonicum symbiotic gene region discovered by competitive DNA-RNA hybridization. J Bacteriol 182:1472-80.

Nogales J., Macchi R., Franchi F., Barzaghi D., Fernandez C., Garcia J.L., Bertoni G., Diaz E. (2007) Characterization of the last step of the aerobic phenylacetic acid degradation pathway. Microbiology 153:357-65. DOI: 153/2/357 [pii]10.1099/mic.0.2006/002444-0.

Nomura M., Mai H.T., Fujii M., Hata S., Izui K., Tajima S. (2006) Phosphoenolpyruvate carboxylase plays a crucial role in limiting nitrogen fixation in Lotus japonicus nodules. Plant Cell Physiol 47:613-21. DOI: pcj028 [pii]10.1093/pcp/pcj028.

Okazaki S., Hattori Y., Saeki K. (2007) The Mesorhizobium loti purB gene is involved in infection thread formation and nodule development in Lotus japonicus. J Bacteriol 189:8347-52. DOI: 10.1128/JB.00788-07.

Olsen A., Jonsson A., Normark S. (1989) Fibronectin binding mediated by a novel class of surface organelles on Escherichia coli. Nature 338:652-5. DOI: 10.1038/338652a0.

Oresnik I.J., Layzell D.B. (1994) Composition and Distribution of Adenylates in Soybean (Glycine max L.) Nodule Tissue. Plant Physiol 104:217-225.

Osteras M., Finan T.M., Stanley J. (1991) Site-directed mutagenesis and DNA sequence of pckA of Rhizobium NGR234, encoding phosphoenolpyruvate carboxykinase: gluconeogenesis and host-dependent symbiotic phenotype. Mol Gen Genet 230:257-69.

Osteras M., O'Brien S.A., Finan T.M. (1997) Genetic analysis of mutations affecting pckA regulation in Rhizobium (Sinorhizobium) meliloti. Genetics 147:1521-31.

Panek H., O'Brian M. (2004) KatG is the primary detoxifier of hydrogen peroxide produced by aerobic metabolism of *Bradyrhizobium japonicum*. . J. Bac. 186:7874-7880.

Panter S., Thomson R., de Bruxelles G., Laver D., Trevaskis B., Udvardi M. (2000) Identification with proteomics of novel proteins associated with the peribacteroid membrane of soybean root nodules. Mol Plant Microbe Interact 13:325-33. DOI: 10.1094/MPMI.2000.13.3.325.

Parke D. (1992) Application of p-Toluidine in Chromogenic Detection of Catechol and Protocatechuate, Diphenolic Intermediates in Catabolism of Aromatic Compounds. Appl Environ Microbiol 58:2694-7.

Parke D., Ornston L.N. (1986) Enzymes of the beta-ketoadipate pathway are inducible in Rhizobium and Agrobacterium spp. and constitutive in Bradyrhizobium spp. J Bacteriol 165:288-92.

Parke D., Rivelli M., Ornston L.N. (1985) Chemotaxis to aromatic and hydroaromatic acids: comparison of Bradyrhizobium japonicum and Rhizobium trifolii. J Bacteriol 163:417-22.

Parniske M., Muller P., Kosch K., Werner D. (1993) *ExoB* mutants of *Bradyrhizobium japonicum* with reduced competitiveness for nodulation of *Glycine max*. Mol Plant Microbe Interact 6:99-106.

Parniske M., Muller P., Kosch K., Werner D. (1994) Plant defense response of host plants with determinate nodules induced by EPS-defective *exoB* mutants of *Bradyrhizobium japonicum*. Mol Plant Microbe Interact 7:631-638.

Patankar A.V., Gonzalez J.E. (2009) An Orphan LuxR Homolog of *Sinorhizobium meliloti* Affects Stress Adaptation and Competition for Nodulation. Applied and Environmental Microbiology 75:946-955.

Patat S.A., Carnegie R.B., Kingsbury C., Gross P.S., Chapman R., Schey K.L. (2004) Antimicrobial activity of histones from hemocytes of the Pacific white shrimp. Eur J Biochem 271:4825-33. DOI: EJB4448 [pii]10.1111/j.1432-1033.2004.04448.x.

Pathirana S.M., Vance C.P., Miller S.S., Gantt J.S. (1992) Alfalfa root nodule phosphoenolpyruvate carboxylase: characterization of the cDNA and expression in effective and plant-controlled ineffective nodules. Plant Mol Biol 20:437-50.

Pauly N., Pucciariello C., Mandon K., Innocenti G., Jamet A., Baudouin E., Hérouart D., Frendo P., Puppo A. (2006) Reactive oxygen and nitrogen species and glutathione:key players in the legume-Rhizobium symbiosis. J. of Exp. Bot. 57:1769-1776.

Peiter E., Schubert S. (2003) Sugar uptake and proton release by protoplasts from the infected zone of Vicia faba L. nodules: evidence against apoplastic sugar supply of infected cells. J Exp Bot 54:1691-700. DOI: 10.1093/jxb/erg191erg191 [pii].

Peoples M.B., Herridge D.F. (1990) Nitrogen fixation by legumes in tropical and subtropical agriculture. Adv. Agron. 44:155-223.

Peralta H., Mora Y., Salazar E., Encarnacion S., Palacios R., Mora J. (2004) Engineering the nifH promoter region and abolishing poly-beta-hydroxybutyrate accumulation in Rhizobium etli enhance nitrogen fixation in symbiosis with Phaseolus vulgaris. Appl Environ Microbiol 70:3272-81. DOI: 10.1128/AEM.70.6.3272-3281.200470/6/3272 [pii].

Perlick A.M., Puhler A. (1993) A survey of transcripts expressed specifically in root nodules of broadbean (Vicia faba L.). Plant Mol Biol 22:957-70.

Pessi G., Ahrens C.H., Rehrauer H., Lindemann A., Hauser F., Fischer H.M., Hennecke H. (2007) Genome-wide transcript analysis of Bradyrhizobium japonicum bacteroids in soybean root nodules. Mol Plant Microbe Interact 20:1353-63. DOI: 10.1094/MPMI-20-11-1353.

Peters N.K., Verma D.P. (1990) Phenolic compounds as regulators of gene expression in plant-microbe relations. Mol Plant Microbe Interact 3:4-8.

Peterson J.B., Evans H.J. (1978) Properties of pyruvate kinase from soybean nodule cytosol. Plant Physiol 61:909-14.

Peterson J.B., Larue T.A. (1981) Utilization of aldehydes and alcohols by soybean bacteroids. Plant Physiol 68:489-93.

Peterson J.B., LaRue T.A. (1982) Soluble aldehyde dehydrogenase and metabolism of aldehydes by soybean bacteroids. J Bacteriol 151:1473-84.

Pladys D., Vance C.P. (1993) Proteolysis during Development and Senescence of Effective and Plant Gene-Controlled Ineffective Alfalfa Nodules. Plant Physiol 103:379-384. DOI: 103/2/379 [pii].

Podila G.K., Kotagiri S., Shantharam S. (1993) Cloning of Protocatechuate 3,4-Dioxygenase Genes from Bradyrhizobium japonicum USDA110. Appl Environ Microbiol 59:2717-9.

Poole P.S., Alloway D.A. (2000) Carbon and nitrogen metabolism in Rhizobium. Adv. Microb. Physiol. (Rio J) 140:2797-2809.

Prell J., Poole P. (2006) Metabolic changes of rhizobia in legume nodules. Trends Microbiol 14:161-8. DOI: S0966-842X(06)00049-7 [pii]10.1016/j.tim.2006.02.005.

Prell J., White J.P., Bourdes A., Bunnewell S., Bonagaerts R.J., Poole P.S. (2009) Legumes Regulate *Rhizobium* Bacteroid Development and Persistence by the Supply of Branched-chain Amino Acids. PNAS USA 106:12477-12482.

Prentki P., Krisch H.M. (1984) In vitro insertional mutagenesis with a selectable DNA fragment. Gene 29:303-13.

Preston G.G., Wall J.D., Emerich D.W. (1990) Purification and properties of acetyl-CoA synthetase from Bradyrhizobium japonicum bacteroids. Biochem J 267:179-83.

Price N.P., Kelly T.M., Raetz C.R., Carlson R.W. (1994) Biosynthesis of a structurally novel lipid A in Rhizobium leguminosarum: identification and characterization of six metabolic steps leading from UDP-GlcNAc to 3-deoxy-D-manno-2-octulosonic acid2-lipid IVA. J Bacteriol 176:4646-55.

Prince J.T., Marcotte E.M. (2008) mspire: mass spectrometry proteomics in Ruby. Bioinformatics 24:2796-7. DOI: 10.1093/bioinformatics/btn513.

Puppo A., Dimitrijevic L., Rigaud J. (1982) Acetylene reduction and superoxide dismutase activities in Sesbania rostrata root and stem nodules. Physiol. Veg. 24:689-696.

Puppo A., Groten K., Bastian F., Carzaniga R., Soussi M., Lucas M.M., de Felipe M.R., Harrison J., Vanacker H., Foyer C.H. (2005) Legume nodule senescence: roles for redox and hormone signalling in the orchestration of the natural aging process. New Phytol 165:683-701. DOI: NPH1285 [pii]10.1111/j.1469-8137.2004.01285.x.

Rabus R., Kube M., Beck A., Widdel F., Reinhardt R. (2002) Genes involved in the anaerobic degradation of ethylbenzene in a denitrifying bacterium, strain EbN1. Arch Microbiol 178:506-16. DOI: 10.1007/s00203-002-0487-2.

Ramirez-Trujillo J.A., S. Encarnacion, E. Salazar, A. Garcia de los Santos, M.F. Dunn, D.W. Emerich, E. Calva, & I. Hernandez-Lucas. (2007) Functional Characterization of the *Sinorhizobium meliloti* Acetate Metabolism Genes *aceA*, SMc00767, and glcB. Journal of Bacteriology 189:5875-5884.

Rastogi V.K., Watson R.J. (1991) Aspartate Aminotransferase Activity is Required for Aspartate Catabolism and Symbiotic Nitrogen Fixation in *Rhizobium meliloti*. Journal of Bacteriology 173:2879-2887.

Raychaudhuri A., Tipton P.A. (2002) Cloning and expression of the gene for soybean hydroxyisourate hydrolase. Localization and implications for function and mechanism. Plant Physiol 130:2061-8. DOI: 10.1104/pp.011049.

Rees D.C., Howard J.B. (2000) Nitrogenase: standing at the crossroads. Curr Opin Chem Biol 4:559-66. DOI: S1367-5931(00)00132-0 [pii].

Reguera G., McCarthy K.D., Mehta T., Nicoll J.S., Tuominen M.T., Lovley D.R. (2005) Extracellular electron transfer via microbial nanowires. Nature 435:1098-101. DOI: 10.1038/nature03661.

Reibach P.H., Streeter J.G. (1983) Metabolism of C-labeled photosynthate and distribution of enzymes of glucose metabolism in soybean nodules. Plant Physiol 72:634-40.

Reynolds P.H., Boland M.J., Blevins D.G., Schubert K.R., Randall D.D. (1982) Enzymes of amide and ureide biogenesis in developing soybean nodules. Plant Physiol 69:1334-8.

Richardson D.J., King G.F., Kelly D.J., McEwan A.G., Ferguson S.J., al. e. (1988) The role of auxiliary oxidants in maintaining redox balance during phototrophic growth of *Rhodobacter capsulatus*. Archive of Microbiology 150:131-137.

Ritz D., Bott M., Hennecke H. (1993) Formation of several bacterial c-type cytochromes requires a novel membrane-anchored protein that faces the periplasm. Mol Microbiol 9:729-40.

Ritz D., Thony-Meyer L., Hennecke H. (1995) The cycHJKL gene cluster plays an essential role in the biogenesis of c-type cytochromes in Bradyrhizobium japonicum. Mol Gen Genet 247:27-38.

Roberts D.M., Tyerman S.D. (2002) Voltage-dependent cation channels permeable to NH(+)(4), K(+), and Ca(2+) in the symbiosome membrane of the model legume Lotus japonicus. Plant Physiol 128:370-8. DOI: 10.1104/pp.010568.

Rodrigues J.L.M., Melloto M., de Abreu Oliveira J.T., da Silveira J.A.G. (1998) Efficiency of soybean nodules in relation to nodulin activities and hydrogenase expression. Revista Brasileira Fisiologia Vegetal 10:173-178.

Romanov V.I., Gordon A.J., Minchin F.R., Witty J.R., Sket L., James C.L., Borisov A.Y., Tikhonovich I.A. (1995) Anatomy, physiology and biochemistry of root nodules of Sprint-2 Fix-; a symbiotically defective mutant of pea (*Pisum sativum* L.) J. Exp. Bot. 46:1809-1816.

Romanov V.I., Hernandez-Lucas I., Martinez-Romero E. (1994) Carbon Metabolism Enzymes of Rhizobium tropici Cultures and Bacteroids. Appl Environ Microbiol 60:2339-42.

Ronson C.W., Lyttleton P., Robertson J.G. (1981) C(4)-dicarboxylate transport mutants of Rhizobium trifolii form ineffective nodules on Trifolium repens. Proc Natl Acad Sci U S A 78:4284-8.

Ronson C.W., Primrose S.B. (1979) Effect of glucose on polyol metabolism by Rhizobium trifolii. J Bacteriol 139:1075-8.

Rosander A., Frykberg L., Ausmees N., Muller P. (2003) Identification of extracytoplasmic proteins in Bradyrhizobium japonicum using phage display. Mol Plant Microbe Interact 16:727-37. DOI: 10.1094/MPMI.2003.16.8.727.

Rosendahl L., Dilworth M.J., Glenn A.R. (1992) Exchange of metabolites across the peribacteroid membrane in pea root nodules. J. Plant Physiol. 139:635-638.

Rosendahl L., Mouritzen P., Rudbeck A. (2001) Nitrogen transfer in the interface between the symbionts in pea root nodules. Plant Soil 230:31-37.

Roth L.E., Stacey G. (1989) Bacterium release into host cells of nitrogen-fixing soybean nodules: the symbiosome membrane comes from three sources. Eur J Cell Biol 49:13-23.

Rudbeck A., Mouritzen P., Rosendahl L. (1999) Characterization of aspartate transport across the symbiosome membrane in pea root nodules. Plant Physiol 155:576-583.

Rudolph G., Semini G., Hauser F., Lindemann A., Friberg M., Hennecke H., Fischer H.M. (2006) The Iron control element, acting in positive and negative control of iron-regulated Bradyrhizobium japonicum genes, is a target for the Irr protein. J Bacteriol 188:733-44. DOI: 188/2/733 [pii]10.1128/JB.188.2.733-744.2006.

Ruiz-Argüeso T., Emerich D.W., Evans H.J. (1979) Characteristics of the hydrogen-oxidizing hydrogenase system in soybean nodule bacteroids. Arch. Microbiol. 121:199-206.

Saalbach G., Erik P., Wienkoop S. (2002) Characterisation by proteomics of peribacteroid space and peribacteroid membrane preparations from pea (Pisum sativum) symbiosomes. Proteomics 2:325-37. DOI: 10.1002/1615-9861(200203)2:3<325::AID-PROT325>3.0.CO;2-W [pii].

Salminen S.O., Streeter J.G. (1986) Enzymes of alpha,alpha-Trehalose Metabolism in Soybean Nodules. Plant Physiol 81:538-41.

Salminen S.O., Streeter J.G. (1990) Factors contributing to the accumlation of glutamate in *Bradyrhizobium japonicum* bacteroids under microaerobic conditions. J. Gen. Microbiol. 136:2119-2126.

Saltikov C.W., Newman D.K. (2003) Genetic identification of a respiratory arsenate reductase. Proc Natl Acad Sci U S A 100:10983-8. DOI: 10.1073/pnas.1834303100 1834303100 [pii].

Sandkvist M. (2001) Type II secretion and pathogenesis. Infect Immun 69:3523-35. DOI: 10.1128/IAI.69.6.3523-3535.2001.

Santos R., Herouart D., Puppo A., Touati D. (2000) Critical protective role of bacterial superoxide dismutase in rhizobium-legume symbiosis. Mol Microbiol 38:750-9. DOI: mmi2178 [pii].

Sarath G., Pfeiffer N.E., Sodhi C.S., Wagner F.W. (1986) Bacteroids Are Stable during Dark-Induced Senescence of Soybean Root Nodules. Plant Physiol 82:346-50.

Sarma A.D., Emerich D.W. (2005) Global protein expression pattern of Bradyrhizobium japonicum bacteroids: a prelude to functional proteomics. Proteomics 5:4170-84. DOI: 10.1002/pmic.200401296.

Sarma A.D., Emerich. D.W. (2006) A comparative proteomic evaluation of culture grown vs nodule isolated *Bradyrhizobium japonicum*. Proteomics 6:3008-3028.

Sarma A.D., Serfozo P., Kahn K., Tipton P.A. (1999) Identification and purification of hydroxyisourate hydrolase, a novel ureide-metabolizing enzyme. J Biol Chem 274:33863-5.

Schmutz J., Cannon S.B., Schlueter J., Ma J., Mitros T., Nelson W., Hyten D.L., Song Q., Thelen J.J., Cheng J., Xu D., Hellsten U., May G.D., Yu Y., Sakurai T., Umezawa T., Bhattacharyya M.K., Sandhu D., Valliyodan B., Lindquist E., Peto M., Grant D., Shu S., Goodstein D., Barry K., Futrell-Griggs M., Abernathy B., Du J., Tian Z., Zhu L., Gill N., Joshi T., Libault M., Sethuraman A., Zhang X.C., Shinozaki K., Nguyen H.T., Wing R.A., Cregan P., Specht J., Grimwood J., Rokhsar D., Stacey G., Shoemaker R.C., Jackson S.A. (2010) Genome sequence of the palaeopolyploid soybean. Nature 463:178-83. DOI: 10.1038/nature08670.

Schubert K.R. (1986) Products of biological nitrogen fixation in higher plants: Synthesis, transport, and metabolism. Ann. Rev. Plant Physiol. 37:539-574.

Schuller K.A., Turpin D.H., Plaxton W.C. (1990) Metabolite regulation of partially purified soybean nodule phosphoenolpyruvate carboxylase. Plant Physiol 94:1429-35.

Schuller K.A., Werner D. (1993) Phosphorylation of Soybean (Glycine max L.) Nodule Phosphoenolpyruvate Carboxylase in Vitro Decreases Sensitivity to Inhibition by L-Malate. Plant Physiol 101:1267-1273. DOI: 101/4/1267 [pii].

Schwinghamer E.A., Evans H.J., Dawson M.D. (1970) Evaluation of Effectiveness in Mutant Strains of Rhizobium by Acetylene Reduction Relative to Other Criteria of N_2 Fixation. Plant and Soil 33:192-212.

Sciotti M.A., Chanfon A., Hennecke H., Fischer H.M. (2003) Disparate oxygen responsiveness of two regulatory cascades that control expression of symbiotic genes in Bradyrhizobium japonicum. J Bacteriol 185:5639-42.

Seaver L.C., Imlay J.A. (2001) Alkyl hydroperoxide reductase is the primary scavenger of endogenous hydrogen peroxide in Escherichia coli. J Bacteriol 183:7173-81. DOI: 10.1128/JB.183.24.7173-7181.2001.

Shah R., Emerich D.W. (2006) Isocitrate dehydrogenase of Bradyrhizobium japonicum is not required for symbiotic nitrogen fixation with soybean. J Bacteriol 188:7600-8. DOI: JB.00671-06 [pii]10.1128/JB.00671-06.

Shah V.K., Davis L.C., Brill W.J. (1975) Nitrogenase. VI. Acetylene reduction assay: Dependence of nitrogen fixation estimates on component ratio and acetylene concentration. Biochim Biophys Acta 384:353-9.

Silvente S., Blanco L., Camas A., Ortega J.L., Ramirez M., Lara-Flores M. (2002) Rhizobium etli mutant modulates carbon and nitrogen metabolism in Phaseolus

vulgaris nodules. Mol Plant Microbe Interact 15:728-33. DOI: 10.1094/MPMI.2002.15.7.728.

Simonsen A.C.W., Rosendahl L. (1999) Origin of *de novo* synthesized proteins in the different compartments of pea-Rhizobium sp. Symbiosomes. Mol. Plant-Microbe Interactions 12:319-327.

Simpson F.B., Burris R.H. (1984) A nitrogen pressure of 50 atmospheres does not prevent evolution of hydrogen by nitrogenase. Science 224:1095-7.

Smallshaw J.E., Kelln R.A. (1992) Cloning, nucleotide sequence and expression of the *Escherichia coli* K-12 *pyrH* gene encoding UMP kinase. Genetics (Life Sci. Adv.) 11:59-65.

Smith M.T., Emerich D.W. (1993a) Alanine dehydrogenase from soybean nodule bacteroids. Kinetic mechanism and pH studies. J Biol Chem 268:10746-53.

Smith M.T., Emerich D.W. (1993b) Alanine dehydrogenase from soybean nodule bacteroids: purification and properties. Arch Biochem Biophys 304:379-85. DOI: S0003-9861(83)71365-2 [pii]10.1006/abbi.1993.1365.

Smith M.T., Preston G.G., Emerich D.W. (1994) Development of acetate and pyruvate metabolic enzyme activities in soybean nodules. Symbiosis 17:33-42.

Snoeck C., Verreth C., Hernandez-Lucas I., Martinez-Romero E., Vanderleyden J. (2003) Identification of a Third Sulfate Activation System in *Sinorhizobium* sp. Strain BR816: the cysDN Sulfate Activation Complex. Applied and Environmental Microbiology 69:2006-2014.

Spampinato C., Modrich P. (2000) The MutL ATPase is required for mismatch repair. J Biol Chem 275:9863-9.

Spector M.P., DiRusso C.C., Pallen M.J., Garcia del Portillo F., Dougan G., Finlay B.B. (1999) The medium-/long-chain fatty acyl-CoA dehydrogenase (fadF) gene of Salmonella typhimurium is a phase 1 starvation-stress response (SSR) locus. Microbiology 145 (Pt 1):15-31.

Stanford A.C., Larsen K., Barker D.G., Cullimore J.V. (1993) Differential expression within the glutamine synthetase gene family of the model legume Medicago truncatula. Plant Physiol 103:73-81. DOI: 103/1/73 [pii].

Steele M.I., Lorenz D., Hatter K., Park A., Sokatch J.R. (1992) Characterization of the mmsAB operon of Pseudomonas aeruginosa PAO encoding methylmalonate-semialdehyde dehydrogenase and 3-hydroxyisobutyrate dehydrogenase. J Biol Chem 267:13585-92.

Steiner D., Forrer P., Stumpp M.T., Pluckthun A. (2006) Signal sequences directing cotranslational translocation expand the range of proteins amenable to phage display. Nat Biotechnol 24:823-31. DOI: 10.1038/nbt1218.

Streeter J.G. (1980) Carbohydrates in Soybean Nodules: II. DISTRIBUTION OF COMPOUNDS IN SEEDLINGS DURING THE ONSET OF NITROGEN FIXATION. Plant Physiol 66:471-6.

Streeter J.G. (1981) Effect of nitrate in the rooting medium on carbohydrate composition of soybean nodules. Plant Physiol 68:840-4.

Streeter J.G. (1982) Enzymes of sucrose, maltose, and α,α-trehalose catabolism in soybean root nodules. Planta 155:112-115.

Streeter J.G. (1987) Carbohydrate, organic Acid, and amino Acid composition of bacteroids and cytosol from soybean nodules. Plant Physiol 85:768-73.

Streeter J.G. (1989) Analysis of periplasmic enzymes in intact cultured bacteria and bacteroids of *Bradyrhizobium japonicum* and *Rhizobium leguminosarium* biovar *phaseoli*. J. Gen. Microbiol. 135:3477-3484.

Streeter J.G., Rudulier D.l. (1990) Release of periplasmic enzymes from *Rhizobium leguminosarium* bv *phaseoli* bacteroids by lysozyme is enhanced by pretreatment of cells at low pH. Curr. Microbiol. 21:169-173.

Streeter J.G., Salminen S.O. (1990) Periplasmic metabolism of glutamate and aspartate by intact *Bradyrhizobium japonicum* bacteroids. Biochemica et Biophysica Acta 1035:257-265.

Streeter J.G., Salminen S.O. (1993) Labeling of bacteroids following incubation of intact nodules with ^{14}C-sucrose for short time periods. Symbiosis 15:15-26.

Strodtman K.N., Franck S., Tindall R., Jensen C., Sarma A.D., Emerich D.W. (2011) *Bradyrhizobium japonicum* bacteroid appendages expressed in senescing and argon-treated nodules. Symbiosis 54:95-100.

Stumpf D.K., Burris R.H. (1979) A micromethod for the purification and quantification of organic acids of the tricarboxylic acid cycle in plant tissues. Anal Biochem 95:311-5. DOI: 0003-2697(79)90221-5 [pii].

Sudtachat N., Ito N., Itakura M., Masuda S., Eda S., Mitsui H., Kawaharada Y., Minamisawa K. (2009) Aerobic vanillate degradation and C1 compound metabolism in Bradyrhizobium japonicum. Appl Environ Microbiol 75:5012-7. DOI: AEM.00755-09 [pii]10.1128/AEM.00755-09.

Suganuma N., Kitou M., Yamamoto Y. (1987) Carbon metabolism in relation to cellular organization of soybean root nodules and respiration of mitochondria aided by leghemoglobin. Plant Cell Physiol 28:113-122.

Suganuma N., Yamamoto A., Itou A., Hakoyama T., Banba M., Hata S., Kawaguchi M., Kouchi H. (2004) cDNA macroarray analysis of gene expression in ineffective nodules induced on the Lotus japonicus sen1 mutant. Mol Plant Microbe Interact 17:1223-33. DOI: 10.1094/MPMI.2004.17.11.1223.

Summers M.L., Botero L.M., Busse S.C., McDermott T.R. (2000) The ++Sinorhizobium meliloti lon protease is involved in regulating exopolysaccharide synthesis and is required for nodulation of alfalfa. J Bacteriol 182:2551-8.

Suzuki F., Zahler W.L., Emerich D.W. (1987) Acetoacetyl-CoA Thiolase of *Bradyrhizobium japonicum* Bacteroids: Purification and Properties. Archives of Biochemistry and Biophysics 254:272-281.

Tajima S., Larue T.A. (1982) Enzymes for acetaldehyde and ethanol formation in legume nodules. Plant Physiol 70:388-92.

Temple S.J., Kunjibettu S., Roche D., Sengupta-Gopalan C. (1996) Total Glutamine Synthetase Activity during Soybean Nodule Development Is Controlled at the Level of Transcription and Holoprotein Turnover. Plant Physiol 112:1723-1733. DOI: 112/4/1723 [pii].

Tesfaye M., Samac D.A., Vance C.P. (2006) Insights into symbiotic nitrogen fixation in Medicago truncatula. Mol Plant Microbe Interact 19:330-41. DOI: 10.1094/MPMI-19-0330.

Thony-Meyer L., Kunzler P. (1996) The Bradyrhizobium japonicum aconitase gene (acnA) is important for free-living growth but not for an effective root nodule symbiosis. J Bacteriol 178:6166-72.

Thony-Meyer L., Ritz D., Hennecke H. (1994) Cytochrome c biogenesis in bacteria: a possible pathway begins to emerge. Mol Microbiol 12:1-9.

Thummler F., Verma D.P. (1987) Nodulin-100 of soybean is the subunit of sucrose synthase regulated by the availability of free heme in nodules. J Biol Chem 262:14730-6.

Tjalsma H., H. Antelmann, J.D.H. Jongbloed, P.G. Braun, E. Darmon, R. Dorenbos, JY.F. Dubois, H. Westers, G. Zanen, W.J. Quax, O.P. Kuipers, S. Bron, M. Hecker, & J.M. van Dijl. (2004) Proteomics of Secretion by *Bacillus subtilis*: Separating the "Secrets" of the Secretome. Microbiology and Molecular Biology 68:207-233.

Todd C.D., Tipton P.A., Blevins D.G., Piedras P., Pineda M., Polacco J.C. (2006) Update on ureide degradation in legumes. J Exp Bot 57:5-12. DOI: erj013 [pii]10.1093/jxb/erj013.

Trinchant J.C., Birot A.M., Rigaud J. (1981) Oxygen supply and energy-yielding substrates for nitrogen fixation (acetylene reduction) by bacteroid preparations. J. Gen. Microbiol. 125:159-165.

Tsien H.C., Cain P.S., Schmidt E.L. (1977) Viability of Rhizobium bacteroids. Appl Environ Microbiol 34:854-6.

Tsukita S., Koyanagi S., Nagata K., Koizuka H., Akashi H., Shimoyama T., Tamura T., Sone N. (1999) Characterization of a cb-type cytochrome c oxidase from Helicobacter pylori. J Biochem 125:194-201.

Tyerman S.D., Whitehead L.F., Day D.A. (1995) A channel-like transporter for NH4+ on the symbiotic interface of N2-fixing plants. Nature (London) 378:629-632.

Udvardi M.K., Day D.A. (1989) Electrogenic ATPase Activity on the Peribacteroid Membrane of Soybean (Glycine max L.) Root Nodules. Plant Physiol 90:982-7.

Udvardi M.K., Day D.A. (1997) Metabolite Transport across Symbiotic Membranes of Legume Nodules. Annu Rev Plant Physiol Plant Mol Biol 48:493-523. DOI: 10.1146/annurev.arplant.48.1.493.

Udvardi M.K., Price G.D., Gresshoff P.M., Day D.A. (1989) A dicarboxylate transporter of the peribacteroid membrane of soybean nodules. . Mol. Plant Micr. Inter. 1:250-254.

Udvardi M.K., Salom C.L., Day D.A. (1988) Transport of L-glutamate across the bacteroid membrane but not the peribacteroid membrane from soybean root nodules. Mol. Plant Micr. Inter. 1:250-254.

Udvardi M.K., Yang L.-J.O., Young S., Day D.A. (1990) Sugar and amino acid transport across symbiotic membranes from soybean nodules. Mol. Plant Micr. Inter. 3:334-340.

Valpuesta V., Botella M.A. (2004) Biosynthesis of L-ascorbic acid in plants: new pathways for an old antioxidant. Trends Plant Sci 9:573-7. DOI: 10.1016/j.tplants.2004.10.002.

Vance C.P. (2000) Amide biosynthesis in root ndoules of temperate legumes Horizon Scientific Press, Wymondham, UK.

Vance C.P., Gantt J.S. (1992) Control of nitrogen and carbon metabolism in root-nodules. Physiol. Plant 85:266-274.

Vance C.P., Gregerson R.G., Robinsson D.B., Miller S.S., Gantt J.S. (1994) Primary assimilation of nitrogen in alfalfa nodules - molecular-features of the enzymes involved. Plant Sci. 101:51-64.

Vance C.P., Heichel G.H. (1991) Carbon in N2 fixation: Limitation or exquisite adaptation. Annual Review in Plant Physiology and Plant Molecular Biology 42:373-392.

Vandenbosch K.A., Newcomb E.H. (1988) The occurrence of leghemoglobin protein in the uninfected interstitial cells of soybean root nodules. Planta 175:422-451.

Vanderlinde E.M., Muszynski A., Harrison J.J., Koval S.F., Foreman D.L., Ceri H., Kannenberg E.L., Carlson R.W., Yost C.K. (2009) Rhizobium leguminosarum biovar viciae 3841, deficient in 27-hydroxyoctacosanoate-modified lipopolysaccharide, is impaired in desiccation tolerance, biofilm formation and motility. Microbiology 155:3055-69. DOI: mic.0.025031-0 [pii]10.1099/mic.0.025031-0.

Vasse J., de Billy F., Camut S., Truchet G. (1990) Correlation between ultrastructural differentiation of bacteroids and nitrogen fixation in alfalfa nodules. J Bacteriol 172:4295-306.

Vattanaviboon P., Tanboon W., Mongkolsuk S. (2007) Physiological and expression analyses of Agrobacterium tumefaciens trxA, encoding thioredoxin. J Bacteriol 189:6477-81. DOI: JB.00623-07 [pii]10.1128/JB.00623-07.

Voegele R.T., Sweet G.D., Boos W. (1993) Glycerol kinase of Escherichia coli is activated by interaction with the glycerol facilitator. J Bacteriol 175:1087-94.

Wadham C., Winter H., Schuller K.A. (1996) Regulation of sobyean nodule phosphoenolpyruvate carboxylase in vivo. Physiol. Plant 97:531-535.

Waheeta H., Mahadevan A. (1997) Degradation of Catechin by *Bradyrhizobium japonicum*. Biodegradation 8:159-165.

Walshaw D.L., Wilkinson A., Mundy M., Smith M., Poole P.S. (1997) Regulation of the TCA cycle and the general amino acid permease by overflow metabolism in Rhizobium leguminosarum. Microbiology 143 (Pt 7):2209-21.

Walthers R.F., Atlas E., Carrigan A., Rouleau Y., Edgecombe A., Visentin L., Lamprecht C., Addicks G.C., Haché R.J.G., Lefebvre Y.A. (2005) A serine-threonine-rich motif is one of three nuclear localization signals that determine unidirectional transport of the mineralocorticoid receptor to the nucleus. J. Biol. Chem. 280:17549-17561.

Wang C., Saldanha M., Sheng X., Shelswell K.J., Walsh K.T., Sobral B.W., Charles T.C. (2007) Roles of poly-3-hydroxybutyrate (PHB) and glycogen in symbiosis of Sinorhizobium meliloti with Medicago sp. Microbiology 153:388-98. DOI: 153/2/388 [pii]10.1099/mic.0.29214-0.

Wang X., Chapman M.R. (2008) Curli provide the template for understanding controlled amyloid propagation. Prion 2:57-60.

Warshaw D.L., Wilkinson A., Mundy M., Shith M., Poole P. (1997) Regulation of the TCA cycle and the general amino acaid permease by overflow metabolism in *Rhizobium leguminosarum*. Microbiol. 143:2209-2221.

Waters J.K., Hughes B.L., 2nd, Purcell L.C., Gerhardt K.O., Mawhinney T.P., Emerich D.W. (1998) Alanine, not ammonia, is excreted from N2-fixing soybean nodule bacteroids. Proc Natl Acad Sci U S A 95:12038-42.

Waters J.K., Karr D.B., Emerich D.W. (1985) Malate dehydrogenase from Rhizobium japonicum 3IIb-143 bacteroids and Glycine max root nodule mitochondria. Biochemistry 24:6479-6486.

Wei M., Yokoyama T., Minamisawa K., Mitsui H., Itakura M., Kaneko T., Tabata S., Saeki K., Omori H., Tajima S., Uchiumi T., Abe M., Ohwada T. (2008) Soybean seed extracts preferentially express genomic loci of Bradyrhizobium japonicum in the initial interaction with soybean, Glycine max (L.) Merr. DNA Res 15:201-14. DOI: dsn012 [pii]10.1093/dnares/dsn012.

Wells D.H., Chen E.J., Fisher R.F., Long. S.R. (2007) ExoR is genetically coupled to the ExoS-Chvl two-component system and located in the periplasm of *Sinorhizobium meliloti*. Mol. Microbiol. 64:647-664.

Wen F., VanEtten H.D., Tsaprailis G., Hawes M.C. (2007) Extracellular proteins in pea root tip and border cell exudates. Plant Physiol 143:773-83. DOI: pp.106.091637 [pii]10.1104/pp.106.091637.

Werner D. (1992) Physiology of Nitrogen-Fixing Legume Nodules: Compartments and Functions Chapman and Hall, New York, NY.

Westenberg D.J., Guerinot M.L. (1999) Succinate dehydrogenase (Sdh) from Bradyrhizobium japonicum is closely related to mitochondrial Sdh. J Bacteriol 181:4676-9.

White J., Prell J., James E.K., Poole P. (2007) Nutrient sharing between symbionts. Plant Physiol 144:604-14. DOI: 144/2/604 [pii]10.1104/pp.107.097741.

White J.P., Prell J., Ramachandran V.K., Poole P.S. (2009) Characterization of a {gamma}-aminobutyric acid transport system of Rhizobium leguminosarum bv.

viciae 3841. J Bacteriol 191:1547-55. DOI: JB.00926-08 [pii]10.1128/JB.00926-08.

Whitehead L.F., Yerman S.D., Salom C.L., Day D.A. (1995) Transport of fixed nitrogen across symbiotic membranes of legume nodules. Symbiosis 19:141-154.

Wienkoop S., Saalbach G. (2003) Proteome analysis. Novel proteins identified at the peribacteroid membrane from Lotus japonicus root nodules. Plant Physiol 131:1080-90. DOI: 10.1104/pp.102.015362.

Wilson D.O., Reisenauer H.M. (1963) Determination of leghemoblobin in legume nodules. Anal. Biochem 6:27-30.

Winzer T., Bairl A., Linder M., Linder D., Werner D., Muller P. (1999) A novel 53-kDa nodulin of the symbiosome membrane of soybean nodules, controlled by Bradyrhizobium japonicum. Mol Plant Microbe Interact 12:218-26. DOI: 10.1094/MPMI.1999.12.3.218.

Wong C.M., Dilworth M.J., Glenn A.R. (1994) Cloning and Sequencing show that 4-hydroxybenzoate hydroxylase (PobA) is required for uptake of 4-hydroxybenzoate in *Rhizobium leguminosarum*. Microbiology 140:2775-2786.

Wong D.W. (2009) Structure and action mechanism of ligninolytic enzymes. Appl Biochem Biotechnol 157:174-209. DOI: 10.1007/s12010-008-8279-z.

Wong P.P., Evans H.J. (1971) Poly-beta-hydroxybutyrate Utilization by Soybean (Glycine max Merr.) Nodules and Assessment of Its Role in Maintenance of Nitrogenase Activity. Plant Physiol 47:750-5.

Yang S.Y., Li J.M., He X.Y., Cosloy S.D., Schulz H. (1988) Evidence that the fadB gene of the fadAB operon of Escherichia coli encodes 3-hydroxyacyl-coenzyme A (CoA) epimerase, delta 3-cis-delta 2-trans-enoyl-CoA isomerase, and enoyl-CoA hydratase in addition to 3-hydroxyacyl-CoA dehydrogenase. J Bacteriol 170:2543-8.

Yoneyama T., Fujihara S., Yagi K. (1998) Natural Abundance of ^{15}N in Amino Acids and Polyamines from Leguminous Nodules: Unique ^{15}N Enrichment in Homospermidine. Journal of Experimental Botany 49:521-526.

Yuan Z.C., Zaheer R., Finan T.M. (2006a) Regulation and properties of PstSCAB, a high-affinity, high-velocity phosphate transport system of Sinorhizobium meliloti. J Bacteriol 188:1089-102. DOI: 188/3/1089 [pii]10.1128/JB.188.3.1089-1102.2006.

Yuan Z.C., Zaheer R., Morton R., Finan T.M. (2006b) Genome prediction of PhoB regulated promoters in Sinorhizobium meliloti and twelve proteobacteria. Nucleic Acids Res 34:2686-97. DOI: 34/9/2686 [pii]10.1093/nar/gkl365.

Zhang K., McKinlay C., Hocart C.H., Djordjevic M.A. (2006) The Medicago truncatula small protein proteome and peptidome. J Proteome Res 5:3355-67. DOI: 10.1021/pr060336t.

Zhang X.Q., Chollet R. (1997) Phosphoenolpyruvate carboxylase protein kinase from soybean root nodules: partial purification, characterization, and up/down-regulation by photosynthate supply from the shoots. Arch Biochem Biophys 343:260-8. DOI: S0003-9861(97)90190-9 [pii]10.1006/abbi.1997.0190.

Zhang X.Q., Li B., Chollet R. (1995) In Vivo Regulatory Phosphorylation of Soybean Nodule Phosphoenolpyruvate Carboxylase. Plant Physiol 108:1561-1568. DOI: 108/4/1561 [pii].

Zhang Y., Hong G. (2009) Post-transcriptional regulation of NifA expression by Hfq and RNase E complex in Rhizobium leguminosarum bv. viciae. Acta Biochim Biophys Sin (Shanghai) 41:719-30.

Zheng L., White R.H., Cash V.L., Jack R.F., Dean D.R. (1993) Cysteine desulfurase activity indicates a role for NIFS in metallocluster biosynthesis. Proc Natl Acad Sci U S A 90:2754-8.

Zipfel C., Kunze G., Chinchilla D., Caniard A., Jones J.D., Boller T., Felix G. (2006) Perception of the bacterial PAMP EF-Tu by the receptor EFR restricts Agrobacterium-mediated transformation. Cell 125:749-60. DOI: S0092-8674(06)00501-0 [pii]10.1016/j.cell.2006.03.037.

VITA

Kent N. Strodtman was born in Marceline, MO and raised in Salisbury, MO, where he attended St. Joseph Catholic Primary School and graduated from Salisbury R-IV High School in May 1999. He completed a B.S. in Biochemistry at Benedictine College (Atchison, KS) in May 2003. He then matriculated to the University of Missouri in the Fall of 2003. Here he was awared the Outstanding Graduate Student Achievement Award in May 2007. He was also the Zahler teaching fellow from Fall 2007 until Fall 2011. This dissertation is in compliance with his completion of a Ph.D. in Biochemistry at the University of Missouri.

Kent is currently employed as an Asst. Prof. of Biology at Columbia Colleg in Columbia, MO and resides in Columbia with his wife of 8 years, Erin and their two daughters, Leslie and Sophia.